Properties of exact density functionals for electronic quantum transport

James David Ramsden

Doctor of Philosophy

University of York

Physics

May, 2013

Abstract

Density functional theory and its extension in the nonequilibrium regime, time-dependent density functional theory, are powerful tools for predicting the structures, energies and dynamics of electronic systems. Their usefulness derives from the Kohn-Sham scheme whereby a system of real, interacting particles is replaced by a fictitious system of non-interacting particles subject to an effective external potential instead of a pairwise particle-particle interaction. The Kohn-Sham universe yields the same observable phenomena as that predicted by standard quantum mechanics so long as the effective external potential is known. However, for the vast majority of systems it is not known, and the usually local (in time and space) functional approximations employed do not capture the physics of true nonlocal interactions.

In this thesis, the exact charge and current densities of model quantum transport devices described by nonlocal potentials are studied and methods for reverse-engineering the corresponding exact Kohn-Sham effective external potential for time-dependent and steady- state density functional theory approaches to the same systems are presented, as well as the resulting exact potentials themselves. Features of improved functionals for calculating approximate Kohn-Sham systems are demonstrated. These functionals are suggested to be very different from existing functionals employed, describing not potentials but electric and magnetic fields, and have a strong dependence on the local and semilocal charge and current density.

I would like to dedicate this thesis to my loving parents . . .

Contents

List of Figures

Acknowledgements

I would like to thank my supervisor Rex Godby for his constant guidance and support throughout the duration of the research detailed in this thesis, and Herve Ness and Louise Dash for their generous assistance and advice. I am also thankful to Peter Bokes for his assistance and for inspiration that was crucial to this work, Phil Hasnip, Robert van Leeuwen and Giovanni Vignale for several illuminating discussions, and Matthew Hodgson for his collaborative spirit.

Finally, I would like to thank my parents Irene and Peter Ramsden for their endless and unconditional support.

Author's Declaration

I declare that the work presented in this thesis, except where otherwise stated, is based on my own research and has not been submitted previously for a degree in this or any other university. Parts of the work reported in this thesis have been published in:

Exact density-functional potentials for time-dependent quasiparticles, J. D. Ramsden and R. W. Godby, Phys. Rev. Lett. **109**, 036402 (2012);

Intrinsic exchange-correlation magnetic fields in exact current density functional theory for degenerate systems, J. D. Ramsden and R. W. Godby, Phys. Rev. B **88**, 195115 (2013).

<div align="right">James Ramsden</div>

Chapter 1

Introduction

The miniaturisation of electronic systems took a giant leap forward in the late 1950's with the introduction of the integrated circuit (IC), a semiconductor chip containing all of the elements of electronic systems integrated into an indivisible single piece. Since then, the number of elements manufacturers have been able to fit onto a chip has approximately doubled every two years: a trend known as Moore's law [12]. Factors that have perpetuated this trend, beyond the invention of the IC itself, include the invention of the complementary metal-oxide-semiconductor (CMOS) technology for constructing dense ICs and the advent of photolithography [13].

Processor chips today may contain tens of millions of transistors: this is the culmination of decades of top-down miniaturisation of electronic components, an approach based on manufacturing the same elements at smaller and smaller scales. The inevitable conclusion of such a venture is the fabrication of devices on the molecular and atomic scales, at which point it becomes necessary to take a bottom-up approach to miniaturisation: to build electronic devices atom-by-atom and molecule-by-molecule.

The bottom-up approach has been suggested since even before the advent of the integrated circuit: an idea known as *molecular engineering* [14] and, in its application to electronics, *molecular electronics*. Throughout the decades to follow and much research into the possibility of fabricating circuits on this scale, the top-down approach continued to achieve beyond expectations, with modern chip features having lengths on the *nanoscale*, or nanometre scale.

Recent perpetuation of Moore's law beyond this has, however, taken on a different character, with a focus on techniques such as multi- and hyper-threading and the integration of previously specialised processors such as graphics processing units. Rather than a continuation of the miniaturisation of components, it has become necessary to

consider instead making circuits larger, more layered and more efficient. One limit-
ing factor is that, at the nanoscale, quantum mechanical effects begin to emerge more
dominantly, and phenomena such as quantum tunnelling will begin to undermine the
operation of electronic circuits as, for instance, electrons leak out of devices.

Rather than limiting such behaviour, the bottom-up approach to molecular elec-
tronics on the nanoscale, or *nanoelectronics*, attempts an incorporation of quantum
mechanical effects into the functional design of electronic components. The field of na-
noelectronics concerns the electron and phonon transport properties of devices on the
nanometre scale, for instance electronic devices as small as a single molecule, and wires
as narrow as one atom thick. A quintessential question of electronic transport concerns
the current-response of an electronic system to the switching on of an externally-applied
electrochemical bias.

Quantum mechanics is a natural tool to answer such questions. In the single-
particle (noninteracting) picture, a quantum mechanical description of a system is given
completely by the wavefunction solution of the time-dependent Schrödinger equation
which, in atomic units (here as throughout this thesis unless otherwise stated), is

$$i\frac{\partial}{\partial t}\psi(\mathbf{r}, t) = \left\{\tfrac{1}{2}\left[\hat{\mathbf{p}} + \mathbf{A}(\mathbf{r}, t)\right]^2 + v(\mathbf{r}, t)\right\}\psi(\mathbf{r}, t). \tag{1.1}$$

The Schrödinger equation encodes all effects of the external potentials $v(\mathbf{r}, t)$ and $\mathbf{A}(\mathbf{r}, t)$
in the wavefunction, and from this wavefunction we can determine any physical property
of interest, including the charge density

$$n(\mathbf{r}, t) = |\psi(\mathbf{r}, t)|^2 \tag{1.2}$$

and the current density

$$\mathbf{j}(\mathbf{r}, t) = \frac{1}{2i}\left[\psi^*(\mathbf{r}, t)\nabla\psi(\mathbf{r}, t) - \psi(\mathbf{r}, t)\nabla\psi^*(\mathbf{r}, t)\right] \tag{1.3}$$

which are related via the continuity equation

$$\frac{\partial}{\partial t}n(\mathbf{r}, t) + \nabla \cdot \mathbf{j}(\mathbf{r}, t) = 0. \tag{1.4}$$

This can be extended to systems of many interacting particles by the inclusion of
interaction terms in the Schrödinger equation, leading to a single many-body wavefunc-

tion for the whole system:

$$i\frac{\partial}{\partial t}\Psi(\mathbf{r},\mathbf{r}_2,\ldots,\mathbf{r}_N,t) = \sum_{j=1}^{N}\left\{\tfrac{1}{2}\left[\hat{\mathbf{p}}_j + \mathbf{A}(\mathbf{r}_j,t)\right]^2 + v(\mathbf{r}_j,t) + \sum_{k>j}^{N}\frac{1}{|\mathbf{r}_j - \mathbf{r}_k|}\right\}. \quad (1.5)$$

The kinds of devices we would be interested in modelling are already being constructed experimentally. The invention of the scanning tunnelling microscope has provided a powerful tool not just for the probing of material surfaces with atomic-scale precision, but also for the manipulation of objects at the atomic scale. Alongside the invention of the atomic force microscope (AFM) and the development of mechanically controllable break-junction (MCBJ) techniques, this paved the way for the fabrication of molecular junctions, atomic-sized point contacts between electronic leads and single-atom-thick nanowires [15]. Examples of molecular junction and nanowires are shown in Fig. 1.1 below.
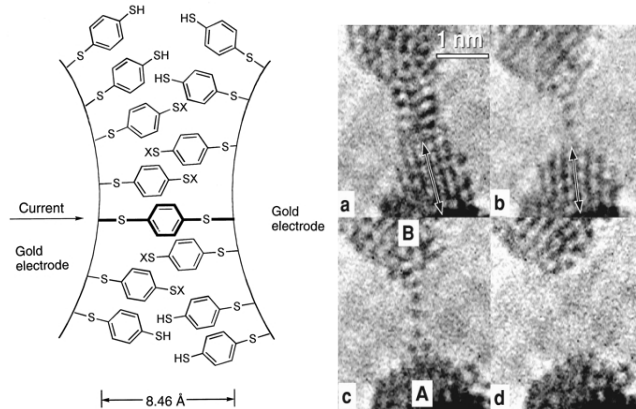
Figure 1.1: **Fabricated molecular electronics devices:** Schematic of a molecular junction of benzene-1,4-dithiolate formed between gold electrodes using the mechanically-controlled break-junction technique [1] (left) and TEM images of gold nanowires of decreasing thickness formed and manipulated with a STM (right) [2]

Fig. 1.2 below demonstrates a purely quantum-mechanical effect in electronics: the quantisation of conductance. Classically, electrical conductance is given by Ohm's law in terms of the voltage across a device and the current passing through it:

$$G = \frac{1}{R} = \frac{I}{V}, \quad (1.6)$$

where R is the resistance of the device, I the current and V the applied voltage. What is clear from Fig. 1.2, and other experimental evidence [16; 17; 18], is that, in reflectionless

3
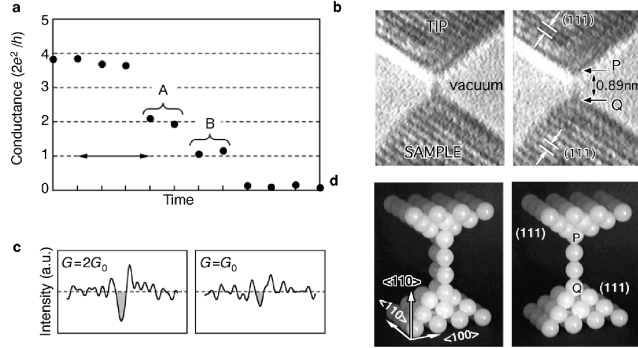
Figure 1.2: Experimental verification of the quantisation of conductance (a) evident in 0-, 1-, 2- and 4-atom-thick gold chains connected to leads. TEM images, corresponding intensity profiles [3] and schematic models of the 1- and 2-atom thick chains are shown in (b)-(d). Image from Nature (1998) [4]

media, the conductance increases in discrete steps of $2e^2/h$ (in S.I. units, or 4π in atomic units). The number of quanta is determined by the width of the contact, hence for the two-atomic-thick chain of gold atoms in Fig. 1.2 the conductance is twice that of the one-atom-thick chain.

Experimental research and fabrication of realistic nanoscale electronic devices continues to develop at a rate that outstrips progress in the computational modelling of such large (in terms of particle numbers) structure, from how one might connect single-molecule devices to metallic leads [19; 20; 21; 22], through the measurement of atomic and electronic structures and conduction of molecular junctions [23; 24], and how the conductance of a molecule can be changed or tuned for precise functionalisation [25; 26].

The computational barrier in modelling such devices and phenomena is the scaling of Eq. 1.5 with increasing particle number. As the number of particles N increases, the number of interaction terms in the Schrödinger equation grows as $\frac{1}{2}(N^2 - N)$. Even without coupling to leads, the number of particles in a molecular junction renders an exact many-body solution unsolvable: the so-called quantum-mechanical many-body problem.

Approaches for applying quantum theory to transport problems are described in the rest of this section. Secs. 1.1 and 1.2 describe the seminal theories for quantum transport that treat particles as noninteracting but rather as tunnelling through and reflecting from a single effective barrier or *scatterer*. Sec. 1.4 describes other approaches to quantum transport such as the statistical description for the electron gas and linear response theory.

In terms of accuracy, the theoretical state-of-the-art is the quasiparticle approach

based on equilibrium and nonequilibrium Green's function approaches described in Sec. 1.6. These approaches incorporate, in principle, all of the quantum-mechanical many-body effects absent in earlier approaches; however, the computational resource required to apply them in practice limits them to small, simple or model systems. The incorporation of many-body effects in a mean-field way is the goal of density-functional theory and time-dependent density-functional theory, a natural extension of noninteracting quantum transport theories, and is described in Chapter 2.

1.1 Two-terminal transport and the Landauer formula

The quantisation of conductance was already a feature in the theory of quantum transport formulated initially by Rolf Landauer in 1957 [27] which is discussed as standard in quantum transport literature, e.g. [15; 28; 29]. Landauer's approach in formulating a theory of quantum transport was to treat it as a scattering problem: that conductance is transmission.

Consider a device connected to two identical, semi-infinite ideal leads of some small cross section such that they act as waveguides, in turn connected to infinite source and sink electron reservoirs held at chemical potentials μ_L and μ_R respectively. Traditional viewpoints on the electric fields in current-carrying systems held that the electric field $\mathbf{E}(\mathbf{r})$ due to an applied bias across a device was the source of the motion of the electrons in it, which accelerated in response to the field as $e\mathbf{E}(\mathbf{r})$. The energy required to add an electron to the device from the source reservoir and the energy required to remove it from the device into the sink reservoir differ by the chemical potential difference between the reservoirs [29]:

$$V = \frac{\mu_L - \mu_R}{e}. \qquad (1.7)$$

For this reason, Landauer maintained the opposite viewpoint [30]: that the establishing of a bias by holding the reservoirs at different chemical potentials is the mechanism by which the charge carriers move, and the aggregation of fluxing charges through the ends of the wires gives rise to the electric field $\mathbf{E}(\mathbf{r}) = \nabla \left(\mu_R(\mathbf{r}) - \mu_L(\mathbf{r}) \right) / e$.

Landauer treats the electrons in the junction connecting the left and right leads as noninteracting. This seemingly crude approximation has some justification: quantum transport is concerned with the behaviour of electrons in devices of very small length scales, and therefore of very low conductance. For conductances large compared with the conductance quantum, electrons are weakly localised (or strongly delocalised) and therefore interact strongly. This is the domain of classical and semiclassical transport.

For conductances very small compared with the conductance quantum, particularly at high energies, conducting electrons are strongly localised. This localisation makes the conducting electrons weakly interacting with each other [28]. (More accurately, the electron *quasiparticles*, accounting for the interaction of the electron with the rest of the non-conducting elements in the wire, are weakly interacting.)

This leaves the interaction with the wire itself: the ions and bound and valence electrons through which the conduction electrons pass. For metals, the screening of the ion lattice by the bound and valence electrons is typically very high, such that the axial variance of the conduction electrons is well approximated by free-space solutions.

The wavefunctions in the leads are of the form

$$\phi_{m,n,k_x}(\mathbf{r}) = \frac{1}{\sqrt{V}} f_{m,n}(y,z) e^{ik_x x} \tag{1.8}$$

where V is the volume the electron occupies, and the dimension x runs along the wire. The function $f_{m,n}(y,z)$ depends on the nature of the cross-sectional confinement and the subband the electron occupies, while the plane-wave term in x is due to the electron being unconfined in that direction. The possible plane wave states form a continuum, each contribution energy

$$E(k_x) = \tfrac{1}{2} k_x^2. \tag{1.9}$$

For an infinite square well confining potential, for instance, we have

$$f_{m,n}(y,z) = 2\cos(k_m y)\cos(k_n z) \tag{1.10}$$

with integer m, n corresponding to the distinct subbands of the system, and energy $E = \tfrac{1}{2}\left(k_y^2 + k_z^2\right)$ yielding a total energy

$$E = \tfrac{1}{2}\left(k_x^2 + k_m^2 + k_n^2\right) = \tfrac{1}{2}k^2. \tag{1.11}$$

These waves form a complete and orthonormal set [31].

The solution of the time-independent Schrödinger equation

$$E\psi(\mathbf{r}) = \left\{ \tfrac{1}{2} \left[\hat{\mathbf{p}} + \mathbf{A}(\mathbf{r},t)\right]^2 + v(\mathbf{r},t) \right\} \psi(\mathbf{r}) \tag{1.12}$$

can then be expanded in terms of incident and outgoing waves in the left and right leads either side of the junction, plus tunnelling waves in the junction itself. If the

junction occupies the region $0 \leq x \leq L$, then the solutions are

$$\psi_L(\mathbf{r}) = \frac{1}{\sqrt{V}} \sum_{n,m,k_x} \left\{ c_{m,n,k_x>0}^{L+} \phi_{m,n,k_x>0}^{L}(\mathbf{r}) + c_{m,n,k_x<0}^{L-} \phi_{m,n,k_x<0}^{L}(\mathbf{r}) \right\} \quad \text{for } x < 0$$

(1.13)

$$\psi_R(\mathbf{r}) = \frac{1}{\sqrt{V}} \sum_{n,m,k_x} \left\{ c_{m,n,k_x<0}^{R-} \phi_{m,n,k_x<0}^{R}(\mathbf{r}) + c_{m,n,k_x>0}^{R+} \phi_{m,n,k_x>0}^{R}(\mathbf{r}) \right\} \quad \text{for } x > L$$

(1.14)

$$\psi_T(\mathbf{r}) = \frac{1}{\sqrt{V}} \sum_{n,m,k_x} \left\{ c_{m,n,ik_x<0}^{T+} \phi_{m,n,ik_x<0}^{T}(\mathbf{r}) + c_{m,n,ik_x>0}^{T-} \phi_{m,n,ik_x>0}^{T}(\mathbf{r}) \right\} \quad \text{for } 0 \leq x \leq L$$

(1.15)

where L, R, T denote the left and right leads and the tunnelling region respectively, and $+, -$ denotes the direction of the wave propagation. Generally, we are interested in the current passing through the device and not the nature of what happens inside it. As such, one solves the above equations for the left and right coefficients.

The coefficients $c^{L+}, c^{L-}, c^{R+}, c^{R-}$ are related via the scattering matrix

$$\begin{pmatrix} c^{L-} \\ c^{R+} \end{pmatrix} = \begin{pmatrix} r & t' \\ t & r' \end{pmatrix} \begin{pmatrix} c^{L+} \\ c^{R-} \end{pmatrix}$$

(1.16)

where r, t are the reflection and transmission coefficients for waves incident from the left lead and r', t' for those incident from the right.

Generally, transmission through and reflection from a scattering barrier depend on the subband (or 'channel'): an electron in subband n (where, for convenience, we denote both y and z subband parameters with a single index) incident upon a scatterer may be transmitted or reflected to a different subband m. The wavefunction coefficients will also be subband-dependent, and thus

$$\begin{pmatrix} c_m^{L-} \\ c_m^{R+} \end{pmatrix} = \begin{pmatrix} r_{m,n} & t'_{m,n} \\ t_{m,n} & r'_{m,n} \end{pmatrix} \begin{pmatrix} c_n^{L+} \\ c_n^{R-} \end{pmatrix} .$$

(1.17)

The reflection and transmission coefficients, $r_{m,n}$ and $t_{m,n}$ may be measured by holding the chemical potential of the sink reservoir such that no electrons flow from the right

in the right-hand region of a given subband. In this case, $c_n^{R-} = 0$, and we have

$$r_{m,n} = \left.\frac{c_m^{L-}}{c_n^{L+}}\right|_{c_n^{R-}=0} \tag{1.18}$$

$$t_{m,n} = \left.\frac{c_m^{R+}}{c_n^{L+}}\right|_{c_n^{R-}=0}. \tag{1.19}$$

For each subband m in the left lead, the fraction of the current from the left reservoir that is transmitted through the junction is the sum of the fractions transmitted from that channel to each of the channels in the right lead:

$$T_m = \sum_n |t_{m,n}|^2; \tag{1.20}$$

the remainder $\sum_n |r_{m,n}|^2$ is reflected back into the left lead. The current per mode is $2e/h$ in S.I. units, where the factor arises due to each mode may be occupied by both spin-up and -down electrons, and thus the current through the system is then the current carried by the electrons transmitted through the junction minus the cancelling current carried by the electrons incoming from the right-hand reservoir:

$$I = \frac{2e}{h} \sum_{m,n} \int_0^\infty dE \; \left[f_L(E) |t_{m,n}(E)|^2 - f_R(E) |t'_{m,n}(E)|^2 \right] \tag{1.21}$$

where $f_L(E)$ and $f_R(E)$ are the Fermi-Dirac distributions for the left and right leads respectively.

The *transmission eigenvalues* $T_m(E) = \sum_n |t_{m,n}(E)|^2$ are typically energy-dependent. However, for chemical potential differences that are small compared with the scale of the energy-dependence, they may be evaluated at the Fermi energy [28]. Thus at zero temperature, where the Fermi-Dirac distribution is a step function at the Fermi energy,

$$\delta I = \frac{2e}{h} \sum_{m,n} |t_{m,n}(\mu)|^2 \, \delta\mu \tag{1.22}$$

and thus

$$G = \frac{\delta I}{\delta V} = e \frac{\delta I}{\delta \mu} = G_0 \sum_{m,n} |t_{m,n}|^2 \tag{1.23}$$

where $G_0 = 2e^2/h$ is the quantum of conductance. Eq. 1.23 is known as the *Landauer formula*.

For a system consisting only of source and sink reservoirs, a scattering device and

two leads connecting them, the actual chemical potential across the device is not well defined [32]. It was soon noted [33]-[34] that real current-carrying devices are connected to multiple leads, rather than just two (measuring the current or voltage across a circuit, for instance, requires additional terminals connected to the measuring device) and that a multi-terminal quantum transport theory was required. While this thesis will focus on two-terminal nanowires, generally one is interested in multi-terminal transport which we will describe in the following section.

1.2 Multi-terminal transport and the Büttiker formalism

The classical current through a device with more than two terminals is given by the generalisation of Ohm's law

$$I_m = \sum_n G_{m,n} \left(V_n - V_m \right), \tag{1.24}$$

where I_m and V_m are the current and voltage across the mth terminal, and $G_{m,n}$ are the elements of the conductance matrix. In a quantum mechanical description, a structure acting as a scattering region is once again connected to ideal leads acting as waveguides, in turn connected this time to N electron reservoirs.

The extension of the Landauer approach to four terminals was first achieved by Engquist and Anderson [35] and was generalised to any number of terminals by Buttiker (1985) [36; 37]. The wavefunctions in each of these waveguides are once again plane waves along the leads within discrete modes or subbands due to the transverse confinement of the leads of finite cross-section.

It is convenient still to refer to the direction of propagation along the leads as the x-direction, with a label denoting which lead a given electron is propagating in, likewise for the corresponding y- and z-directions:

$$\psi(\mathbf{r}_\alpha) = \frac{1}{V_\alpha} \sum_n f_n(y_\alpha, z_\alpha) \left[c^{\alpha+} e^{ik_{x,\alpha} x_\alpha} + c^{\alpha-} e^{-ik_{x,\alpha} x_\alpha} \right] \tag{1.25}$$

where $\alpha+$ is taken to be propagating *from* the reservoir *to* the junction. n once again denotes the subband that the electron is in, and $f_n(y_\alpha, z_\alpha)$ is the transverse component of the wavefunction in terminal α, determined by the cross-sectional confinement in that terminal. Each of the reservoirs is held at a chemical potential μ_α, and the leads connected to them have Fermi-Dirac distributions of $f_\alpha(E)$.

The fraction of electrons propagating to reservoir α then consists of contributions

from all of the leads, including reflections in lead α. If we index with n the channels of lead α and m those of an arbitrary lead β, then we may define a transmission tensor

$$T_{\alpha,\beta}(E) = \sum_{\beta,m} \sum_{\alpha,n} T_{m,n}(E) \tag{1.26}$$

where $T_{m,n}(E)$ is defined as in the two-terminal case [29]. The current passing through the α lead is then

$$I = \sum_{\beta} \frac{2e}{h} \int_0^\infty dE \ [f_\alpha(E)T_{\alpha,\beta}(E) - f_\beta(E)T_{\beta,\alpha}(E)] . \tag{1.27}$$

A more rigorous proof of the Landauer-Büttiker formula has been derived [38] and the application of the formula to quantum transport has been remarkably successful compared to experiment in its description of mesoscopic systems, including of course the prediction of the quantisation of conductance, but also good agreement with experiment on the quantum Hall effect [39; 40; 41; 42], universal conductance fluctuations [43] and the Aharonov-Bohm effect [44; 45].
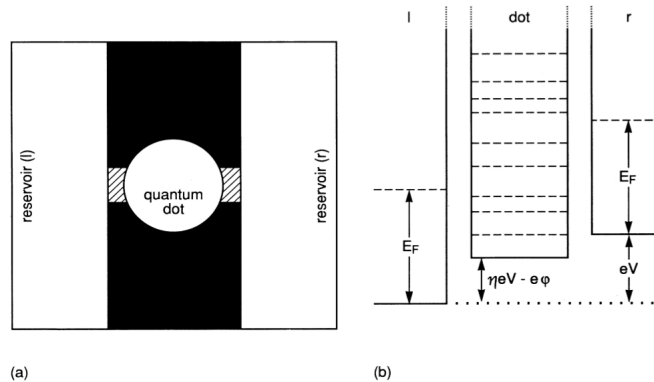
Figure 1.3: Schematic representation of a quantum dot used as a Coulomb blockade device by connecting it to two reservoirs by ideal leads (left), and a representation of the blockade in it's open state. Electrons incident from the leads cannot tunnel through the barrier into the island unless the applied bias between them is sufficiently high. Once tunnelling occurs, the electron in the island will repel other electrons from tunnelling in unless a sufficiently higher bias is applied. Image from [5]

While the approach of treating the details of the device as negligible to determine the current through otherwise noninteracting leads is well-justified, if one wishes to know how the current flows through the actual device, for instance for the creation of functional molecular electronics devices, one needs to know about the electric and electrochemical potentials within the device itself. Details of the actual potentials

outside and inside perfectly conducting devices with currents driven by a perfect battery have been examined for various geometries by Payne [46], and the application of density-functional theory (see Sec. 2.1 and Chapter 2) to quantum transport for interacting systems of electrons largely concerns the study and calculation of potentials within the device itself.

Another issue with the Landauer-Büttiker formalism is that it does not take into account many-body effects. It has been shown by Vignale and Di Ventra [47] that such effects cannot be included in the single-particle transmission probabilities employed in the scattering approach to transport and yet have a direct effect on the conductance of transport devices. Dissipative electron-electron interactions within the device lead to small increases in its resistivity [48; 49] which were identified by Vignale and Di Ventra as arising from the viscosity of the electron fluid.

Thus a full treatment of quantum mechanical systems must take into account such electron-electron (as well as electron-phonon) interactions which are absent in the Landauer-Büttiker approach. Such effects are often substantial, as seen for instance in the Coulomb blockade (Fig. 1.3). The Coulomb blockade, or single-electron transistor (SET) consists of a small island connected to leads in such a way as to form a potential barrier between the island and the leads. For sufficiently small applied biases, electrons in the leads do not have enough energy to tunnel through the barriers and the conductance of the device is zero (Fig. 1.4).
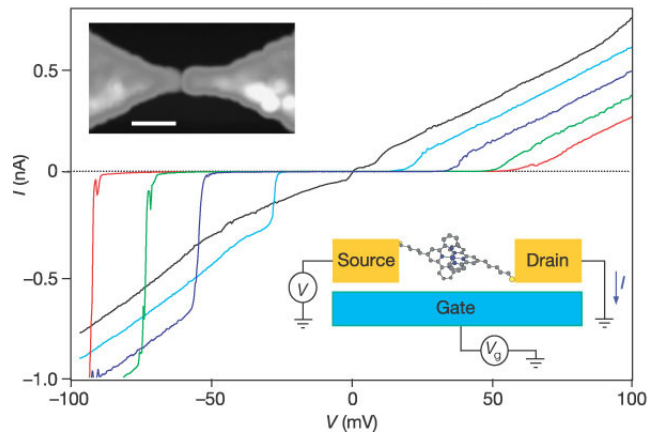
Figure 1.4: STM image of a functioning single-electron transistor (SET) consisting of a molecule of $\left[\mathrm{Co}\left(\mathrm{tpy} - (\mathrm{CH}_2)_5 - \mathrm{SH}\right)_2\right]$ connected to two leads and its conductance as a function of applied voltage for gate voltages between $-0.4V$ (red) and $-1V$ (black). For sufficiently low voltages at low gate voltages for which the tunnelling rate is lower, the device does not conduct. [6]

With increased bias, the tunnelling rates of the incident electrons are higher and

thus higher-energy electrons may tunnel through a barrier and occupy the island. The Coulomb repulsion of the occupied barrier then seen by the other electrons in the system then lowers the probability of other electrons tunnelling, again reducing the conductance of the device until the occupying electron tunnels back out. This way, one may control the flux of electrons through a device on a particle-by-particle level.

Without electron-electron interactions, the Coulomb blockade phenomena cannot be observed. Many different methods for incorporating interactions within the Landauer approach of treating the device as a scatterer have been investigated since the inception of quantum transport theory including density-functional approaches, Green's function methods and others. Density-functional methods for quantum transport will be discussed in Chapter 2. The remainder of this Chapter will discuss other theoretical methods for modelling quantum transport.

1.3 The interaction picture of quantum mechanics

In addition to the Schrödinger picture of quantum mechanics, in which operators are treated as time-independent and thus all time-dependence originates from the wavefunctions, and the Heisenberg picture, in which the state of the system is considered as time-independent with all of the time-dependence attributed to the operators, it is often convenient in treating perturbations, such as in Sections 1.4 and 1.6.5 below, to let both operators and wavefunctions as carrying part of the time-dependence of a system.

As in many-body perturbation theory, in the *interaction* (or Dirac) picture of quantum mechanics, the Hamiltonian in the Schrödinger picture is typically decomposed into a solvable part (for instance: noninteracting terms) and a perturbation (e.g. interaction terms):

$$\hat{H}_{\mathrm{S}}(t) = \hat{H}_0(t) + \hat{V}(t). \tag{1.28}$$

The interaction picture states and operators are then defined in terms of their Schrödinger picture counterparts as

$$|\Psi_{\mathrm{I}}(t)\rangle = e^{iH_0 t}|\Psi_{\mathrm{S}}(t)\rangle = e^{i\hat{H}_0 t}e^{-i\hat{H}t}|\Psi_{\mathrm{S}}(0)\rangle \tag{1.29}$$

$$\hat{O}_{\mathrm{I}}(t) = e^{iH_0 t}\hat{O}_{\mathrm{S}}e^{-iH_0 t}. \tag{1.30}$$

Expectation values of operators are unchanged by this transformation:

$$\langle O \rangle = \frac{\left\langle \Psi_{\mathrm{I}} \left| \hat{O}_{\mathrm{I}} \right| \Psi_{\mathrm{I}} \right\rangle}{\left\langle \Psi_{\mathrm{I}} \mid \Psi_{\mathrm{I}} \right\rangle} = \frac{\left\langle \Psi_{\mathrm{S}} \left| \hat{O}_{\mathrm{S}} \right| \Psi_{\mathrm{S}} \right\rangle}{\left\langle \Psi_{\mathrm{S}} \mid \Psi_{\mathrm{S}} \right\rangle}, \tag{1.31}$$

and likewise the solvable part of the Hamiltonian is unchanged:

$$e^{iH_0 t} \hat{H}_0(t) e^{-iH_0 t} = \hat{H}_0(t). \tag{1.32}$$

From Eq. 1.29, the time-dependence of the wavefunction is then

$$i\frac{\partial}{\partial t} \left| \Psi_{\mathrm{I}}(t) \right\rangle = e^{i\hat{H}_0 t} \left(\hat{H} - \hat{H}_0 \right) \left| \Psi_{\mathrm{S}}(t) \right\rangle = \hat{V}_{\mathrm{I}}(t) \left| \Psi_{\mathrm{I}}(t) \right\rangle \tag{1.33}$$

meaning that only the time-dependence of the perturbation is included in the wavefunction. This is now the Schrödinger equation of the interaction picture: all of the remaining time-dependence is now included in the operators.

We can take the perturbation $\hat{V}(t)$ to be, for instance, the many-electron interaction and switch this on perturbatively at $t = -\infty$. If we denote the unperturbed wavefunction as $|\Psi_0\rangle$, this yields the time-dependent operator (for instance, pertaining to a measurement) expectation values

$$\langle O \rangle = \frac{\left\langle \Psi_0 \left| \hat{U}_{\mathrm{I}}(-\infty, t) \hat{O}_{\mathrm{I}} \hat{U}_{\mathrm{I}}(t, -\infty) \right| \Psi_0 \right\rangle}{\left\langle \Psi_0 \left| \hat{U}_{\mathrm{I}}(-\infty, t) \hat{U}_{\mathrm{I}}(t, -\infty) \right| \Psi_0 \right\rangle} \tag{1.34}$$

where $\hat{U}_{\mathrm{I}}(t, t_0)$ is the time-evolution operator that propagates the wavefunction from time t_0 to time t, related to the time-evolution operator of the Schrödinger picture by Eq. 1.30.

1.4 Other quantum transport methods

1.4.1 The Boltzmann equation

In formulating a quantum-mechanical description of transport, it was natural to take the prevailing statistical theory of *classical* transport and apply it to quantum-mechanical systems. Macroscopic fluids out of equilibrium are amenable to description by the *Boltzmann equation* wherein the traditional notions of known positions and momenta of particles in the fluid is replaced by a statistical description, i.e. the *probability* of the system containing a particle with position $\mathbf{r}(t)$ and momentum $\mathbf{p}(t)$ at time t.

The possible values of $\mathbf{r}$ and $\mathbf{p}$ for particles in a system is the *phase space* of the system, and the statistical probabilities of a particle having a 6-dimensional coordinate $(\mathbf{r}(t), \mathbf{p}(t))$ is the probability density function $f(\mathbf{r}, \mathbf{p}, t)$ which obeys

$$\int_{-\infty}^{\infty} d\mathbf{r} \int_{-\infty}^{\infty} d\mathbf{p} \ f(\mathbf{r}, \mathbf{p}, t) = N, \qquad (1.35)$$

where N is the number of particles in the system.

The classical Liouville equation relates the derivatives of this function with respect to its coordinates and in terms of the velocity and force fields across the system:

$$\frac{df}{dt} = \frac{\partial f}{\partial t} + \mathbf{v} \cdot \frac{\partial f}{\partial \mathbf{r}} + \mathbf{F} \cdot \frac{\partial f}{\partial \mathbf{p}} = 0, \qquad (1.36)$$

assuming that any scattering of the particles is elastic.

While, due to the Heisenberg uncertainty principle, a given particle cannot be described by a position $\mathbf{r}$ and a momentum $\mathbf{p}$ simultaneously, a statistical *ensemble* of quantum particles is a function of these coordinates. Thus the Boltzmann equation can be used to describe time-dependence of a nonequilibrium quantum-mechanical system [28] where, in terms of a system described by N single-particle wavefunctions, the Wigner function is

$$f(\mathbf{r}, \mathbf{p}) = \frac{1}{(2\pi)^3} \sum_{n=1}^{N} \int_{-\infty}^{\infty} d\mathbf{r}' \ \psi_n^*(\mathbf{r} + \tfrac{\hbar}{2}\mathbf{r}') \psi_n(\mathbf{r} - \tfrac{\hbar}{2}\mathbf{r}') e^{i\mathbf{p}\cdot\mathbf{r}'}. \qquad (1.37)$$

Generally, $f(\mathbf{r}, \mathbf{p})$ is the Wigner transform of the density matrix (see next section)

$$f(\mathbf{r}, \mathbf{p}) = \frac{1}{(2\pi)^3} \int_{-\infty}^{\infty} d\mathbf{r}' \ \langle \mathbf{r} + \tfrac{\hbar}{2}\mathbf{r}' | \hat{\rho} | \mathbf{r} - \tfrac{\hbar}{2}\mathbf{r}' \rangle e^{-i\mathbf{p}\cdot\mathbf{r}'} \qquad (1.38)$$

and correctly has the properties that, when integrated over momentum, yields the probabilities of finding electrons at particular positions and, when integrated over space, yields the probabilities of finding electrons with particular momenta [50].

In the presence of inelastic scattering, the probabilities of scattering between states of different momenta must be included explicitly. If the rate at which particles with momentum $\mathbf{p}$ are scattered into states with momentum $\mathbf{p}'$ is $W_{p,p'}$, then the full Boltzmann equation is

$$\frac{\partial f}{\partial t} = -\mathbf{v} \cdot \frac{\partial f}{\partial \mathbf{r}} - \mathbf{F} \cdot \frac{\partial f}{\partial \mathbf{p}} + \int_{-\infty}^{\infty} d\mathbf{p}' \ \frac{1}{2\pi} \left[W_{p',p} f_{p'} - W_{p,p'} f_p \right]. \qquad (1.39)$$

14

Generally, the scattering rates must be calculated using quantum mechanics, for instance using Fermi's golden rule for a given impurity potential. However, if the scattering potential is nearly constant, the scattering is characterised by the *relaxation time* τ: the characteristic time it takes for the system to relax into an equilibrium state $\langle f \rangle$ through inelastic scattering which is directly related to the weighted probabilities of scattering angles: generally, the higher the scattering angle, the shorter the relaxation time and the faster the system attains equilibrium [51].

For such "white noise scattering", the Boltzmann equation reads

$$\frac{\partial f}{\partial t} = -\mathbf{v} \cdot \frac{\partial f}{\partial \mathbf{r}} - \mathbf{F} \cdot \frac{\partial f}{\partial \mathbf{p}} - \frac{f - \langle f \rangle}{\tau}. \tag{1.40}$$

This form of the Boltzmann equation will be used when we come to study the decay of nonequilibrium "quasiparticle" states in Chapter 5.

1.4.2 Linear response and density matrices

An alternative method of calculating the time-dependent properties of a quantum mechanical system is by the use of *density matrices*. Density matrices are used to describe systems in *mixed states*: a *ensemble* of states each with an associated statistical likelihood as opposed to a particular eigenstate or linear combination of eigenstates of the Hamiltonian. The one-particle density matrix of a state $|\Psi(t)\rangle$ is

$$\hat{\rho}(\mathbf{r}, \mathbf{r}', t) = |\Psi(t)\rangle \langle \Psi(t)| = \int_{-\infty}^{\infty} d\mathbf{r}_2 ... \int_{-\infty}^{\infty} d\mathbf{r}_N \ \Psi(\mathbf{r}, \mathbf{r}_2, ..., \mathbf{r}_N, t)\Psi^*(\mathbf{r}', \mathbf{r}_2, ..., \mathbf{r}_N, t) \tag{1.41}$$

where N is the number of particles in the system. In a statistical ensemble of such systems, each having a state vector $|\Psi_n(t)\rangle$ where n labels the system, the density matrix is

$$\hat{\rho}(\mathbf{r}, \mathbf{r}', t) = \sum_n p_n |\Psi_n(t)\rangle \langle \Psi_n(t)| \tag{1.42}$$

where $p_n > 0$ is the probability that the state n is occupied such that

$$\sum_n p_n = 1. \tag{1.43}$$

Using the density matrix, the expectation value of any operator is

$$\langle O(t) \rangle = \frac{1}{Z_0} \text{Tr} \left[\hat{\rho}(t) \hat{O} \right] = \sum_n p_n \left\langle \Psi(t) \left| \hat{O} \right| \Psi(t) \right\rangle \tag{1.44}$$

where $Z_0 = \text{Tr}\,[\hat{\rho}]$ is the partition function.

If the system is described by a time-independent Hamiltonian plus a perturbation,

$$\hat{H}(t) = \hat{H}_0 + \hat{V}(t), \tag{1.45}$$

then in the interaction picture, the system state may be written as

$$
\begin{aligned}
|\Psi_n(t)\rangle &= e^{i\hat{H}_0 t}\hat{U}(t,t_0)e^{-i\hat{H}_0 t_0}|\Psi_n(t_0)\rangle \\
&= \hat{U}_{\text{I}}(t,t_0)|\Psi_n(t_0)\rangle.
\end{aligned} \tag{1.46}
$$

To linear order in $\hat{V}(t)$, the time-evolution operator is

$$\hat{U}_{\text{I}}(t,t_0) = 1 - i\int_{t_0}^{t} dt'\ \hat{V}_{\text{I}}(t') \tag{1.47}$$

where $\hat{V}_{\text{I}}(t) = e^{i\hat{H}_0 t}\hat{V}(t)e^{-i\hat{H}_0 t_0}$.

Inserting 1.46 into Eq. 1.44 yields

$$
\begin{aligned}
\langle O \rangle\,(t) &= \langle O \rangle_0 - i\int_{t_0}^{t} dt'\ \frac{1}{Z_0}\sum_n p_n \left\langle \Psi_n(t_0) \left| \hat{O}(t)\hat{V}_{\text{I}}(t') - \hat{V}_{\text{I}}(t')\hat{O}(t) \right| \Psi_n(t_0) \right\rangle \\
&= \langle O \rangle_0 - i\int_{t_0}^{t} dt'\ \left\langle \left[\hat{O},\hat{V}_{\text{I}}(t')\right] \right\rangle,
\end{aligned} \tag{1.48}
$$

where $\hat{V}_{\text{I}}(t) = e^{i\hat{H}_0 t}e^{-i\hat{H}(t)t}\hat{V}(t)e^{i\hat{H}(t)t}e^{-i\hat{H}_0 t}$ is the perturbation operator in the interaction picture (see Sec. 1.3 below), $\left[\hat{O},\hat{V}_{\text{I}}\right] = \hat{O}\hat{V}_{\text{I}} - \hat{V}_{\text{I}}\hat{O}$ is the commutator of $\hat{O}$ and $\hat{V}_{\text{I}}$, and $\langle O \rangle_0$ is defined for Hamiltonian $\hat{H}_0$ as per Eq. 1.44.

Eq. 1.48 is the *Kubo formula*, a linear-response formula yielding the response of a measurable to an external perturbation to first order, and thus is suited to slowly-varying or small perturbations. Prior to the formulation of multi-terminal Landauer-Büttiker theory, the Kubo formula was the foremost theory of quantum transport, and it has been shown [52; 53] that the Landauer formula can be derived from the Kubo approach, and indeed early multi-terminal extensions to the Landauer approach were based on derivations from the Kubo formula.

While we will not study the Kubo formula any further here, density matrices to describe statistical ensembles can be used in conjunction with the Boltzmann equation for studying the time-evolution of nonequilibrium systems, particularly those undergoing

relaxation, which, for a system governed by the Hamiltonian $\hat{H}$, is

$$i\frac{\partial\hat{\rho}}{\partial t} = \left[\hat{H}, \hat{\rho}\right].$$ (1.49)

Eq. 1.49 is called the *Liouville-von Neumann equation* and can be derived directly from the Schrödinger equation [54]. The Liouville-von Neumann equation is the quantum-mechanical analogue of the Liouville equation for classical statistical mechanics in which the time-evolution of the probability density function $f(\mathbf{r}, \mathbf{p}, t)$ is

$$\frac{\partial f}{\partial t} = -\sum_{i=1}^{n} \left(\mathbf{v}_i \cdot \frac{\partial f}{\partial \mathbf{r}_i} + \mathbf{F_i} \cdot \frac{\partial f}{\partial \mathbf{p}_i}\right) = 0$$ (1.50)

where $\mathbf{r}_i, \mathbf{p}_i$ are the positions and momenta of the ith particle.

In general, the Hamiltonian in Eq. 1.49 will be the full Hamiltonian of the system, including scattering potentials. From Eq. 1.40, we know that, under certain conditions, the scattering potential can be treated separately as

$$i\frac{\partial\hat{\rho}}{\partial t} = \left[\hat{H}_0, \hat{\rho}\right] - \frac{\hat{\rho} - \hat{\rho}_0}{\tau},$$ (1.51)

where $\hat{H}_0$ now is the Hamiltonian minus the terms responsible for inelastic scattering, $\hat{\rho}_0$ is the average equilibrium ensemble to which the system relaxes and τ is the relaxation time to reach equilibrium. We will investigate the effects of Eq. 1.51 in Chapter 5.

1.5 Limitations of noninteracting models

In the absence of particle-particle interactions and neglecting the spin degrees of freedom, the Hamiltonian of a system with external potential v may be written in terms of *creation and annihilation operators* as

$$\hat{H}_0 = \sum_{ij} \hat{c}_i^\dagger t_{ij} \hat{c}_j + \hat{H}_v$$ (1.52)

where $\hat{c}_j$ removes an electron from state j and $\hat{c}_i^\dagger$ adds an electron to state i, together describing a "hopping" event. (Generally, the creation operator is defined by the requirement that $\hat{c}_i^\dagger |1, 2, ..., i, ...\rangle = 0$ and $\hat{c}_i^\dagger |1, 2, ..., 0, ...\rangle = 1$ where i indexes a particular state. The annihilation operator is the Hermitian conjugate of the creation operator and acts in the opposite manner.) The probability amplitude of this hopping occurs is t_{ij}: the *hopping parameter*. $\hat{H}_v$ is the potential energy term of the Hamiltonian. In

direct space, for instance, the potential term is $\hat{H}_v = \sum_i \, v(\mathbf{r}_i)\hat{c}_i^\dagger(\mathbf{r})\hat{c}_i(\mathbf{r})$.

In the presence of electron-electron interactions, the probability of an electron hopping from one state to another can be greatly affected by the presence of other electrons on those sites. The interacting Hamiltonian is

$$\hat{H} = \sum_{ij} \, \hat{c}_i^\dagger t_{ij} \hat{c}_j + \sum_{ijkl} U_{ijkl} \hat{c}_i^\dagger \hat{c}_j^\dagger \hat{c}_k \hat{c}_l, \qquad (1.53)$$

where

$$U_{ijkl} = \frac{1}{2} \int_{-\infty}^{\infty} \, d\mathbf{r} \, \int_{-\infty}^{\infty} \, d\mathbf{r}' \, \psi_i^*(\mathbf{r})\psi_j^*(\mathbf{r}')\hat{U}(\mathbf{r},\mathbf{r}')\psi_k(\mathbf{r}')\psi_l(\mathbf{r}) \qquad (1.54)$$

and $\hat{U}(\mathbf{r},\mathbf{r}')$ is the usual Coulomb interaction operator.

This is called the *tight-binding representation*, and in the position basis has the Hamiltonian

$$\hat{H} = \sum_{ij} \, \hat{\psi}^\dagger(\mathbf{r}_i)t_{ij}\hat{\psi}(\mathbf{r}_j) + \sum_i \, v_i \hat{c}_i^\dagger \hat{c}_i + \sum_{ijkl} U_{ijkl}\hat{\psi}^\dagger(\mathbf{r}_i)\hat{\psi}^\dagger(\mathbf{r}_j)\hat{\psi}(\mathbf{r}_k)\hat{\psi}(\mathbf{r}_l), \qquad (1.55)$$

where $\psi^\dagger(\mathbf{r})$ and $\psi(\mathbf{r})$ are the *field creation and annihilation operators* which add and remove respectively one electron to and from site ($\mathbf{r}$).

Typically, one approximates the Coulomb term by limiting the number of nonzero elements of U to nearest neighbour interactions or, in the case of the *Hubbard* model, on-site interactions only, suited to describe systems with a large interatomic spacing such that the Coulomb interaction is negligible between sites [55].

The tight-binding method has been employed within the field of quantum transport theory to study one-atom contacts, single-atom chains and stacking faults [56], the effects of impurities on conductance in quantum wires [57]

Relatively recently, Kurth *et al* [7] applied the tight-binding model to the Coulomb blockade (described in Sec. 1.2 above) to determine if the often assumed notion that systems driven out of equilibrium eventually achieve a microscopic steady state. They simulated a quantum dot with an on-site charging energy connected to two ideal leads with an externally-controlled gate voltage across the dot. The system was prepared in equilibrium then perturbed from $t > 0$ by an external potential bias.

Fig. 1.5 shows the time-dependent charge and current densities of the system for varying applied biases. As can be seen, the system does not tend to a steady state with time, but rather continues to undergo current oscillations as electrons hop into and out of the Coulomb blockade. Only away from the quantum dot does the current, after transient effects have subsided, diminish with time.
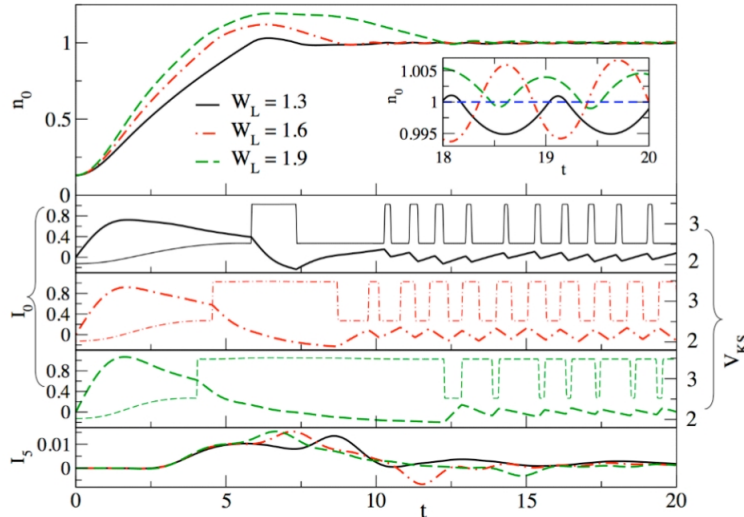
Figure 1.5:   **Time-dependent Coulomb blockade**: The time-dependent charge density (top) and current density (middle three) of a quantum dot connected to reservoirs via ideal leads for three different externally-applied biases. Also shown (bottom) is the time-dependent current density in the lead five sites from the dot. The dot does not settle to a steady-state with time, but rather undergoes perpetual current oscillations as the dot charges and discharges, however the current away from the dot does diminish with time. The KS potential required to reproduce the system in a TDDFT calculation is also shown (middle three) and contains discontinuous steps as the dot charges and discharges due to the local change in electron number. [7]

This discovery illuminates something of the nature of electrons in quantum transport systems, that even when a circuit as a whole is varying little with time, the precise nature of the current through the circuit depends on highly dynamic behaviour in some of its components, which in turn depends on the precise nature of the device. The varying of the state of the quantum dot with time, as it charges and discharges, is evident in the dynamics of the effective time-dependent potential of a single-particle (noninteracting) representation required to reproduce the same time-dependent charge and current density.

This single-particle picture is based on the idea that we can replace particle-particle interactions with additional fictitious external fields acting on independent electrons. As we can see in Fig. 1.5, these effective potentials can be rather complex: in the case of the quantum dot, the local field discontinuously jumps up or down whenever the dot is charging or discharging, i.e. when the integer number of electrons in the dot changes. This is a consequence of the *derivative discontinuity* in the energy with increasing electron number in the noninteracting model [58], and will be discussed further in Sec. 2.2.4.

1.6 Green's function approaches to quantum transport

1.6.1 Quantum-mechanical Green's functions

Green's functions are mathematically defined as the inverses of differential operators. Since the Hamiltonian is a differential operator, one can solve it (in principle) by means of Green's functions:

$$EG(\mathbf{r}, \mathbf{r}', E) - \int_{-\infty}^{\infty} \hat{H}(\mathbf{r}, \mathbf{r}'')G(\mathbf{r}'', \mathbf{r}', E) \, d\mathbf{r}'' = \delta(\mathbf{r} - \mathbf{r}'). \quad (1.56)$$

Eq. 1.56 will generally have multiple solutions depending on the boundary conditions of the problem. For instance, the free-electron solutions are

$$G^r(\mathbf{r}, \mathbf{r}', E) = -\frac{e^{i\mathbf{k}\cdot|\mathbf{r}-\mathbf{r}'|}}{4\pi |\mathbf{r} - \mathbf{r}'|} \quad (1.57)$$

$$G^a(\mathbf{r}, \mathbf{r}', E) = -\frac{e^{-i\mathbf{k}\cdot|\mathbf{r}-\mathbf{r}'|}}{4\pi |\mathbf{r} - \mathbf{r}'|} = G^{r\dagger} \quad (1.58)$$

where $k = \sqrt{2E}$.

The first of these solutions is called the *retarded* Green's function and in many-body perturbation theory may be employed to represent an electron added to the system. The second is the *advanced* Green's function and represents an electron removed from the system, or, equivalently, a "hole" added to it. One can select which of the two solutions one wishes to find by adding a small, imaginary infinitesimal to the energy:

$$\lim_{\eta\to 0} [E \pm i\eta] \, G^{r,a}(\mathbf{r}, \mathbf{r}', E) - \int_{-\infty}^{\infty} \hat{H}G^{r,a}(\mathbf{r}'', \mathbf{r}', E)d\mathbf{r}'' = \delta(\mathbf{r} - \mathbf{r}'). \quad (1.59)$$

The Green's function for interacting electrons is generally difficult to solve directly, and the typical approach is to calculate an noninteracting Green's function exactly and self-consistently calculate perturbations to it due to interactions. From the closure relation

$$\sum_n |\psi_n\rangle \langle\psi_n| = \hat{I}, \quad (1.60)$$

where $\hat{I}$ is the identity operator, and the noninteracting time-independent Schrödinger equation $\hat{H}_0 |\psi_n\rangle = \varepsilon_n |\psi_n\rangle$, one can write the noninteracting Green's function in terms

of the single-particle solutions of $\hat{H}_0$:

$$G_0^{r,a}(E) = \sum_n \frac{|\psi_n\rangle \langle\psi_n|}{E - \varepsilon_n \pm i\eta}. \tag{1.61}$$

Defining the fully perturbed Hamiltonian as

$$\hat{H} = \hat{H}_0 + \Sigma(\mathbf{r}, \mathbf{r}', E), \tag{1.62}$$

the interacting Green's function is then given by

$$G^{r,a}(\mathbf{r}, \mathbf{r}', E) = G_0^{r,a}(\mathbf{r}, \mathbf{r}', E)$$
$$+ \int_{-\infty}^{\infty} d\mathbf{r}_2 \int_{-\infty}^{\infty} d\mathbf{r}_2' \, G_0^{r,a}(\mathbf{r}, \mathbf{r}_2, E)\Sigma^{r,a}(\mathbf{r}_2, \mathbf{r}_2', E)G^{r,a}(\mathbf{r}_2', \mathbf{r}', E), \tag{1.63}$$

or, in shorthand notation of $(1) = \mathbf{r}_1, t_1$, etc. and $A(1,2)B(1,3) = \int_{-\infty}^{\infty} A(1,2)B(1,3)d1$,

$$G^{r,a}(1,1') = G_0^{r,a}(1,1') + G_0^{r,a}(1,2)\Sigma^{r,a}(2,2')G^{r,a}(2',1'). \tag{1.64}$$

Eq. 1.64 is called the *Dyson equation*, and the perturbation that incorporates interaction is called the *self-energy operator*. The noninteracting Green's function can be calculated from a DFT calculation (see Sec. 2.1) with either no interaction terms (in which case the self-energy (SE) will include all interaction) or with only the Hartree potential (in which case the SE will be defined to provide exchange-correlation effects).

The two unknowns – the interacting Green's function and the self-energy – may be calculated self-consistently (via Hedin's equations [59]). The self-energy operator describes all of the exchange and correlation many-body quantum mechanical effects and is generally too complicated a quantity to calculate exactly: it is nonlocal in space, energy-dependent and non-Hermitian, and one usually terminates the calculation at a given order of the perturbation expansion.

A similar equation relates the *screened* two-particle Coulomb interaction $W(1, 1', 2, 2')$ to the polarisation operator $P(1, 1', 2, 2')$ and the usual (unscreened) Coulomb operator, here denoted $V(1, 1', 2, 2')$:

$$W(1,1',2,2') = V(1,1',2,2') + W(1,1',3,3')P(3'3,4'4)V(4,4',2,2'). \tag{1.65}$$

Three further equations relate the polarisation operator to the Green's function and the self-energy operator, resulting in a set of five equations which, in principle, may be solved self-consistently.

In practise, solution of the full Hedin equations is rarely computationally feasible. However, the equations permit an order expansion of the self-energy operator about the screened Coulomb expansion. In real spacetime, this is

$$\Sigma(\mathbf{r}t, \mathbf{r}'t') = iG(\mathbf{r}t, \mathbf{r}'t')W(\mathbf{r}t + i\delta, \mathbf{r}'t') - \int_{-\infty}^{\infty} d\mathbf{r}''dt'' \, d\mathbf{r}'''dt''' \, G(\mathbf{r}t, \mathbf{r}''t'')G(\mathbf{r}''t'', \mathbf{r}'''t''')$$

$$\times \, G(\mathbf{r}'''t''', \mathbf{r}'t')W(\mathbf{r}t, \mathbf{r}'''t''')W(\mathbf{r}''t'', \mathbf{r}'t') + \text{...} \tag{1.66}$$

where $W(E)$ is the screened Coulomb potential. The usual approximation for the self-energy terminates the expansion after the first term so that $\Sigma = iGW$: the so-called GW approximation [60]. From the quantum mechanical Green's function, all properties of interest concerning the excitation can then be calculated.

1.6.2 Quasiparticle theory

By means of Green's functions, one is able to calculate the electronic properties of systems excited by the addition, removal or excitation of an electron to, from or within a system that may be modelled by other means. Such elementary excitations are called *quasiparticles*, so-called because they share properties such as charge, spin and crystal momentum with elementary particles. However, other properties such as their mass and the electric fields they produce may differ strikingly from, for instance, those of an electron.

The benefit of the quasiparticle approach to excited systems is that, while individual electrons strongly interact with each other, quasiparticles are usually weakly interacting. The elementary electron in a material repels other electrons around it, creating around itself a positively-charged cloud of polarisation that screens the quasiparticle from others around it by effectively reducing the Coulomb interaction between them.

The residual interaction between the quasiparticle and its surroundings is the self-energy; as such, the quasiparticle is governed by a wave equation similar to the non-interacting Schrödinger equation which, with the inclusion of the self-energy, provides an effective single-particle theory of excitations:

$$\varepsilon_{\text{QP}}\psi_{\text{QP}}(\mathbf{r}) = \hat{H}_0\psi_{\text{QP}}(\mathbf{r}) + \int_{-\infty}^{\infty} \Sigma(\mathbf{r}, \mathbf{r}', E)\psi_{\text{QP}}(\mathbf{r}') \, d\mathbf{r}'. \tag{1.67}$$

The quasiparticle energies appear as peaks in the spectral function, which is related to the Green's function as

$$A(E) = \frac{1}{\pi}\left|\text{Im } G^{r,a}(E)\right| \tag{1.68}$$

such as is shown for an electron and a hole in Fig. 1.6 below.
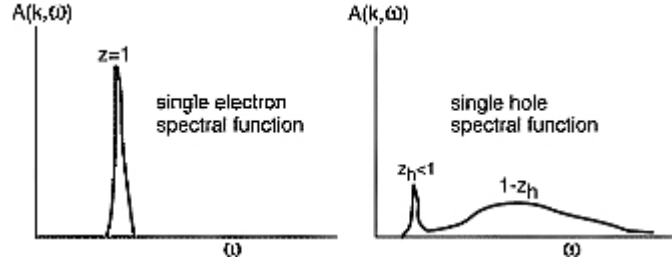
Figure 1.6: **Quasiparticle peaks in spectral functions.** Spectral functions near Fermi energy of nearly-empty band (left) and nearly-full band (right) corresponding to electron and hole quasiparticles respectively. (Illustration from [8].)

The combined approach of the quasiparticle concept and the quantum-mechanical Green's function formalism have been found to predict features of excited systems that are qualitatively different or sometimes completely absent in other approximations that implement no or only partial many-body effects (e.g. [60; 61; 62; 63; 64]) that agree better with experimental than predictions based on DFT band structures. However, such systems are typically very small compared to the sizes of systems that DFT can, in principle, cope with.

1.6.3 Embedded nonequilibrium Green's functions

A quintessential test of the Green's function technique for quantum transport is that of a molecular junction coupled to semi-infinite leads. If we take the simplest case of a single-energy-level junction and assume that the two leads do not interact with each other, we can write down the Hamiltonian in the tight-binding approach [15; 65] which, in equilibrium, is (neglecting spin):

$$\hat{H} = \hat{H}_{\mathrm{L}} + \hat{H}_{\mathrm{R}} + \varepsilon \hat{c}_{\mathrm{C}}^{\dagger} c_{\mathrm{C}} + t_{\mathrm{L}} \left(\hat{c}_{\mathrm{C}}^{\dagger} c_{\mathrm{L}} + \hat{c}_{\mathrm{L}}^{\dagger} c_{\mathrm{C}} \right) + t_{\mathrm{R}} \left(\hat{c}_{\mathrm{C}}^{\dagger} c_{\mathrm{R}} + \hat{c}_{\mathrm{R}}^{\dagger} c_{\mathrm{C}} \right) \tag{1.69}$$

where the first three terms on the right-hand side are the uncoupled Hamiltonians of the left lead, right lead and junction respectively, and $\hat{c}^{\dagger}$ and $\hat{c}$ are once again the creation and annihilation operators respectively (see Sec. 1.5). The couplings are introduced by the hopping parameters t_{L} and t_{R} which give the probabilities of electrons moving between the junction and the left and right leads respectively. One can see that the probability of hopping from a lead to the junction are the same as hopping from the junction to the lead, as required in equilibrium.

The unperturbed Hamiltonian is then taken to be $\hat{H}_{0} = \hat{H}_{\mathrm{L}} + \hat{H}_{\mathrm{R}} + \varepsilon \hat{c}_{\mathrm{C}}^{\dagger} c_{\mathrm{C}}$, and the

perturbation is therefore

$$\Sigma = t_{\mathrm{L}} \left(\hat{c}_0^\dagger c_{\mathrm{L}} + \hat{c}_{\mathrm{L}}^\dagger c_0 \right) + t_{\mathrm{R}} \left(\hat{c}_{\mathrm{C}}^\dagger c_{\mathrm{C}} + \hat{c}_{\mathrm{R}}^\dagger c_{\mathrm{C}} \right). \tag{1.70}$$

The Dyson equation then yields the Green's function for the junction

$$G_{CC}(E) = g_{\mathrm{C}}(E) + g_{\mathrm{C}}(E) t_{\mathrm{L}} G_{\mathrm{LC}}(E) + g_{\mathrm{C}}(E) t_{\mathrm{R}} G_{\mathrm{RC}}(E) \tag{1.71}$$

where g_{C} is the uncoupled Green's function of the central junction,

$$G_{\mathrm{LC}}(E) = g_{\mathrm{L}}(E) t_{\mathrm{L}} G_{\mathrm{CC}}(E) \tag{1.72}$$

$$G_{\mathrm{RC}}(E) = g_{\mathrm{R}}(E) t_{\mathrm{R}} G_{\mathrm{CC}}(E), \tag{1.73}$$

and $g_{\mathrm{L}}(E)$ and $g_{\mathrm{R}}(E)$ are the surface Green's function matrix elements of the uncoupled left and right leads respectively.

Substituting Eqs. 1.72 and 1.73 into Eq. 1.71 gives the self-energy operator as

$$\Sigma_{\mathrm{C}}(E) = t_{\mathrm{L}}^2 g_{\mathrm{L}}(E) + t_{\mathrm{R}}^2 g_{\mathrm{R}}(E) \tag{1.74}$$

from which we obtain the Green's functions

$$G_{\mathrm{CC}}^{r,a}(E) = \frac{1}{E - \varepsilon - \Sigma_{\mathrm{C}}(E)} \tag{1.75}$$

from which we can calculate the energy, charge density and density of states of the system.

Due to the quantum transport approach of treating the leads as noninteracting, the procedure is a remarkably straightforward extension of Green's function methods, and even simple approaches such as embedding the *GW* self-energy in the central region and employing a local DFT exchange-correlation potential for the rest of the self-energy shows considerable improvement over pure DFT calculations in comparison with experiment [66]. Extending the range of the interaction to include the connections to the leads is more computationally difficult, however, and the approach still neglects dynamic many-body effects and we have seen that, even in a macroscopic steady state, electron transport is a fundamentally dynamic phenomenon. As such, a full Green's function approach to quantum transport must incorporate time-dependence.

One aspect of the self-energy operator that incorporates many-body effects difficult to incorporate in any other many-body quantum theory is its non-Hermitian nature:

electron quasiparticles corresponding to excited state generally have a finite lifetime due to scattering events between the added electron and the rest of the system (for instance, via Auger transitions). It is only as $\varepsilon \to E_\mathrm{F}$, where E_F is the Fermi energy of the ground-state system, that the quasiparticle lifetime tends toward infinite and these finite lifetime effects vanish.

While the Green's function determines how the quasiparticle decays, it does not contain information about what happens to the added electron as it de-excites, for instance: what happens to the elementary charge of quasiparticle? To access this sort of information, we need to know how the system as a whole evolves with time.

1.6.4 Time-dependent Green's functions

The energy-dependence of the equilibrium Green's function demonstrates that they are generally time-dependent quantities, as can be seen by taking the Fourier transform of $G(\mathbf{r}, \mathbf{r}', E)$ into real time. The definition of the time-dependent Green's function is broader than that of the equilibrium functions discussed above. It is usual (e.g. [15; 29]) to define the time-dependent Green's function in the Heisenberg picture of quantum mechanics wherein all of the time-dependence of a system is incorporated into the operators rather than the wavefunction. In this representation, the *causal* Green's function for a system is defined in the position basis as

$$G^\mathrm{c}(xt, x't') = -i \left\langle \Psi_0 \left| \hat{T} \hat{\psi}(xt) \hat{\psi}^\dagger(x't') \right| \Psi_0 \right\rangle \tag{1.76}$$

where $|\Psi_0\rangle$ is the N-body system's ground-state wavefunction, $\hat{\psi}^\dagger$ is the field creation operator, $\hat{\psi}$ is the field annihilation operator, and $\hat{T}$ the time-ordering operator that will order the field operators depending on the sign of $t-t'$. The retarded and advanced components are

$$G^r(xt, x't') = -i\theta(t-t') \left\langle \Psi_0 \left| \left\{ \hat{\psi}(xt), \hat{\psi}^\dagger(x't') \right\} \right| \Psi_0 \right\rangle \tag{1.77}$$

$$G^a(xt, x't') = i\theta(t'-t) \left\langle \Psi_0 \left| \left\{ \hat{\psi}(xt), \hat{\psi}^\dagger(x't') \right\} \right| \Psi_0 \right\rangle \tag{1.78}$$

where

$$\theta(t-t') = \begin{cases} 1 & \text{for} \quad t > t' \\ 0 & \text{for} \quad t < t' \end{cases} \tag{1.79}$$

and vice versa for $\theta(t'-t)$, and $\left\{ \hat{A}, \hat{B} \right\} = \hat{A}\hat{B} + \hat{B}\hat{A}$ is the anticommutator of $\hat{A}$ and $\hat{B}$.

Two other types of Green's function – the *lesser* and *greater* Green's functions – are also useful quantities insofar as they are directly associated with physical observables such as the current density. They are defined as

$$G^{<}(xt, x't') = \pm i \left\langle \Psi_0 \left| \hat{\psi}^{\dagger}(x't') \hat{\psi}(xt) \right| \Psi_0 \right\rangle \tag{1.80}$$

$$G^{>}(xt, x't') = -i \left\langle \Psi_0 \left| \hat{\psi}(xt) \hat{\psi}^{\dagger}(x't') \right| \Psi_0 \right\rangle \tag{1.81}$$

and are related to the retarded and advanced Green's functions via the relations

$$G^{r}(xt, x't') = \theta(t - t') \left(G^{>}(xt, x't') - G^{<}(xt, x't') \right) \tag{1.82}$$

$$G^{a}(xt, x't') = -\theta(t' - t) \left(G^{>}(xt, x't') - G^{<}(xt, x't') \right). \tag{1.83}$$

Including spin, the coordinate $x = (\mathbf{r}, \sigma)$ with $\sigma = \uparrow, \downarrow$ the spin coordinate. All instantaneous properties can then be calculated from the system's Green's functions, including the spin-up, spin-down and total charge densities

$$n_{\sigma}(\mathbf{r}, t) = -iG^{<}(\mathbf{r}\sigma t, \mathbf{r}\sigma t) \tag{1.84}$$

current density

$$\mathbf{j}_{\sigma}(\mathbf{r}, t) = \tfrac{1}{2} \lim_{\mathbf{r}' \to \mathbf{r}} \left(\nabla' - \nabla \right) G^{<}(\mathbf{r}\sigma t, \mathbf{r}'\sigma t), \tag{1.85}$$

total energy

$$E = \frac{1}{2} \int_{-\infty}^{\infty} \left[\frac{\partial}{\partial t} - ih(x) \right] G(xt, xt + \eta) \, dx, \tag{1.86}$$

and spectral function

$$A(x, x', \omega) = \frac{1}{\pi} \left| \text{Im } G^{r}(x, x', \omega) \right| \tag{1.87}$$

where $h(x)$ is the part of the Hamiltonian that is independent of the charge density, and $G(\omega)$ is the Fourier- transform (in time) of the Green's function.

The evolution of fully time-dependent Green's functions was first formulated by Kadanoff and Baym [67], who derived the time-evolution of the Green's functions as

$$\left[i\frac{\partial}{\partial t} - h(t) \right] G^{r,a}(t, t') = \delta(t - t')\hat{I} + \int_{C} dt'' \, \Sigma^{r,a}(t, t'') G^{r,a}(t'', t') \tag{1.88}$$

$$\left[i\frac{\partial}{\partial t} - h(t) \right] G^{>,<}(t, t') = \int_{C} dt'' \, \Sigma^{r}(t, t'') G^{>,<}(t'', t') + \Sigma^{>,<}(t, t'') G^{a}(t'', t'), \tag{1.89}$$

the so-called Kadanoff-Baym equations. This approach has been used to determine properties of stable excitations such as optical spectra of semiconductors [68; 69] and

quantum wells [70].

An alternative formulation for nonequilibrium Green's functions was proposed independently and shortly after the Kadanoff-Baym approach by Keldysh which has enjoyed considerable success in quantum transport theory. This approach – called the *Keldysh formalism* – is the subject of the next section.

1.6.5 The Keldysh formalism

Eq. 1.34 is certainly too convoluted to evaluate directly, replacing as it does one time-evolution operator with, effectively, several. However Keldysh [71] showed that one can evaluate the expression if one adopts a novel time line over which one evolves the system.

Exploiting the fact that, as well as switching on the perturbation at $t = -\infty$, we may also switch it off again at $t = \infty$, Keldysh proposed a time contour for propagation in which runs from $-\infty$ to ∞ along a real time axis in one branch before running back from ∞ to $-\infty$ in a parallel branch. This is known as the *Keldysh contour* and is shown in Fig. 1.7 below. Further, if the perturbation $\hat{V}(t) = 0$ for $t < t_0$ and $t > t_1'$, then one can perform the evolution between these finite times.
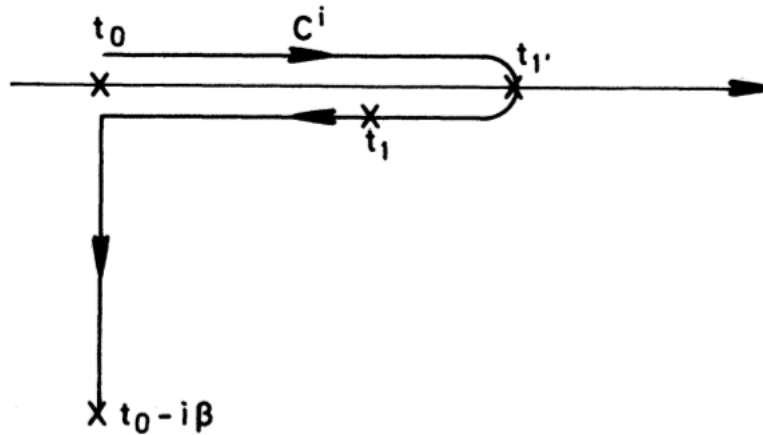
Figure 1.7: **The Keldysh contour.** Evolution from some initial time t_0 to some desired time t_1 runs via the upper branch to some final time t_1' before making a U-turn back to t_1. If the perturbation is always on, then $t_0 = -\infty$ and $t_1' = \infty$. Image from Rev. Mod. Phys. (1986) [9].

Expectations values at some time t_1 may then be written in terms of time-evolution from some initial, unperturbed state, along the Keldysh time contour to the desired time. The exact expression for the expectation value depends on whether the desired

time is on the upper or lower branch of the contour:

$$\langle O \rangle = \frac{\left\langle \Psi_0 \left| \hat{U}_-(-\infty, \infty)\hat{U}_+(\infty, t)\hat{O}_\mathrm{I}(t)\hat{U}_+(t, -\infty) \right| \Psi_0 \right\rangle}{\left\langle \Psi_0 \left| \hat{U}_-(-\infty, \infty)\hat{U}_+(\infty, t)\hat{U}_+(t, -\infty) \right| \Psi_0 \right\rangle} \quad \text{if } t \text{ in upper branch} \quad (1.90)$$

$$\langle O \rangle = \frac{\left\langle \Psi_0 \left| \hat{U}_-(-\infty, t)\hat{O}_\mathrm{I}(t)\hat{U}_-(t, \infty)\hat{U}_+(\infty, -\infty) \right| \Psi_0 \right\rangle}{\left\langle \Psi_0 \left| \hat{U}_-(-\infty, t)\hat{U}_-(t, \infty)\hat{U}_+(\infty, -\infty) \right| \Psi_0 \right\rangle} \quad \text{if } t \text{ in lower branch} \quad (1.91)$$

where $\hat{U}_+$ propagates along the upper branch and $\hat{U}_-$ propagates along the lower branch. This may be written more succinctly using the time-ordering operator:

$$\langle O \rangle = \frac{\left\langle \Psi_0 \left| \hat{T}_\mathrm{c} \left[\hat{O}_\mathrm{I}(t)\hat{U}_\mathrm{c}(\infty, -\infty) \right] \right| \Psi_0 \right\rangle}{\left\langle \Psi_0 \left| \hat{U}_\mathrm{c}(\infty, -\infty) \right| \Psi_0 \right\rangle} \quad (1.92)$$

where $\hat{U}_\mathrm{c}(\infty, -\infty) = \hat{U}_-(-\infty, \infty)\hat{U}_+(\infty, -\infty)$.

From Eq. 1.92, one can calculate the causal Green's function:

$$G^\mathrm{c}(\mathbf{r}t, \mathbf{r}'t') = -i \left\langle \Psi_0 \left| \hat{T}_\mathrm{c} \left[\hat{\Psi}(\mathbf{r}t)\hat{\Psi}^\dagger(\mathbf{r}'t') \right] \right| \Psi_0 \right\rangle. \quad (1.93)$$

There are four distinct solutions to this equation corresponding to which of the two branches each of the two time coordinates is evaluated at.

$$G^{++}(\mathbf{r}t, \mathbf{r}'t') = -i \left\langle \Psi_0 \left| \hat{T} \left[\hat{\Psi}(\mathbf{r}t)\hat{\Psi}^\dagger(\mathbf{r}'t') \right] \right| \Psi_0 \right\rangle \quad \text{if } t = t_+ \text{ and } t' = t'_+ \quad (1.94)$$

$$G^{+-}(\mathbf{r}t, \mathbf{r}'t') = i \left\langle \Psi_0 \left| \hat{\Psi}^\dagger(\mathbf{r}'t')\hat{\Psi}(\mathbf{r}t) \right| \Psi_0 \right\rangle \quad \text{if } t = t_+ \text{ and } t' = t'_- \quad (1.95)$$

$$G^{-+}(\mathbf{r}t, \mathbf{r}'t') = -i \left\langle \Psi_0 \left| \hat{\Psi}(\mathbf{r}t)\hat{\Psi}^\dagger(\mathbf{r}'t') \right| \Psi_0 \right\rangle \quad \text{if } t = t_- \text{ and } t' = t'_+ \quad (1.96)$$

$$G^{--}(\mathbf{r}t, \mathbf{r}'t') = -i \left\langle \Psi_0 \left| \hat{T}_- \left[\hat{\Psi}(\mathbf{r}t)\hat{\Psi}^\dagger(\mathbf{r}'t') \right] \right| \Psi_0 \right\rangle \quad \text{if } t = t_- \text{ and } t' = t'_- \quad (1.97)$$

where $\hat{T}_-$ time-orders its arguments in reverse.

The full Green's function may then be written as

$$\mathbf{G}(\mathbf{r}t, \mathbf{r}'t') = \begin{pmatrix} G^{++}(\mathbf{r}t, \mathbf{r}'t') & G^{+-}(\mathbf{r}t, \mathbf{r}'t') \\ G^{-+}(\mathbf{r}t, \mathbf{r}'t') & G^{--}(\mathbf{r}t, \mathbf{r}'t') \end{pmatrix}. \quad (1.98)$$

This obeys a Dyson equation of the same form as for the equilibrium Green's function:

$$\mathbf{G} = \mathbf{g} + \mathbf{g}\boldsymbol{\Sigma}\mathbf{G} \quad (1.99)$$

where

$$\mathbf{\Sigma} = \left(\begin{array}{cc} \Sigma^{++} & \Sigma^{+-} \\ \Sigma^{-+} & \Sigma^{--} \end{array} \right). \tag{1.100}$$

In application to electron transport, one scheme that is frequently employed was introduced by Caroli *et al* in 1971 [72; 73] in which the leads are initially disconnected and in equilibrium with the chemical potentials of their respective reservoirs. The part of the Hamiltonian describing the junction is then turned on adiabatically and a steady-state is allowed to form, a scheme later extended [74] to include electron-electron interactions. A second approach was introduced by Cini in 1980 [75] in which the leads and junction are initially connected but the whole system is in equilibrium, with the perturbation then taking the form of a time-dependent external potential. It has been shown [76] that, for noninteracting electrons, both schemes yield the same long-term steady-state currents.

The current through an interacting scattering region connected to noninteracting leads has been calculated in terms of the NEGFs [74] and has been shown to exhibit peaks in the conductance around the Fermi energy due to resonant tunnelling that do not appear in the Landauer theory but have been established [77] as necessary to conform to experimental trends in temperature-dependence. More recently [78], it was seen that the NEGF current can be thought of consisting of a Landauer term plus additional many-body terms, and that peaks in the conductance are typically underestimates by the Landauer formula.

The Keldysh formalism has been successfully applied to a broad variety of dynamic systems, including fully-correlated transport through nanojunctions [79; 80], equilibrium and nonequilibrium electronic properties in vibron coupling in molecular junctions [81; 82], spin transport through quantum dots [83], and phonon transport and scattering in resonant-tunnelling diodes [84] and carbon nanotubes [85]. Typically, however, such calculations do not consider full electron-electron interactions in the device, but rather treat the NEGF scheme as a means of embedding the device to ideal leads by use of self-energy operators that handle only the device-lead coupling (see e.g. [86]) and not fully interacting many-body effects such as exchange and correlation.

It is only more recently that computational resources have allowed for the calculation of fully interacting, dynamic systems using the Kadanoff-Baym equations [87; 88], and such models are typically constrained to be small, finite and approximate.

The treatment of exchange and correlation (XC) effects in both ground-state and time-dependent systems has had a long and difficult history. It has been established that the XC energy of a system is uniquely determined by its charge density (see Sec.

2.1 below), but the precise nature of the relationship is nonanalytic and good approximations to it in the nonequilibrium regime have proven generally elusive. One could, in principle, do without the computational complexities of time-dependent Green's function approaches altogether, and indeed move beyond the necessary approximations of NEGF approaches to quantum transport, if one had access to exact or good approximations to the XC energy as a functional of the system density. This constitutes a major part of the active research within time-dependent density-functional theoretical, which shall be introduced in the next chapter.

While considerably more tractable than solving the many-body Schrödinger equation directly for systems of more than a few particles (even with the additional time coordinate), Green's functions approaches are still much more computationally expensive than density-functional approaches, both in terms of the numbers of coordinates of the fundamental variables and the computational effort required to calculate them. However, for sufficiently small systems or under suitable approximations that preserve the important physical features of an excited system, Green's functions and quasiparticle calculations can provide a useful basis by which to construct and test density-functionals for DFT and TDDFT calculations. Since this thesis concerns the calculations of exact density-functional potentials for quantum transport that include such physics, this is the approach I adopt in this research.

Chapter 2

Density and current-density functional theories

2.1 Density-functional theory

Density functional theory (DFT) dates back to the 1920's albeit without a rigorous theoretical foundation. Thomas-Fermi (TF) theory [89; 90] neatly sidestepped the problem of the many-body Schrödinger equation by taking as its basic variable the electronic density $n(\mathbf{r})$ which is a function of only 3 (rather than $3N$ as is the case with the N-body wavefunction) spatial coordinates.

Density-functional theory was given a firm theoretical footing by Hohenberg and Kohn [91] who demonstrated that, for a given electron-electron interaction strength, there exists both a one-to-one relationship between the external potential and the charge density of a ground-state system, and a variational procedure for finding the correct ground-state charge density for its corresponding potential.

If we consider a system of N electrons in their ground state configuration in an external scalar potential $v_{\text{ext}}(\mathbf{r})$, the system is uniquely defined by the many-body Hamiltonian which, in atomic units, is:

$$\hat{H} = \sum_{i=1}^{N} \left\{ -\frac{1}{2}\nabla_i^2 + v_{\text{ext}}(\mathbf{r}_i) + \frac{1}{2}\sum_{j\neq i}^{N} \frac{1}{|\mathbf{r}_i - \mathbf{r}_j|} \right\}. \tag{2.1}$$

The ground-state energy of this system is

$$E_0 = \left\langle \Psi_0 \left| \hat{H} \right| \Psi_0 \right\rangle \tag{2.2}$$

where $|\Psi_0\rangle$ is the ground-state N-particle wavefunction which, for fermionic systems such as the electronic systems under consideration, is exchange-antisymmetric.

From the Rayleigh-Ritz variational principle [92], it follows that any arbitrary, exchange-antisymmetric N-electron state $|\Psi\rangle$ must obey

$$E_0 \leq \left\langle \Psi \left| \hat{H} \right| \Psi \right\rangle \tag{2.3}$$

For systems of more than a few particles, the number of wavefunction coordinates makes such a minimisation procedure impractical however.

2.1.1 The Hohenberg-Kohn theorems

The DFT of Hohenberg and Kohn [91] (HK) still involves a minimisation procedure, but because it takes as its basic variable the charge density rather than the many-body wavefunction, it is a much smaller procedure than that involved in solving the ground state of the time-independent many-body Schrödinger equation.

The HK theorems are:

1. For a nondegenerate ground-state system subject only to a time-independent scalar potential, all physical quantities are unique functionals of the ground-state charge density.

2. For a given external scalar potential, the ground-state density is that which minimises the system energy.

Proving the first of these relies on establishing a unique mapping between the density and potential. This is shown via unique maps with an intermediate quantity: the ground-state many-body wavefunction. The HK hypothesis can be summarised as:

$$v(\mathbf{r}) \quad \xleftarrow{\text{HK}} \quad n(\mathbf{r})$$

$$A^{-1} \diagdown A \qquad B^{-1} \diagup B$$

$$|\Psi_0\rangle \tag{2.4}$$

Maps A and B follow from the definitions of nondegeneracy and the many-body charge density. The inverse of map A is proven to within an additive constant in $v(\mathbf{r})$, since if two potentials $v_1(\mathbf{r})$ and $v_2(\mathbf{r})$ yield the same ground-state wavefunction $|\Psi_0\rangle$

with energies E_1 and E_2 respectively, it follows that

$$(E_1 - E_2) |\Psi_0\rangle = \left(\hat{H}_{v_1} - \hat{H}_{v_2} \right) |\Psi_0\rangle = (v_1(\mathbf{r}) - v_2(\mathbf{r})) |\Psi_0\rangle \qquad (2.5)$$

and thus that $v_1(\mathbf{r}) - v_2(\mathbf{r})$ equals a constant.

The inverse of map B follows from the Rayleigh-Ritz variational theorem. If two different ground-state wavefunctions $|\Psi_1\rangle$ and $|\Psi_2\rangle$ have the same density $n(\mathbf{r})$, then the ground-state energies of each obey the inequalities

$$E_1 < \left\langle \Psi_2 \left| \hat{H}_{v_1} \right| \Psi_2 \right\rangle = E_2 + \int_{-\infty}^{\infty} d\mathbf{r} \; n(\mathbf{r}) \left[v_1(\mathbf{r}) - v_2(\mathbf{r}) \right] \qquad (2.6)$$

$$E_1 < \left\langle \Psi_1 \left| \hat{H}_{v_2} \right| \Psi_1 \right\rangle = E_1 + \int_{-\infty}^{\infty} d\mathbf{r} \; n(\mathbf{r}) \left[v_2(\mathbf{r}) - v_1(\mathbf{r}) \right]. \qquad (2.7)$$

Summing over the two inequalities yields

$$E_1 + E_2 < E_2 + E_1 \qquad (2.8)$$

and thus the unique mapping between $v(\mathbf{r})$ and $n(\mathbf{r})$ is proven *reductio ad absurdum*.

The potential may then be written as:

$$v(\mathbf{r}) = v\left[n\right](\mathbf{r}), \qquad (2.9)$$

i.e. as a *functional* of the density, and thus the Hamiltonian and its ground-state wavefunction are also uniquely defined by the density:

$$|\Psi_0\rangle = |\Psi_0\rangle \left[n\right]. \qquad (2.10)$$

All other physical quantities of interest can be derived from these two functionals, and thus, in principle, from the charge density. The energy of a system with charge density $n(\mathbf{r})$ subject to a scalar potential $v(\mathbf{r})$ is

$$E_v\left[n\right] = F\left[n\right] + \int_{-\infty}^{\infty} d\mathbf{r} \; n(\mathbf{r}) v(\mathbf{r}) \qquad (2.11)$$

where $F\left[n\right]$ is a universal (insofar as it does not depend on the external potential) functional of the density:

$$F\left[n\right] = \left\langle \Psi_0\left[n\right] \left| \hat{T} + \hat{U} \right| \Psi_0\left[n\right] \right\rangle \qquad (2.12)$$

where $\hat{T}$ and $\hat{U}$ are once again the kinetic-energy and electron-electron interaction operators.

The second theorem of a variational procedure to find the ground-state charge density n_0 of a given external potential v_{ext} also follows from Eq. 2.3 and 2.4:

$$\int_{-\infty}^{\infty} n(\mathbf{r}) v_{\text{ext}}(\mathbf{r}) \, d\mathbf{r} + F[n] \geq \int_{-\infty}^{\infty} n_0(\mathbf{r}) v_{\text{ext}}(\mathbf{r}) \, d\mathbf{r} + F[n_0(\mathbf{r})] , \qquad (2.13)$$

thus the total energy density-functional for a given external potential v has its minimum when the density is the ground-state density of that potential:

$$\left. \frac{\partial E}{\partial n(\mathbf{r})} \right|_{n=n_0} = 0. \qquad (2.14)$$

The variational procedure above is limited insofar as the n we are varying must be V-representable (or "interacting V-representable"), i.e. it must be the ground-state charge density of some external potential v'_{ext}. There are densities for which no such ground-state wavefunction exists, for instance certain excited atomic state densities having nodes, and densities of statistical ensembles encountered in G-fold degenerate systems with density matrices

$$\rho(\mathbf{r}, \mathbf{r}') = \sum_{i}^{G} p_i \, |\Psi_i\rangle \langle \Psi_i| \qquad (2.15)$$

where p_i is the statistical likelihood of measuring each state in the ensemble such that $\sum_i p_i = 1$, and with ensemble densities

$$n^{\text{e}}(\mathbf{r}) = \rho(\mathbf{r}, \mathbf{r}). \qquad (2.16)$$

The variational theorem was therefore extended by Levy [93] and Lieb [94] to accept searches over all wavefunctions and ensembles having charge density n. This variational procedure is then over

$$E[n] = \inf_{\Psi \to n} \left\langle \Psi \left| \hat{T} + \hat{U} \right| \Psi \right\rangle + \int_{-\infty}^{\infty} d\mathbf{r} \, n(\mathbf{r}) v(\mathbf{r}), \qquad (2.17)$$

where $\Psi \to n$ indicates that the infimum is to be taken over all N-particle states having density n. (For all intents and purposes, the infimum is the global minimum. For infinite sets, it does not generally hold that a minimum exists. The infimum of $\left\langle \Psi \left| \hat{T} + \hat{U} \right| \Psi \right\rangle$ is the largest number inside or outside the set of integrals that is less

than or equal to the all of the values in the set. Since the ground-state energy *is* given by one of the integrals in the set, the infimum is the minimum [95]. However, it does not follow that there are not other minima satisfying $\partial_n E\,|_{n_0} = 0$.)

While the procedure is simple in principle, in practice the universal functional $F[n]$ is unknown and must be approximated. Finding good approximations to F, both in this density-functional theory and its extensions, has formed a large part of the research into its applications and efficacy [96]. The next section will look at the most popular scheme in which to make such approximations.

2.1.2 The Kohn-Sham formulation of DFT

While the HK proofs establish a unique relationship between the external potential and its N-electron ground-state density, and allows us in principle to find the correct ground-state density for a given potential for a given approximate universal functional, it does not offer any guidance on how one might construct the approximate functional, without which the variational procedure is effectively useless.

The Kohn-Sham (KS) formulation of DFT [97] resolves this beautifully. It relies in part on the HK theorem being insensitive to the Coulomb strength of the true electron-electron interaction that is within the universal functional $F[n]$. While the unique relationship between external potential and charge density holds only for a given Coulomb strength, a choice of different strength simply yields a different universal functional and so a different potential.

Thus KS realised that one may construct an auxiliary system of noninteracting electrons subject to an effective external potential – the KS potential – with the same charge density as the interacting system it represents. Since the universal functional is a unique functional *only* of the density, it may be calculated as the sum of single-particle densities of the noninteracting system.

First, the universal functional is decomposed into three separate components

$$F[n] = T_{\mathrm{S}}[n] + E_{\mathrm{H}}[n] + E_{\mathrm{xc}}[n] \tag{2.18}$$

where

$$E_{\mathrm{H}}[n] = \tfrac{1}{2} \int_{-\infty}^{\infty} d\mathbf{r} \int_{-\infty}^{\infty} d\mathbf{r}' \, \frac{n(\mathbf{r})n(\mathbf{r}')}{|\mathbf{r} - \mathbf{r}'|} \tag{2.19}$$

is the classical electron-electron interaction energy (the Hartree energy), E_{xc} is the exchange-correlation (XC) energy, and T_{S} is the noninteracting kinetic energy of an

auxiliary system of noninteracting electrons having ground-state density

$$n(\mathbf{r}) = \sum_{k=1}^{N} |\psi_k|^2 \qquad (2.20)$$

where $\{\psi_k\}$ are the solutions of the single-particle time-independent wave equation

$$\hat{H}\psi_k = \left(\hat{T} + v_{\text{ext}}(\mathbf{r}) + v_{\text{H}}[n](\mathbf{r}) + v_{\text{xc}}[n](\mathbf{r})\right)\psi_k = \varepsilon_k\psi_k \qquad (2.21)$$

where $v_{\text{xc}}[n](\mathbf{r}) = \delta E_{\text{xc}}[n]/\delta n(\mathbf{r})$ by definition.

Equations (2.20) and (2.21) are the *Kohn-Sham* equations, whose self-consistent solution for a known external potential $v_{\text{ext}}(\mathbf{r})$ and an appropriate approximate XC functional $v_{\text{xc}}[n](\mathbf{r})$ is equivalent to the minimisation of the total energy of the interacting system. The XC potential is, like the universal functional, generally unknown. The usual approximations employed for ground-state electronic structure calculations are local or semilocal functionals of the density, such as the local density approximation (LDA)

$$E_{\text{xc}}^{\text{LDA}}[n] = \int_{-\infty}^{\infty} d\mathbf{r}\, n(\mathbf{r})\epsilon_{\text{xc}}(n(\mathbf{r})) \qquad (2.22)$$

which takes the potential at position $\mathbf{r}$ to be that of a ground-state homogeneous electron gas whose density is everywhere equal to $n(\mathbf{r})$ [98], or the generalised gradient approximation (GGA) which incorporates the spatial variation of the charge density via an explicit functional dependence of the density gradient [99; 100; 101; 102].

Generally, the XC potential is not a local or semilocal functional of the ground-state density, except in the limit of the density gradient going to zero, i.e. the homogeneous electron gas, and for high densities at short wavelengths [103]. Despite the seeming crudeness of local and semilocal functional approximations, density-functional theory in the Kohn-Sham scheme has enjoyed a great deal of success in the calculation of ground-state energy and electronic structure calculations [96].

However, the theory is concerned with nondegenerate ground states subject only to a scalar potential, and such systems are not generally current-carrying. To be applied to quantum transport, a density-functional theory must account for the current in steady-state and nonequilibrium systems. Density-functional theory for ground-state current-carrying systems will be studied in Sec. 2.3 and Chapter 3. For nonequilibrium systems, the current density can be decomposed into two parts: a longitudinal part

and a transverse part whose sum is the total physical current:

$$\mathbf{j}(\mathbf{r}, t) = \mathbf{j}_L(\mathbf{r}, t) + \mathbf{j}_T(\mathbf{r}, t), \tag{2.23}$$

with each part defined via the identities

$$\nabla \times \mathbf{j}_L(\mathbf{r}, t) = 0 \tag{2.24}$$

$$\nabla \cdot \mathbf{j}_T(\mathbf{r}, t) = 0. \tag{2.25}$$

From the continuity equation

$$\frac{\partial}{\partial t} n(\mathbf{r}, t) + \nabla \cdot \mathbf{j}(\mathbf{r}, t), \tag{2.26}$$

we see that the time-dependent density fully determines the longitudinal current for given boundary conditions. An extension of DFT to the time-dependent regime therefore would provide a theory that explicitly accounts for the current, so long as the current is longitudinal. In Sec. 2.2 we shall see that such an extension exists and is called time-dependent density-functional theory. There are also multiple extensions of density-functional theory to ground-state systems subject to both external scalar *and* vector potentials, which will be discussed in depth in Sec. 2.3 and Chapter 3.

2.2 Time-dependent density-functional theory

2.2.1 Uniqueness in the time-dependent regime

The success of density functional theory in the ground state made it appealing to extend to excited systems and, in particular, to time-dependent systems. Clearly the proofs of the Hohenberg-Kohn theorems have no application here since for any given excited system $|\Psi\rangle$ time-evolving under an external potential $v(\mathbf{r}, t)$ at time t, one can generally construct an alternative system at that time that has a lower energy, most especially the ground-state of v at t.

But in 1984, Runge and Gross (RG) [104] detailed an equivalent existence theorem for time-dependent systems described by the N-body Schrödinger equation:

$$i\frac{\partial}{\partial t} \Psi(\mathbf{r}_1, \mathbf{r}_2, ..., \mathbf{r}_N, t) = \sum_{k=1}^{N} \left\{ -\frac{1}{2}\nabla_k^2 + v_{\text{ext}}(\mathbf{r}_k) + \frac{1}{2}\sum_{j \neq k} \frac{1}{|\mathbf{r}_k - \mathbf{r}_j|} \right\} \Psi(\mathbf{r}_1, \mathbf{r}_2, ..., \mathbf{r}_N, t). \tag{2.27}$$

If the system begins in some initial state $|\Phi_0\rangle$ (which, if a ground state, can be found by via the time-independent Schrödinger equation for $v(t=0)$), then the Schrödinger equation uniquely defines a map – map A – from the time-dependent external potential of the system $v_{\text{ext}}(\mathbf{r}, t)$ and the time-dependent many-body wavefunction $|\Psi(t)\rangle$. Likewise for a given time-dependent state, the instantaneous time-dependent charge density is uniquely defined (map B):

$$n(\mathbf{r}, t) = \langle \Psi |\hat{n}(\mathbf{r})| \Psi \rangle |_t \tag{2.28}$$

where

$$\hat{n}(\mathbf{r}) = \sum_{i=1}^{N} \delta(\mathbf{r} - \mathbf{r}_i) \tag{2.29}$$

is the number density operator.

The Runge-Gross theorem states that maps A and B are invertible. They hypothesise that

$$v(\mathbf{r}, t) \xleftarrow{\hspace{1.5em}\text{RG}\hspace{1.5em}} (n(\mathbf{r}, t), |\Phi_0\rangle)$$
$$A^{-1} \diagdown A \qquad B^{-1} \diagup B$$
$$|\Psi(\mathbf{r}, t)\rangle \tag{2.30}$$

and demonstrated that this was true so long as the system under study is finite and external potential is Taylor-expandable in time its initial time. Within these restrictions, the initial state and time-dependent density were shown *reductio ad absurdum* to uniquely define the external electric field $\mathbf{E}_{\text{ext}}(\mathbf{r}, t) = -\nabla v_{\text{ext}}(\mathbf{r}, t)$, and thus the external scalar potential up to a time-dependent constant which affects only on the time-dependent phase of the wavefunction and does affect any physical quantity.

The necessity that the external potential be Taylor-expandable arises due to the fact that one could consider two external potentials $v_1(\mathbf{r}, t)$ and $v_2(\mathbf{r}, t)$ which are distinct and nonetheless equal for some unlimited duration. Likewise, their first time-derivatives, second time-derivatives, and so on may also be identical. However, so long as the two potentials do diverge at *some* time, the Taylor expansions of each must contain terms that differ at some order of the expansion. This is a vital component of the RG uniqueness proof.

Within the linear response regime, where the rate of change of the system is small, proof of uniqueness has since been extended to finite intervals of time-evolution under small but arbitrary perturbations [105], and to potentials that are Laplace-

transformable in time when the initial state of the system is the ground state [106]. Maitra, Todorov, Woodward and Burke [107] have demonstrated a proof of uniqueness for non-Taylor-expandable potentials and densities via nonlinear formulations of the Schrödinger equation consisting of the coupled equations:

$$i\frac{\partial}{\partial t}\left|\Psi(t)\right\rangle = \hat{H}_v(t)\left|\Psi(t)\right\rangle \tag{2.31}$$

$$\nabla \cdot [n(\mathbf{r}, t)\nabla v(\mathbf{r}, t)] = \frac{\partial^2}{\partial t^2}n(\mathbf{r}, t) + \nabla \cdot \mathbf{a}\left[\Psi(t)\right] \tag{2.32}$$

where $\mathbf{a}\left[\Psi(t)\right] = -i\left\langle \Psi(t) \left| \left[\hat{\mathbf{j}}_{\mathrm{p}}, \hat{H}_0\right] \right| \Psi(t)\right\rangle$ is the stress-momentum tensor functional, $\hat{H}_0 = \hat{T} + \hat{U}$, and one solves Eq. 2.32 iteratively for $v(\mathbf{r}, t)$ for a given time-dependent charge density.

Ruggenthaler and van Leeuwen [108] replaced the Taylor expansion with an iterative procedure by which one approaches the unique potential for a given time-dependent density and initial state. Nonlinear Schrödinger equation approaches to both the Taylor-expandability and noninteracting-V-representability problems have been assessed for both TDDFT and time-dependent current-density-functional theory (see Sec. 2.2.5).

No general uniqueness proof exists that does not replace the condition of Taylor-expandability with another limitation; however, taken as a whole, the uniqueness proofs established cover most physical situations of interest.

2.2.2 Variational theorem and the action functional

Since there exists no variational procedure for excited systems to find the correct time-dependent charge density by minimisation of the energy, an alternative quantity is required: the quantum-mechanical action. This is defined for an interval of time $t_2 - t_1$ as:

$$Q(t_1, t_2) = \int_{t_1}^{t_2} dt \left\langle \Psi(t) \left| i\frac{\partial}{\partial t} - \hat{H}(t) \right| \Psi(t)\right\rangle \tag{2.33}$$

and has a stationary point when $\left|\Psi(t)\right\rangle$ is precisely the wavefunction being time-evolved from an initial state $\left|\Phi_0\right\rangle$ with the Hamiltonian $\hat{H}$. To be able to find the correct time-dependent charge density, then, one must be able to write the action as a functional of the density such that its stationary points may be found by varying that density:

$$\left.\frac{\delta}{\delta n'}Q\left[n'\right]\right|_{n'=n} = 0. \tag{2.34}$$

At first glance, it would seem, since the density only defines the wavefunction up to a time-dependent phase factor, there should be an infinite number of possible actions all corresponding to the same density. However, this phase factor is caused by a time-dependent constant in the scalar potential, and these two quantities exactly cancel. If we define $v_0(\mathbf{r}, t)$ such that $v_{\text{ext}}(\mathbf{r}, t) = v_0(\mathbf{r}, t) + c(t)$, then:

$$
\begin{aligned}
Q(t_1, t_2) &= \int_{t_1}^{t_2} dt \, \left\langle e^{-ic(t)}\Psi(t) \left| i\frac{\partial}{\partial t} - \hat{T} - \hat{U} - v_{\text{ext}}(\mathbf{r}, t) \right| e^{-ic(t)}\Psi(t) \right\rangle \\
&= \int_{t_1}^{t_2} dt \, \left\langle \Psi(t) \left| i\frac{\partial}{\partial t} - \hat{T} - \hat{U} - v_0(\mathbf{r}, t) - c(t) + c(t) \right| \Psi(t) \right\rangle.
\end{aligned} \tag{2.35}
$$

Thus $Q(t_1, t_2)$ is a unique functional of the density and, since only the term involving the potential depends on the nature of the system, the remainder forms part of a universal action functional:

$$
Q[n] = B[n] - \int_{t_1}^{t_2} dt \int_{-\infty}^{\infty} d\mathbf{r} \, n(\mathbf{r}, t)v(\mathbf{r}, t). \tag{2.36}
$$

A trial time-dependent density can then be varied until equation 2.34 holds at which point the exact density has been found.

2.2.3 TDDFT in the Kohn-Sham scheme

The Kohn-Sham scheme can be extended to the time-dependent regime so long as there exists a mapping from interacting densities $n(\mathbf{r}, t)$ to KS potentials $v_{\text{KS}}(\mathbf{r}, t)$ for some given initial many-body state $|\Psi(t = 0)\rangle$. The proof of the existence of this mapping was provided by van Leeuwen in 1999 [109] for Taylor-expandable potentials that vanish at infinity, while the existence proof for broader classes of potentials was provided alongside the proof of uniqueness in 2011 [108]. To this extent, the Kohn-Sham scheme as applied to time-dependent densities has a much stronger theoretical foundation than for the ground-state systems originally considered by KS for which there is no general proof of noninteracting-V-representability.

The conditions on the initial states of the interacting and noninteracting systems are reasonable. First, they must yield the same initial charge density:

$$
\langle \Phi_0 | \hat{n}(\mathbf{r}) | \Phi_0 \rangle = \langle \Psi_0 | \hat{n}(\mathbf{r}) | \Psi_0 \rangle = n(\mathbf{r}, 0), \tag{2.37}
$$

where $|\Psi_0\rangle$ is the initial interacting state and $|\Phi_0\rangle$ the initial noninteracting state. That they must be the same is already necessitated by the fact that the two share the same

time-dependent density at *all* times.

Second, the time-derivatives of the two initial densities must be the same which, from the continuity equation, yields

$$\left\langle \Phi_0 \left| \nabla \cdot \hat{\mathbf{j}}(\mathbf{r}) \right| \Phi_0 \right\rangle = \left\langle \Psi_0 \left| \nabla \cdot \hat{\mathbf{j}}(\mathbf{r}) \right| \Psi_0 \right\rangle = \nabla \cdot \mathbf{j}(\mathbf{r}, 0). \tag{2.38}$$

This implies that the longitudinal parts of the current densities of the two representations must also be the same.

In the case of Taylor-expandable external potentials, van Leeuwen showed that one can evaluate the difference between the two external potentials and the differences between their time-derivatives for the two interaction strengths at the initial time t_0 and construct the time-dependent noninteracting potential from its Taylor series.

The universal action functional can then be expressed in terms of single-particle wavefunctions as:

$$B[n] = \int_{t_0}^{t_1} dt \left\langle \Phi(t) \left| i\frac{\partial}{\partial t} - \hat{T}_{\mathrm{S}} - v_{\mathrm{H}}(\mathbf{r}, t) - v_{\mathrm{xc}}(\mathbf{r}, t) \right| \Phi(t) \right\rangle \tag{2.39}$$

where

$$v_{\mathrm{xc}}(\mathbf{r}, t) = \left. \frac{\partial Q_{\mathrm{xc}}[n]}{\partial n(\mathbf{r}, t')} \right|_{n=n(\mathbf{r}, t)} \tag{2.40}$$

is now defined to be the time-dependent exchange-correlation potential.

The time-dependent XC potential has been shown to have a nonlocal functional dependence on the charge density in both space and time, not least because of its intrinsic and important dependence on the initial state [110] and, as such, it is a much more difficult quantity to approximate than the XC potential functional of ground-state DFT. The simplest approximation is the adiabatic approximation:

$$v_{\mathrm{xc}}^{\mathrm{adiabatic}}[n](\mathbf{r}, t) = \left. v_{\mathrm{xc}}[n](\mathbf{r}) \right|_{n=n(\mathbf{r}, t)} \tag{2.41}$$

where $v_{\mathrm{xc}}[n](\mathbf{r})$ is the XC potential of the *ground-state* system having charge density $n(\mathbf{r}) = n(\mathbf{r}, t)$. Since even the ground-state potential is not generally known, it must be approximated. Just as in ground-state DFT the most frequently used approximation is the local density approximation, as is the case here. The resulting approximation for the time-dependent XC potential:

$$v_{\mathrm{xc}}^{\mathrm{ALDA}}[n](\mathbf{r}, t) = v_{\mathrm{xc}}^{\mathrm{LDA}}[n(\mathbf{r}, t)] \tag{2.42}$$

is the adiabatic local density approximation (ALDA). As can be seen from equation 2.42, the ALDA has a local functional dependence in time as well as in space on the charge density, and so does not incorporate any memory effects in the exact time-dependent XC potential such as initial state dependence.

Likewise one can construct adiabatic GGA and adiabatic meta-GGA approximations [111] which re-introduce some spatial nonlocality, the latter with some success, and adiabatic exact-exchange potentials (or "optimised effective potentials" [112]). However, all of these approximations yield XC functionals that are local in time.

2.2.4 Density-functional theory for quantum transport

The application of density functional theory for quantum transport simulations was pioneered by Hirose & Tsukada in 1994 for tunnelling junctions [113] and by Lang in 1995 for nanojunctions [114]. Lang used the formalism to calculate the single-particle wavefunctions of noninteracting leads subject to a potential bias. These wavefunctions and the Green's function for the scattering device were then used to calculate the single-particle wavefunction for the whole system as the solution of, in the Lippmann-Schwinger [115] form,

$$\psi(\mathbf{r}) = \psi^{\text{leads}}(\mathbf{r}) + \int_{-\infty}^{\infty} d\mathbf{r}' \int_{-\infty}^{\infty} d\mathbf{r}'' \ G^{\text{leads}}(\mathbf{r}, \mathbf{r}') v(\mathbf{r}', \mathbf{r}'') \psi(\mathbf{r}''), \qquad (2.43)$$

where

$$v(\mathbf{r}, \mathbf{r}') = v_{\text{ps}}(\mathbf{r}, \mathbf{r}') + \delta(\mathbf{r} - \mathbf{r}') \left\{ v_{\text{H}} \left[n - n^{\text{leads}} \right](\mathbf{r}) + v_{\text{xc}} \left[n \right](\mathbf{r}) - v_{\text{xc}} \left[n^{\text{leads}} \right](\mathbf{r}) \right\} \quad (2.44)$$

and $v_{\text{ps}}(\mathbf{r}, \mathbf{r}')$ is the sum of nonlocal pseudopotentials representing the electric potential of the underlying ions or atomic cores.

Typical approximations such as LDA and GGA (see Sec. 2.1) are continuous in $n(\mathbf{r})$ and $\nabla n(\mathbf{r})$, but we have seen in Fig. 1.5, the true XC energy has a discontinuous dependence on the local electron number (see Fig. 2.1). The necessity of incorporating derivative discontinuities is very apparent in the case of the Coulomb blockade, and it has been noted in the past by Toher *et al* [10] that the usual approximations for exchange and correlation cannot be applied to quantum transport. One consequence of the lack of a derivative continuity in the XC potential is that a Kohn-Sham description of even a ground-state system does not predict the correct band structure of the material it represents, for instance yielding metallic band structures for semiconductor densities [116]. Toher *et al* proposed a scheme that reintroduced an approximation to the correct

derivative discontinuity by removing the self-interaction introduced by the Hartree potential which, for each KS electron, is

$$v_{\text{SIC},i}(\mathbf{r}) = -\frac{1}{2} \int_{-\infty}^{\infty} d\mathbf{r}' \, \frac{n_i(\mathbf{r}')}{|\mathbf{r} - \mathbf{r}'|}. \tag{2.45}$$
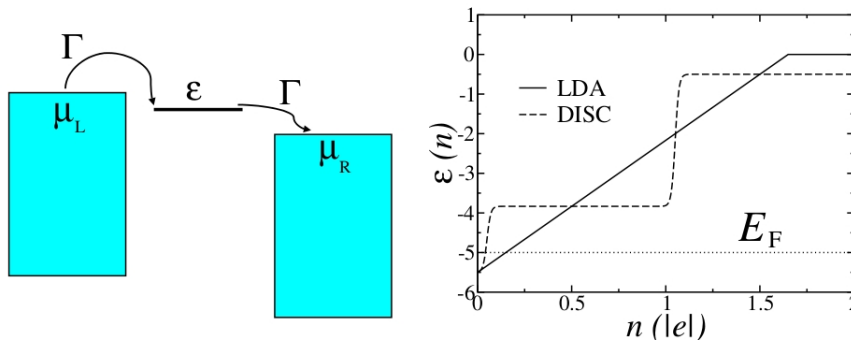
Figure 2.1: **The derivative discontinuity:** The dependence of the energy of a state, such as the single-level transport region shown here, has a step-like dependence on the number of electrons in that state. Usual DFT approximations such as the LDA have a continuous dependence on the electron density. [10].

Derivative discontinuities play a major role in open quantum systems such as those studied in quantum transport. Since the particle number in a device is allowed to vary with time, the total electron number passes through an integer continuously. The need to deal with fractional particle numbers in density-functional theory was treated by Perdew *et al* [117]. They found that the dependence of the total energy E on the electron number N is linear in N, but goes through a discontinuous change in the coefficient of proportionality whenever N passes through an integer. Likewise for applications of density-functional theory they argued that the XC potential must be dependent on the energy of the single-particle state it is acting on [118].

Another difficulty of applying density-functional theory to quantum transport problems is that of dealing with the infinite quantum systems required to maintain a current (or else the even less appealing modelling of infinite electron reservoirs or a fully quantum-mechanical description of a battery). How one deals with this problem comes down to a choice of the boundary conditions of the system being simulated.

The application of time-dependent density functional theory to nonequilibrium quantum transport was performed by Kurth *et al* in 2005 [119]. They took as their point of departure the NEGF scheme of Cini [75] and so, like in the Cini approach,

one begins for $t < 0$ with the system in equilibrium and carrying no current, i.e. in its ground state which is amenable to a density-functional description as demonstrated by the Hohenberg-Kohn theorem.

This provides an unambiguous initial state for a TDDFT calculation, wherein it has been shown that the time-dependent potential is a functional of both the time-dependent charge density *and* the initial state. For $t \geq 0$, the system is driven out of equilibrium by the turning on of an externally-applied electric potential bias.

Generally, since the system being described is infinite, the spatial extent of the electron wavefunctions and the Hamiltonian governing them will also be infinite. An approach that had been commonly employed for NEGF treatments of steady-state transport (e.g. [120]) was to partition the system into left- and right-lead components and the central scattering region, which includes the device and the portions of the leads that couple to it. Rather than attempt to calculate the wavefunction for the entire system, one instead calculates a finite wavefunction equal to the exact within the region of interest: the so-called *transparent boundary condition* [121].

The Hamiltonian and electron wavefunctions, partitioned into the left-lead, central region and right-lead components, with the two lead components noninteracting, yields the time-dependent Schrödinger equation:

$$i\frac{\partial}{\partial t}\begin{bmatrix} \psi_{\mathrm{L}} \\ \psi_{\mathrm{C}} \\ \psi_{\mathrm{R}} \end{bmatrix} = \begin{bmatrix} \hat{H}_{\mathrm{LL}} + \hat{U}_{\mathrm{L}}(t) & \hat{H}_{\mathrm{LC}} & 0 \\ \hat{H}_{\mathrm{CL}} & \hat{H}_{\mathrm{CC}}(t) & \hat{H}_{\mathrm{CR}} \\ 0 & \hat{H}_{\mathrm{RC}} & \hat{H}_{\mathrm{RR}} + \hat{U}_{\mathrm{R}}(t) \end{bmatrix}\begin{bmatrix} \psi_{\mathrm{L}} \\ \psi_{\mathrm{C}} \\ \psi_{\mathrm{R}} \end{bmatrix}, \qquad (2.46)$$

where $U_{\mathrm{L}}(t) - U_{\mathrm{R}}(t)$ is the time-dependent potential drop across the central region that perturbs the system.

The components of the Hamiltonian are generally dependent on position as well as time. Because the KS potential is local in space, $\hat{U}_{\alpha}$ can depend on only one spatial coordinate. Further, the potentials of the left and right leads may differ, but for metallic leads the potential is constant within each one, thus

$$\hat{U}_{\alpha}(\mathbf{r}, t) = U_{\alpha}(t)\mathbf{1}_{\alpha} \qquad (2.47)$$

where $\mathbf{1}_L = 1$ for coordinates in the left lead and 0 otherwise, and $\mathbf{1}_R = 1$ for coordinates in the right lead and 0 otherwise.

From an initial state determined in DFT, the time-evolution of the KS wavefunction

in the central region of the wire then yields

$$\psi_{\mathrm{C}}(\mathbf{r}, t) = \hat{U}_{\mathrm{eff}}(t, t_0)\psi_{\mathrm{C}}(\mathbf{r}, t_0) + S + M, \tag{2.48}$$

where S is a source term describing the injection of electrons into the central region and M is a memory term that must be calculated recursively. The propagator $\hat{U}_{\mathrm{eff}}$ is that for an effective central Hamiltonian that incorporates the time-varying left and right lead wave functions and the coupling thereto. Generally the on-site Hamiltonian $\hat{H}_{\mathrm{CC}}(t)$ depends on the KS potential that yields $\psi_{\mathrm{C}}(\mathbf{r}, t)$ which itself depends on the effective Hamiltonian, thus $\hat{H}_{\mathrm{CC}}(t)$ too must be calculated iteratively.

2.2.5 Time-dependent current density functional theory

Since the current density is proportional to the *gradient* of the wavefunction, a density-functional theory based on the *current* density instead of or as well as the charge density would introduce a more spatially nonlocal dependence on the charge density itself. In the time-dependent regime, the current density also encodes temporally nonlocal information about the charge density via the continuity equation. Since adiabatic approximations to the XC potential are blind to the time-evolution of the charge density, there is a strong case for a *time-dependent* current-density functional theory. An illustration of how important such a theory might be is the slab of electric charge moving back and forth in a confining potential referred to in the Introduction.
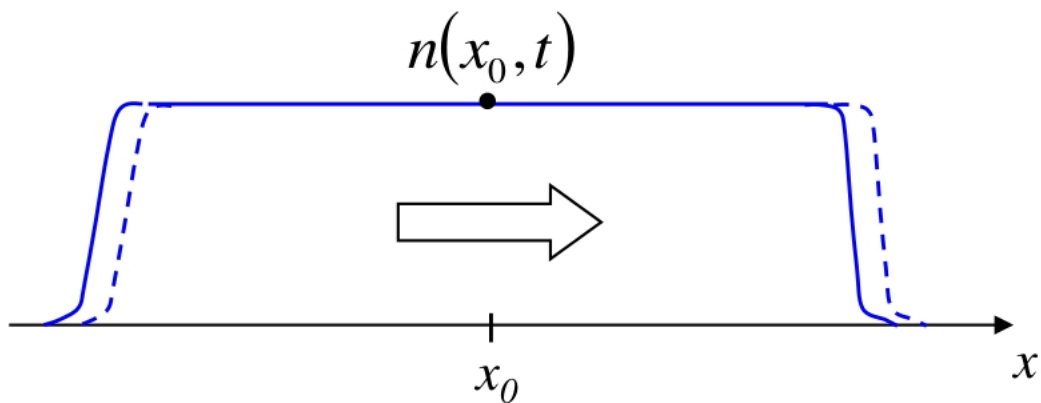
Figure 2.2: Any local or semilocal functional of the time-dependent charge density such as the ALDA or adiabatic GGA will be unable to see the direction of the current in the centre of the slab. A practical functional of the charge density must therefore be very long-ranged. However, a local functional of the *current* density will capture the correct physics. (Illustration from [11].)

In the centre of the moving slab, the charge density is time-independent: $\partial n/\partial t = 0$. However, the slab as a whole is moving with time with $\mathbf{j} \neq 0$. Taking the current density as well as or instead of the charge density will make more information accessible to local and adiabatic functional approximations.

Time-dependent current-density functional theory (TDCDFT) was originally formulated by Ghosh and Dhara in 1988 [122]. The hypothesis they prove is that there exists a one-to-one relationship between the time-dependent (physical) current density and the time-dependent external scalar and vector potentials $v(\mathbf{r}, t)$ and $\mathbf{A}(\mathbf{r}, t)$ for a given initial state $|\Phi_0\rangle$ of the system:

$$
(v(t), \mathbf{A}(t)) \xleftarrow[\hspace{2.5cm}]{\text{RG}} (\mathbf{j}(t), |\Phi_0\rangle)
$$
$$
A^{-1} \diagdown A \qquad B^{-1} \diagup B
$$
$$
|\Psi(t)\rangle \tag{2.49}
$$

The choice of the physical current as a basic variable was a logical one: first, because the uniqueness relation between external scalar potentials and current densities was already established in part by Runge and Gross in their uniqueness proof for TDDFT; second, because the current density contains information not available to the time-dependent charge density (namely the transverse part of the time-dependent current); and third, because it allowed for the extension of TDDFT to time-dependent systems subject to both electric and magnetic fields via scalar and vector potentials.

The action functional for a system evolved from a given initial state by time-dependent external scalar and vector potentials may be written as

$$
Q\left[\mathbf{j}\right] = B\left[\mathbf{j}\right] + \int_{t_1}^{t_2} dt \int_{-\infty}^{\infty} d\mathbf{r} \ \left\{ n(\mathbf{r}, t) \left(v(\mathbf{r}, t) - \tfrac{1}{2}A^2(\mathbf{r}, t) \right) + \mathbf{A}(\mathbf{r}, t) \cdot \mathbf{j}(\mathbf{r}, t) \right\} \tag{2.50}
$$

where $n(\mathbf{r}, t)$ is accessible via the continuity equation from $\mathbf{j}(\mathbf{r}, t)$ and the initial state, and $B\left[\mathbf{j}\right]$ is the same universal functional as in Eq. 2.36, now uniquely identified by the current. For a given set of external potentials $(v(\mathbf{r}, t), \mathbf{A}(\mathbf{r}, t))$, this allows one, with a suitable approximation for B, to find the stationary point of the action, i.e. $\delta Q/\delta \mathbf{j} = \mathbf{0}$,

by varying $\mathbf{j}$. Defining instead the action functional as

$$Q\left[n, \mathbf{j}\right] = B\left[\mathbf{j}\right] + \int_{t_1}^{t_2} dt \int_{-\infty}^{\infty} d\mathbf{r} \left\{ n(\mathbf{r}, t)\left(v(\mathbf{r}, t) - \tfrac{1}{2}A^2(\mathbf{r}, t)\right) + \mathbf{A}(\mathbf{r}, t) \cdot \mathbf{j}(\mathbf{r}, t) \right\},$$
(2.51)

one can vary $n(\mathbf{r}, t)$ and $\mathbf{j}(\mathbf{r}, t)$ independently, loosening the constraints on the choice of current density which may then be reintroduced via a constrained search.

Ghosh and Dhara further derived a unique equation of motion for the current density

$$\frac{\partial}{\partial t}\mathbf{j}(\mathbf{r}, t) = -i\left\langle \Psi(t) \left| \left[\hat{\mathbf{j}}_{\mathrm{p}}, \hat{H}_0 \right] \right| \Psi(t) \right\rangle + \mathbf{E}(\mathbf{r}, t)n(\mathbf{r}, t) + \mathbf{B}(\mathbf{r}, t) \times \mathbf{j}(\mathbf{r}, t)$$
(2.52)

where the first term on the RHS is the stress-momentum tensor, $\hat{H}_0 = \hat{T} + \hat{U}$, and $\mathbf{E}(\mathbf{r}, t)$ and $\mathbf{B}(\mathbf{r}, t)$ are the external electric and magnetic fields, related to the external scalar and vector potentials as

$$\mathbf{E}(\mathbf{r}, t) = -\nabla v(\mathbf{r}, t) - \frac{\partial}{\partial t}\mathbf{A}(\mathbf{r}, t)$$
(2.53)

$$\mathbf{B}(\mathbf{r}, t) = \nabla \times \mathbf{A}(\mathbf{r}, t).$$
(2.54)

That the above uniqueness and minimisation theorems hold true regardless of the interaction strength of the many-body system allows us to consider the construction of noninteracting approximations to the universal action functional, so long as time-dependent currents are generally noninteracting-V-representable.

2.2.6 TDCDFT in the Kohn-Sham scheme

The universal action functional $B\left[\mathbf{j}\right]$ is unknown without access to the many-body wave-function. As with earlier versions of DFT, then, one still has to calculate the wave-function explicitly in order to exploit the unique relation between the time-dependent current density and the external potentials and, also as before, one may do so in a system of noninteracting Kohn-Sham particles.

As van Leeuwen achieved within the TDDFT framework, Vignale [123] established that, under similar mild restrictions of the densities and potentials noted by van Leeuwen for TDDFT, the time-dependent current density $\mathbf{j}(\mathbf{r}, t)$ of an interacting system subject to external potentials $(v(\mathbf{r}, t), \mathbf{A}(\mathbf{r}, t))$ could always be reproduced by a noninteracting Kohn-Sham system subject to a different set of external potentials $(v_{\mathrm{KS}}(\mathbf{r}, t), \mathbf{A}_{\mathrm{KS}}(\mathbf{r}, t))$.

The self-consistent KS equations for a N-electron system are:

$$i\frac{\partial}{\partial t}\phi_k(\mathbf{r},t) = \left\{\frac{1}{2}\left[-i\nabla + \mathbf{A}_{\mathrm{KS}}(\mathbf{r},t)\right]^2 + v_{\mathrm{KS}}(\mathbf{r},t)\right\}\phi_k(\mathbf{r},t) \tag{2.55}$$

$$\mathbf{j}(\mathbf{r},t) = \sum_{k=1}^{N}\frac{1}{2i}\left(\phi_k^*(\mathbf{r},t)\nabla\phi_k(\mathbf{r},t) - \phi_k(\mathbf{r},t)\nabla\phi_k^*(\mathbf{r},t)\right) + \mathbf{A}_{\mathrm{KS}}(\mathbf{r},t)n(\mathbf{r},t)$$

$$\tag{2.56}$$

where $\phi_k(\mathbf{r},t)$ is the single-particle wavefunction of the kth electron in the KS system. The KS scalar and vector potentials are the effective external potentials which reproduce the N-electron charge and current density of a real interacting system subject to physical external potentials $v_{\mathrm{ext}}(\mathbf{r},t)$ and $\mathbf{A}(\mathbf{r},t)$. The forms of the effective KS potentials are determined by Ghosh and Dhara to be:

$$\mathbf{A}_{\mathrm{KS}}(\mathbf{r},t) = \mathbf{A}_{\mathrm{ext}}(\mathbf{r},t) + \mathbf{A}_{\mathrm{BS}}(\mathbf{r},t) + \frac{\delta E_{\mathrm{xc}}}{\delta\mathbf{j}}, \tag{2.57}$$

$$v_{\mathrm{KS}}(\mathbf{r},t) = v_{\mathrm{ext}}(\mathbf{r},t) + v_{\mathrm{H}}(\mathbf{r},t) + \frac{\delta E_{\mathrm{xc}}}{\delta n} + \frac{1}{2}\left(A_{\mathrm{KS}}^2(\mathbf{r},t) - A_{\mathrm{ext}}^2(\mathbf{r},t)\right). \tag{2.58}$$

The term $v_{\mathrm{H}}(\mathbf{r},t)$ is the time-dependent Hartree potential:

$$v_{\mathrm{H}}(\mathbf{r},t) = \int_{-\infty}^{\infty} d\mathbf{r}'\, \frac{n(\mathbf{r}',t)}{|\mathbf{r}-\mathbf{r}'|}, \tag{2.59}$$

and $\delta E_{\mathrm{xc}}/\delta\mathbf{A}$ and $\delta E_{\mathrm{xc}}/\delta n$ define the exchange-correlation vector and scalar potentials respectively. The new term, $\mathbf{A}_{\mathrm{BS}}(\mathbf{r},t)$, is the Biot-Savart vector potential

$$\mathbf{A}_{\mathrm{BS}}(\mathbf{r},t) = \int_{-\infty}^{\infty} d\mathbf{r}'\, \frac{\mathbf{j}(\mathbf{r}',t)}{|\mathbf{r}-\mathbf{r}'|}. \tag{2.60}$$

associated to the Biot-Savart magnetic field, and is usually included within the XC vector potential as, for instance, by Vignale and Rasolt [124] in time-independent current-density functional theory (CDFT). The explicit introduction of it by Ghosh and Dhara is by way of analogy with the explicit introduction of the Hartree potential: the classical electric potential due to a charge density $n(\mathbf{r})$. In this thesis, the convention of including the Biot-Savart vector potential in the definition of the XC vector potential *a la* Vignale and Kohn [125] will be adopted.

As in TDDFT, the exchange-correlation scalar and vector potentials are unknown and must be approximated. The most widely used approximation for the scalar potentials remains the adiabatic LDA. For the vector potential, the most widely-used

approximation is the Vignale-Kohn functional [125]. The general expression for the vector potential is long and complex, and it will not be employed in this research, but for systems where the velocity field $\mathbf{u}(\mathbf{r}, t) = \mathbf{j}(\mathbf{r}, t)/n(\mathbf{r}, t)$ is a constant in space, the Fourier transform (in time) of the VK vector potential simplifies to:

$$\mathbf{A}(\mathbf{r}, \omega) = -\frac{1}{\omega^2} \nabla \left[f^h_{\mathrm{xc,L}}(\mathbf{r}, \mathbf{r}', \omega) \nabla \cdot \mathbf{j}(\mathbf{r}, \omega) - \delta f^h_{\mathrm{xc,L}}(\mathbf{r}, \mathbf{r}', \omega) \nabla n(\mathbf{r}, \omega) \cdot \mathbf{u}(\mathbf{r}, \omega) \right], \quad (2.61)$$

where f^h_{xc} is the exchange-correlation kernel for the homogeneous electron gas, $f^h_{\mathrm{xc,L}}$ is its longitudinal part, and

$$\delta f^h_{\mathrm{xc,L}}(\omega) = f^h_{\mathrm{xc,L}}(\omega) - f^h_{\mathrm{xc,L}}(0). \quad (2.62)$$

The general form of the XC kernel is

$$f_{\mathrm{xc}}(\mathbf{r}, \mathbf{r}', t, t') = \frac{\delta v_{\mathrm{xc}}(\mathbf{r}, t)}{\delta n(\mathbf{r}', t')}. \quad (2.63)$$

The reliance on this kernel limits the VK functional to systems that are slowly-varying in time, while the use of the kernel of the homogeneous gas limits it to systems that are slowly-varying in space, but it nonetheless introduces effects that have some nonadiabatic dependence on the charge density and that are completely absent in the ALDA.

As per the treatment of TDDFT uniqueness by Maitra *et al*, an alternative formulation of TDCDFT yields the external potential functionals from a nonlinear Schrödinger equation [126]. Noting first that the time-dependent scalar potential may be implemented instead as a time-dependent vector potential via the gauge transformation

$$v(\mathbf{r}, t) \to v(\mathbf{r}, t) - \frac{\partial}{\partial t} \lambda(\mathbf{r}, t) \quad (2.64)$$

$$\mathbf{A}(\mathbf{r}, t) \to \mathbf{A}(\mathbf{r}, t) + \nabla \lambda(\mathbf{r}, t), \quad (2.65)$$

with $\partial_t \lambda(\mathbf{r}, t) = v(\mathbf{r}, t)$, the vector potential of the system is then

$$\mathbf{A}(\mathbf{r}, t) = \frac{1}{n(\mathbf{r}, t)} \left(\mathbf{j}(\mathbf{r}, t) - \left\langle \Psi(t) \left| \hat{\mathbf{j}}_{\mathrm{p}}(\mathbf{r}) \right| \Psi(t) \right\rangle \right). \quad (2.66)$$

The nonlinear Schrödinger equation is then constructed by inserting Eq. 2.66 into the Schrödinger equation

$$i \frac{\partial}{\partial t} \Psi(t) = \tfrac{1}{2} \sum_k \left[\hat{\mathbf{p}}_k + \mathbf{A}(\mathbf{r}_k, t) \right]^2 \Psi(t). \quad (2.67)$$

As in the special case of $\mathbf{A}(\mathbf{r}, t) = \mathbf{0}$ for TDDFT, no general proof of uniqueness for arbitrary external potentials yet exists for TDCDFT. However, the various treatments of potentials beyond the Taylor-expandable cover most physical situations of interest.

2.3 Current-density functional theory

Density-functional theory as formulated by Hohenberg and Kohn, and developed by Kohn and Sham, applies only to ground-state systems free from external magnetic fields. The inclusion of such fields introduces additional terms in the total energy of the system due to the ways the magnetic field can couple to the charge density, any ground-state current density, and the net spin density of the system.

The Hamiltonian for such systems is the Pauli Hamiltonian

$$\hat{H} = \frac{1}{2} \left[\hat{\boldsymbol{\sigma}} \cdot (\hat{\mathbf{p}} + \mathbf{A}(\mathbf{r})) \right]^2 + v(\mathbf{r}) \tag{2.68}$$

which, in the absence of spin-orbit coupling, may be rewritten as

$$\hat{H} = \frac{1}{2} \left[\mathbf{p} + \mathbf{A}(\mathbf{r}) \right]^2 + v(\mathbf{r}) - \mu_{\mathrm{B}} \hat{\boldsymbol{\sigma}} \cdot \mathbf{B}(\mathbf{r}) \tag{2.69}$$

where μ_{B} is the Bohr magneton (which is equal to $1/2$ is atomic units), $\hat{\boldsymbol{\sigma}} = (\sigma_{\mathrm{x}}, \sigma_y, \sigma_z)$ is the spin vector, the components of which are the two-by-two Pauli matrices, and

$$\mathbf{B}(\mathbf{r}) = \nabla \times \mathbf{A}(\mathbf{r}) \tag{2.70}$$

is the corresponding external magnetic field. The first two terms of Eq. 2.69 is the Schrödinger equation for a spinless massive charged particle in external electromagnetic fields, while the final term describes the coupling of the external magnetic field to the spin and is thus known as the *Stern-Gerlach* term.

The total energy of the ground-state system is then given by

$$
\begin{aligned}
E &= \left\langle \Psi_0 \left| \hat{H} \right| \Psi_0 \right\rangle \\
&= \left\langle \Psi_0 \left| \hat{T} + \hat{U} \right| \Psi_0 \right\rangle + \int_{-\infty}^{\infty} d\mathbf{r} \, \mathbf{j}_{\mathrm{p}}(\mathbf{r}) \cdot \mathbf{A}(\mathbf{r}) + \int_{-\infty}^{\infty} d\mathbf{r} \, n(\mathbf{r}) \left(v(\mathbf{r}) + \frac{1}{2} A^2(\mathbf{r}) \right) \\
&\quad - \int_{-\infty}^{\infty} d\mathbf{r} \, \mathbf{m}(\mathbf{r}) \cdot \mathbf{B}(\mathbf{r}) \\
&= \left\langle \Psi_0 \left| \hat{T} + \hat{U} \right| \Psi_0 \right\rangle + \int_{-\infty}^{\infty} d\mathbf{r} \, \mathbf{j}(\mathbf{r}) \cdot \mathbf{A}(\mathbf{r}) + \int_{-\infty}^{\infty} d\mathbf{r} \, n(\mathbf{r}) \left(v(\mathbf{r}) - \frac{1}{2} A^2(\mathbf{r}) \right)
\end{aligned}
\tag{2.71}
$$

where $\mathbf{j}$ is the physical current density:

$$\mathbf{j}(\mathbf{r}) = \mathbf{j}_\mathrm{p}(\mathbf{r}) + \mathbf{j}_\mathrm{d}(\mathbf{r}) + \mathbf{j}_\mathrm{m}(\mathbf{r}) \tag{2.72}$$

comprising the paramagnetic term $\mathbf{j}_\mathrm{p}$, the diamagnetic term $\mathbf{j}_\mathrm{d}$ and the magnetisation term $\mathbf{j}_\mathrm{m}$:

$$\mathbf{j}_\mathrm{p}(\mathbf{r}) = \frac{1}{2i} \left\langle \Psi_0 \left| \sum_{k=1}^{N} \nabla_k \delta(\mathbf{r}_k - \mathbf{r}) + \delta(\mathbf{r}_k - \mathbf{r})\nabla_k \right| \Psi_0 \right\rangle$$
$$\mathbf{j}_\mathrm{d}(\mathbf{r}) = \mathbf{A}(\mathbf{r})n(\mathbf{r})$$
$$\mathbf{j}_\mathrm{m}(\mathbf{r}) = \nabla \times \mathbf{m}(\mathbf{r}), \tag{2.73}$$

with

$$\mathbf{m}(\mathbf{r}) = \langle \Psi_0 \left| \hat{\mathbf{m}}(\mathbf{r}) \right| \Psi_0 \rangle, \tag{2.74}$$

where

$$\hat{\mathbf{m}}(\mathbf{r}) = -\mu_\mathrm{B} \sum_{i=1}^{N} \boldsymbol{\sigma}_i \delta(\mathbf{r} - \mathbf{r}_i) \tag{2.75}$$

is the magnetisation density operator and $\mu_\mathrm{B} = \frac{1}{2}$ is the Bohr magneton in atomic units.

By extending DFT to include magnetic fields as well as electric fields, one can no longer consider the charge density alone as a basic variable, since the energy functional of any current-carrying or magnetised system will contain couplings between the magnetic field and the current density and magnetisation which therefore must be included as basic variables.

2.3.1 The paramagnetic current as basic variable

The first proposal for a theoretical basis of a current-density functional theory for systems subject to both external scalar *and* vector potentials was by Vignale and Rasolt (VR) in 1988 [124], which, incorporating spin, consisted of eight basic potentials and eight basic densities.

The hypothesis they sought to prove was:

$$(v_{\uparrow,\downarrow}, \mathbf{A}_{\uparrow,\downarrow}) \xleftarrow{\quad\quad \text{HK} \quad\quad} (n_{\uparrow,\downarrow}, \mathbf{j}\text{p}_{,\uparrow,\downarrow})$$
$$A^{-1} \diagdown A \quad\quad B^{-1} \diagup B$$
$$(|\Phi_0\rangle_{\uparrow,\downarrow}) \tag{2.76}$$

where the $\uparrow$ and $\downarrow$ indices denote the spin-up and spin-down elements of the associated quantity. The external scalar potential is given by

$$v(\mathbf{r}) = \tfrac{1}{2}\left[v_\uparrow(\mathbf{r}) + v_\downarrow(\mathbf{r})\right], \tag{2.77}$$

the magnetic field by

$$B(\mathbf{r}) = \tfrac{1}{2}\left[v_\uparrow(\mathbf{r}) - v_\downarrow(\mathbf{r})\right], \tag{2.78}$$

and the external vector potential by

$$\mathbf{A}(\mathbf{r}) = \mathbf{A}_\uparrow(\mathbf{r}) = \mathbf{A}_\downarrow(\mathbf{r}). \tag{2.79}$$

The total charge density is the sum of its spin-dependent components:

$$n(\mathbf{r}) = n_\uparrow(\mathbf{r}) + n_\downarrow(\mathbf{r}) \tag{2.80}$$

while the magnetisation is the difference:

$$m(\mathbf{r}) = n_\uparrow(\mathbf{r}) - n_\downarrow(\mathbf{r}). \tag{2.81}$$

Since the spin-up, -down and total vector potentials are identical, each of the spin-components of the paramagnetic current density couple to their corresponding vector potentials in the same way.

The uniqueness theorem Eq. 2.76 appears to hold because of the assumption that two sets of external potentials $(v_1, \mathbf{A}_1)$ and $(v_2, \mathbf{A}_2)$ will necessarily yield different ground-state wavefunctions $|\Phi_1\rangle$ and $|\Phi_2\rangle$. However, as discovered by Capelle and Vignale in 2002 [127], this isn't necessarily the case.

Capelle and Vignale provide a counterexample in which a system of N electrons is subject to an external, uniform magnetic field $\mathbf{B} = B\hat{\mathbf{e}}_z$ and a scalar potential $v(\mathbf{r})$, a version of which [95] will be detailed next. For the case where the Stern-Gerlach term

vanishes, the Hamiltonian may be written as:

$$\hat{H} = \hat{T} + \hat{U} + \int_{-\infty}^{\infty} d\mathbf{r} \ \left\{ \hat{n}(\mathbf{r}) \left(v(\mathbf{r}) + \frac{1}{2} A^2(\mathbf{r}) \right) + \hat{\mathbf{j}}_{\mathrm{p}}(\mathbf{r}) \cdot \mathbf{A}(\mathbf{r}) \right\} \tag{2.82}$$

where $\hat{n}$ is the number density operator as before,

$$\hat{\mathbf{j}}_{\mathrm{p}} = -\tfrac{1}{2} i \sum_{i=1}^{N} \ \boldsymbol{\nabla}_i \delta(\mathbf{r} - \mathbf{r}_i) + \delta^{(3)}(\mathbf{r} - \mathbf{r}_i) \boldsymbol{\nabla}_i \tag{2.83}$$

is the paramagnetic current density operator, and $\mathbf{B} = \nabla \times \mathbf{A}$ as always. The ground state of this Hamiltonian is $|\Phi_0\rangle$.

They consider next a second N-electron system subject to a uniform magnetic field $\mathbf{B}'(\mathbf{r}) = (B + \Delta B)\hat{\mathbf{e}}_z$ and scalar potential $v'(\mathbf{r})$, and ask: is it possible to choose a v' such that the ground state solution of the corresponding Hamiltonian $\hat{H}' = \hat{H} + \Delta\hat{H}$ is still $|\Phi_0\rangle$? The answer is yes, so long as $\Delta\hat{H}$ commutes with $\hat{H}$ such that:

$$\Delta\hat{H} |\Phi_0\rangle = \Delta E_0 |\Phi_0\rangle , \tag{2.84}$$

where ΔE_0 is the difference in ground-state energies of $\hat{H}$ and $\hat{H} + \Delta\hat{H}$.

One example of an operator that commutes with the Hamiltonian is the angular momentum operator:

$$\hat{L}_z = m \int_{-\infty}^{\infty} d\mathbf{r} \ (\hat{\mathbf{e}}_z \times \mathbf{r}) \cdot \hat{\mathbf{j}}_{\mathrm{p}}(\mathbf{r}). \tag{2.85}$$

Vector and scalar potentials in the second system which differ from those in the first by:

$$\Delta\mathbf{A}'(\mathbf{r}) = \frac{1}{2} \Delta B \ (\hat{\mathbf{e}}_z \times \mathbf{r}) \tag{2.86}$$

$$\Delta v'(\mathbf{r}) = -\frac{1}{2} \left((\Delta A(\mathbf{r}))^2 + 2\Delta\mathbf{A}(\mathbf{r}) \cdot \mathbf{A}(\mathbf{r}) \right) \tag{2.87}$$

will then have $|\Phi_0\rangle$ as an eigenstate. If we call $|\Phi_0'\rangle$ and $|\Phi_1'\rangle$ the ground and first excited states of $\hat{H}'$ respectively, then so long as:

$$\Delta E_0 \ll \left\langle \Phi_1' \left| \hat{H}' \right| \Phi_1' \right\rangle - \left\langle \Phi_0 \left| \hat{H} \right| \Phi_0 \right\rangle , \tag{2.88}$$

this eigenstate must also be the ground-state.

This counterexample to the bijectivity of external potentials and charge and paramagnetic current densities applies to both interacting and Kohn-Sham systems, therefore

even if the external potentials of a real system are uniquely defined by its densities, it does not follow that the auxiliary *Kohn-Sham system* used to calculate the universal functional in the minimisation procedure is uniquely determined.

This exemplifies the problem in the choice of basic variables for CDFT. The charge and paramagnetic current densities do not contain all of the physical information about a system subject to external electromagnetic fields, thus we cannot expect that all combinations of those fields will yield unique densities. Another issue is that the paramagnetic current density isn't a measurable quantity in the regime in which CDFT applies, since the presence of the nonzero vector potential $\mathbf{A}(\mathbf{r})$ will necessarily yield a diamagnetic current density $\mathbf{j}_d(\mathbf{r}) = \mathbf{A}(\mathbf{r})n(\mathbf{r})$, and it is only the total current density that can be measured.

It is precisely within the diamagnetic part of the current density that one could account for the different vector potentials in the two systems described above, since:

$$\mathbf{j}'_d(\mathbf{r}) = \mathbf{j}_d(\mathbf{r}) + \frac{1}{2}\Delta B \left(\hat{\mathbf{e}}_z \times \mathbf{r}\right) n(\mathbf{r}) \neq \mathbf{j}_d(\mathbf{r}). \tag{2.89}$$

Thus for a full uniqueness proof, and a firm theoretical foundation for CDFT, one must have a theory that incorporates diamagnetism.

2.3.2 The physical current as basic variable

A second theoretical basis for CDFT in the absence of Stern-Gerlach coupling was proposed by Pan and Sahni (PS) in 2010 [128] and is in terms of the physical current density

$$\mathbf{j}(\mathbf{r}) = \mathbf{j}_p(\mathbf{r}) + n(\mathbf{r})\mathbf{A}(\mathbf{r}) \tag{2.90}$$

and will thus be referred to hereafter as "physical CDFT" to differentiate it from Vignale and Rasolt's formulation of the theory. The hypothesis PS seek to prove is:

$$(v, \mathbf{A}) \xleftarrow{\quad \text{HK} \quad} (n, \mathbf{j})$$

$$A^{-1} \diagdown A \qquad B^{-1} \diagup B$$

$$|\Phi_0\rangle \tag{2.91}$$

The PS proof is applied to a given gauge, characterised by the scalar function $\alpha(\mathbf{r})$ defined by the gauge transformation

$$\mathbf{A}'(\mathbf{r}) = \mathbf{A}(\mathbf{r}) + \nabla\alpha(\mathbf{r}), \tag{2.92}$$

with respect to some reference gauge but which otherwise plays no part in the proof.

Vignale *et al* [129] pointed out that the mapping in Eq. 2.91, which includes within it the map:

$$|\Phi_0\rangle \to (n, \mathbf{j}). \tag{2.93}$$

cannot possibly be true. From [124] and [127], it is clear that this is map is not unique in the case of nonzero diamagnetic current, and indeed this would be the case with any CDFT that incorporates either explicitly or implicitly the diamagnetic current. However, it does not necessarily spell the end of a CDFT based on the physical current, since $|\Phi_0\rangle$ is only an intermediate quantity: it does not appear in the ultimate mapping that one wishes a HK proof to confirm. This suggests that any HK proof that goes beyond the paramagnetic current must also go beyond the ground-state wavefunction as an intermediate quantity.

A second and far more terminal criticism came from Tellgren *et al* [130]: the proof of the uniqueness theorem contained mathematical errors that, when eliminated, meant that the *reductio ad absurdum* was not achieved. The PS proof relied on the Hohenberg-Kohn-like approach of considering two sets of external potentials, $(v_1, \mathbf{A}_1)$ and $(v_2, \mathbf{A}_2)$ that yield ground states $|\Phi_1\rangle$ and $|\Phi_2\rangle$ with the same densities $(n, \mathbf{j})$. The ground-state energies are then

$$E_1 = F\left[|\Phi_1\rangle\right] + \int_{-\infty}^{\infty} d\mathbf{r} \ \left\{ \mathbf{j} \cdot \mathbf{A}_1 + n \left(v_1 - \tfrac{1}{2} A_1^2 \right) \right\} \tag{2.94}$$

$$E_2 = F\left[|\Phi_2\rangle\right] + \int_{-\infty}^{\infty} d\mathbf{r} \ \left\{ \mathbf{j} \cdot \mathbf{A}_2 + n \left(v_2 - \tfrac{1}{2} A_2^2 \right) \right\} \tag{2.95}$$

where F is the usual universal part of the energy.

PS evaluated the excited energies of each state subject to the potentials of the other as

$$E_1' = F\left[|\Phi_1\rangle\right] + \int_{-\infty}^{\infty} d\mathbf{r} \ \left\{ \mathbf{j} \cdot \mathbf{A}_2 + n \left(v_2 - \tfrac{1}{2} A_2^2 \right) \right\} \tag{2.96}$$

$$E_2' = F\left[|\Phi_2\rangle\right] + \int_{-\infty}^{\infty} d\mathbf{r} \ \left\{ \mathbf{j} \cdot \mathbf{A}_1 + n \left(v_1 - \tfrac{1}{2} A_1^2 \right) \right\}, \tag{2.97}$$

however, this is not the case, since when subject to $(v_2, \mathbf{A}_2)$, the state $|\Phi_1\rangle$ has physical current density

$$\mathbf{j}_1'(\mathbf{r}) = \left\langle \Phi_1 \left| \hat{\mathbf{j}}_{\mathrm{P}} \right| \Phi_1 \right\rangle + n(\mathbf{r}) \mathbf{A}_2(\mathbf{r}) = \mathbf{j}(r) + n(\mathbf{r}) \left[\mathbf{A}_2(\mathbf{r}) - \mathbf{A}_1(\mathbf{r}) \right], \tag{2.98}$$

and similarly for the current of $|\Phi_2\rangle$ subject to $(v_1, \mathbf{A}_1)$.

When the appearance of the vector potential in the energy functional is properly account for, the PS proof under the assumption of two sets of potentials having the same ground-state densities yields the inequality

$$E_1 + E_2 < E_1 + E_2 + \int_{-\infty}^{\infty} d\mathbf{r} \, n(\mathbf{r}) \left[\mathbf{A}_2(\mathbf{r}) - \mathbf{A}_1(\mathbf{r})\right]^2. \tag{2.99}$$

Since the last term must necessarily be positive everywhere for two different vector potentials, the inequality is perfectly sensible, and the hypothesis that two sets of external potentials *can* yield the same physical densities has not been disproven.

Indeed, one should not expect the ground-state physical densities of a system to uniquely determine the external potentials that yielded them at all. While PS state that the proof is intended to hold within a chosen gauge, there is nothing in the mathematics of their HK-like proof that distinguishes between sets of potentials that differ by a gauge transform (having $\nabla \times \Delta\mathbf{A} = \mathbf{0}$) and those that differ due to differing magnetic fields (having $\nabla \cdot \Delta\mathbf{A} = 0$).

However, it was precisely for the removal of the tricky integral of $n(\mathbf{r})\Delta A^2(\mathbf{r})$ term in Eq. 2.99 that Diener [131] formulated his version of physical CDFT, although almost 20 years earlier.

Writing the expectation value of the energy of an arbitrary wavefunction subject to fields $(v, \mathbf{A})$ as

$$\left\langle \Psi \left| \hat{H}_{v,A} \right| \Psi \right\rangle = \left\langle \Psi \left| \hat{T} + \hat{U} - \sum_k \tfrac{1}{2} a^2(\mathbf{r}_k) \right| \Psi \right\rangle$$
$$+ \int_{-\infty}^{\infty} d\mathbf{r} \, \{\mathbf{j}(\mathbf{r}) \cdot \mathbf{A}(\mathbf{r}) + n(\mathbf{r})v(\mathbf{r})\} + \tfrac{1}{2} \int_{-\infty}^{\infty} d\mathbf{r} \, n(\mathbf{r}) \left[\mathbf{A}(\mathbf{r}) - \mathbf{a}(\mathbf{r})\right]^2 \tag{2.100}$$

one can see that, when

$$\mathbf{a} = \frac{\mathbf{j} - \left\langle \Psi \left| \hat{\mathbf{j}}_{\mathrm{p}} \right| \Psi \right\rangle}{n} \tag{2.101}$$

the right-hand side of Eq. 2.100 is identical to Eq. 2.82.

Given a set of external potentials, this allows one, in principle, to set up a variational procedure by which one can vary trial charge and physical current densities $(n', \mathbf{j}')$ by ensuring that a pair of trial densities $(n', \mathbf{j}'_{\mathrm{p}})$ has, by definition, the correct trial physical current density. When the trial density corresponds to the minimum of the energy –

the ground state – then it follows that $\mathbf{a} = \mathbf{A}$.

Since $\mathbf{a}$ is entirely defined by the trial wavefunction $|\Psi\rangle$ and the trial current density $\mathbf{j}'$, it does not depend at all on the external potentials of the system, rather it is an inference about the external potentials of the system that has $|\Psi\rangle$ as its ground state and $(n', \mathbf{j}')$ as its corresponding ground-state physical densities.

Diener thus defines a universal functional, independent of the external fields, as

$$F\left[n, \mathbf{j}\right] = \inf_{\Psi \to n, j} \left\langle \Psi \left| \hat{H}_a \right| \Psi \right\rangle, \tag{2.102}$$

where

$$\hat{H}_a = \hat{T} + \hat{U} - \tfrac{1}{2} \sum_{k=1}^{N} a^2(\mathbf{r}_k), \tag{2.103}$$

and an energy functional

$$E_{v,A}\left[n, \mathbf{j}\right] = F\left[n, \mathbf{j}\right] + \int_{-\infty}^{\infty} d\mathbf{r} \ \{\mathbf{j}(\mathbf{r}) \cdot \mathbf{A}(\mathbf{r}) + n(\mathbf{r})v(\mathbf{r})\} \tag{2.104}$$

which, Diener finds, leads to the inequality

$$E_{v,A}\left[n, \mathbf{j}\right] \leq \left\langle \Psi \left| \hat{H}_{v,A} \right| \Psi \right\rangle - \tfrac{1}{2} \int_{-\infty}^{\infty} d\mathbf{r} \ n(\mathbf{r}) \left[\mathbf{A}(\mathbf{r}) - \mathbf{a}(\mathbf{r})\right]^2. \tag{2.105}$$

It should be noted here that the energy functional Eq. 2.105 is not minimised by the ground-state densities (in fact it is generally unbounded) but rather yields the stationary point

$$\left.\frac{\delta E_{v,A}\left[n, \mathbf{j}\right]}{\delta n, \mathbf{j}}\right|_{n_0, \mathbf{j}_0} = 0. \tag{2.106}$$

Diener then proposed a HK-like theorem of bijectivity between the physical densities $(n, \mathbf{j})$ and the external potentials $(v, \mathbf{A})$. He first considered the opposite scenario: that two systems with the same ground-state charge density and physical current density could be yielded by different sets of external potentials $(v_1, \mathbf{A}_1) \neq (v_2, \mathbf{A}_2)$. One can note here that such a scenario, should it exist, demands that the two systems be described by two different ground-state wavefunctions $|\Psi_1\rangle$ and $|\Psi_2\rangle$: were they the same, the resulting charge and paramagnetic current densities of the two systems must also be the same, thus for the physical currents to also be the same, it follows that $\mathbf{A}_2 = \mathbf{A}$ and thus this reduces the problem to the original Hohenberg-Kohn proof.

Starting from Eq. 2.105, we find that

$$E_1 < \left\langle \Psi_2 \left| \hat{H}_1 \right| \Psi_2 \right\rangle - \int_{-\infty}^{\infty} d\mathbf{r} \; n \left[\mathbf{A}_1 - \mathbf{a} \right]^2$$

$$= E_2 + \int_{-\infty}^{\infty} d\mathbf{r} \; \left\{ \mathbf{j} \cdot \left[\mathbf{A}_1 - \mathbf{A}_2 \right] + n \left[v_1 - v_2 + \tfrac{1}{2} \left(A_1^2 - A_2^2 \right) \right] \right\} \qquad (2.107)$$

$$E_2 < \left\langle \Psi_1 \left| \hat{H}_2 \right| \Psi_1 \right\rangle - \int_{-\infty}^{\infty} d\mathbf{r} \; n \left[\mathbf{A}_2 - \mathbf{a} \right]^2$$

$$= E_1 + \int_{-\infty}^{\infty} d\mathbf{r} \; \left\{ \mathbf{j} \cdot \left[\mathbf{A}_2 - \mathbf{A}_1 \right] + n \left[v_2 - v_1 + \tfrac{1}{2} \left(A_2^2 - A_1^2 \right) \right] \right\}, \qquad (2.108)$$

where the universal functionals in the integral $\left\langle \Psi \left| \hat{H}_a - \hat{H}_b \right| \Psi \right\rangle$ have cancelled, as have the integrals over $n \left[\mathbf{A} - \mathbf{a} \right]^2$. Summing the two inequalities yields the *reductio ad absurdum* of the HK proof:

$$E_1 + E_2 < E_2 + E_1 \qquad (2.109)$$

thus disproving the possibility of two systems with the same charge and physical current densities being the ground states of two different sets of external potentials.

It is surprising that both the Diener and the Pan and Sahni formulations of CDFT both take as their basic variables the charge and physical current densities, both employ a Hohenberg-Kohn-like approach to proving the bijectivity of those variables with the external potentials of which they are the ground-state properties, and yet both yield very different results, especially considering that the expressions considered in the Diener case are simple algebraic rearrangements of those employed in the PS case. While the energy functional of Diener is written differently, all occurrences in some Hamiltonian $\hat{H}_{v,A}$ of a vector potential different to $\mathbf{A}$ cancel when properly accounted for. Once again, this is a matter of accounting properly for the vector potential, and this issue will be investigated again in the next chapter.

It remains to be seen if there exists another method of proving the uniqueness theorem for a physical CDFT, beyond a Hohenberg-Kohn-like proof. Restricting ourselves to the question: 'What *can* a HK proof show?', it is apparent that, if any CDFT proof exists:

1. it must have key current quantities that go beyond the paramagnetic current density;

2. it must have intermediate quantities that go beyond the ground-state wavefunction;

3. it cannot deal with the physical current directly as a fundamental quantity.

In the next chapter and the Appendix, uniqueness proofs for alternative formulations of CDFT will be detailed that meet the above three criteria.

2.3.3 The exchange-correlation vector potential

The new quantity in CDFT is the exchange-correlation vector potential which, from considerations of gauge-invariance and the steady-state condition, Vignale and Rasolt provided much insight into. Under a gauge transform:

$$\mathbf{A}(\mathbf{r}) \rightarrow \mathbf{A}(\mathbf{r}) - \nabla\Lambda(\mathbf{r}), \qquad (2.110)$$

the paramagnetic current becomes:

$$\mathbf{j}'_\mathrm{p}(\mathbf{r}) \rightarrow \mathbf{j}'_\mathrm{p}(\mathbf{r}) + \nabla\Lambda(\mathbf{r})n(\mathbf{r}) \qquad (2.111)$$

and the wavefunction:

$$|\Psi\rangle\left[n', \mathbf{j}'_\mathrm{p} + n'\nabla\Lambda\right] = \exp\left(i\sum_{k=1}^{N} \Lambda(\mathbf{r}_k)\right)|\Psi\rangle\left[n', \mathbf{j}'_\mathrm{p}\right]. \qquad (2.112)$$

The universal functional is then

$$\begin{aligned}
F\left[n', \mathbf{j}'_\mathrm{p} + n'\nabla\Lambda\right] &= \left\langle\Psi\left|\hat{T} + \hat{U} + \tfrac{1}{2}\left[\hat{\mathbf{p}}, \nabla\Lambda\right] + \tfrac{1}{2}\nabla\Lambda^2\right|\Psi\right\rangle \\
&= F\left[n', \mathbf{j}'_\mathrm{p}\right] + \int_{-\infty}^{\infty} d\mathbf{r} \left\{\mathbf{j}'_\mathrm{p}\cdot\nabla\Lambda + \frac{1}{2}n'\left|\nabla\Lambda\right|^2\right\}
\end{aligned} \qquad (2.113)$$

and likewise a single-particle kinetic energy functional:

$$T_\mathrm{s}\left[n', \mathbf{j}'_\mathrm{p} + n'\nabla\Lambda\right] = T_\mathrm{s}\left[n', \mathbf{j}'_\mathrm{p}\right] + \int_{-\infty}^{\infty} d\mathbf{r} \left\{\mathbf{j}'_\mathrm{p}\cdot\nabla\Lambda + \frac{1}{2}n'\left|\nabla\Lambda\right|^2\right\} \qquad (2.114)$$

and thus the XC energy functional must remain unchanged after gauge transform:

$$E_\mathrm{xc}\left[n', \mathbf{j}'_\mathrm{p} + n'\nabla\Lambda\right] = E_\mathrm{xc}\left[n', \mathbf{j}'_\mathrm{p}\right]. \qquad (2.115)$$

This means that E_xc cannot depend on the longitudinal part of the vector potential: only any transverse parts.

Furthermore, in the real, interacting system, the continuity equation demands that,

for a steady-state system,

$$\nabla \cdot [\mathbf{j}_{\mathrm{p}}(\mathbf{r}) + n(\mathbf{r})\mathbf{A}_{\mathrm{ext}}(\mathbf{r})] = 0 \tag{2.116}$$

where $n(\mathbf{r})\mathbf{A}_{\mathrm{ext}}(\mathbf{r})$ is the diamagnetic current. In the KS scheme, this becomes:

$$\nabla \cdot [\mathbf{j}_{\mathrm{p}}(\mathbf{r}) + n(\mathbf{r})\mathbf{A}_{\mathrm{ext}}(\mathbf{r})] + \nabla \cdot [n(\mathbf{r})\mathbf{A}_{\mathrm{xc}}(\mathbf{r})] = 0. \tag{2.117}$$

From the previous equation, we know the left-hand term must be zero, and thus:

$$\nabla \cdot [n(\mathbf{r})\mathbf{A}_{\mathrm{xc}}(\mathbf{r})] = 0. \tag{2.118}$$

Thus E_{xc} can only depend on the charge density and the quantity:

$$\nabla \times \frac{\mathbf{j}_{\mathrm{p}}'(\mathbf{r})}{n(\mathbf{r})}. \tag{2.119}$$

In application to a homogeneous electron gas carrying a small steady-state current, Vignale and Rasolt calculated expressions for the XC potentials based on a second-order expansion of the universal functional about the paramagnetic current density $\mathbf{j}_{\mathrm{p}}'(\mathbf{r})$ and linear response theory for small currents. The approximations they derive [124; 132] are

$$\mathbf{A}_{\mathrm{xc}}(\mathbf{r}) = \frac{b}{n(\mathbf{r})}\nabla \times \left[\nabla \times \frac{\mathbf{j}_{\mathrm{p}}(\mathbf{r})}{n(\mathbf{r})} \right] \tag{2.120}$$

$$v_{\mathrm{xc}}(\mathbf{r}) = v_{\mathrm{xc}}^{\mathrm{LDA}}(\mathbf{r}) - \mathbf{A}_{\mathrm{xc}}(\mathbf{r}) \cdot \frac{\mathbf{j}_{\mathrm{p}}(\mathbf{r})}{n(\mathbf{r})}, \tag{2.121}$$

where b is a constant of proportionality that depends on the magnetic susceptibility of the gas, and $v_{\mathrm{xc}}^{\mathrm{LDA}}(\mathbf{r})$ is the usual XC scalar potential of DFT.

Because of the success of *ab initio* KS DFT in predicting the ground-state properties on non-magnetic systems, it has become common to employ the Kohn-Sham scheme beyond the minimisation principle by modelling physical, interacting systems with KS noninteracting ones from first principles. The two approaches, while equivalent in DFT, are very different in CDFT. The KS representation in paramagnetic CDFT is constructed to yield the same charge and paramagnetic current density as a real interacting system. The presence of the exchange-correlation vector potential dictates that the KS diamagnetic current must differ from its interacting counterpart:

$$\mathbf{j}_{\mathrm{KS,d}}(\mathbf{r}) = [\mathbf{A}_{\mathrm{ext}}(\mathbf{r}) + \mathbf{A}_{\mathrm{xc}}(\mathbf{r})]\, n(\mathbf{r}) \neq \mathbf{j}_{\mathrm{d}}(\mathbf{r}). \tag{2.122}$$

Since the KS and interacting paramagnetic currents are the same and their diamagnetic currents differ, it follows that the KS physical current is not that of the interacting system:

$$\mathbf{j}_{KS}(\mathbf{r}) = \mathbf{j}_p(\mathbf{r}) + \mathbf{j}_{KS,d}(\mathbf{r}) \neq \mathbf{j}(\mathbf{r}). \tag{2.123}$$

The KS system employed in the minimisation procedure is physical different to the interacting system it stands in for in the calculation of the universal functional. This is not a problem with the minimisation procedure itself so long as the XC energy is chosen to yield the correct universal functional, but it does mean that the KS system cannot be used to model the interacting system accurately. Alternatively, one could choose a KS system which has the same physical current density as the interacting system and a different XC functional, since the varying physical current is well defined by the charge and paramagnetic current being varied and the fixed vector potential.

However, there are more fundamental issues with this formulation of CDFT that render the construction of a unique KS system for a given combination of charge and paramagnetic current densities not generally possible, as we will see in the next subsection.

This thesis will focus on the calculation of exact KS potentials for excited and degenerate nanowires without an applied electric potential and for time-independent electrochemical potentials. This simplifies the many of the complications described in Sec. 2.2.4. Rather than studying finite nanowires attached to infinite ideal leads, this research will instead treat the nanowire itself as being infinitely long, and coupled to reservoirs only at infinity. The simplifications to the calculations this yields are twofold: first, one may replace the transparent boundary conditions typical of quantum transport theory with periodic boundary conditions; second, one may remove terms coupling the wavefunction in the central region to the leads such that, for instance, the quasiparticles of the nanowire may be described by the isolated quasiparticle equation (Eq. 1.67).

Chapter 3

Unique and exact KS fields in current-carrying systems

Steady-state currents pose a particular problem for density functional theory. Whereas in time-dependent DFT the longitudinal part of the time-dependent current density is accessible from the time-dependent charge density via the continuity equation, and there are many systems where this is sufficient, steady-state currents are not defined by the charge density beyond the fact that they must be divergence-free.

However, even before one can consider the external potentials that are necessary to yield particular charge and current densities in the steady-state regime, one needs to establish a uniqueness relation between the potentials and the densities. Secs. 2.3.1 and 2.3.2 in the previous chapter reviewed three existing formulations of ground-state current-density functional theory, one based on the paramagnetic current density, the other two based on the physical current density.

Both approaches appear to have their strengths and weaknesses. A CDFT based on the paramagnetic current has a uniquely-determined ground-state wavefunction, but it has been demonstrated that different sets of potentials can yield that wavefunction, with the difference accounted for in the diamagnetic part of the physical current density. A CDFT based on the physical current avoids this problem since the diamagnetic part is included; however, the chosen basic densities do not uniquely determine the ground-state wavefunction and, worse, the ground-state wavefunction does not uniquely determine the densities.

Tellgren *et al* concluded that there is no functional that both is universal and admits a practical minimisation procedure (as distinct from a proof of a variational theorem in principle). This research has concluded that such a theory does exist, so long as one

is suitably flexible regarding the definition of the basic and intermediate variables of a Hohenberg-Kohn-like proof.

Peculiarly, one formulation of CDFT based on the physical current appears to accept both a uniqueness proof and a minimisation scheme, and does so by algebraic manipulation of the Hamiltonian. The minimisation scheme, however, is unbounded. Furthermore, the breakdown of equivalence to the Pan and Sahni approach has yet to be examined. This will be the subject of the next section.

Sec. 3.2 will make a case for new choices of basic variables, and Sec. 3.3 will demonstrate a proof of a uniqueness theorem for a particular choice of basic densities. Sec. 3.4 provides a proof of a variational procedure, and Sec. 3.5 will detail and prove a practical energy-minimisation scheme. Once we have determined which basic densities a set of potentials is a unique functional *of*, we will examine the question of how one might calculate these potentials exactly for a given charge (and current) density. 3.6 will provide a means to calculate those potentials in the steady-state regime where the charge and current density are known, and 3.7 will extend this procedure to the nonequilibrium regime.

For interest, Secs. A.2.1 and A.2.2 will extend the theory to magnetised and degenerate ground-state systems respectively. The remainder of the Appendix is dedicated to an alternative CDFT formulation that has equal numbers of basic potentials and basic densities.

3.1   Does the physical current determine the system?

As a test of their uniqueness theorem, Pan and Sahni [128] considered the possibility of two different sets of external potentials $(v_1, \mathbf{A}_1)$ and $(v_2, \mathbf{A}_2)$ having the same ground-state densities $(n, \mathbf{j})$, where the physical current for a system with zero net spin density is

$$\mathbf{j}(\mathbf{r}) = \left\langle \Psi \left| \hat{\mathbf{j}}_{\mathrm{p}} \right| \Psi \right\rangle + \mathbf{A}(\mathbf{r})n(\mathbf{r}). \tag{3.1}$$

When one accounts properly for the appearance of the vector potential in the energy functional, Tellgen *et al* [130] found that one arrives at the perfectly sensible inequality

$$E_1 + E_2 < E_2 + E_1 + \int_{-\infty}^{\infty} d\mathbf{r}\, n(\mathbf{r}) \left[\mathbf{A}_2 - \mathbf{A}_1 \right]^2. \tag{3.2}$$

In order to avoid the appearance of the difficult final term, Diener [131] had already derived a new inequality that is stated as being more strict than the Rayleigh-Ritz

principle:

$$E_0[v, \mathbf{A}] = F_a[|\Psi_0\rangle, \mathbf{j}] + \int_{-\infty}^{\infty} d\mathbf{r}\, \mathbf{j} \cdot \mathbf{A} \leq \left\langle \Psi \left| \hat{H}_{v,A} \right| \Psi \right\rangle - \tfrac{1}{2} \int_{-\infty}^{\infty} d\mathbf{r}\, n\, (\mathbf{A} - \mathbf{a})^2, \quad (3.3)$$

where E_0 is the ground-state energy of the system having scalar potential $v(\mathbf{r})$, vector potential $\mathbf{A}(\mathbf{r})$ (indexed here by subscript A), charge density $n(\mathbf{r})$, current density $\mathbf{j}(\mathbf{r})$ and wavefunction $|\Psi_0\rangle$, and $|\Psi\rangle$ is some trial wavefunction and $\mathbf{a}(\mathbf{r})$ (indexed here by subscript a) is a vector quantity defined by the trial wavefunction and the ground-state current density to yield the current physical current under any ambient vector potential

$$\mathbf{a}[|\Psi\rangle, \mathbf{j}](\mathbf{r}) = \frac{1}{n(\mathbf{r})} \left[\mathbf{j}(\mathbf{r}) - \left\langle \Psi \left| \hat{\mathbf{j}}_{\mathrm{p}}(\mathbf{r}) \right| \Psi \right\rangle \right], \quad (3.4)$$

where $\hat{\mathbf{j}}_{\mathrm{p}}(\mathbf{r})$ is the usual paramagnetic current density operator.

Nominally, in accordance with the definition Eq. 3.4 and the fact that the final term on the right-hand side of inequality 3.3 arises due to being subtracted from both sides, $\mathbf{a}(\mathbf{r})$ should be defined in terms of the ground-state wavefunction and current, yielding $\mathbf{a} = \mathbf{A}$, and thus the final term vanishes.

On the other hand, allowing $\mathbf{a}(\mathbf{r})$ to differ from $\mathbf{A}$, i.e. to be defined in terms of the *trial* wavefunction and current, ensures that the final term is not generally zero (it is zero when the trial wavefunction is the true ground state) and that, since the term is positive semidefinite, the inequality always holds. However, it is clear that, in this case, the quantity on the left-hand side of the inequality is no longer the ground-state energy, but is a lesser quantity which henceforth we shall denote

$$E_0' = E_0 - \tfrac{1}{2} \int_{-\infty}^{\infty} d\mathbf{r}\, n(\mathbf{r}) \left[\mathbf{A}(\mathbf{r}) - \mathbf{a}(\mathbf{r}) \right]^2. \quad (3.5)$$

As such, this is not a more strict inequality than the Rayleigh-Ritz inequality: it is simply the Rayleigh-Ritz theorem with a positive semidefinite quantity subtracted from both sides.

Diener then employs the usual Hohenberg-Kohn approach to proving that the assumption of nonunique potentials leads to a contradiction. Assuming two different ground-state wavefunctions $|\Psi_1\rangle$ and $|\Psi_2\rangle$ for the two sets of potentials $(v_1, \mathbf{A}_1)$ and

$(v_2, \mathbf{A}_2)$, one has a pair of inequalities for each:

$$E_1' < \left\langle \Psi_2 \left| \hat{H}_2 \right| \Psi_2 \right\rangle + \left\langle \Psi_2 \left| \hat{H}_1 - \hat{H}_2 \right| \Psi_2 \right\rangle - \tfrac{1}{2} \int_{-\infty}^{\infty} d\mathbf{r} \, n \left[\mathbf{A}_1 - \mathbf{A}_2 \right]^2 \qquad (3.6)$$

$$E_2' < \left\langle \Psi_1 \left| \hat{H}_1 \right| \Psi_1 \right\rangle + \left\langle \Psi_1 \left| \hat{H}_2 - \hat{H}_1 \right| \Psi_1 \right\rangle - \tfrac{1}{2} \int_{-\infty}^{\infty} d\mathbf{r} \, n \left[\mathbf{A}_2 - \mathbf{A}_1 \right]^2 \qquad (3.7)$$

where $\hat{H}_i$ is the Hamiltonian defined by external potentials $(v_i, \mathbf{A}_i)$.

The first terms on the right-hand sides of inequalities 3.6 and 3.7 are the true ground-state energies E_2 and E_1 respectively, independent of the appearance of any vector quantities $\mathbf{a}(\mathbf{r})$ within the definition of the Hamiltonians. To arrive at Diener's *reductio ad absurdum*, the universal functionals in the second terms must cancel, i.e. the same vector quantity $\mathbf{a}_{1,2} = \mathbf{A}_{2,1}$ must appear in each. This yields

$$E_1' < E_2 + \int_{-\infty}^{\infty} d\mathbf{r} \, \left\{ \mathbf{j} \cdot [\mathbf{A}_1 - \mathbf{A}_2] + n \left(v_1 - v_2 + \tfrac{1}{2} [\mathbf{A}_1 - \mathbf{A}_2]^2 \right) - \tfrac{1}{2} n [\mathbf{A}_1 - \mathbf{A}_2]^2 \right\}$$
$$(3.8)$$

$$E_2' < E_1 + \int_{-\infty}^{\infty} d\mathbf{r} \, \left\{ \mathbf{j} \cdot [\mathbf{A}_2 - \mathbf{A}_1] + n \left(v_2 - v_1 + \tfrac{1}{2} [\mathbf{A}_2 - \mathbf{A}_1]^2 \right) - \tfrac{1}{2} n [\mathbf{A}_2 - \mathbf{A}_1]^2 \right\}.$$
$$(3.9)$$

As desired, the integrals over $n(\Delta \mathbf{A})^2$ cancel, and summing up over both inequalities yields

$$E_1' + E_2' < E_2 + E_1. \qquad (3.10)$$

Diener finds that there is a contradiction here because he identifies the primed energies with the unprimed ones. This is, however, incorrect: if the primed and unprimed quantities were the same, this would yield the equality

$$E' = \left\langle \Psi \left| \hat{H} \right| \Psi \right\rangle - \int_{-\infty}^{\infty} d\mathbf{r} \, n \left[\mathbf{A} - \mathbf{a} \right]^2 = \left\langle \Psi \left| \hat{H} \right| \Psi \right\rangle = E \qquad (3.11)$$

which holds only for $\mathbf{a}(\mathbf{r}) = \mathbf{A}(\mathbf{r})$, leaving nothing to cancel with the tricky integrals over $n(\mathbf{r}) (\Delta \mathbf{A})^2$. In fact substituting Eq. 3.5 into inequality 3.10 yields

$$E_1 + E_2 - \int_{-\infty}^{\infty} d\mathbf{r} \, n(\mathbf{r}) \left[\mathbf{A}_2 - \mathbf{A}_1 \right]^2 < E_1 + E_2, \qquad (3.12)$$

which is exactly equivalent to the inequality 3.2 which Tellgren *et al* arrived at in the Pan-Sahni approach.

In summary, while it remains unproven that two different sets of external potentials

may yield the same ground-state charge and physical current densities, the converse also remains unproven. The choice of the physical current as a basic density, while logical, cannot be justified by a Hohenberg-Kohn proof. This is an expected problem so long as the HK proof does not distinguish between vector potentials that differ by a transverse component corresponding to a different magnetic field and those that differ by a longitudinal component corresponding merely to a change in gauge, since there are of course an infinite number of pairs of external potentials which yield the same ground-state charge and physical current densities in the latter case.

In the following sections and the Appendix, we shall see which unique mappings the Hohenberg-Kohn approach *can* determine for CDFT. Clearly, in order to resolve the nonuniqueness in Vignale-Rasolt theory, such a formulation must go beyond the paramagnetic current density, and yet to resolve the nonuniqueness of Pan-Sahni and Diener theories, it cannot rely on the physical current density, i.e. the choice of basic variables must be *gauge-variant* in order to uniquely determine the gauge-variant potentials.

3.2 The choice of basic variables in CDFT

A vital decision in any density functional theory therefore is the choice of basic variables. Once the basic variables are chosen, we may proceed with a Hohenberg-Kohn-like theorem based on those variables. The purpose of a HK theorem like Eq. 3.13 is to uniquely map density quantities to external potentials and vice-versa: $\mathscr{V} \leftrightarrow \mathscr{N}$. In the original HK proof of this theorem for DFT, and in the two varieties of CDFT, this is achieved via an intermediate quantity $\mathscr{G}$ which is always chosen to be the ground-state wavefunction.

$$
\begin{array}{ccc}
\mathscr{V} & \xleftarrow{\quad\text{HK}\quad}\dashrightarrow & \mathscr{N} \\
A^{-1}\diagdown\;A & & B^{-1}\diagup\;B \\
& \mathscr{G} &
\end{array}
\tag{3.13}
$$

If one can show, as Hohenberg and Kohn did, that $\mathscr{V} \leftrightarrow \mathscr{G}$ and that $\mathscr{N} \leftrightarrow \mathscr{G}$, then one has fully proven that $\mathscr{V} \leftrightarrow \mathscr{N}$. To this extent, the inclusion of $\mathscr{G}$ in the maps is purely utilitarian, and $\mathscr{G}$ may, in principle, be anything at all so long as it yields a unique map.

Let us then consider the content of $\mathscr{G}$ first. The uniqueness theorem of paramagnetic CDFT fails when two different sets of potentials ($v_2 \neq v_1, \mathbf{A}_2 \neq \mathbf{A}_1$) corresponding to

two different sets of electromagnetic fields $(\mathbf{E}_2 \neq \mathbf{E}_1, \mathbf{B}_2 \neq \mathbf{B}_1)$ share the same ground-state wavefunction:

$$(v_1(\mathbf{r}), \mathbf{A}_1(\mathbf{r})) \rightarrow |\Psi_0\rangle \leftarrow (v_2(\mathbf{r}), \mathbf{A}_2(\mathbf{r})). \qquad (3.14)$$

This map is not invertible, i.e. the ground-state wavefunction alone does not uniquely define the external potentials. The question then is: what further information must $\mathscr{G}$ contain in order to make the map invertible without destroying it?

If we define $\mathscr{G}$ as

$$\mathscr{G} = \{(|\Psi_0\rangle, \mathbf{A})\}, \qquad (3.15)$$

it is nothing more than a truism to state that $(v, \mathbf{A})$ uniquely defines the $\mathbf{A}$, and that it also uniquely defines $|\Psi_0\rangle$ is necessary from the condition of nondegeneracy, thus map A is still unique. Likewise, it is a truism to state that $(|\Psi_0\rangle, \mathbf{A})$ uniquely defines $\mathbf{A}$. This reduces map A^{-1} to the standard HK proof of ground-state DFT, the proof of which will be demonstrated in section 3.3.

We can use a similar procedure to suggest a choice of basic densities. One immediate observation is that $\mathscr{V}$ and $\mathscr{G}$ are gauge-variant sets, and so $\mathscr{N}$ should also be a gauge-variant set if a unique relationship is to be established. Since $|\Psi_0\rangle$ alone determines the charge and paramagnetic current density, these two density quantities cannot fully determine the vector potential. To achieve this, the density set needs to include more information about the physical current density. Given that we cannot replace $\mathbf{j}_p$ with $\mathbf{j}$, the physical current, the explicit diamagnetic current density is required.

This yields two possible choices of basic densities: $\mathscr{N} = \{n, \mathbf{j}_d\}$, and $\mathscr{N} = \{n, \mathbf{j}_p, \mathbf{j}_d\}$. The first of these does uniquely determine the external potentials, since $n(\mathbf{r})$ and $\mathbf{j}_d(\mathbf{r})$ together uniquely determine the external vector potential, after which the uniqueness problem reduces to the first theorem of Hohenberg and Kohn. Further, it admits a minimisation procedure, once again that of the second HK theorem since $\mathbf{j}_d(\mathbf{r})$ may not be varied independently of $n(\mathbf{r})$ under fixed external vector potential $\mathbf{A}(\mathbf{r})$.

Another advantage of the choice of $(n, \mathbf{j}_d)$ as basic densities is that the mapping

$$(v, \mathbf{A}) \leftrightarrow (n, \mathbf{j}_d) \qquad (3.16)$$

is balanced: neither set overdefines or underdefines the other.

However, any practical minimisation scheme employing auxiliary Kohn-Sham systems of noninteracting electrons relies on a mapping of some choice of ground-state properties – typically the basic densities – between the interacting and Kohn-Sham

systems. Since we should not expect the noninteracting vector potential to be generally identical to the interacting external vector potential, if follows that the KS diamagnetic current will differ from the interacting system under study.

For this reason in this chapter we shall focus on the second choice of basic densities: $(n, \mathbf{j}_\text{p}, \mathbf{j}_\text{d})$ with the understanding that trial densities are not chosen independently and are restricted to those that are interacting-V-representable (V-representability here implying the ground state of some set of external potentials $(v, \mathbf{A})$). While this makes the uniqueness and variational theorems more cumbersome, it is more suited to practical minimisation and self-consistent calculations.

The proofs of uniqueness and variational theorems, along with some recommendations about how one would practically implement them, for the minimal set of basic densities $(n, \mathbf{j}_\text{d})$ are given in the Appendix. In this chapter, the uniqueness theorem for the larger set of densities is proven in Sec. 3.3, the corresponding variational theorem is proven in Sec. 3.4, and a practical minimisation and self-consistent Kohn-Sham scheme is described in Sec. 3.5.

3.3   A proof of uniqueness for CDFT

The theorem we wish to prove in this section is that all physical ground-state properties of interest are unique functionals of the set of V-representable, nondegenerate ground-state densities $(n, \mathbf{j}_\text{p}, \mathbf{j}_\text{d})$. In particular, we wish to prove that the external potentials $(v, \mathbf{A})$ (of which the densities are the ground-state densities) are uniquely determined, from which all other properties may, in principle, be derived.

This map is broken down into maps to an intermediate quantity consisting of the ground-state wavefunction $|\Psi\rangle$ and the vector potential $\mathbf{A}(\mathbf{r})$. Proving these intermediate one-to-one relationships implies a one-to-one relationship between the densities and the potentials. We aim to prove, therefore, that

$$
\begin{array}{ccc}
(v, \mathbf{A}) & \xleftarrow{\quad\text{HK}\quad} & (n, \mathbf{j}_\text{p}, \mathbf{j}_\text{d}) \\
{}_{A^{-1}}\diagdown{}^{A} & & {}^{B^{-1}}\diagup{}_{B} \\
& (|\Psi_0\rangle, \mathbf{A}) &
\end{array}
\tag{3.17}
$$

Map $A : (v, \mathbf{A}) \to (|\Psi_0\rangle, \mathbf{A})$ is immediately evident from the solution of the Schrödinger equation for nondegenerate systems, while map $B : (|\Psi_0\rangle, \mathbf{A}) \to (n, \mathbf{j}_\text{p}, \mathbf{j}_\text{d})$ is immedi-

ately evident from the definitions of the charge and current densities:

$$n(\mathbf{r}) = \langle \Psi \left| \hat{n}(\mathbf{r}) \right| \Psi \rangle \tag{3.18}$$

$$\mathbf{j}_{\mathrm{p}}(\mathbf{r}) = \left\langle \Psi \left| \hat{\mathbf{j}}_{\mathrm{p}}(\mathbf{r}) \right| \Psi \right\rangle \tag{3.19}$$

$$\mathbf{j}_{\mathrm{d}}(\mathbf{r}) = \mathbf{A}(\mathbf{r}) \langle \Psi \left| \hat{n}(\mathbf{r}) \right| \Psi \rangle . \tag{3.20}$$

This leaves the inverse maps A^{-1} and B^{-1} to be proven.

The vector potential in both $\mathscr{V}$ and $\mathscr{G}$ is uniquely determined by the charge and diamagnetic current densities as

$$\mathbf{A}(\mathbf{r}) = \mathbf{A}\left[n, \mathbf{j}_{\mathrm{d}}\right](\mathbf{r}) = \frac{\mathbf{j}_{\mathrm{d}}(\mathbf{r})}{n(\mathbf{r})}, \tag{3.21}$$

thus if mapping B^{-1} is nonunique, there must exist two ground-state wavefunctions defined by the same vector potential but different scalar potentials that yield the same charge density. The original HK proof demonstrates otherwise. Let there be two sets of potentials $(v_1, \mathbf{A}_1)$ and $(v_2, \mathbf{A}_2)$ such that:

$$v_2(\mathbf{r}) \neq v_1(\mathbf{r}) + \mathrm{constant} \tag{3.22}$$

$$\mathbf{A}_2(\mathbf{r}) = \mathbf{A}_1(\mathbf{r}) = \mathbf{A}(\mathbf{r}) \tag{3.23}$$

whose corresponding Hamiltonians $\hat{H}_1$ and $\hat{H}_2$ yield ground-state wavefunctions $|\Psi_1\rangle$ and $|\Psi_2\rangle$ with corresponding ground-state energies:

$$E_1 = F_1\left[\Psi_1\right] + \int_{-\infty}^{\infty} d\mathbf{r}\ \mathbf{j}_{\mathrm{p}}(\mathbf{r}) \cdot \mathbf{A}(\mathbf{r}) + \int_{-\infty}^{\infty} d\mathbf{r}\ n(\mathbf{r}) \left(v_1(\mathbf{r}) + \tfrac{1}{2}A^2(\mathbf{r})\right) \tag{3.24}$$

$$E_2 = F_2\left[\Psi_2\right] + \int_{-\infty}^{\infty} d\mathbf{r}\ \mathbf{j}_{\mathrm{p}}(\mathbf{r}) \cdot \mathbf{A}(\mathbf{r}) + \int_{-\infty}^{\infty} d\mathbf{r}\ n(\mathbf{r}) \left(v_2(\mathbf{r}) + \tfrac{1}{2}A^2(\mathbf{r})\right) . \tag{3.25}$$

From the Ritz principle we know that:

$$E_1' = \left\langle \Psi_1 \left| \hat{H}_2 \right| \Psi_1 \right\rangle = \left\langle \Psi_1 \left| \hat{H}_1 \right| \Psi_1 \right\rangle + \left\langle \Psi_1 \left| \hat{H}_2 - \hat{H}_1 \right| \Psi_1 \right\rangle \tag{3.26}$$

$$= E_1 + \int_{-\infty}^{\infty} d\mathbf{r}\ n(\mathbf{r}) \left[v_2(\mathbf{r}) - v_1(\mathbf{r})\right] > E_2. \tag{3.27}$$

Likewise:

$$E_2 + \int_{-\infty}^{\infty} d\mathbf{r}\ n(\mathbf{r}) \left[v_1(\mathbf{r}) - v_2(\mathbf{r})\right] > E_1. \tag{3.28}$$

Summing the two inequalities together yields the contradiction of the HK proof:

$$E_1 + E_2 > E_2 + E_1, \tag{3.29}$$

and thus the uniqueness of the ground-state wavefunction for a given set of densities $(n, \mathbf{j}_\mathrm{p}, \mathbf{j}_\mathrm{d})$ and the invertibility of map B has been proven *reductio ad absurdum*.

The remaining part of the proof, that of map A^{-1}, concerns two different sets of potentials $(v_1, \mathbf{A}_1)$ and $(v_2, \mathbf{A}_2 = \mathbf{A}_1)$ as per equations 3.22 that share the same ground-state wavefunction $|\Psi_0\rangle$ with different ground-state energies E_1 and E_2. Then:

$$\left[\hat{H}_1 - \hat{H}_2\right]|\Psi_0\rangle = [v_1(\mathbf{r}) - v_2(\mathbf{r})]|\Psi_0\rangle = (E_1 - E_2)|\Psi_0\rangle. \tag{3.30}$$

It follows that the two scalar potentials differ by only a constant.

Thus it has been shown that the external potentials uniquely determine and are uniquely determined by $(n, \mathbf{j}_\mathrm{p}, \mathbf{j}_\mathrm{d})$:

$$(v, \mathbf{A}) \leftrightarrow (n, \mathbf{j}_\mathrm{p}, \mathbf{j}_\mathrm{d}). \tag{3.31}$$

The number of scalar fields on each side of the map is uneven, reflecting the fact that the paramagnetic current was not required in the proof of uniqueness (rather we require it for minimisation), and that the densities together are constrained to be V-representable (see Appendix).

The issue of V-representability is less of a concern for uniqueness proofs than for variational procedure proofs where, ideally, one wishes to be free to vary the trial basic densities independently and still evaluate the resulting energy. We shall see in the next section that the diamagnetic current density, so vital to the proof of uniqueness, is maximally constrained in the variational procedure, and the balance between the number of basic potentials and basic densities is restored.

3.4 Proof of variational theorem

The theorem to be proven in this section is that, for a given set of external potentials $(v, \mathbf{A})$, we may construct an energy functional of the basic densities $(n, \mathbf{j}_\mathrm{p}, \mathbf{j}_\mathrm{d})$ (for brevity denoted by the seven-component quantity $\underline{\mathbf{N}}$) which has its minimum for the ground-state densities $(n_0, \mathbf{j}_{\mathrm{p},0}, \mathbf{j}_{\mathrm{d},0})$ (denoted $\underline{\mathbf{N}}_0$).

We first make use of the uniqueness theorem proven in the previous section to show that the ground-state energy is a unique functional of the ground-state densities. Since

the densities uniquely determine their corresponding external potentials, the potentials may be used to construct the Hamiltonian operator

$$\hat{H}[\underline{\mathbf{N}}] = \tfrac{1}{2} \left(\hat{\mathbf{p}} + \mathbf{A}[\underline{\mathbf{N}}_0] \right)^2 + v[\underline{\mathbf{N}}_0]. \tag{3.32}$$

The ground-state wavefunction $|\Psi_0\rangle$ was also proven to be a unique functional of the densities, thus the ground-state energy is

$$E_0\left[\underline{\mathbf{N}}_0\right] |\Psi_0\left[\underline{\mathbf{N}}_0\right]\rangle = \hat{H}[\underline{\mathbf{N}}_0] |\Psi_0\left[\underline{\mathbf{N}}_0\right]\rangle. \tag{3.33}$$

From the Rayleigh-Ritz theorem, it follows that any arbitrary wavefunction $|\Psi\rangle$ that is uniquely determined by a set of densities $\underline{\mathbf{N}}$ must, when subject to the same external potentials, have an energy greater than or equal to that yielded by the ground-state densities:

$$E_0\left[\underline{\mathbf{N}}_0\right] \leq \left\langle \Psi[\underline{\mathbf{N}}] \left| \hat{H}[\underline{\mathbf{N}}_0] \right| \Psi[\underline{\mathbf{N}}] \right\rangle = E_{v,A}\left[\underline{\mathbf{N}}\right]. \tag{3.34}$$

The right-hand side of Eq. 3.34 can be expanded as a functional of the external potentials and input densities as

$$E_{v,A}[\underline{\mathbf{N}}] = F[\underline{\mathbf{N}}] + \int_{-\infty}^{\infty} d\mathbf{r} \ \left\{ \mathbf{j}_{\mathrm{p}}(\mathbf{r}) \cdot \mathbf{A}(\mathbf{r}) + n(\mathbf{r}) \left[v(\mathbf{r}) + \tfrac{1}{2} A^2(\mathbf{r}) \right] \right\} \tag{3.35}$$

where

$$F\left[\underline{\mathbf{N}}\right] = \left\langle \Psi[\underline{\mathbf{N}}] \left| \hat{T} + \hat{U} \right| \Psi[\underline{\mathbf{N}}] \right\rangle \tag{3.36}$$

is a universal functional of $\underline{\mathbf{N}}$ that does not depend directly on the external potentials.

One can note already from the form of Eq. 3.35 that the energy functional under fixed $(v, \mathbf{A})$ does not depend on the diamagnetic current density as an independent variable. Thus we may write

$$E_0\left[n_0, \mathbf{j}_{\mathrm{p},0}\right] \leq E_{v,A}\left[n, \mathbf{j}_{\mathrm{p}}\right]. \tag{3.37}$$

This follows from the fact that, under a fixed vector potential $\mathbf{A}(\mathbf{r})$, the trial charge density fully determines the trial diamagnetic current density, i.e. the diamagnetic current is maximally constrained. This alleviates part of the problem of restricting ourselves to V-representable trial densities.

The remainder of the problem concerns the V-representability of combinations of n and $\mathbf{j}_{\mathrm{p}}$. There are some densities which cannot be yielded from a single ground-state wavefunction, such as certain excited states of atoms containing nodes, and density

ensembles of, for instance, degenerate ground-states. Furthermore, there are constraints on the selection of densities concerning electron number and the continuity equation.

For any density $n(\mathbf{r})$ that is non-negative and normalisable, there generally exists an antisymmetric, normalisable function $|\Psi\rangle$ [133; 134; 135; 136] such that

$$n(\mathbf{r}) = \langle \Psi | \hat{n}(\mathbf{r}) | \Psi \rangle . \tag{3.38}$$

It follows from the Rayleigh-Ritz theorem that any such densities must therefore obey inequality 3.37, freeing the constraint of the densities being those of ground states. The energy functional then obeys

$$
\begin{aligned}
E_{v,A}\left[\underline{\mathbf{N}}\right] &= \inf_{\Psi \to n, \mathbf{j}_{\mathrm{p}}} \left\langle \Psi[\underline{\mathbf{N}}] \left| \hat{T} + \hat{U} \right| \Psi[\underline{\mathbf{N}}] \right\rangle + \int_{-\infty}^{\infty} d\mathbf{r} \ \left\{ \mathbf{j} \cdot \mathbf{A} + n \left[v - \tfrac{1}{2}A^2 \right] \right\} \\
&\geq E_{v,A}\left[\underline{\mathbf{N}}_0\right] .
\end{aligned}
\tag{3.39}
$$

The search may be extended to density ensembles following the approach of Levy [93] for ensembles, such as densities of statistical combinations of degenerate ground states. We may consider a density matrix

$$\rho(\mathbf{r}, \mathbf{r}') = \sum_k p_k |\Psi_k\rangle \langle \Psi_k| \tag{3.40}$$

with an associated ensemble charge and paramagnetic current densities

$$n(\mathbf{r}) = \rho(\mathbf{r}, \mathbf{r}) \tag{3.41}$$

$$\mathbf{j}_{\mathrm{p}}(\mathbf{r}) = \frac{1}{2i} \left(\nabla_{\mathbf{r}'} - \nabla_{\mathbf{r}''} \right) \rho(\mathbf{r}', \mathbf{r}'') \big|_{\mathbf{r}''=\mathbf{r}'=\mathbf{r}} . \tag{3.42}$$

We can then construct an energy functional for the density matrix when subject to external potentials $(v, \mathbf{A})$:

$$E\left[n(\mathbf{r}), \mathbf{j}_{\mathrm{p}} \right] = F\left[\rho\right] + \int_{-\infty}^{\infty} d\mathbf{r} \ \left\{ \mathbf{j}_{\mathrm{p}} \cdot \mathbf{A} + n \left[v + \tfrac{1}{2}A^2 \right] \right\} . \tag{3.43}$$

where

$$F\left[\rho\right] = \mathrm{Tr} \left[\rho \left(\hat{T} + \hat{U} \right) \right] \tag{3.44}$$

is a universal functional of the density matrix, and therefore the densities. As pointed out by Lieb [94], $F[\rho] = F[n]$ and thus likewise has its minimum at $\rho_0(\mathbf{r}, \mathbf{r}')$ where $\rho_0(\mathbf{r}, \mathbf{r}) = n_0(\mathbf{r})$.

The above procedures for finding the ground-state densities of a set of external potentials rely on knowledge of the universal functional. Generally, the universal functional is unknown and must be approximated. A practical scheme for doing so will be discussed in the next section. This scheme is markedly different from previous practical minimisation schemes for current-density functional theories.

3.5 Practical minimisation scheme

The proof of a variational procedure is only useful if we may construct a practical scheme for performing it. In all previous ground-state density-functional theories, this has been achieved by decomposing the universal part of the energy functional into parts that may be expressed in terms of an auxiliary system of noninteracting electrons – the Kohn-Sham system – having the same basic variables and yielding the correct universal functional value by definition.

In the Vignale-Rasolt formulation of CDFT, this held even when the basic variable was a gauge-dependent variable, resulting in the construction of KS systems that were not physically identical to the real systems they represented. As such, the CDFT of Vignale and Rasolt is not approached by time-dependent current-density functional theory in the limit of $\omega \to 0$. For this reason, such an approach is not desired here.

Further, it has been proven that the charge density, paramagnetic current density and diamagnetic current density together, $((n_0(\mathbf{r}), \mathbf{j}_{\mathrm{p},0}(\mathbf{r}), \mathbf{j}_{\mathrm{d},0}(\mathbf{r}),)$ uniquely determines the set of external scalar and vector potentials $(v(\mathbf{r}), \mathbf{A}(\mathbf{r}))$ that yield those densities as a nondegenerate ground state, and vice versa.

We have also seen that, in an ideal minimisation scheme under fixed external potentials where an expression (or at least a good approximation) for the universal functional $F[n(\mathbf{r}), \mathbf{j}_{\mathrm{p}}(\mathbf{r}), \mathbf{j}_{\mathrm{d}}(\mathbf{r})]$ is known, it is sufficient to vary only $n(\mathbf{r})$ and $\mathbf{j}_{\mathrm{p}}(\mathbf{r})$ since, under fixed $\mathbf{A}(\mathbf{r})$, the choice of a trial density n fixes the diamagnetic current density $\mathbf{j}_{\mathrm{d}}(\mathbf{r}) = \mathbf{A}(\mathbf{r})n(\mathbf{r})$.

Adopting the conventions

$$(a(\mathbf{r}) \mid b(\mathbf{r})) = \int_{-\infty}^{\infty} d\mathbf{r} \ a(\mathbf{r})b(\mathbf{r}) \tag{3.45}$$

$$(\mathbf{A}(\mathbf{r}) \mid \mathbf{B}(\mathbf{r})) = \int_{-\infty}^{\infty} d\mathbf{r} \ \mathbf{A}(\mathbf{r}) \cdot \mathbf{B}(\mathbf{r}), \tag{3.46}$$

the energy functional of some set of trial densities subject to a fixed set of external

potentials can be written as

$$E_{v,A}[n, \mathbf{j}_{\mathrm{p}}, \mathbf{j}_{\mathrm{d}}] = F[n, \mathbf{j}_{\mathrm{p}}, \mathbf{j}_{\mathrm{d}}] + (\mathbf{j}_{\mathrm{p}} \mid \mathbf{A}) + (\mathbf{j}_{\mathrm{d}} \mid \mathbf{A}) + (n \mid u) \tag{3.47}$$

$$= F[n, \mathbf{j}_{\mathrm{p}}, \mathbf{j}_{\mathrm{d}}] + (\mathbf{j} \mid \mathbf{A}) + (n \mid u) \tag{3.48}$$

where $u(\mathbf{r}) = v(\mathbf{r}) - \frac{1}{2}A^2(\mathbf{r})$. Here $\mathbf{j}_{\mathrm{d}}(\mathbf{r})$ is the diamagnetic current density of the system when subject to the ambient vector potential $\mathbf{A}(\mathbf{r})$.

Since, under fixed external vector potential, varying $n(\mathbf{r})$ is equivalent to varying $\mathbf{j}_{\mathrm{d}}(\mathbf{r})$, the ideal minimisation scheme quickly reduces to that of Vignale and Rasolt [124] discussed in Sec. 2.3. However, it has been seen that, in the usual practical (Kohn-Sham) scheme of calculating the universal functional F via an auxiliary system of noninteracting electrons subject to effective external scalar and vector potentials $(v_{\mathrm{KS}}, \mathbf{A}_{\mathrm{KS}}(\mathbf{r}))$ and having the same charge and paramagnetic current density, those effective external potentials are not uniquely determined: we need knowledge also of the diamagnetic current density of the interacting system.

Generally, the KS vector potential will not be that of the interacting system, and therefore we cannot choose

$$(n_{\mathrm{KS}}(\mathbf{r}), \mathbf{j}_{\mathrm{p,KS}}(\mathbf{r}), \mathbf{j}_{\mathrm{d,KS}}(\mathbf{r})) = (n(\mathbf{r}), \mathbf{j}_{\mathrm{p}}(\mathbf{r}), \mathbf{j}_{\mathrm{d}}(\mathbf{r})) . \tag{3.49}$$

As such, we need an alternative scheme for mapping the densities of interacting systems onto their KS representations.

Recalling the definition of the basic seven-component density vector as

$$\underline{\mathbf{N}}(\mathbf{r}) = (n(\mathbf{r}), \mathbf{j}_{\mathrm{p}}(\mathbf{r}), \mathbf{j}_{\mathrm{d}}(\mathbf{r})) \tag{3.50}$$

and defining the *physical* density and external potential four-component vectors as

$$\mathbf{N}(\mathbf{r}) = (\mathbf{j}(\mathbf{r}), n(\mathbf{r})) \tag{3.51}$$

$$\mathbf{V}(\mathbf{r}) = (\mathbf{A}(\mathbf{r}), u(\mathbf{r})) , \tag{3.52}$$

then because the basic density uniquely determines the physical density, the variational theorem for a given external potential may be rewritten as

$$F[\underline{\mathbf{N}}] + (\mathbf{N} \mid \mathbf{V}) \geq F[\underline{\mathbf{N}}_0] + (\mathbf{N}_0 \mid \mathbf{V}) \tag{3.53}$$

where $\mathbf{N}(\mathbf{r}) = \mathbf{N}[\underline{\mathbf{N}}]$.

Because the diamagnetic current is fixed by $n(\mathbf{r})$ and $\mathbf{A}(\mathbf{r})$, a unique choice of $\underline{\mathbf{N}}$ is equivalent to a unique choice of $\mathbf{N}(\mathbf{r})$. (Note, this is *only* true under fixed $\mathbf{A}(\mathbf{r})$: generally, there are multiple wavefunctions that yield the same $\mathbf{N}(\mathbf{r})$.)

The general energy functional may then be written as

$$E_V[\underline{\mathbf{N}}] = F[\underline{\mathbf{N}}] + (\mathbf{N}[\underline{\mathbf{N}}] \,|\, \mathbf{V}). \tag{3.54}$$

Defining the four-component density operators as

$$\hat{\mathbf{N}}_1(\mathbf{r}) = \left(\hat{\mathbf{j}}_{\mathrm{p}}(\mathbf{r}), \hat{n}(\mathbf{r})\right) \tag{3.55}$$

$$\hat{\mathbf{N}}_2(\mathbf{r}) = (\hat{n}(\mathbf{r})\mathbf{A}(\mathbf{r}), 0) \tag{3.56}$$

and noting that the first of these and the universal functional $F[\underline{\mathbf{N}}]$ do not depend on the external potential, the functional derivative of the energy functional with respect to the external potential is evaluated as

$$
\begin{aligned}
\frac{\delta E_V}{\delta \mathbf{V}(\mathbf{r})} &= \frac{\delta F}{\delta \mathbf{V}(\mathbf{r})} + \frac{\delta}{\delta \mathbf{V}(\mathbf{r})} \left(\hat{\mathbf{N}}_1(\mathbf{r}') \,|\, \mathbf{V}(\mathbf{r}')\right) + \frac{\delta}{\delta \mathbf{V}(\mathbf{r})} \left(\hat{\mathbf{N}}_2(\mathbf{r}') \,|\, \mathbf{V}(\mathbf{r}')\right) \\
&= \left(\hat{\mathbf{N}}_1(\mathbf{r}') \,|\, \frac{\delta \mathbf{V}(\mathbf{r}')}{\delta \mathbf{V}(\mathbf{r})}\right) + \frac{\delta}{\delta \mathbf{V}(\mathbf{r})} \left(\hat{n}(\mathbf{r}') \,|\, \tfrac{1}{2}\mathbf{A}(\mathbf{r}') \cdot \mathbf{A}(\mathbf{r}')\right) \\
&= \left(\hat{\mathbf{N}}_1(\mathbf{r}') \,|\, \delta(\mathbf{r}, \mathbf{r}')\right) + \left(\hat{\mathbf{N}}_2 \,|\, \delta(\mathbf{r}, \mathbf{r}')\right) \\
&= (\mathbf{j}_{\mathrm{p}}(\mathbf{r}), n(\mathbf{r})) + (\mathbf{j}_{\mathrm{d}}(\mathbf{r}), 0) \\
&= \mathbf{N}(\mathbf{r}).
\end{aligned}
\tag{3.57}
$$

Thus we see that the conjugate variable to the external potential is the four-component *physical* density, making it a sensible choice for the variable in a minimisation scheme.

Rearranging Eq. 3.54, we have

$$F[\underline{\mathbf{N}}] = E_{V'}[\underline{\mathbf{N}}] - \left(\mathbf{N}(\mathbf{r}') \,|\, \mathbf{V}'(\mathbf{r}')\right), \tag{3.58}$$

where $\mathbf{V}'(\mathbf{r})$ is the potential which has $\mathbf{N}(\mathbf{r})$ as its ground-state density, and its func-

tional derivative with respect to the physical density is

$$
\begin{aligned}
\frac{\delta F}{\delta \mathbf{N}(\mathbf{r})} &= \frac{\delta E_V}{\delta \mathbf{N}(\mathbf{r})} - \left(\delta(\mathbf{r}, \mathbf{r}') \,|\, \mathbf{V}'(\mathbf{r}')\right) - \left(\mathbf{N}(\mathbf{r}') \,|\, \frac{\delta \mathbf{V}'(\mathbf{r}')}{\delta \mathbf{N}(\mathbf{r})}\right) \\
&= \left(\frac{\delta E_V}{\delta \mathbf{V}'(\mathbf{r}')} \,|\, \frac{\delta \mathbf{V}'(\mathbf{r}')}{\delta \mathbf{N}(\mathbf{r})}\right) - \mathbf{V}'(\mathbf{r}) - \left(\mathbf{N}(\mathbf{r}') \,|\, \frac{\delta \mathbf{V}'(\mathbf{r}')}{\delta \mathbf{N}(\mathbf{r})}\right) \\
&= \left(\mathbf{N}(\mathbf{r}') \,|\, \frac{\delta \mathbf{V}'(\mathbf{r}')}{\delta \mathbf{N}(\mathbf{r})}\right) - \mathbf{V}'(\mathbf{r}) - \left(\mathbf{N}(\mathbf{r}') \,|\, \frac{\delta \mathbf{V}'(\mathbf{r}')}{\delta \mathbf{N}(\mathbf{r})}\right) \\
&= -\mathbf{V}'(\mathbf{r}).
\end{aligned}
\tag{3.59}
$$

The universal functional may then be decomposed as

$$
F = T_{\mathrm{S}} + E_{\mathrm{H}} + E_{\mathrm{xc}}
\tag{3.60}
$$

where T_{S} is the single-particle kinetic energy, E_{H} the Hartree energy as usual, and E_{xc} the exchange-correlation (XC) energy (i.e. remainder of the universal energy).

In standard DFT, T_{S} is defined as the kinetic energy of a system of noninteracting particles having the same charge density as the interacting system and as such is uniquely determined by the density, while in the CDFT of Vignale and Rasolt, it is the kinetic energy of a noninteracting system having the same charge and paramagnetic current density as the interacting system. In both cases, since the noninteracting system is chosen to have the same basic densities as the interacting system, T_{S} is a unique functional of those densities. Here, however, the noninteracting and interacting systems do not share the same basic densities.

We may note that the universal functional $F[\underline{\mathbf{N}}]$ is always exactly equal to a non-universal functional $F^A[\mathbf{N}]$ during energy minimisation:

$$
F^A[\mathbf{N}] = F[\underline{\mathbf{N}}]\big|_{\mathbf{j}_{\mathrm{d}} = n\mathbf{A}},
\tag{3.61}
$$

where A uniquely indexes the external vector potential $\mathbf{A}$, since knowledge of $\mathbf{N}(\mathbf{r})$ and $\mathbf{A}(\mathbf{r})$ yields $\mathbf{j}_{\mathrm{d}}(\mathbf{r})$. Decomposing the $\mathbf{A}$-dependent functional as before, we have

$$
F^A = T_{\mathrm{S}}^A + E_{\mathrm{H}} + E_{\mathrm{xc}}^A.
\tag{3.62}
$$

We consider now a system of an equal number N of noninteracting electrons whose density $\mathbf{N}_{\mathrm{KS}}(\mathbf{r})$ satisfies the identity

$$
\mathbf{N}_{\mathrm{KS}}(\mathbf{r}) = \mathbf{N}(\mathbf{r})
\tag{3.63}
$$

via the equations

$$\left\{ \tfrac{1}{2} \left[\hat{\mathbf{p}} + \mathbf{A}_{\text{KS}}(\mathbf{r}) \right]^2 + v_{\text{KS}}(\mathbf{r}) \right\} \phi_i(\mathbf{r}) = \epsilon_i \phi_i(\mathbf{r}) \tag{3.64}$$

$$n_{\text{KS}}(\mathbf{r}) = \sum_{i=1}^{N} \langle \phi_i(\mathbf{r}) | \hat{n}(\mathbf{r}) | \phi_i(\mathbf{r}) \rangle \tag{3.65}$$

$$\mathbf{j}_{\text{KS}}(\mathbf{r}) = \mathbf{A}_{\text{KS}}(\mathbf{r}) n_{\text{KS}}(\mathbf{r}) + \sum_{i=1}^{N} \left\langle \phi_i \left| \hat{\mathbf{j}}_{\text{p}}(\mathbf{r}) \right| \phi_i \right\rangle \tag{3.66}$$

$$\mathbf{N}_{\text{KS}}(\mathbf{r}) = (\mathbf{j}_{\text{KS}}(\mathbf{r}), n_{\text{KS}}(\mathbf{r})) . \tag{3.67}$$

For the noninteracting system subject to the effective external field

$$\mathbf{V}_{\text{KS}}(\mathbf{r}) = (\mathbf{A}_{\text{KS}}(\mathbf{r}), u_{\text{KS}}(\mathbf{r})) , \tag{3.68}$$

we require that

$$F^{A_{\text{KS}}}[\mathbf{N}] = T_{\text{S}}^{A}[\mathbf{N}]. \tag{3.69}$$

Applying the Hellman-Feynman [137]-[138] theorem and taking the functional derivative of Eq. 3.62 with respect to the physical density as before, we have that

$$\begin{aligned}
\frac{\delta F^A}{\delta \mathbf{N}} &= \frac{\delta F^{A_{\text{KS}}}}{\delta \mathbf{N}} + \frac{\delta E_{\text{H}}}{\delta \mathbf{N}} + \frac{\delta E_{\text{xc}}^{A_{\text{KS}}}}{\delta \mathbf{N}} = -\mathbf{V}'(\mathbf{r}) \\
&= -\mathbf{V}_{\text{KS}}(\mathbf{r}) + (\mathbf{0}, v_{\text{H}}(\mathbf{r})) + \mathbf{V}_{\text{xc}}(\mathbf{r}) \\
&= -\mathbf{V}(\mathbf{r}),
\end{aligned} \tag{3.70}$$

where we have defined

$$\mathbf{V}_{\text{xc}}(\mathbf{r}) = \frac{\delta E_{\text{xc}}^{A_{\text{KS}}}}{\delta \mathbf{N}}. \tag{3.71}$$

Thus we have an expression for the noninteracting potential

$$\mathbf{V}_{\text{KS}}(\mathbf{r}) = \mathbf{V}(\mathbf{r}) + (\mathbf{0}, v_{\text{H}}(\mathbf{r})) + \mathbf{V}_{\text{xc}}(\mathbf{r}) \tag{3.72}$$

which, from Eq. 3.52, has scalar and vector components which defined the exchange-correlation potentials

$$\mathbf{A}_{\text{KS}}(\mathbf{r}) = \mathbf{A}(\mathbf{r}) + \mathbf{A}_{\text{xc}}(\mathbf{r}) \tag{3.73}$$

$$u_{\text{KS}}(\mathbf{r}) = u(\mathbf{r}) + v_{\text{H}}(\mathbf{r}) + v_{\text{xc}}(\mathbf{r}) \tag{3.74}$$

and thus

$$v_{\text{KS}}(\mathbf{r}) = v(\mathbf{r}) + v_{\text{H}}(\mathbf{r}) + v_{\text{xc}}(\mathbf{r}) + \tfrac{1}{2}\left[A_{\text{KS}}^2(\mathbf{r}) - A^2(\mathbf{r})\right]. \tag{3.75}$$

This is the KS scalar potential of the physical current-density-functional theory of Pan and Sahni, rather than that of the paramagnetic CDFT of Vignale and Rasolt, arising as a consequence of our insistence that the KS system have the same physical charge and current densities as the interacting system it represents, rather than the same charge and paramagnetic current densities as in paramagnetic CDFT.

From the stationary property of the ground-state energy of the interacting system, the definition of the universal functional, and the condition

$$\int_{-\infty}^{\infty} \delta\mathbf{N}(\mathbf{r})d\mathbf{r} = \mathbf{0} \tag{3.76}$$

we obtain

$$\begin{aligned}
\int \delta\mathbf{N}(\mathbf{r})\frac{\delta E_{v,A}}{\delta\mathbf{N}(\mathbf{r})} &= \int \delta\mathbf{N}(\mathbf{r})\left\{\frac{\delta F}{\delta\mathbf{N}(\mathbf{r})} + u(\mathbf{r})\right\} \\
&= \int \delta\mathbf{N}(\mathbf{r})\left\{\frac{\delta}{\delta\mathbf{N}(\mathbf{r})}\left[T_{\text{S}} + E_{\text{H}} + E_{\text{xc}}\right] + u(\mathbf{r})\right\} \\
&= \int \delta\mathbf{N}(\mathbf{r})\left\{\frac{\delta T_{\text{S}}}{\delta\mathbf{N}(\mathbf{r})} + v_{\text{H}}(\mathbf{r}) + v_{\text{xc}}(\mathbf{r}) + u(\mathbf{r})\right\} >= \mathbf{0}. \tag{3.77}
\end{aligned}$$

From the definition of the KS system we obtain

$$\int \delta\mathbf{N}(\mathbf{r})\left\{\frac{\delta T_{\text{S}}}{\delta\mathbf{N}(\mathbf{r})} + u_{\text{KS}}(\mathbf{r})\right\} \geq \mathbf{0}. \tag{3.78}$$

From the Hohenberg-Kohn theorem, this is equivalent to solving the ground-state, many-body Schrödinger equation self-consistently for a noninteracting system of electrons subject to external fields $u_{\text{KS}}(\mathbf{r})$ and $\mathbf{A}_{\text{KS}}(\mathbf{r})$, i.e. the Kohn-Sham equations Eq. 3.64-3.67. The Kohn-Sham equations and the definitions of the KS potentials allow one to take a self-consistent approach equivalent to the minimisation procedure, and the resulting KS system (with the appropriate XC functionals) is approached by TDCDFT as the perturbation of the ground-state goes to zero.

It should be noted that, while $\mathbf{V}_{\text{KS}}(\mathbf{r})$ is a unique functional of

$$\underline{\mathbf{N}}_{\text{KS}}(\mathbf{r}) = (n(\mathbf{r}), \mathbf{j}_{\text{p,KS}}(\mathbf{r}), \mathbf{j}_{\text{d,KS}}(\mathbf{r})), \tag{3.79}$$

it is not a unique functional of $\mathbf{N}(\mathbf{r})$. The single-particle kinetic energy is only uniquely

defined for a specific definition of E_{xc} and the condition that

$$F^A[\mathbf{N}] - E_{\mathrm{H}}[\mathbf{N}] = T_{\mathrm{S}}^A[\mathbf{N}] + E_{\mathrm{xc}}^A[\mathbf{N}]. \tag{3.80}$$

Such a condition allows for a gauge-dependence in the XC functional. One can eliminate this entirely by implementing the further conditions that

$$\boldsymbol{\nabla} \cdot \mathbf{A}_{\mathrm{xc}}(\mathbf{r}) = 0 \tag{3.81}$$

and that v_{xc} go to zero infinitely far from the system. This ensures that $\boldsymbol{\nabla} \cdot \mathbf{A}_{\mathrm{KS}}(\mathbf{r}) = \boldsymbol{\nabla} \cdot \mathbf{A}(\mathbf{r})$ and that $v_{\mathrm{xc}}(\mathbf{r})$ does not add an arbitrary constant to the energy of the trial density.

Beyond gauge-dependence, if there exist multiple choices of $\mathbf{V}_{\mathrm{xc}}[\mathbf{N}]$ that yield the same universal functional, all are equivalent since they do not effect energy minimisation. On the other hand, the XC functional must be constructed (e.g. from *ab initio* calculations) in such a way as that, if multiple choices of $\mathbf{V}_{\mathrm{xc}}[\mathbf{N}]$ exist that yield the same physical densities but different universal functionals, the correct one is selected.

Further, by taking the physical current of the system into account, one explicitly avoids the problems described by Capelle and Vignale [127] and Engel and Dreizler [95] since two sets of external potentials that share the same ground-state wavefunction, and thus the same ground-state charge and paramagnetic current densities, will not share the same physical current density. Likewise no two sets of KS potentials yielding the same ground-state wavefunction may yield the same physical densities. It is important to remember, though, that it is the gauge-variant KS current densities that determine the KS wavefunction. Nonetheless, minimising the system energy with respect to the physical current is equivalent to minimising with respect to the paramagnetic current, and thus it falls to the precise form of the XC potentials to ensure the correct $\mathbf{j}(\mathbf{r})$ is achieved in self-consistency.

Other approaches to the problem of a practical minimisation scheme for a CDFT founded on a proven uniqueness theorem and which makes contact with TDCDFT in the adiabatic limit as outlined in the Appendix.

3.6 Reverse-engineering algorithm for steady-state systems

Section 3.3 demonstrated that, for any fixed interaction strength, the external potentials are unique functionals of the charge and paramagnetic and diamagnetic current densities. However, the effective external potentials of the KS representation will generally differ from those of the real systems they represent, and thus the KS diamagnetic current will also vary from its real-world counterpart.

The only measurable current quantity is the physical current, but a CDFT in terms of the physical current density has already been discounted. Thus a scheme is required whereby the measurable physical densities of a real system can be reproduced in a KS system whose effective potentials are uniquely defined for the charge and gauge-variant *components* of the current density.

Let us consider a KS system of N electrons subject to an effective external scalar potential, found either approximately by a functional such as the LDA or by an exact method such as the van Leeuwen-Baerends procedure [139] or similar (e.g. [140], [141]), and an effective external vector potential which might be simply the external vector potential of the interacting system, that reproduces the charge density of a real system of N interacting electrons but does not reproduce the physical current density.

$$v_{KS}(\mathbf{r}) = v_{KS}^{(0)}(\mathbf{r})$$

$$\mathbf{A}_{KS}(\mathbf{r}) = \mathbf{A}_{KS}^{(0)}(\mathbf{r})$$

$$n_{KS}(\mathbf{r}) = n(\mathbf{r}) \tag{3.82}$$

$$\mathbf{j}_{KS}(\mathbf{r}) \neq \mathbf{j}(\mathbf{r}) \tag{3.83}$$

$$\mathbf{j}_{d,KS}(\mathbf{r}) = \mathbf{j}_{d,KS}^{(0)}(\mathbf{r}). \tag{3.84}$$

What is required is a procedure by which the KS potentials can be varied to yield the exact physical densities of the real system. For now, we will consider small variations that leave the KS charge density approximately unchanged. In order to reproduce the physical current density, the KS vector potential at least must be modified, and this will yield a correction to the KS diamagnetic current:

$$\mathbf{A}^{(i+1)}(\mathbf{r}) = \mathbf{A}_{KS}^{(i)}(\mathbf{r}) + \Delta\mathbf{A}_{KS}^{(i+1)}(\mathbf{r})$$

$$\mathbf{j}_{d,KS}^{(i+1)}(\mathbf{r}) = \mathbf{j}_{d,KS}^{(i)}(\mathbf{r}) + n(\mathbf{r})\Delta\mathbf{A}_{d,KS}^{(i+1)}(\mathbf{r}).$$

If the paramagnetic current remained unchanged after such a correction, then the reverse-engineering of the exact KS vector potential would require only one iteration with

$$\mathbf{A}_{\text{KS}}(\mathbf{r}) = \mathbf{A}_{\text{KS}}^{(0)}(\mathbf{r}) + \frac{\mathbf{j}(\mathbf{r}) - \mathbf{j}_{\text{KS}}^{(0)}(\mathbf{r})}{n(\mathbf{r})}. \tag{3.85}$$

However, the presence of the corrected vector potential will generally lead to changes in both the paramagnetic current density *and* (if the correction to the vector potential has a transverse component) the charge density. The former is accounted for by making the procedure iterative:

$$\mathbf{A}_{\text{KS}}^{(i+1)}(\mathbf{r}) = \mathbf{A}_{\text{KS}}^{(i)}(\mathbf{r}) + \frac{\mathbf{j}(\mathbf{r}) - \mathbf{j}_{\text{KS}}^{(i)}(\mathbf{r})}{n(\mathbf{r})}. \tag{3.86}$$

After each correction, one can recalculate the KS eigenstates and thus the KS physical charge and current densities and repeat to find further corrections, so long as the KS charge density is held approximately constant from iteration to iteration which may require a recalculation of the scalar potential for each recalculation of the vector potential.

Generally, however, the KS charge density will also respond to the presence of a revised KS potential. For this reason, it is necessary to correct both the vector *and* scalar potentials when tuning a KS system to reproduce exact physical densities. This is because the initial KS system, with $\mathbf{A}(\mathbf{r}) = \mathbf{A}^{(0)}(\mathbf{r})$ is still only an approximate KS system even if it reproduces the charge density of the interacting system exactly, and thus the scalar potential it is subject to is also only an approximation. As $\mathbf{A}^{(i)} \to \mathbf{A}_{\text{KS}}$, i.e. the exact KS vector potential, one must ensure, via the van Leeuwen-Baerends procedure or similar, that the scalar potential $v^{(i)}(\mathbf{r})$ is also allowed to approach the exact KS scalar potential.

Fig. 3.1 shows a schematic diagram of the iterative reverse-engineering algorithm for steady-state systems. In this scheme, the algorithm only proceeds to make corrections to the KS current density when the KS charge density $n_{\text{KS}}(\mathbf{r})$ is exactly that of the interacting system $n(\mathbf{r})$. Each time the vector potential is corrected by $(\mathbf{j} - \mathbf{j}_{\text{KS}})/n$, both the charge and the current density of the KS system are recalculated. If the revised KS charge density has diverged from that of the interacting system, the KS scalar potential must be recalculated once more. This would typically be done by some iterative scheme, such as the van Leeuwen-Baerends procedure or other optimisation algorithm, which will have its own termination criteria for the main algorithm. Due to the fact that the KS charge density is constantly updated in this way, the replacing
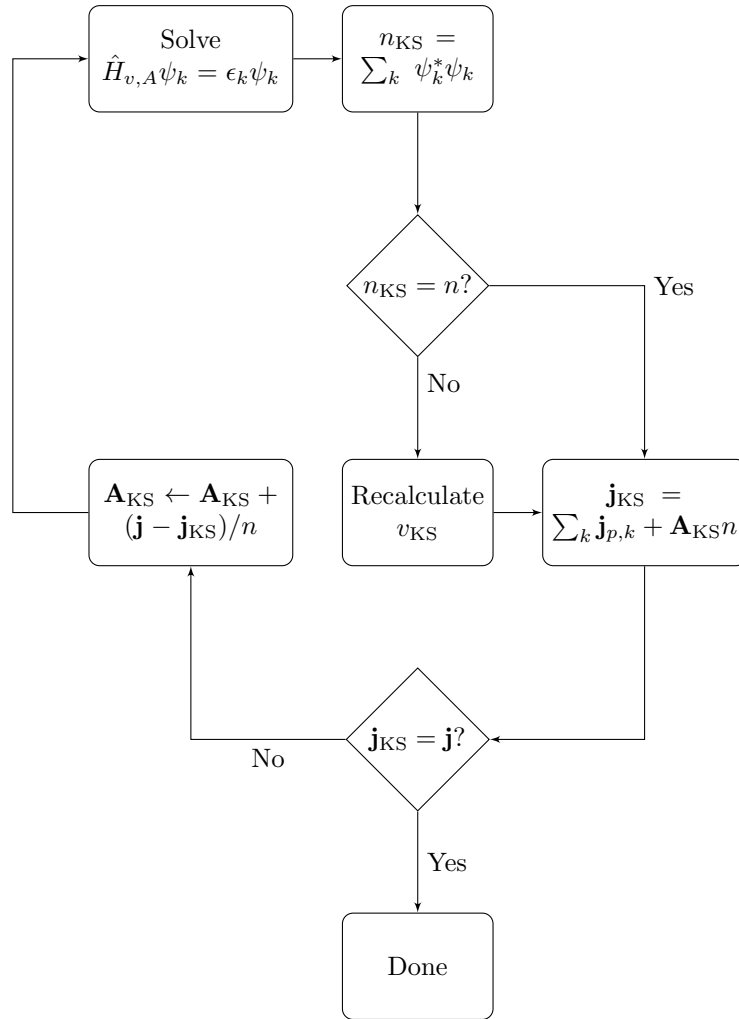
Figure 3.1: A schematic diagram of a reverse-engineering algorithm for the calculation of exact KS potentials that reproduce the physical charge and current densities of a real system. The details of the calculation of the scalar potential are not covered, but there are existing algorithms that are compatible with this approach such as the van Leeuwen-Baerends procedure.

of the KS charge density with the exact charge density in the corrections to the vector potential is justified.

The KS vector potential and current are uniquely determined by the charge density (found via methods such as the van Leeuwen-Baerends procedure) and the diamagnetic current density (see previous sections of this chapter and the Appendix). Thus, even while we may not know the target diamagnetic current density, we know that, as we approach it, we also approach the exact KS vector potential so long as the charge density is held fixed to that of the interacting system.

The steady-state reverse-engineering algorithm allows us to scan the space of $(n, \mathbf{j}_\mathrm{d})$ limited in range by the difference between the true current density and that of a trial or partially-converged KS system. While the corrections to the KS vector potential will have an inconsequential longitudinal component

$$\boldsymbol{\nabla} \cdot \Delta \mathbf{A}_\mathrm{KS}^{i+1}(\mathbf{r}) = \frac{\Delta \mathbf{j}^i(\mathbf{r}) \cdot \boldsymbol{\nabla} n(\mathbf{r})}{n^2(\mathbf{r})}, \tag{3.87}$$

it is guaranteed to have a transverse component

$$\boldsymbol{\nabla} \times \Delta \mathbf{A}_\mathrm{KS}^{i+1}(\mathbf{r}) = \frac{n(\mathbf{r})\boldsymbol{\nabla} \times \Delta \mathbf{j}^i(\mathbf{r}) - \boldsymbol{\nabla} n(\mathbf{r}) \times \Delta \mathbf{j}^i(\mathbf{r})}{n^2(\mathbf{r})} \tag{3.88}$$

since any steady-state current is purely transverse from the continuity equation, and thus any difference between the true and unconverged KS current densities will also be purely transverse, and thus yield a correction to the KS magnetic field $\mathbf{B}_\mathrm{KS}(\mathbf{r})$.

3.7 Reverse-engineering in the nonequilibrium regime

As in the steady-state case, we now seek a means of calculating *time-dependent* potentials for Kohn-Sham systems defined to have the same physical charge and current densities as a real interacting system.

Let us consider a real ground-state system $|\Psi(0)\rangle$ of interacting electrons with charge and current densities $n(\mathbf{r})$ and $\mathbf{j}(\mathbf{r})$ whose corresponding KS representation $|\Psi_\mathrm{KS}(0)\rangle$ can be calculated from the reverse-engineering algorithm of the previous section. This ground-state system is then perturbed by a time-dependent external vector potential $\mathbf{A}(\mathbf{r}, t)$ at $t = 0$. Assuming the KS scalar potential is likewise static, we can time-evolve our initial KS state with the initial KS Hamiltonian $\hat{H}_\mathrm{KS}$ using the time-evolution operator:

$$|\psi_{\mathrm{KS},k}(t)\rangle = \hat{U}(t, 0) |\psi_{\mathrm{KS},k}(0)\rangle \tag{3.89}$$

If the time over which the system is evolving is not small, the time-evolution can be broken down into finite intervals:

$$\psi_{KS,i}(\mathbf{r}, t + \Delta t) = e^{-i\hat{H}_{\mathrm{KS}}\Delta t}\psi(\mathbf{r}, t). \tag{3.90}$$

This will yield a (undoubtedly incorrect) set of gauge-invariant and gauge-variant densities:

$$n^{(0)}(\mathbf{r}, t) = \sum_k |\psi_{\mathrm{KS},k}(\mathbf{r}, t)|^2 \neq n(\mathbf{r}, t) \tag{3.91}$$

$$\mathbf{j}_{\mathrm{p}}^{(0)}(\mathbf{r}, t) = \frac{1}{2i}\sum_k \left(\psi_{\mathrm{KS},k}^*(\mathbf{r}, t)\boldsymbol{\nabla}\psi_{\mathrm{KS},k}(\mathbf{r}, t) - \psi_{\mathrm{KS},k}(\mathbf{r}, t)\boldsymbol{\nabla}\psi_{\mathrm{KS},k}^*(\mathbf{r}, t)\right) \tag{3.92}$$

$$\mathbf{j}_{\mathrm{d}}^{(0)}(\mathbf{r}, t) = \mathbf{A}^{(0)}(\mathbf{r}, 0)n^{(0)}(\mathbf{r}, t) \tag{3.93}$$

$$\mathbf{j}^{(0)}(\mathbf{r}, t) = \mathbf{j}_{\mathrm{p}}^{(0)}(\mathbf{r}, t) + \mathbf{j}_{\mathrm{d}}^{(0)}(\mathbf{r}, t) \neq \mathbf{j}(\mathbf{r}, t). \tag{3.94}$$

One can improve on the KS physical current density if one could force the system to carry an additional diamagnetic current $\Delta\mathbf{j}_{\mathrm{d}}^{(1)}(\mathbf{r}, t)$. If this improvement could be performed in one iteration, then the associated vector potential must be:

$$\mathbf{A}^{(1)}(\mathbf{r}, t) = \frac{\Delta\mathbf{j}_{\mathrm{d}}^{(0)}(\mathbf{r}, t)}{n(\mathbf{r}, t)}. \tag{3.95}$$

Recalculating the time-evolution of the KS system from time 0 to time t with this vector potential should then reproduce the charge and current density of the real system, so long as t is sufficiently small that the KS vector potential and charge density are approximately constant.

After calculating the exact vector potential for $t = \Delta t$, one may then begin the reverse-engineering algorithm once again, using the KS Hamiltonian $\hat{H}_{\mathrm{KS}}(\Delta t)$, to determine the exact vector potential that reproduces the time-dependent current density at time $2\Delta t$. From the continuity equation, as long as the time-dependent current density is correct, it follows that the time-derivative of the charge density must also be correct and, since the initial charge density is known and is exact, the time-dependent charge density of the KS system is that of the real, interacting system.

Generally, an improvement of the KS vector potential by $\Delta\mathbf{j}_{\mathrm{d}}/n$ will lead to a different paramagnetic current density at time t, meaning that the total KS physical current is yet again different to the real system. Successive improvements to the KS physical current, via additions to the diamagnetic current with associated corrections to

the KS vector potential, will lead to successive improvements to the KS charge density. When, after the ith iteration, $\mathbf{j}^{(i)}(\mathbf{r}, t) = \mathbf{j}(\mathbf{r}, t)$, the procedure is complete and can start again for the next stage of the time-evolution.

However, systems subject to a time-dependent vector potential and static scalar potential are very limited, and even if the external scalar potential of the interacting system were static, the KS effective scalar potential would not be: it includes the Hartree and XC potentials which are necessarily time-dependent for time-dependent densities. However, one has the gauge-freedom in a time-dependent system to include time-dependent electric and magnetic fields either via a scalar potential *or* a vector potential. This holds true in both the interacting and KS descriptions.

Thus, if our interacting system has time-dependent potentials $v(\mathbf{r}, t)$ and $\mathbf{A}(\mathbf{r}, t)$, we may choose a scalar field $\Lambda(\mathbf{r}, t)$ such that:

$$v'(\mathbf{r}, t) = v(\mathbf{r}, t) + \frac{\partial}{\partial t}\Lambda(\mathbf{r}, t) = v_0(\mathbf{r}) \tag{3.96}$$

$$\mathbf{A}'(\mathbf{r}, t) = \mathbf{A}(\mathbf{r}, t) - \boldsymbol{\nabla}\Lambda(\mathbf{r}, t) \tag{3.97}$$

where $v_0(\mathbf{r}) = v(\mathbf{r}, t = 0)$. Substituting these potentials into the time-dependent many-body Schrödinger equation will yield the same time-dependent physical charge and current densities, but different gauge-dependent component densities.

The same can be applied to the KS representation. Since, in our considerations above, we knew the initial scalar and vector potentials of the KS system, we may choose a gauge such that all of the time-dependence – including the Hartree and XC potentials – occurs in the vector potential. This makes the time-dependent reverse-engineering approach described above generally valid.

Furthermore, a vector potential calculated in this way need not be used in the same way to time-evolve the KS system: one need only be aware of what the time-dependent vector potential *would* be in this gauge to continue calculating corrections to it, but one still has the freedom to make an additional gauge-transform when time-evolving the KS system. A schematic representation of the reverse-engineering algorithm for time-dependent systems in this gauge is shown in Fig. 3.2.

An alternative choice of gauge is the Coulomb gauge, having $\nabla \cdot \mathbf{A}(\mathbf{r}, t) = 0$. In this gauge, the time-dependent vector potential is uniquely determined by the scalar
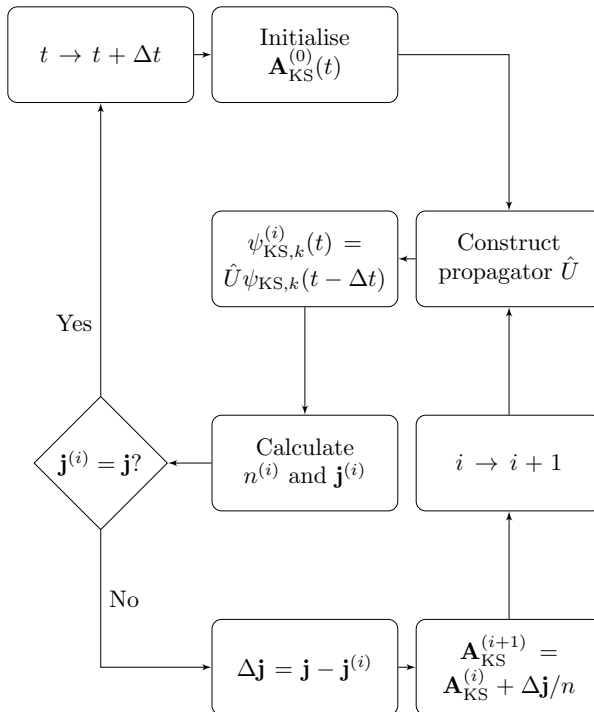
Figure 3.2: **The time-dependent reverse-engineering algorithm.** An initial guess for the KS vector potential is iteratively corrected by calculating the resultant KS physical current density and taking the difference with the exact physical current. The difference is the new correction to the diamagnetic current density which has associated with it a correction to the vector potential. This procedure is repeated until the physical current density, and thus the charge density, is that of the interacting system.

potential and the electric and magnetic fields via

$$\mathbf{E}(\mathbf{r}, t) = -\boldsymbol{\nabla} v(\mathbf{r}, t) - \dot{\mathbf{A}}(\mathbf{r}, t) \tag{3.98}$$

$$\mathbf{B}(\mathbf{r}, t) = \boldsymbol{\nabla} \times \mathbf{A}(\mathbf{r}, t). \tag{3.99}$$

Further, it is possible to make a gauge transformation between scalar and vector potential implementations of the electric field via Eq. 3.96-3.97. For instance, for a system subject to scalar and vector potentials $(v(\mathbf{r}, t), \mathbf{A}_\text{L}(\mathbf{r}, t) + \mathbf{A}_\text{T}(\mathbf{r}, t))$ where $\mathbf{A}_\text{L}(\mathbf{r}, t)$ is a longitudinal vector potential and $\mathbf{A}_\text{T}(\mathbf{r}, t)$ the transverse, one may make a gauge transformation

$$v(\mathbf{r}, t) \to v(\mathbf{r}, 0)$$

$$\mathbf{A}_\text{L}(\mathbf{r}, t) \to \mathbf{A}_\text{L}(\mathbf{r}, t) + \int_{-\infty}^{t} dt' \, \boldsymbol{\nabla} v(\mathbf{r}, t) \tag{3.100}$$

to implement the electric field entirely via the vector potential, or alternatively

$$v(\mathbf{r}, t) \to v(\mathbf{r}, t) + \int_{-\infty}^{\mathbf{r}} d\mathbf{r}' \, \dot{\mathbf{A}}_{\mathrm{L}}(\mathbf{r}', t) \tag{3.101}$$

$$\mathbf{A}_{\mathrm{L}}(\mathbf{r}, t) \to \mathbf{0} \tag{3.102}$$

to implement the electric field entirely via a scalar potential alone. Fig. 3.3 illustrates this algorithm schematically for the latter case.
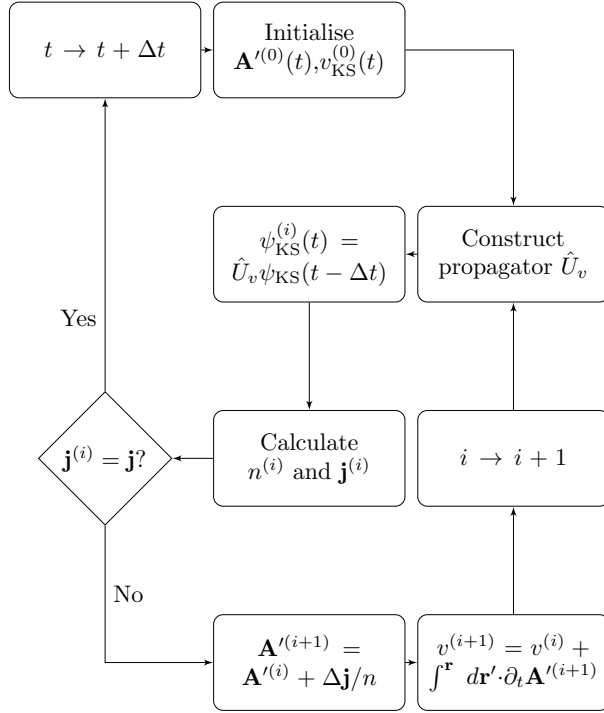
Figure 3.3: **Electric field reverse-engineering algorithm.** An initial guess for the KS vector potential is iteratively corrected by calculating the error in the resultant KS current density. Where the ratio of the error to the charge density is purely longitudinal, the result can be gauge-transformed to yield a corrected scalar potential. The vector potential in this case is an auxiliary quantity for calculation purposes only, and is not included in the time-propagation. This is particularly useful for 1D calculations where there can be no KS magnetic fields.

In conclusion, an iterative scheme for the calculation of the exact time-dependent KS potentials that reproduce the charge and current densities of a nonequilibrium interacting system has been formulated. This reverse-engineering algorithm has the correct stop-condition and is, in principle, applicable to all systems in the absence of magnetic fields. Both this and the steady-state reverse-engineering algorithm will be employed to calculate the exact KS potentials of different kinds of interacting current-

carrying system in the following two chapters.

Chapter 4

Steady-state quantum transport

A steady-state electronic system is one whose physical properties, including the charge and the current density, are not changing with time:

$$\frac{\partial n}{\partial t} = 0 \tag{4.1}$$

$$\frac{\partial \mathbf{j}}{\partial t} = \mathbf{0}, \tag{4.2}$$

either because the system is in its ground state, or else because all transient effects due to a preceding perturbation or disturbance have since decayed.

The steady-state current density is thus limited to being time-independent and, via the continuity equation, in being divergence-free:

$$\nabla \cdot \mathbf{j}(\mathbf{r}) = -\frac{\partial n(\mathbf{r})}{\partial t} = 0. \tag{4.3}$$

The actual current density can be given by the boundary conditions for finite systems, but for periodic structures we can gain no information about the current density without calculating it directly from the electronic wavefunction, which is not practically solvable for systems of more than a few particles. However, because of the time-independence of a steady-state system, which removes the possibility of excitation or de-excitation without external stimulus, the particular case of steady-state systems where the net current is carried by one or two electrons lends itself to representation in quasiparticle theory: the (in principle) exact calculation of elementary excitations of ground-state systems. In this chapter, the excitation we shall study is the addition of a single electron to the lowest-energy unoccupied state of a ground-state N-electron periodic nanowire.

The model self-energy operator governing the quasiparticle will be described in Sec.

4.1 and will be employed throughout. Section 4.2 will study the steady-state quantum wire in 1D and identify a major obstacle of DFT for 1D quantum transport. Section 4.3 will study a three-dimensional nanowire wherein these obstacles may be overcome. The reverse-engineering algorithm for steady-state system described in the previous chapter will be applied to the 3D nanowire where it will be found that the physics involved in exact KS system are strikingly different from those involved in the interacting systems they represent.

4.1   The model self-energy operator

The self-energy operator $\Sigma(\mathbf{r}, \mathbf{r}', \omega)$ remains a difficult quantity to calculate from first principles due to its complexity. Typically, one would begin with a DFT calculation in the local density approximation and employ the resulting wavefunctions and energies as an initial guess for a full GW calculation.

An alternative approach is to model the self-energy operator directly for use in the quasiparticle equation. Godby *et al* [142] found that the difference between LDA-DFT energies and GW quasiparticle energies for silicon and diamond are energy-dependent and take the approximate form of a step function. However, the inclusion of the energy dependence acted only to slightly reduce the band gaps of the two materials, thus they deduced that the most significant character of the self-energy operator that led to band gap errors [143] between GW and DFT calculations of band structures was its nonlocal dependence on position: while $\Sigma(\mathbf{r}, \mathbf{r}', \omega)$ is a function of pairs of spatial coordinates, the exchange-correlation potential $v_{\mathrm{xc}}(\mathbf{r})$ is a function of only one. Indeed, it is typical that DFT potentials that reproduce the correct charge density of a ground-state system do not reproduce also the correct band structure [116].

They further found that the self-energy operators for silicon and diamond were dominated by approximately spherically-symmetric exchange holes centred around $\mathbf{r}' = \mathbf{r}$ whose amplitude was position-dependent. Based on these findings, they proposed the following model form of the operator:

$$\Sigma(\mathbf{r}, \mathbf{r}', \omega) = \frac{f(\mathbf{r}, \omega) + f(\mathbf{r}', \omega)}{2} g(|\mathbf{r} - \mathbf{r}'|) \tag{4.4}$$

where $f(\mathbf{r})$ is chosen to reproduce the correct symmetry. The function $g(|\mathbf{r} - \mathbf{r}'|)$ was shown to be approximately that of the corresponding function for a homogeneous electron gas with the same average electronic density, while f introduces the position-dependence. This hole was found to account for the majority of the nonlocality of the

self-energy operator.

Godby *et al* also found that, to good approximation, the energy-dependence of the self-energy is separable from its nonlocal spatial dependence, such that 4.4 may be further decomposed into

$$\Sigma(\mathbf{r}, \mathbf{r}', \omega) = \frac{f(\mathbf{r}) + f(\mathbf{r})}{2} g(|\mathbf{r} - \mathbf{r}'|) h(\omega). \tag{4.5}$$

One of the benefits of the model self-energy operator is that, whereas the Σ derived from a GW or even full many-body calculation is done so purely numerically, here its physical ingredients are apparent in the construction.

The use of the model self-energy in the GKS scheme was examined by Sanchez-Friera and Godby (2000) [144] and found to improve in many respects on LDA DFT calculations, for instance in linear response theory of the homogeneous electron gas. They demonstrated that the calculation overheads of a GKS calculation using an energy-independent ($h(\omega) = 1$) model self-energy operator were small, with the matrix elements of the operator in reciprocal space given very simply as

$$\langle \mathbf{k} |\Sigma| \mathbf{k}' \rangle = f(\mathbf{k} - \mathbf{k}') \frac{g(|\mathbf{k}|) + g(|\mathbf{k}'|)}{2}, \tag{4.6}$$

where $f(\mathbf{k})$ and $g(k)$ are the spatial Fourier transforms of the real-space functions $f(\mathbf{r})$ and $g(r)$ above. These matrix-elements will be employed later in calculating the self-energy operator for steady-state and nonequilibrium current-carrying systems from whose densities the exact potentials of their Kohn-Sham representations will be reverse-engineered.

In the following study, we consider an infinite wire connected to sink and source electron reservoirs at $z = \pm\infty$ held at the same chemical potential at zero temperature such that the wire has zero current. We raise the chemical potential of the source reservoir slightly with respect to the sink such that an electron propagates through the wire. We model one supercell of this wire, close to the source, via the addition of an electron quasiparticle into the lowest-energy unoccupied state.

Since the electron is added to the lowest-energy state above the Fermi energy, one expects no possibility of inelastic scattering of the electron. Furthermore, in the absence of any time-dependence, while the true self-energy for such a system would be energy-dependent, one would not expect any qualitative difference in the resultant charge and current densities, only small quantitative differences due, for instance, to the modified band gap. As such, we make the approximation that the self-energy operator

is Hermitian and energy-independent, and has a position-dependent nonlocal spatial dependence of the form of Eq. 4.5.

4.2   The one-dimensional nanowire

A nanowire is a structure whose thickness is of the order of the nanometre (10^{-9} m) but whose length is unconfined. As such, all of the current of such a system is constrained to be directed along the axial direction (along the length of the wire) in a steady-state system.

If one ignores or suppresses subband excitations such that all current-carrying electrons are in the lowest subband of the system, nanowires are *pseudo*-one-dimensional systems which are amenable to approximation in one-dimensional calculations. For the purpose of reverse-engineering Kohn-Sham systems, we may consider that the additional degrees of freedom are common between the interacting and the KS systems.

To obtain the charge and current densities of the interacting system from which we may reverse-engineer a Kohn-Sham system, we consider the model self-energy operator of Sec. 4.1 whose matrix elements are given by Eq. 4.6 for a supercell of 10 unit cells of a periodic semiconductor based on silicon, with a self-energy amplitude $F_0 = 4.1$ eV, nonlocal range $w = 2$ a.u and periodicity $a = 4$ a.u.

$$\Sigma(z, z') = \tfrac{1}{2} \left(f(z) + f(z') \right) g \left(|z - z'| \right) \tag{4.7}$$

$$f(z) = -F_0 \left[1 - \cos(2\pi z/a) \right] \tag{4.8}$$

$$g(x) = \frac{e^{-(x^2/w^2)}}{\sqrt{\pi} w}. \tag{4.9}$$

Since the external potential due to the silicon lattice and the Hartree potential will be the same in both the interacting and KS systems, we take $(v_{\mathrm{ext}} + v_{\mathrm{H}} = 0)$. Periodic boundary conditions are applied such that the coupling to the reservoirs occurs at $x = \pm\infty$ and has no effect on the dynamics of the supercell under study other than the injection of the quasiparticle electron. While the system constitutes an open quantum system, insofar as electrons are passing into and out of the supercell, the rate at which electrons enter and exit the supercell are identical and the electron number remains fixed throughout.

The quasiparticle energies and wavefunctions are given by

$$\left(-\frac{1}{2} \frac{\partial^2}{\partial z^2} - \varepsilon_{\mathrm{QP},i} \right) \psi_{\mathrm{QP},i}(z) + \int_{-\infty}^{\infty} dz' \, \Sigma(z, z') \psi_{\mathrm{QP},i}(z') = 0. \tag{4.10}$$

The quasiparticle band structure for these parameters, sampled at the Γ-point (which, here, are integer multiples of $2\pi/L$ where $L = 10 \times a = 40$ a.u.), for the supercell is shown in Fig. 4.1.
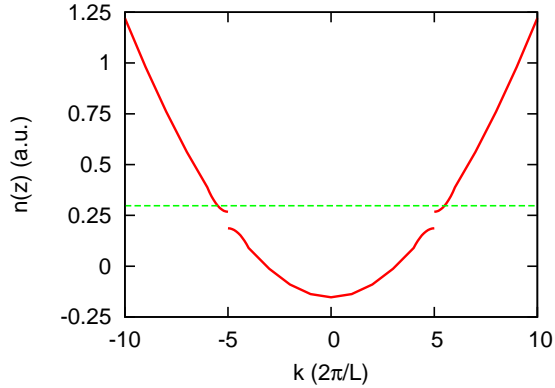
Figure 4.1: **Band structure of 1D model semiconductor.** The ground-state density of Fig. 4.2 is found by summing over all of the single-particle densities for electrons occupying states below the dashed line. The system is filled beyond the band gap, and as such is in a metallic state.

On a discretised grid, the energy spacing between the QP and the Fermi energy will be finite, corresponding to the chemical potential difference between the two reservoirs, μ, which nominally gives the QP a finite, if very long, lifetime. However, on such a grid there are no states for which the QP to decay into, and it is sufficient to note that as the characteristic grid spacing $\Delta \to 0$, the state the electron is added to approaches the Fermi energy.

Fig. 4.2 shows the ground-state charge density of the 1D supercell, where each unit cell contributes one spin-up and one spin-down electron to the ground-state density, with two additional (spin-up and -down) electrons occupying the standing wave at the bottom of the conduction band, giving a total of $N = 22$ electrons in the ground state.

To this ground-state system, an electron quasiparticle is added to the right-going (positive z-direction), lowest-energy unoccupied state. Because of the symmetry of the band structure, this is one of a pair of degenerate 23-electron ground states, the other being the left-propagating (negative z-direction) state. All of the current through the system is then carried by the additional quasiparticle ψ_{QP}.

The current density of a quasiparticle is given by the continuity equation and the
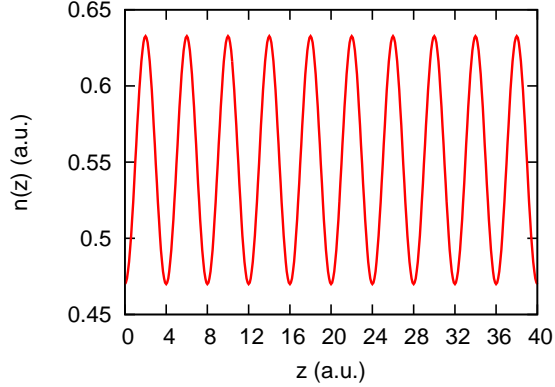
Figure 4.2: **Electron density of one-dimensional ground-state quantum wire.** The supercell consists of 10 unit cells, each contributing 2 electrons (one spin-up, one spin-down) in addition to the two electrons occupying the standing state at the bottom of the conduction band, giving a total of $N = 22$ electrons in the ground state.

quasiparticle equation [145; 146]:

$$
\begin{aligned}
\frac{\partial}{\partial t} n(z) &= \frac{\partial}{\partial t} \psi_{\mathrm{QP}}^*(z) \psi_{\mathrm{QP}}(z) = \psi_{\mathrm{QP}}^*(z) \frac{\partial}{\partial t} \psi_{\mathrm{QP}}(z) + \psi_{\mathrm{QP}}(z) \frac{\partial}{\partial t} \psi_{\mathrm{QP}}^*(z) \\
&= i \left(\psi_{\mathrm{QP}}(z) \left\{ -\frac{1}{2} \frac{\partial^2}{\partial z^2} \right\} \psi_{\mathrm{QP}}^*(z) - \psi_{\mathrm{QP}}^*(z) \left\{ -\frac{1}{2} \frac{\partial^2}{\partial z^2} \right\} \psi_{\mathrm{QP}}(z) \right) \\
&\quad + \int_{-\infty}^{\infty} dz' \ \left(-i \psi_{\mathrm{QP}}^*(z) \Sigma(z, z') \psi_{\mathrm{QP}}(z') + \mathrm{c.c} \right) \\
&= -\frac{\partial}{\partial z} j(z).
\end{aligned} \tag{4.11}
$$

The first bracketed term is the divergence of the standard paramagnetic current density; the second is unique to the self-energy operator. Integrating both sides yields

$$
\begin{aligned}
j(z) &= \frac{1}{2i} \left(\psi_{\mathrm{QP}}^*(z) \frac{\partial}{\partial z} \psi_{\mathrm{QP}}(z) - \psi_{\mathrm{QP}}(z) \frac{\partial}{\partial z} \psi_{\mathrm{QP}}^*(z) \right) \\
&\quad + \int_{-\infty}^{z} dz' \int_{-\infty}^{\infty} dz'' \ \left(i \psi_{\mathrm{QP}}^*(z') \Sigma(z', z'') \psi_{\mathrm{QP}}(z'') + \mathrm{c.c.} \right).
\end{aligned} \tag{4.12}
$$

The resultant current density of the model wire is 0.0234 a.u., and the charge density is shown in Fig. 4.3.

To calculate the Kohn-Sham scalar potential which reproduces the 23-electron charge density of the model interacting system, we employ the van Leeuwen-Baerends procedure [139] in which one begins with an initial guess $v_{\mathrm{KS}}^{(0)}(\mathbf{r})$ which is everywhere

greater than zero and then iteratively corrects it by solving the Kohn-Sham equations:

$$\varepsilon_k \phi_k(\mathbf{r}) = \left\{ -\tfrac{1}{2}\nabla^2 + v_{\mathrm{KS}}^{(i)}(\mathbf{r}) \right\} \phi_k(\mathbf{r}) \tag{4.13}$$

$$n^{(i)}(\mathbf{r}) = \sum_k |\phi_k(\mathbf{r})|^2 \tag{4.14}$$

$$v_{\mathrm{KS}}^{(i+1)}(\mathbf{r}) = \frac{n^{(i)}(\mathbf{r})}{n(\mathbf{r})} v_{\mathrm{KS}}^{(i)}(\mathbf{r}) \tag{4.15}$$

until the error in the KS charge density $n^{(i)}(\mathbf{r})$ falls below a desired tolerance. Since $v_{\mathrm{ext}} + v_{\mathrm{H}} = 0$ for the ground state for both the interacting and KS systems, total KS scalar potential required is comprised of the additional Hartree potential Δv_{H} due to the presence of the electron quasiparticle, and the exchange-correlation potential of the whole system:

$$v_{\mathrm{KS}}(z) = \Delta v_{\mathrm{H}}(z) + v_{\mathrm{xc}}(z). \tag{4.16}$$

Using the above procedure, the accuracy of the KS charge density is such that, for any position z, the error is never in excess of 5×10^{-5} %.

Since there is no external vector potential in the model system, one might expect that the KS representation would also have no KS vector potential, in which case the DFT calculation above would be exact. In fact, this is not the case. Fig. 4.4 shows the current density carried by the quasiparticle and by the KS systems. As can be seen, the physical current density predicted by the DFT calculation falls short of the physical quasiparticle current density by 2.5%, which is very large compared with the typical 10^{-5} % error in the charge density, and is due to the fact that even exact density-functional theory fails to reproduce the semiconductor band structure [118] and thus the electron group velocities.

We can assure ourselves that the error arises from the nonlocality of the self-energy operator by allowing the nonlocal range, w, of the operator to go to zero. Fig. 4.5 shows that, as the nonlocal range is reduced, the error in the DFT current is also reduced. The DFT KS system becomes exact when the nonlocal range is zero and the interacting and KS bands are identical.

Thus the QP system cannot be reproduced by a KS scalar potential alone: if it can be reproduced at all, a vector potential is also necessary, even though there is no equivalent phenomenon in the interacting nanowire. Fig. 4.4 shows the exact vector potential which, within the traditional paramagnetic current-based CDFT of Vignale and Rasolt, along with the DFT scalar potential of Fig. 4.3, reproduces both the charge density and paramagnetic current density (also shown) of the model system. (In the
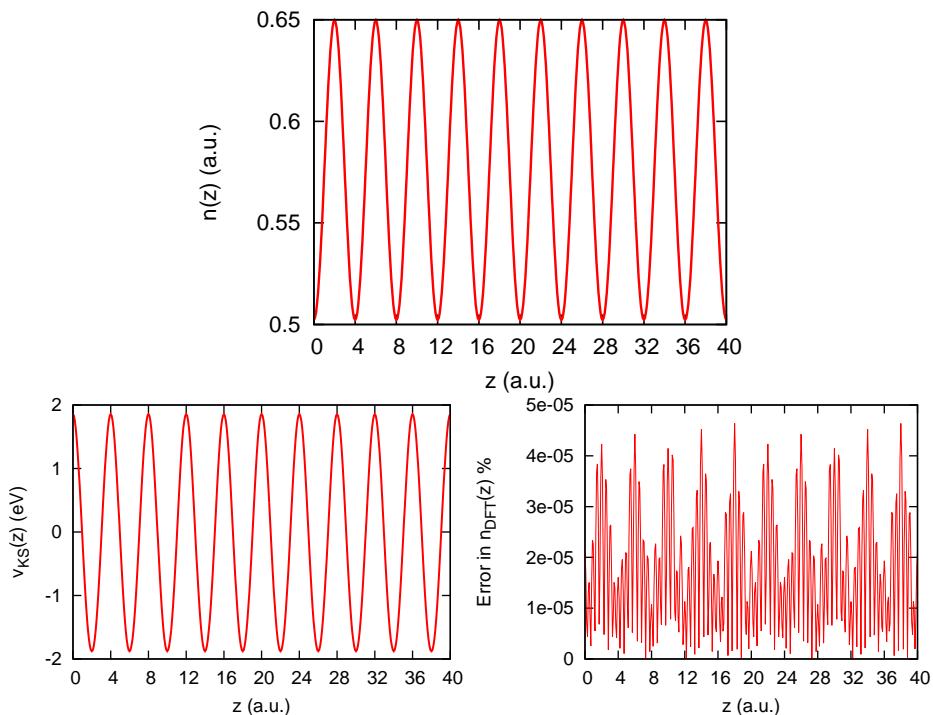
Figure 4.3: The electron density of the model 1D nanowire with the current-carrying electron quasiparticle added (top), and the exact DFT scalar potential which reproduces it (middle). The exact DFT scalar potential was determined by applying the van Leeuwen-Baerends procedure for 250 iterations, with the resulting spatially-dependent percentage error shown (bottom).

absence of an external vector potential, the physical and paramagnetic QP current densities are identical.) However, the *physical* current density of the KS-CDFT system remains that of the KS-DFT system: nothing physical has actually changed because the vector potential corresponds to nothing more than a gauge-transform.

This must always be the case for one-dimensional steady-state systems, since any 1D vector potential may always be written as

$$A_{\mathrm{KS}}(z) = -\frac{\partial}{\partial z}\lambda(z) \tag{4.17}$$

and thus has no nonzero divergence-free contributions. For this reason, steady-state Kohn-Sham systems in one-dimension are unlikely to be accurate when there is any significant difference between the KS band structure and that of the interacting system being modelled, as is often the case. This could potentially make the 1D approximation, which one might expect to capture most of the physics of a pseudo-1D interacting system, very poor in steady-state density-functional theories.

96
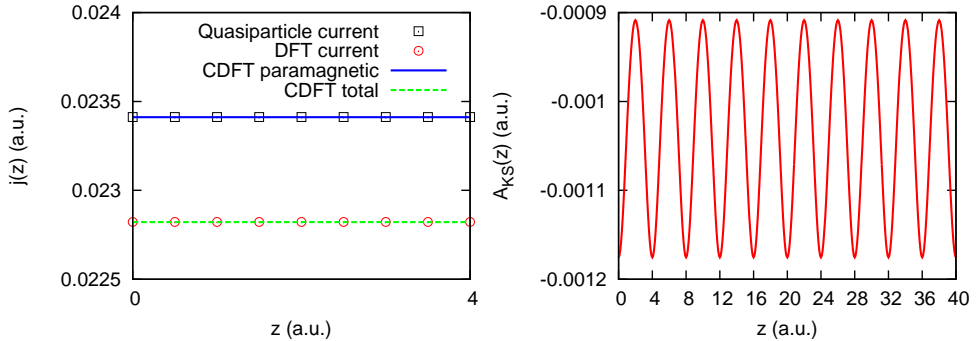
Figure 4.4: **Quasiparticle and DFT steady-state current densities:** The total current densities (left) carried by the quasiparticle (black squares) and the exact KS-DFT system (red circles). The current predicted by exact DFT – which yields the correct charge density – underestimates the true current. Applying the CDFT of Vignale and Rasolt, the paramagnetic current (blue solid) in the presence of a vector potential (right) reproduces the QP paramagnetic current, but the physical current (green dashed) remains unimproved: the vector potential corresponds only to a change of gauge, not to any physical electric or magnetic fields.

4.3   The three-dimensional nanowire

Whereas in a one-dimensional wire there can be no divergence-free nonzero vector potentials, the same is not true in two- and three-dimensional systems. This section will consider a cylindrically-symmetric three-dimensional nanowire similar to the one-dimensional case above but confined radially by a strong but finite r^6 external potential.

We consider again the model self-energy operator, this time of the form

$$\Sigma(\mathbf{r}, \mathbf{r}') = \tfrac{1}{2} \left(f(\mathbf{r}) + f(\mathbf{r}') \right) g(\left| \mathbf{r} - \mathbf{r}' \right|) \tag{4.18}$$

$$f(\mathbf{r}) = -F_0 \left(1 - \cos(2\pi z/a) \right) \tag{4.19}$$

$$g(r) = \frac{e^{-(r^2/w^2)}}{\sqrt{\pi} w}. \tag{4.20}$$

The model self-energy operator is defined for all three dimensions but the periodic part depends only on the axial dimension z. For the nanowire under study, the parameters $F_0 = 4.1$ eV and $a = 4$ a.u. are chosen once again to resemble a silicon nanowire, but a smaller nonlocality of $w = 0.5$ a.u.: approximately the Wigner-Seitz radius $r_{\mathrm{s}} = (3/4\pi n)^{1/3}$ given by the average charge density of the wire.

Mirroring the 1D wire, a supercell of 10 unit cells is defined, each contributing two electrons (one spin-up, one spin-down) with an additional two electrons in the standing state at the bottom of the conduction band, yielding a ground state of $N = 22$ electrons.

As with the 1D wire, we assume that the longitudinal variation of the external
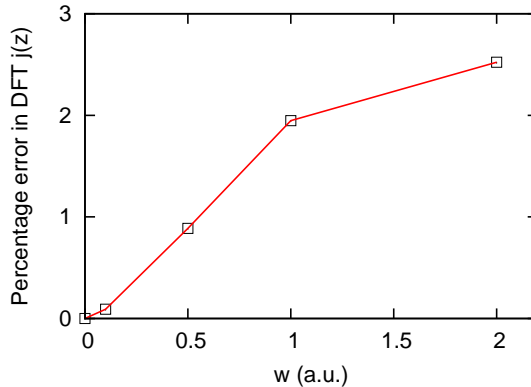
Figure 4.5:   **Current effects of the DFT band-gap error:** The error in the current density predicted by exact DFT. As the nonlocal range, w, of the self-energy operator is reduced, the error in the DFT current density is likewise reduced. At $w = 0$, the two bands converge.

potential will be approximately screened by the electronic charge, and any variation that does exist will be the same in both the interacting system and the KS representation: since we are only interested in the *differences* between the two representations, any contributions to the scalar potential that are the same in both may be ignored. The stronger, confining part of the external potential will *not* be expected to be cancelled completely by the Hartree potential, and thus the sum of the external and Hartree potentials of the ground-state system is taken to be of the form $v_{\text{ext}}(\mathbf{r}) + v_{\text{H}}(\mathbf{r}) = Hr^6$, where H is a parameter controlling the strength of the confinement. H is chosen to high enough to ensure that neither the 22 ground-state electrons, nor the additional quasiparticle, are in any subband other than the lowest: $H = 2\text{eV}/\text{a.u.}^6$ suffices.

As in the 1D case, the electron quasiparticle is added to the lowest-energy, right-propagating unoccupied state. The resulting charge and physical current densities of the model system are shown in Fig. 4.6. As can be seen, the r^6 confining potential
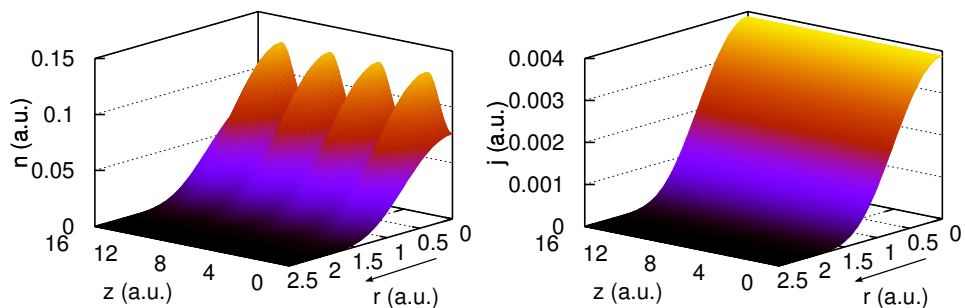
Figure 4.6:   The charge (left) and physical current (right) density of a 3D nanowire comprised of a current-carrying electron quasiparticle added to a ground-state wire. The wire is cylindrically-symmetric, and the outward radial direction is parallel to the arrow.

ensures that the charge and current density decay quickly to zero with increasing radial distance r from the centre of the wire such that we may focus on the region $r \leq 2$ a.u.

The Kohn-Sham scalar potential which reproduces the model nanowire electron density is found again by the van Leeuwen-Baerends procedure, starting from an initial guess that is equal to the self-energy operator when the nonlocal range $w = 0$. Because the charge densities of both the model and KS systems decay to zero, convergence with the van Leeuwen-Baerends procedure alone is more difficult, so the procedure is augmented by a simple, practical iterative scheme which gives corrections to the potential of

$$v_{\text{KS}}^{(i+1)}(\mathbf{r}) = v^{(i)} + \mu \left(n_{\text{KS}}^{(i)}(\mathbf{r}) - n(\mathbf{r}) \right),$$ (4.21)

where μ is a controllable parameter, $n(\mathbf{r})$ is the exact charge density of the model system, and $n_{\text{KS}}^{(i)}(\mathbf{r})$ is the charge density of the KS system having zero vector potential and a scalar potential $v^{(i)}(\mathbf{r})$. The algorithm behaves asymptotically convergent for a fixed μ, but gives much better convergence when used in conjunction with the van Leeuwen-Baerends procedure, taking us sufficiently close to the exact DFT potential.

The two procedures described above were applied iteratively until the maximum spatially-dependent error in the KS charge density was reduced to 0.005%. The KS scalar potential which reproduces the model system electron density is shown in Fig. 4.7.
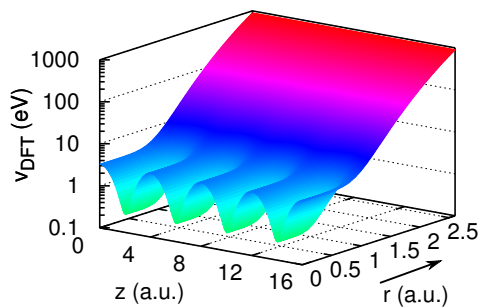
Figure 4.7: The KS scalar potential which, in the absence of a KS vector potential, reproduces the model system's electron density to an accuracy of, at worst, 0.005%.

The error in the KS charge density at each iteration of the calculation of the KS scalar potential can be quantified as

$$\epsilon_n = \sqrt{\frac{\int d\mathbf{r} \left(n(\mathbf{r}) - n_{\text{KS}}^{(i)}(\mathbf{r}) \right)^2}{V}}.$$ (4.22)

where V is the volume of the supercell. Fig. 4.8 shows a logarithmic plot of how this quantity changes with each iteration, first via the van Leeuwen-Baerends procedure, then, from $i = 133$ onwards, via Eq. 4.21. One can see that, whereas in the 1D case the van Leeuwen-Baerends procedure was quickly convergent for all iterations, the fact that the charge density is finite in the radial direction and the procedure depends inversely on this quantity limits the improvements made by it very early on, at about $i = 10$.

The resultant KS current density again falls short of the current density of the model system governed by the nonlocal self-energy operator by 5%, an even larger error than in the one-dimensional case. This is again due to the differences in the band structures of the two systems: the gradient of the band structure in vicinity of the electron quasiparticle determines the group velocity of the quasiparticle and thus the current density (see Fig. 4.9).

Applying the steady-state reverse-engineering algorithm to the nanowire we can now find corrections to the KS vector potential that have divergence-free contributions, corresponding to a magnetic field, with the aim of reproducing the *physical* current density of the nanowire.

Once again, we can quantify the error in the KS current density at each iteration of the reverse-engineering algorithm as

$$\epsilon_j = \sqrt{\frac{\int_V \; d\mathbf{r} \; \left(\mathbf{j}(\mathbf{r}) - \mathbf{j}_{\text{KS}}^{(i)}(\mathbf{r})\right)^2}{V}}. \tag{4.23}$$

This error is shown in Fig. 4.10 for each iteration of, first, the DFT calculation and, from $i = 150$, the CDFT reverse-engineering calculation. During the DFT calculation, the current density very quickly becomes insensitive to any improvement in the charge density. The reverse-engineering algorithm, on the other hand, provides sudden and exponential improvement to the current density, and the final accuracy of the KS current density is 10^{-4} %.

Fig. 4.11 shows the vector potential calculated via this procedure that ensures that both the charge and *physical* current density are those of the model system, along with the corresponding magnetic field $\nabla \times \mathbf{A}$. (In general, it would be necessary to recalculate the scalar potential as well, since the presence of a magnetic field will change the charge density of the system. As it happens, in this case the deformation of the charge density due to the magnetic field is very small, and the scalar potential of the DFT calculation is correct to a very good approximation, with $\epsilon_n = 1.3 \times 10^{-7}$, compared to the exact DFT value of 2.6×10^{-8}.)
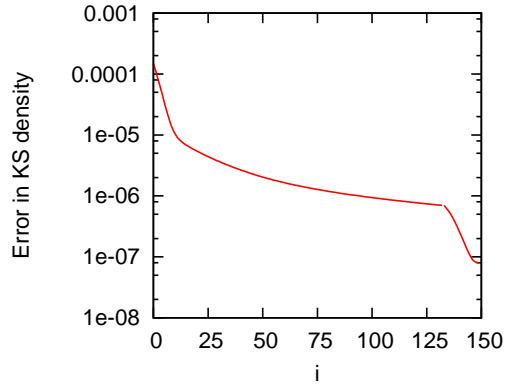
Figure 4.8: The error ϵ in the KS charge density as the exact DFT calculation converges to within the accepted error. The van Leeuwen-Baerends procedure becomes limited very quickly (around $i = 10$) but does not diverge. At $i = 130$, the calculation switches from the van Leeuwen-Baerends procedure to that of Eq. 4.21 to bring us sufficiently close to the exact DFT potential.
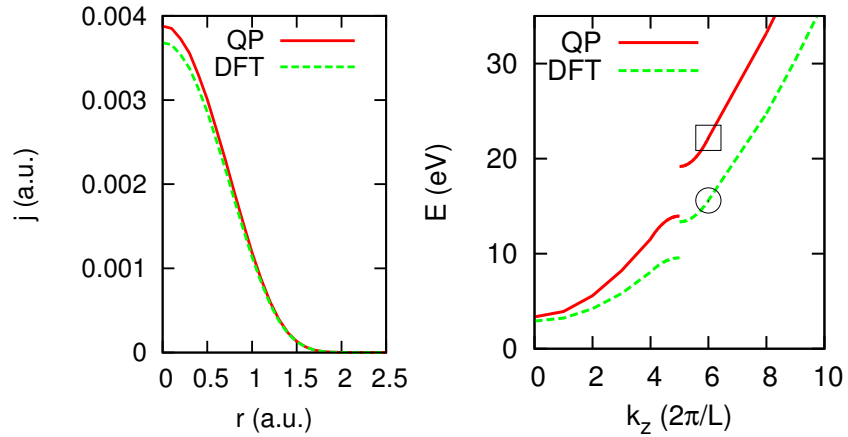
Figure 4.9: The radial dependence of the physical current density (left) for the quasiparticle (red solid) and KS-DFT system (green dashed). The DFT calculation underestimates the current density by 5%. This underestimate is caused by the difference in band structures (right) of the two systems: the QP and KS band structures have different gradients in the vicinity of the highest occupied electron state (denoted by a square and circle respectively.
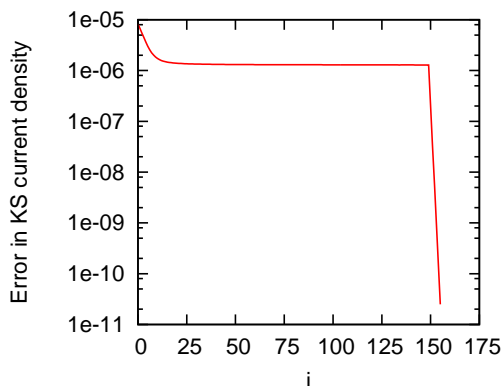
Figure 4.10: The error ϵ_j for each iteration of the DFT calculation ($i < 150$) and of the CDFT reverse-engineering algorithm ($i \geq 150$). As can be seen, the current density quickly becomes insensitive to corrections in the scalar potential in the absence of an XC vector potential, and converges suddenly and exponentially toward the desired accuracy as that vector potential is calculated.

Like the interacting nanowire, the exact KS state which reproduces its charge and current density is degenerate: there is a left-propagating KS state that has the same energy subject to the same KS external potentials. However, unlike the interacting nanowire, this left-propagating degenerate state does not have the same current density with the opposite sign: that is, it is not the corresponding left-propagating state of the interacting nanowire itself. The degeneracy of the nanowire has been lifted by the current-sensitivity of the KS vector potential, but the vector potential has introduced a new KS degeneracy (see Fig. 4.12).

This can be compared to the XC vector potential which is given by the Vignale-Rasolt functional in Eq. 2.120 by fitting the magnetic susceptibility of the functional to yield the best approximation to the actual current density. Finding an approximate susceptibility of $b = 0.35$ a.u., the resulting VR vector potential is shown in Fig. 4.13. While the VR functional correctly predicts that the vector potential is parallel to the current density, and fitting the magnetic susceptibility ensures that the potential will be on a similar scale to the exact, it is qualitatively very different to the potential yielded by the reverse-engineering algorithm, demonstrating a much stronger radial dependence that would have a much stronger associated XC magnetic field. However, the VR functional was derived from considering the homogeneous electron gas and, as such, is ill-suited to finite systems, particularly due to the inverse square relationship to the charge density which very quickly goes to zero with increasing radius.

While the individual electrons in a KS system have no physical meaning in and of themselves, properties of the electronic states, such as the energy level differences probed in absorption and emission calculations, are often taken to be analogous to
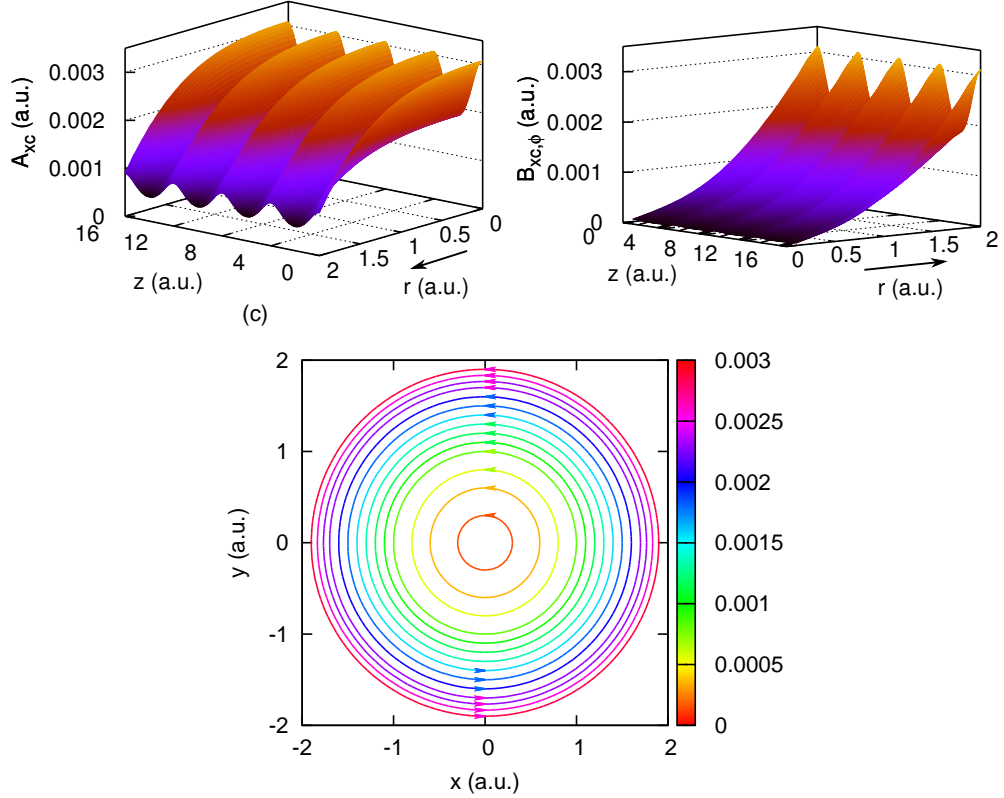
Figure 4.11: The exchange-correlation vector potential of the exact KS-CDFT representation of the model nanowire (top left). Only the axial (z-) component of the vector potential is nonzero. This corresponds to a purely azimuthal XC magnetic field (top right). The field resembles a Biot-Savart magnetic field arising due to the current, but is oppositely-directed (bottom) and increases radially outward. The radial increase in the strength of the field is due to the similarly radially-increasing electric field of the confining potential.

their real, interacting counterparts. Given that there were no external magnetic fields in the model system, it is striking how different the KS electrons are to those of the model system, engaging as they do in qualitatively different phenomena. Two cases in point are the sources of the physical KS current density and the electrons involved in carrying it. In the interacting nanowire, the net current was purely paramagnetic and carried only by the quasiparticle. In the KS representation of the same system, part of the current is paramagnetic and part of it is diamagnetic. Furthermore, electrons in *all* of the KS energy levels carry some of the paramagnetic current density, not just the highest-energy occupied state, as can be seen in Fig. 4.14 which plots the total current density $\mathbf{j}_{z,\mathrm{val}}(\mathbf{r})$ of the 22 lowest-energy electrons.

The distribution of the current across the electrons in the system is not the only
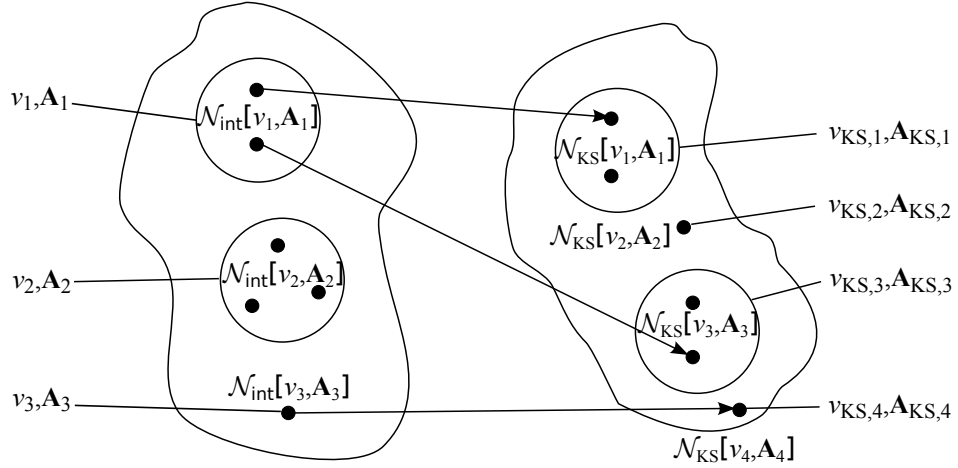
Figure 4.12: **Degeneracies in interacting systems and their Kohn-Sham representations.** Certain external potentials have multiple ground-state solutions with the same energies but different ground-state densities. In their KS representations, systems that are degenerate in the interacting world are not necessarily degenerate with each other in the KS world, but may be degenerate with other KS states. For example, the external potentials $v_1, \mathbf{A}_1$ yield two degenerate states in the set $\mathcal{N}_{\text{int}}[v_1, \mathbf{A}_1]$. The KS representations of these states are not degenerate with each other, however are yielded by KS potentials, here $v_{\text{KS},1}, \mathbf{A}_{\text{KS},1}$ and $v_{\text{KS},3}, \mathbf{A}_{\text{KS},3}$ that themselves have degenerate KS ground states.

major qualitative difference between the KS electrons and those of the model system. In the model system, the ground state to which the electron quasiparticle is added consists of equal numbers of spin-up and spin-down electrons yielding, in the absence of any external magnetic fields, no net magnetisation. The electron quasiparticle then carries all of the net magnetisation of the system. Since there are no external magnetic fields coupling to quasiparticle spin via a Stern-Gerlach interaction, and in the absence of spin-orbit interactions, the nanowire is spin-degenerate: the spin does not enter into the quasiparticle equation.

In the KS representation, there is both a net magnetisation and an external magnetic field. Thus if the quasiparticle magnetisation is such that $\mathbf{B} \cdot \mathbf{m}$ is nonzero, there will be a Stern-Gerlach interaction in the KS system: a phenomenon completely absent in the interacting system. (Because $\mathbf{B}_{\text{xc}}$ is purely azimuthal, the radial and axial components of the spin will not couple to it and may be neglected.) The KS equations for the
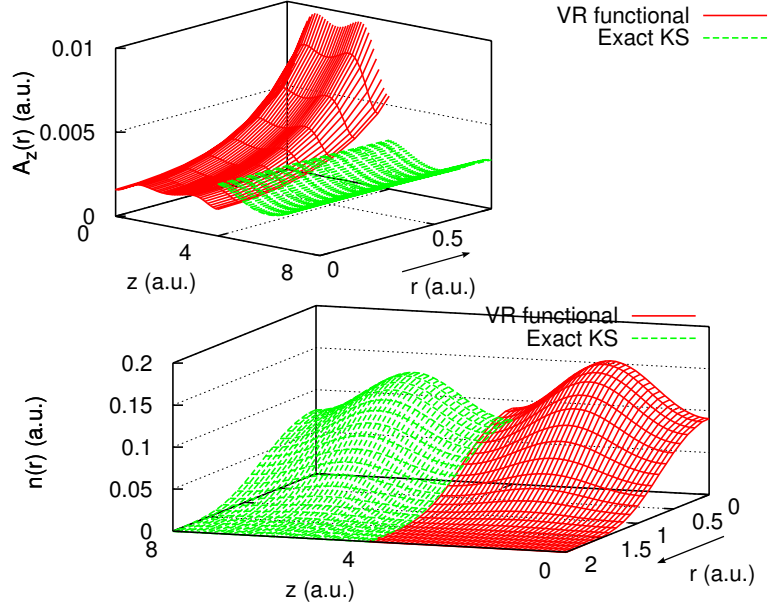
Figure 4.13: **Comparison of the exact vector potential and the VR approximation.** The XC vector potential (top) predicted by the Vignale-Rasolt functional for a fitted magnetic susceptibility of $b = 0.35$ a.u. over a single unit cell with the reverse-engineered potential also shown for comparison. The predicted vector potential is qualitatively different from the exact, showing much more radial dependence corresponding to a much stronger XC magnetic field, dwarfing the radial variation of the exact potential. The VR functional is based on the homogeneous electron gas and is ill-suited to finite systems, especially strongly-confined ones. As a result, it does not predict the correct charge density for the system (bottom).

system are now

$$\left(\tfrac{1}{2} \left[\hat{\mathbf{p}} + \mathbf{A}_{\mathrm{KS}}(\mathbf{r}) \right]^2 + v_{\mathrm{KS}}(\mathbf{r}) + \mu_{\mathrm{B}} \mathbf{B}_{\mathrm{KS}}(\mathbf{r}) \cdot \hat{\boldsymbol{\sigma}} \right) \psi_{\mathrm{KS},i}(\mathbf{r}) = \varepsilon_i \psi_{\mathrm{KS},i}(\mathbf{r}) \tag{4.24}$$

$$n(\mathbf{r}) = \sum_{i=1}^{N} |\psi_{\mathrm{KS},i}(\mathbf{r})|^2 \tag{4.25}$$

$$\mathbf{j}_{\mathrm{KS,d}}(\mathbf{r}) = \mathbf{A}_{\mathrm{KS}}(\mathbf{r})n(\mathbf{r}) \tag{4.26}$$

$$\mathbf{m}(\mathbf{r}) = \mu_{\mathrm{B}} \sum_{i=1}^{N} \psi_{\mathrm{KS},i}^*(\mathbf{r}) \hat{\boldsymbol{\sigma}} \psi_{\mathrm{KS},i}(\mathbf{r}), \tag{4.27}$$

where $\mathbf{m}(\mathbf{r})$ is the magnetisation of the KS system, equal to that of the quasiparticle. Thus the KS Hamiltonian that has, as its N-electron ground state, a charge and physical current density equal to that of the model nanowire must have spin-dependent terms in order to cancel the effect of the Stern-Gerlach interaction. Since the vector potential is fixed via the charge and diamagnetic current densities, the presence of a nonzero
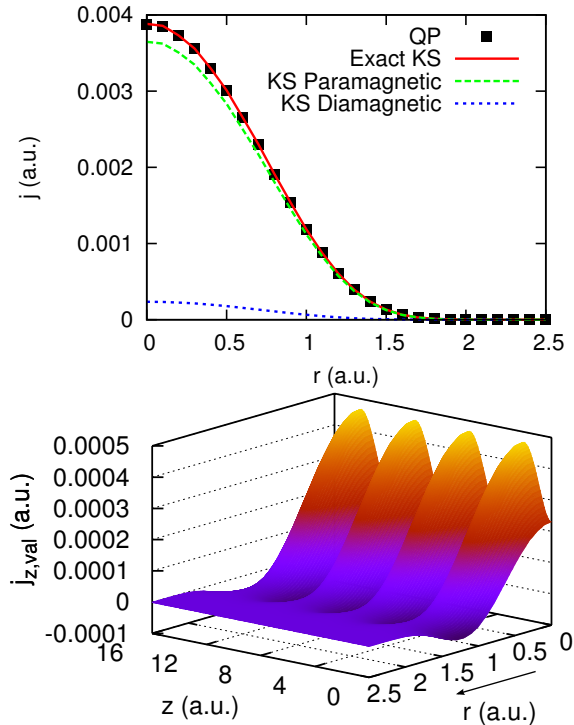
Figure 4.14: The physical current (top) of both the quasiparticle (squares) and exact KS (red solid line) systems. While the quasiparticle current is purely paramagnetic, in the KS system which reproduces it the current is composed of both paramagnetic (green dashed) and diamagnetic (blue dotted) components. A small part of the net KS paramagnetic current density is now also carried by the electrons that carried no net current in the model system or the ground-state KS or current-carrying KS-DFT representations (bottom).

Stern-Gerlach term must be accompanied by an additional contribution to the KS scalar potential that depends both on the net KS spin and the current density, as well as the charge density.

Generally, any nonzero contribution to the Stern-Gerlach interaction will depend on the spatial position, however for a simple illustration we will take the magnetisation of the quasiparticle to be such that the total spin of the KS system has an azimuthal component that is independent of position and with a value of $s_{\mathrm{KS},\theta} = \frac{1}{2}$. Figure 4.15 shows the resulting additional KS scalar potential required to counteract the effects of the Stern-Gerlach interaction, leaving the ground-state KS physical densities as per the interacting model system.

As can be seen, the effect is small because the magnetisation of the nanowire and the XC magnetic field are small, and therefore in this case can be neglected with little loss of accuracy. For more highly magnetised systems or those requiring stronger
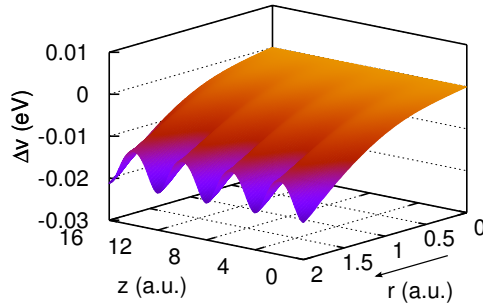
Figure 4.15: **Exchange-correlation Stern-Gerlach effects:** The additional KS scalar potential required for $s_{\mathrm{KS},\theta} = \frac{1}{2}$ due to a spin-dependent Stern-Gerlach interaction in the presence of the effective external KS vector potential $\mathbf{A}_{\mathrm{KS}}$. The XC scalar potential has an intrinsic functional dependence on the current density and the magnetisation, as well as the charge density.

XC magnetic fields due to greater DFT underestimates (or, possibly, overestimates) in Kohn-Sham current density, the effect will be proportionally larger, meaning that the XC scalar potential has a potentially strong functional dependence on the current density and magnetisation, as well as the charge density.

In conclusion, the exact KS system which reproduces the charge and current density (and, more generally, the magnetisation) of an interacting steady-state system is qualitatively and strikingly different from that interacting system even in a very simple case. In the absence of external magnetic fields, the KS representation will generally require an effective external magnetic field that depends on both the charge and the current density. Degenerate interacting systems where different states will correspond to different current densities will therefore not yield likewise-degenerate states of the same KS Hamiltonian. Furthermore, the presence of the intrinsic KS magnetic field will yield a Stern-Gerlach interaction that may be entirely absent in the interacting system. In order to reproduce the correct charge and current density in the presence of such an effective Stern-Gerlach interaction, a spin- and current-dependent KS scalar potential is required and thus spin-degenerate states in the interacting system have KS representations that are not degenerate states of the same KS Hamiltonian. The Stern-Gerlach interaction gives XC scalar potential a potentially strong functional dependence on the current density and magnetisation, as well as the charge density.

All of this is in stark contrast to the approach one would take in simply matching the paramagnetic current densities of the interacting and KS systems which, as we have seen, might result in nothing more than a gauge-transformation of a DFT calculation. The above study demonstrates the consequences of the scheme by which we map Kohn-Sham potentials onto densities. The XC energy functional, for instance, is gauge-

invariant [124] and thus the XC vector potential functional Eq. 2.120 is likewise gauge-invariant, and yet the choice of mapping gauge-variant densities onto KS potentials may yield XC vector potentials that are purely longitudinal.

This contradiction is removed when we map physical, gauge-invariant densities to KS potentials, since longitudinal vector potentials do not enter into such maps. This does introduce an ambiguity into the KS potentials: for a given KS system such as the one calculated above there exists an infinitum number of alternatives which yield the same physical densities and XC energy, analogous to the additive constant in the scalar potential. It remains unshown, however, whether there might exist an alternative set of KS electromagnetic fields that yield the same physical densities but different ground-state wavefunctions, a question that has been shown in the previous two chapters to be immune to a Hohenberg-Kohn-like treatment.

Chapter 5

Time-dependent quantum transport

In the previous chapter we saw that, even for interacting systems free from magnetic fields, a Kohn-Sham magnetic field is generally required to describe them exactly using the KS scheme. We also saw the application of the time-independent form of the reverse-engineering algorithm to the realm of steady-state current-carrying systems, and found that it was very quickly convergent and highly accurate.

This chapter will focus on the description of systems that are time-dependent without being subject to time-dependent external fields, extending the studies of the one-dimensional steady-state nanowire which was found to be not describable exactly in the KS scheme. Because 1D steady-state currents cannot be reproduced exactly in 1D KS systems, we shall only consider the longitudinal part of the current density.

The systems under study will once more be based on quasiparticle calculations employing the model self-energy operator. To ensure that the current density has no nonzero time-independent parts, and that the system will be in the nonequilibrium regime even in the absence time-dependent external potentials, we will consider localised quasiparticle wavepackets with positive crystal momentum added to a ground-state infinite, semiconducting wire, again based on the properties of silicon. The quasiparticle wavepacket will be able to propagate through the wire due to its intrinsic momentum and in the absence of applied fields.

In an exact calculation, a quasiparticle added to a ground-state system should be in an eigenstate of the time-independent quasiparticle equation, a criterion which yielded the steady-state systems studied in the previous chapter. However, the electron wavepacket is a more realistic description of electrons in devices. In order to construct

a nonequilibrium system based on the addition of a quasiparticle wavepacket, we relax this restriction slightly and construct the wavepacket as a weighted sum over a small range of pure quasiparticle states. So long as the range of eigenstates summed over is small, the quasiparticle still approximately has the crystal momentum of a pure state and we remain in the quasiparticle approximation.

The criteria of time-independent fields and time-dependent densities also necessitates that we choose an initial time $t = 0$ at which the system is already in an excited state. This is fully consistent with the Runge-Gross theorem, which states that the time-dependent external potential is a unique functional of the time-dependent charge density and the initial wavefunction of the system which need not be a ground state. As has been demonstrated by Maitra and Burke [110], the full wavefunction at any given time t_1 encodes within it all memory of the history of the system from $t < t_1$: if we consider a system described by an initial states $\Psi(t_0)$ and a time-dependent charge density $n(t \geq t_0)$, the time-dependent potential is uniquely defined for $t \geq t_0$. If that system passes through the state $\Psi(t_1)$ at time t_1, we could also uniquely define the time-dependent potential over $t \geq t_1$ from that state and the charge density $n(t \geq t_1)$ without access to the wavefunction at times $t < t_1$.

This freedom to choose an initial state with the correct charge density will be exploited here. However, in not starting from a ground state, this freedom also introduces an initial-state dependence for our potentials: a different initial state with the same density will yield a different time-dependent potential. That said, the choice of a ground state for our system at $t = t_0$ is hardly less arbitrary unless we wish to study transient effects in perturbed ground states (which, here, we do not) since the freedom of choice of an initial state at t_1 corresponds to the myriad ways we might time-evolve a t_0 system into that state, including a potentially infinite number of means by which one could reach that state from a ground state system.

The self-energy operator employed in the steady-state calculation was nonlocal but Hermitian, appropriate for a quasiparticle added to the lowest unoccupied energy level above the Fermi energy. The nonequilibrium quasiparticle will not occupy the lowest available energy level but a range of states. As such, one would expect such a QP to have a finite lifetime, however large. In order to separate out the effects of the nonlocal dependence of the SE and those pertaining to correlations, we will first investigate the behaviour of QP under the assumption of approximately infinite lifetime.

This will then be compared to a more realistic QP model that incorporates finite-lifetime effects. Within the restrictions of conservation of energy, momentum and electron number, we can calculate the final state to which the system tends with time

as a statistical distribution, i.e. an ensemble represented by a density-matrix, given by Fermi-Dirac statistics. Separating out the Hermitian and non-Hermitian parts of the self-energy operator, we can then calculate the equation of motion for the time-dependent density matrix, from which we can calculate the time-dependent charge and current densities as inputs to the time-dependent reverse-engineering algorithm.

First, in Sec. 5.1, we will introduce the stable but nonlocally-interacting system being modelled using quasiparticle theory, including the ground-state system the quasiparticle will be added to. Then in Sec. 5.2 we will examine the means by which we can, in the Kohn-Sham scheme, reproduce the ground and initial states of the model wire, the latter of which, as has been discussed above, has multiple solutions. We will also see that the KS system will be unable to reproduce the correct time-dependent charge density of the interacting system, which is itself free from time-dependent external fields, without a time-dependent KS potential. In Sec. 5.3 we will investigate how the time-dependent form of the reverse-engineering algorithm operates in the nonequilibrium regime, what obstacles there are to overcome, how it converges. Sec. 5.4 will look at the resultant time-dependent KS scalar potentials for a given initial KS state, its physical meaning (in the Kohn-Sham universe), which aspects are captured by existing functionals and how it might be approximated by future functionals as well as a cursory examination of the initial-state-dependence of the potential.

In Sec. 5.5, we will calculate the time-dependent charge and current densities of a QP subject to a non-Hermitian, nonlocal but energy-independent self-energy operator. The KS potentials required to reproduce these densities will be separated into two kinds: the first, studied in Sec. 5.7, will be based on a QP that is already decaying at $t = 0$ with a corresponding initial KS state, and the time-dependent KS potentials required to ensure the wavepacket decays with the correct time-dependence; the second, studied in Sec. 5.6, will study a QP that is decaying infinitesimally after $t = 0$ with a corresponding KS state, the KS potential that is required to induce the correct decay, and the initial-state-dependence of the time-dependent KS potential.

A modified version of this work appeared in Ramsden and Godby, 2012 [147].

5.1   The nonequilibrium quasiparticle

The work in this chapter will focus on the study of a single time-dependent system comprised of a localised quasiparticle wavepacket added to a ground-state, 1D semi-conducting nanowire modelled on silicon. We employ once more the model self-energy

operator used in the previous chapter

$$\Sigma(x, x') = \frac{f(x) + f(x')}{2} g(|x - x'|) \tag{5.1}$$

where

$$f(x) = -F_0 \left[1 - \cos(2\pi x/a)\right] \tag{5.2}$$

$$g(x) = \frac{1}{w\sqrt{\pi}} \exp\left(-\left(\frac{x}{w}\right)^2\right). \tag{5.3}$$

$f(x)$ introduces the periodicity of the self-energy operator present in periodic systems, with amplitude $F_0 = 4.1$ eV and unit cell length $a = 4$ a.u., and $g(x)$ introduces the nonlocality of the self-energy via a Gaussian broadening function of average range $w = 2$ a.u.

The model nanowire consists this time of a supercell of 20 unit cells, modelling an infinite wire via the use of periodic boundary conditions, each contributing one spinless electron to the total ground-state charge density. The system is sampled at the Γ-point, thus each electron is normalised to a region the size of the supercell, and the occupied states exactly fill the semiconductor valence band. The single-particle electronic states of the system are given by the quasiparticle equation which is, once again,

$$\left[-\tfrac{1}{2}\nabla^2 + v_{\text{ext}}(x) + v_{\text{H}}(x) - \epsilon_k\right] \phi_k(x) + \int_{-\infty}^{\infty} dx' \, \Sigma(x, x')\phi_k(x). \tag{5.4}$$

As before, since the external and Hartree terms are the same in both the QP and KS systems, we take $v_{\text{ext}} + v_{\text{H}} = 0$.

The band structure of this system is identical to that of the 1D steady-state system shown in 4.1. However, the longer supercell length and the choice of spinless electrons in the ground state being employed here yield a different charge density (more precisely, exactly half the ground-state density of the steady-state system for twice as many unit cells), which is shown in Fig. 5.1.

Into the centre of the supercell, the quasiparticle wavepacket is injected and allowed to propagate under its own finite crystal momentum. The wavepacket is constructed as a weighted sum over the right-propagating states of the first excited band of the semiconductor. Sampling at the Γ-point for a 20-atom supercell gives a choice of nine such available unoccupied states. The occupation numbers for the quasiparticle were selected via numerical optimisation using Powell's conjugate direction method [148], minimising the density of the resulting wavepacket for only the first two and last two
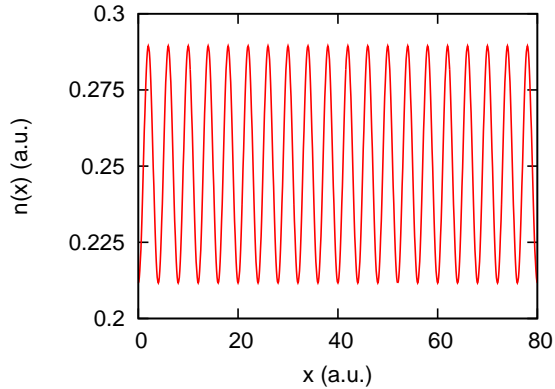
Figure 5.1:   **Charge density of the ground-state semiconducting nanowire.** The ground state is defined over a supercell of 20 unit cells with periodic boundary conditions, each unit cell corresponding to a silicon ion which contributes one spinless electron to the total density.

unit cells of the supercell. This allows the quasiparticle to nbe localised enough to ensure a localisation of the current density, but large enough to ensure the quasiparticle has a well-defined crystal momentum. The coefficients of the right-going pure quasiparticle states are shown in Fig. 5.2 and yield the wavefunction

$$\psi_{\mathrm{QP}}(x, t_0) = \sum_k c_k \phi_k(x). \tag{5.5}$$

The density of the initial quasiparticle wavepacket is shown in Fig. 5.3 below.
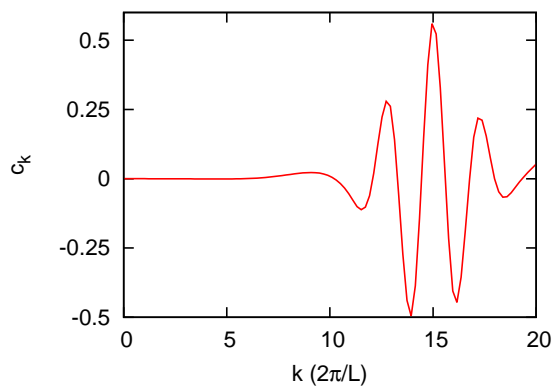
Figure 5.2:   **The quasiparticle wavepacket coefficients of pure Bloch states.** The quasiparticle wavepacket is constructed as a weighted sum of pure Bloch-wave quasiparticle states whose coefficients, shown here, are calculated by minimising the quasiparticle density in the first and last two unit cells of the supercell.

Thus constructed, only the wavepacket need be time-evolved via the time-dependent
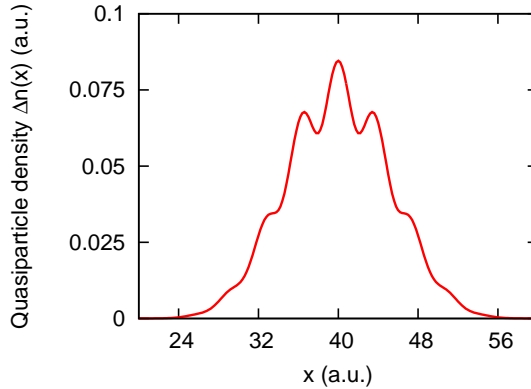
Figure 5.3: **The initial quasiparticle wavepacket density.** The quasiparticle wavepacket is constructed as a weighted sum over right-propagating eigenstates of the quasiparticle equation for the chosen self-energy operator. The wavepacket begins in the centre of the supercell and is allowed to propagate freely.

quasiparticle equation

$$i\frac{\partial \psi_{\mathrm{QP}}(x,t)}{\partial t} = -\tfrac{1}{2}\nabla^2 \psi_{\mathrm{QP}}(x,t) + \int_{-\infty}^{\infty} dx' \; \Sigma(x,x')\psi_{\mathrm{QP}}(x',t) = \hat{H}_{\mathrm{QP}}\psi_{\mathrm{QP}}(x) \qquad (5.6)$$

since the electrons in the valence band are already in eigenstates of the quasiparticle equation and, as such, will only change in time by a physically meaningless phase. The Crank-Nicolson method [149; 150; 151] is employed to solve the time-dependent quasiparticle equation such that, for a known wavefunction at time t, the unknown wavefunction at time $t + \Delta t$ is given by

$$\left(1 + \left(\tfrac{1}{2}i\Delta t \hat{H}_{\mathrm{QP}}\right)\right)\psi_{\mathrm{QP}}(x, t+\Delta t) = \left(1 - \left(\tfrac{1}{2}i\Delta t \hat{H}_{\mathrm{QP}}\right)\right)\psi_{\mathrm{QP}}(x, t). \qquad (5.7)$$

The Crank-Nicolson method was chosen for its unconditional stability [152] and norm-conservation. It is also second-order in time, and thus can be made highly accurate with a sufficiently small time-step Δt. In this calculation, $\Delta t = 4 \times 10^{-3}$ a.u. is chosen. A second benefit of using such a small time-step is that, with such a fine discretisation of the timeline, the continuity equation still holds to good approximation.

The charge density of the time-dependent quasiparticle at a given time t is, as usual, the absolute square of the quasiparticle wavefunction $|\psi_{\mathrm{QP}}|^2$, while the physical current

density of the quasiparticle, as in Sec. 4.2, is

$$j_{\mathrm{QP}}(x,t) = \frac{1}{2i}\left(\psi_{\mathrm{QP}}^*(x,t)\partial_x\psi_{\mathrm{QP}}(x,t) - \psi_{\mathrm{QP}}(x,t)\partial_x\psi_{\mathrm{QP}}^*(x,t)\right)$$
$$+ \int_{-\infty}^{x} dx' \int_{-\infty}^{\infty} dx'' \; i\psi_{\mathrm{QP}}^*(x',t)\Sigma(x',x'')\psi_{\mathrm{QP}}(x'',t) + \text{c.c..} \qquad (5.8)$$

Snapshots of the resulting time-dependent charge density of the quasiparticle, as well as the corresponding time-dependent current density, after 1, 75 and 150 time-steps is shown in Fig. 5.4. Over this small amount of time, the quasiparticle has not propagated very far, but the manner by which it does so is already evident. The wavepacket does not move as a rigid mass, or even approximately so; rather the propagation arises due to the density to the right of the centre of mass growing and the density to the left attenuating with time. The current density, on the other hand, maintains its shape at all times and simply translates along the wire rigidly with time.
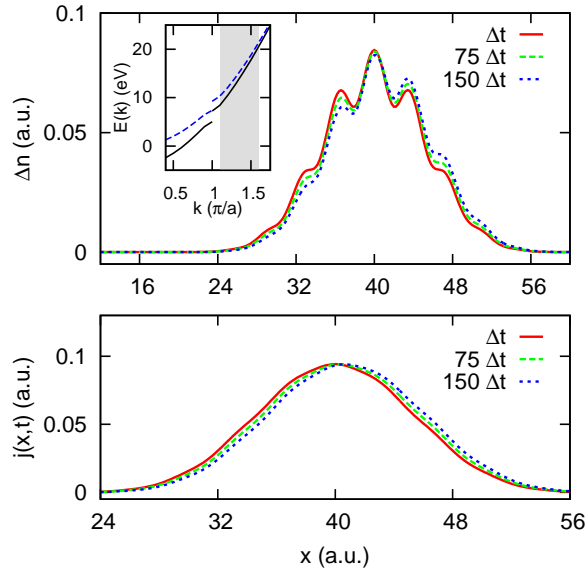
Figure 5.4: **Time-dependence of the quasiparticle wavepacket.** The quasiparticle wavepacket is time-evolved under fixed conditions and the density is captured at snapshots (above) in time at $t = \Delta t$ (red solid), $75\Delta t$ (greed dashed) and $150\Delta t$ (blue dotted). The construction of the wavepacket, over only right-propagating eigenstates of the quasiparticle equation (inset) ensures that quasiparticle remains localised and propagates in the positive x-direction. The density propagates not by rigid translation but by growing to the right of the centre of mass and receding to the left. The current density (bottom) on the other hand propagates rigidly across the wire, and is shown here at the same snapshots in time.

Having propagated across one unit cell, the dispersion of the quasiparticle wavepacket is sufficiently small (see Fig. 5.6 below) that the charge and current densities of the

system are almost identical to those at $t = t_0$ except for a translation by one unit cell spacing. As such, we can focus on the behaviour of the system within this interval. The calculations above then provide the time-dependent charge and current densities that, along with some specified initial Kohn-Sham state, we need to uniquely identify the corresponding KS potentials.

The supercell is sufficiently large compared with the unit cell length and the wave-packet width that the number of electrons in the sampled part of the system does not change over the simulation time: at all times, there are 21 electrons in the supercell. Further, due to the periodic boundary conditions of the quasiparticle calculation, there will remain 21 electrons even after the studied quasiparticle wavepacket has started to propagate out of the supercell. (To this extent, we may consider the infinite wire as comprised of an infinite number of supercells to each of which an identical quasiparticle wavepacket is added at $t = 0$. Each of the quasiparticles are expected to act very weakly with one another [28] and so are treated as noninteracting. This is consistent with the application of quasiparticle theory to quantum transport, described in Sec. 1.1.)

As such, there is never a change in the number of electrons in the supercell as a whole. However, we have seen in Sec. 1.5 that derivative discontinuities in the XC energy occur even when local regions of the system have time-dependent electron numbers that pass through integers. As such, while problems of fractional charges associated with open quantum systems [153] do not pose a problem in our study, one might expect localised discontinuities as the number of electrons per *unit* cell passes through integers.

If so, one cannot assume periodic boundary conditions in the Kohn-Sham system even if all physical quantities of interest are periodic, since the dynamics of the Kohn-Sham electrons may very well depend on a difference between the potential either side of the wavepacket. This poses a challenge to the KS representation of the system: the structure is periodic and therefore not necessarily amenable to a real-space representation, and yet the potentials may be non-periodic and therefore not amenable to a reciprocal-space representation. We shall investigate this problem further in Sec. 5.3 below.

5.2 The initial Kohn-Sham state

As was discussed in the introduction to this chapter, the choice of initial Kohn-Sham state with the correct initial charge density will affect which time-dependent KS po-

tential will be required to reproduce the time-dependent charge density. An immediate choice to be made is whether, in the initial state, only the KS electron wavepacket (corresponding to the quasiparticle wavepacket) is in an excited state or whether there are other electrons in excited states. It is certainly possible to construct such a system, however a localised quasiparticle wavepacket was chosen as a more realistic representation of an added electron: i.e. we consider at $t = 0$ the electron to be added to the ground-state supercell.

In a TDDFT representation of the system, such an addition will have an immediate (at $t = 0$) effect on the KS potential, but the KS electrons won't yet have been affected by it, thus it is reasonable to construct the initial state such that the valence band is unperturbed. For this reason, we shall choose to assign all of the initial quasiparticle charge and current density to the conduction electron. Nonetheless, this is only one of an infinite number of ways of preparing the KS system, and an alternative approach will be studied later in this section.

Because the initial KS state has been chosen to have the density of the quasiparticle, t_0 KS potential in the regions of the wire away from the quasiparticle is identical to the ground-state KS potential. The KS potential which reproduces the 20-electron ground-state density of the model wire, calculated once more using the van Leeuwen-Baerends procedure, is shown in Fig. 5.5.
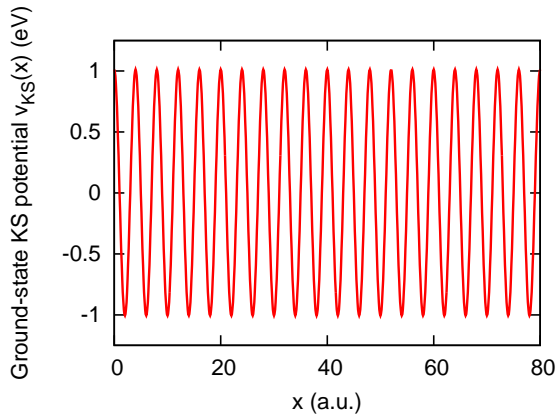
Figure 5.5: **KS potential of the ground-state semiconducting nanowire.** The KS potential, found using the val Leeuwen-Baerends procedure, that reproduces the $N = 20$ electron ground-state wire of Fig. 5.1.

Since the KS wavepacket has the same charge and current density as the QP wavepacket $\Delta n(x, t_0)$, its wavefunction may be written as

$$\psi_{\mathrm{KS,WP}}(x, t_0) = \sqrt{\Delta n(x, t_0)} \exp\left(i\lambda(x)\right) \tag{5.9}$$

117

where

$$\lambda(x) = \int_{-\infty}^{x} dx' \; \frac{j(x', t_0)}{\Delta n(x', t_0)}.$$ (5.10)

The $\sqrt{\Delta n(x, t_0)}$ term carries no current but gives the wavepacket the correct density, while the position-dependence complex phase function modifies the real part to yield the correct current at time t_0.

Generally, one would have to be careful that the constructed KS wavepacket does not have contributions from the already fully occupied electronic states in the ground state. However, because the ground state exactly fills the valence band while the electron wavepacket occupies the conduction band with approximately the same crystal momentum as the QP wavepacket it represents, the wavepacket is inhibited from having significant contributions from states below the band gap, with the total overlap between the KS wavepacket and the valence band of 0.0002 a.u. As such, the KS electron wavepacket is still a weighted sum over excited states of the ground-state KS potential:

$$\psi_{\text{KS,WP}}(x, t_0) = \sum_k c_{\text{KS},k} \phi_{\text{KS},k}(x).$$ (5.11)

These are not, however, the same weightings as used in the QP construction; indeed, the KS wavepacket may be comprised of a larger or different range of eigenstates of the ground-state Hamiltonian. As such, while the KS system has the same charge and current density as the model nanowire at time t_0, we might expect the dynamics of the two systems to differ during time-evolution under fixed fields such that their time-dependent charge and current densities diverge thereafter. This is indeed the case, as can be seen in Fig. 5.6 below.

Very shortly after the two systems have been time-evolved, it becomes clear that the KS electron wavepacket propagates with a lower group velocity than its QP counterpart. Thus, interestingly, even when the interacting system being modelled is free from time-dependent fields, the KS system that represents it cannot reproduce its time-dependent charge and current density without time-dependent KS potentials. The next question is: What *are* those time-dependent potentials? How we may calculate these using the time-dependent reverse-engineering algorithm is the subject of the next section.

5.3 Reverse-engineering in the nonequilibrium regime

For systems described by a time-dependent external potential that is Taylor-expandable in time acting on a system of N interacting electrons, it was proven by van Leeuwen
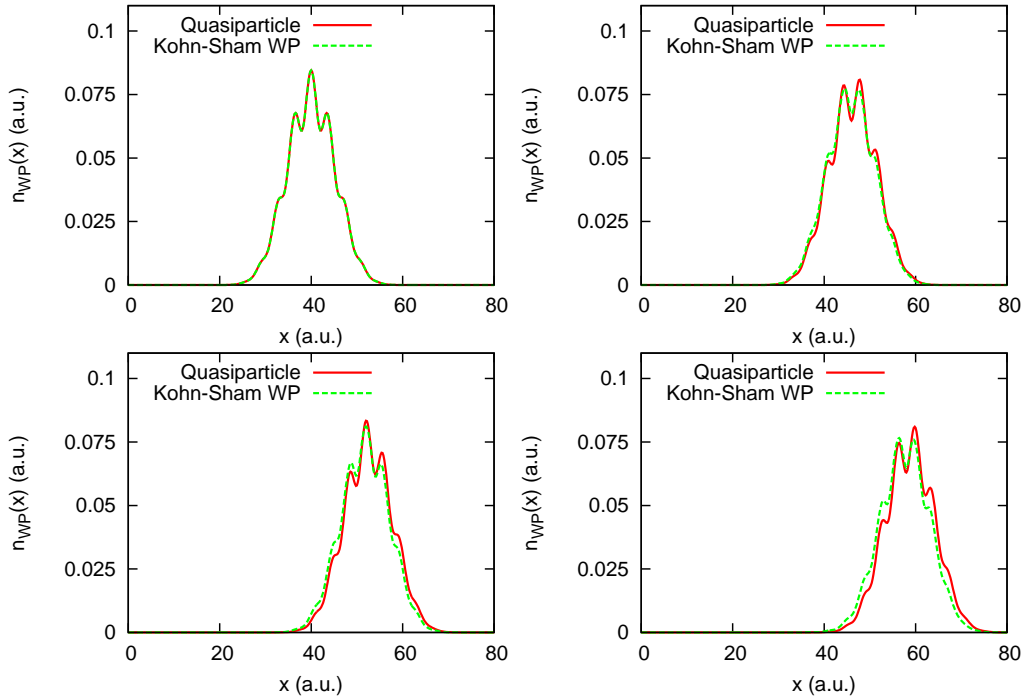
Figure 5.6: **QP and KS wavepacket densities for time-independent external fields.** The QP and KS wavepackets are constructed such that they have the same charge and current density at time t_0. The remaining electrons have no net current and yield the same charge densities in the two representations. Time-evolving both systems according to their ground-state external fields gives rise to deviations in the two time-dependent charge (and therefore current) densities. It is clear that, having moved three unit cells along the wire, the KS wavepacket is substantially falling behind its QP counterpart. This is because the band structures of the two systems differ in their gradients in the vicinity of the wavepacket.

[109] that there exists an effective external potential – the Kohn-Sham potential – which produces the same time-dependent density when acting on a system of N noninteracting electrons. In the model interacting system described in the previous section, the external potential is zero at all times, thus we can be confident that there exists a Kohn-Sham potential that reproduces its density history.

A proposed method of calculating the exact time-dependent KS potentials for a given time-dependent density was detailed in Sec. 3.7, particularly Fig. 3.3. One crucial ingredient is the time-dependent current density, which may either be provided in addition or, if the current has no nonzero, divergence-free components, may be calculated from the charge density via the continuity equation.

The time-dependent KS potential, as was proven in Chapter 2, is uniquely defined by the time-dependent charge density $n(x, t \geq t_0)$, which, along with the corresponding current density $j(x, t \geq t_0)$, was calculated in Sec. 5.1 for the quasiparticle wavepacket,

and the initial KS wavefunction $|\Psi_{\mathrm{KS}}(t_0)\rangle$, which was calculated in Sec. 5.2.

The reverse-engineering algorithm is applied to calculate the KS potential that is required to propagate the KS system for one time-step Δt, from state $|\Psi_{\mathrm{KS}}(t_0)\rangle$ to the state $|\Psi_{\mathrm{KS}}(t_0 + \Delta t)\rangle$ which has the correct current density $j(x, t_0 + \Delta t)$.

Once the state $|\Psi_{\mathrm{KS}}(t_0 + \Delta t)\rangle$ is found, the algorithm may be applied once again to find the state $|\Psi_{\mathrm{KS}}(t_0 + 2\Delta t)\rangle$ having the correct current density $j(x, t_0 + 2\Delta t)$ and so on. In this calculation, the Coulomb gauge has been chosen and, since this is a 1D calculation, no KS magnetic fields can be yielded by the algorithm. As such, the KS vector potential is always zero.

The reverse-engineering algorithm employed was limited to 1000 iterations per timestep and remained convergent throughout. The corrections found by the algorithm diminished in size with each iteration, so one might employ far fewer iterations in practice – generally the correct potential to within around 0.001 % was found within 20 iterations, but the algorithm was allowed to continue to improve upon it, by however small a correction, for the full 1000 for every time-step. The errors in the KS charge and current densities were quantified as

$$\epsilon_n(t) = \sqrt{\int_0^L dx \ (n(x,t) - n_{\mathrm{KS}}(x,t))^2 / L} \tag{5.12}$$

$$\epsilon_j(t) = \sqrt{\int_0^L dx \ (j(x,t) - j_{\mathrm{KS}}(x,t))^2 / L} \tag{5.13}$$

and are shown in Fig. 5.7 below.

The error in the time-dependent charge, approximately linear in time, is to be expected from the numerical methods employed to calculate it, namely the discretisation of the both the spatial axis and time-line of the system, and the Crank-Nicolson propagation scheme. Errors associated with discretised propagation are cumulative and, as such, the total error tends to increase linearly with time. More pathological are the small and periodic gains and losses in accuracy of the current density. These occur because, if the reverse-engineering algorithm *can* find an improvement, it will, even if it is simply making corrections due to earlier losses in accuracy associated with the propagation scheme. As such, the error associated with the current density will tend to decrease even as the error in the charge increases. Since, from the continuity equation, it is not possible for the current density to be arbitrarily and highly accurate while the charge density loses accuracy linearly with time, one cannot expect the algorithm to maintain that level of accuracy indefinitely. On average, however, the current density
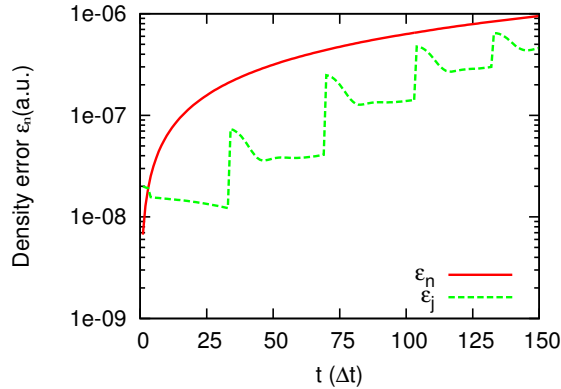
Figure 5.7: **Quantified errors in time-dependent charge and current densities.** The error quantities ϵ_n (red solid) associated with the charge density, and ϵ_j (green dashed) associated with the current density as a function of time for $t \leq 125\Delta t$. Both are, on average linear with time which is to be expected from any numerical scheme for propagation based on a discretised grid. One pathological element is the alternate gains and losses in accuracy the current density attains due to the reverse-engineering algorithm's focus on that quantity. If an improvement can be made to the current density via a correction to the potential, the algorithm will do so, even if the error it is correcting is due to numerical errors in the propagation scheme rather than missing elements of the scalar potential.

loses accuracy approximately linearly with time, mirroring the accuracy of the charge density.

Fig. 5.8 shows snapshots of the additional time-dependent KS scalar potential $\Delta v_{\mathrm{KS}}(x, t)$ which, in addition to the ground-state KS potential of Fig. 5.5, reproduces the time-dependent charge and current density of the model nanowire. The snapshots are taken at the same times as the charge and current densities of the corresponding QP in Fig. 5.4.

The potential is observed to have three main features:

1. a small potential barrier;

2. a time-dependent periodic component;

3. a time-dependent potential step.

The small potential barrier is localised with the charge and current density of the wavepacket and corresponds to the Hartree potential of the quasiparticle. (Since the external potential is unchanged by the addition of the electron wavepacket, the total potential $v_{\mathrm{ext}} + v_{\mathrm{H}}$ is no longer zero, and indeed is time-dependent. This effect is included in the self-energy operator of the quasiparticle and so was not explicitly included in the quasiparticle equation.) The time-varying periodic component superposed onto the barrier is also localised with the wavepacket density: note that the periodicity of
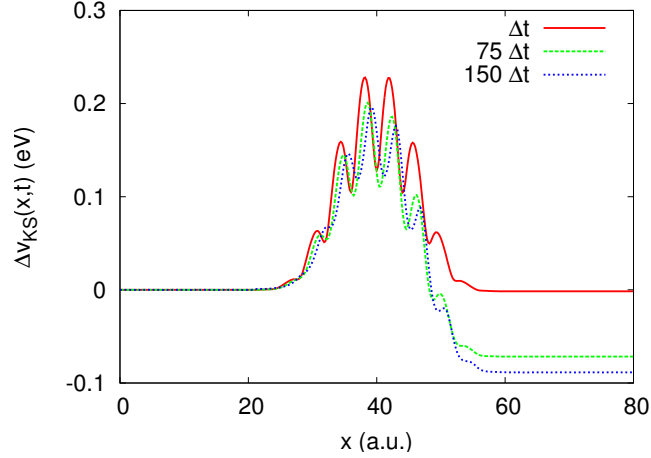
Figure 5.8: **The time-dependent KS potential of the semiconducting nanowire.** The additional time-dependent KS potential required, in addition to the ground-state KS potential, to reproduce the dynamic charge and current densities of the nonequilibrium semiconducting nanowire at snapshots in time of Δt (red solid), $75\Delta t$ (green dashed) and $150\Delta t$ (blue dotted) with $\Delta t = 4 \times 10^{-3}$ a.u. The potential consists of three main components: a small Hartree-like potential barrier, a time-dependent periodic component that tunes the local band structure, and a time-dependent potential step which has an ultranonlocal functional dependence on the charge and current density.

the potential in the vicinity of wavepacket is not fixed, essentially locally modifying the nature of the underlying semiconductor lattice and so tuning the local band structure. Since the gradient of the band structure determines the group velocity of the eigenstates (see Fig. 5.9 below), this changes, in a position- and time-dependent way, the group velocity of the wavepacket.

The third and most striking component is the time-dependent potential difference between the left and right sides of the wavepacket, equivalent to having a time-dependent potential bias across the entire (infinite) wire. Away from the localised wavepacket, the charge density is time-independent and remains that of the ground-state system. Despite this, the relative values of the potential behind and ahead of the propagating wavepacket differ, and in a time-dependent way, creating a dynamic effective exchange-correlation electrochemical potential across the wavepacket.

The step, like the rest of the KS potential, is sensitive to the initial conditions of the simulation. However, at later times, the potential step appears to obey an approximately periodic time-dependence, as shown in Fig. 5.10. It is not possible to state whether the deviation from periodicity, appearing here as a small attenuation of the step amplitude, is numerical or physical: on the one hand, the periodic deviations from a smoothly-varying step, approximately coincident with the afore-mentioned steps
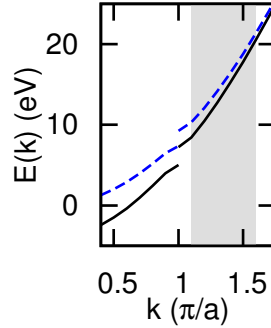
Figure 5.9: **Band structures of the QP and ground-state KS systems in the vicinity of the wavepacket.** The QP (solid black) and ground-state KS (dashed blue) systems have band structures with different gradients in the region where the wavepacket is defined (shaded region), yielding Bloch states with different group velocities. Since the localised conduction electrons are composed of similar weighted sums over these states, the resulting wavepackets have different velocities. The periodic part of the time-dependent KS potential (see Fig. 5.8) "tunes" the local band structure in the wavepacket region such that, in conjunction with the other features of the potential, the KS wavepacket obtains the correct velocity.

in the current density error, while small, generally increase in duration over time; on the other, the wavepacket is dispersing as it propagates, thus one would not expect a temporally periodic potential. Importantly, however, the step does not increase in size indefinitely – consistent with the approximate periodicity of the system in the wavepacket's frame of reference – nor does it settle to a constant size, i.e. it is not a transient effect but a genuine dynamic one.
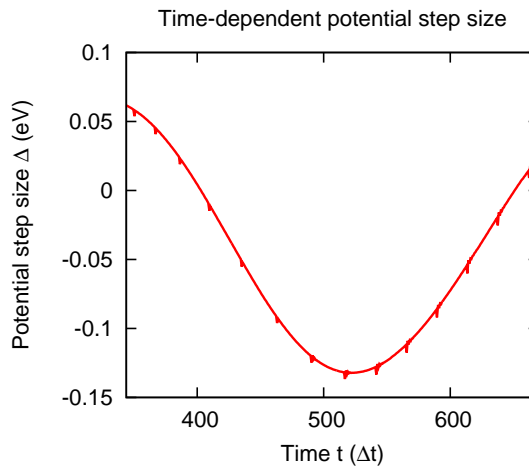
Figure 5.10: **Long-time alternation of the time-dependent potential step:** Time-dependence of the potential step after initial transient effects have subsided. The step amplitude appears approximately periodic, as one might expect as the quasiparticle moves from one unit cell to the next.

It is the interplay between these three components which force the wavepacket

123

to propagate with the correct group velocity: the barrier acting as a local source of resistance, the periodic part raising and lowering the group velocities of the underlying Bloch states of which the wavepacket is comprised and thus raising and lowering the group velocity of the wavepacket itself in a position- and time-dependent way, and the time-dependent potential step in turn accelerating and decelerating the KS wavepacket externally.

The correct physics clearly cannot be captured with an approximate potential that is a local and adiabatic functional of the charge density: a functional such as the ALDA or the adiabatic GGA would predict that the regions ahead of and behind the wavepacket would have exactly the same potential and fail to predict the necessary time-dependent potential step.

A related difficulty to overcome in employing KS schemes to realistically model quantum transport phenomena is that, quite clearly, systems whose time-dependent charge and current densities obey periodic boundary conditions have corresponding KS potentials do not: enforcing periodic boundary conditions in the KS description of the nanowire would destroy the time-dependent potential step and lose some of the necessary physics. While the quasiparticle description that produced the input densities was calculated in reciprocal space, the KS system here had to be calculated in real space which, for a periodic system, introduces significant computational difficulties in applying the Crank-Nicolson method of propagation.

One saving grace is that, while the KS potential is nonperiodic, the electron wavepacket is zero at the edges of the supercell and thus the KS wavefunctions still obey the Bloch condition there such that, add the edges of the supercell,

$$\phi_{\mathrm{KS},k}(x + a, t) = e^{i\alpha}\phi_{\mathrm{KS},k}(x, t). \tag{5.14}$$

This allows one to adopt a *mixed* approach: here, we perform the time-evolution of the wavefunctions in real space as we would a finite system, but we enforce the correct periodicity without destroying the potential step by, at each time-step, extending the supercell beyond the simulation region ($0 \leq x \leq L$) with left and right "buffer regions" extrapolated from the Bloch condition. This allows one to propagate the KS system on the larger grid, with any errors associated with the finite difference scheme of the Crank-Nicolson method remaining within the buffer regions which are then discarded. This approach holds for as long as the KS wavepacket remains zero at the edges of the supercell which, since we are studying a sufficiently small interval of time, in this case it will. (For longer times, one may extend the buffer region further to the right of the

supercell and discard unit cells to the left.)

The Coulomb gauge employed in the above calculation highlights is not the only sensible choice of gauge, nor is it the most computational efficient. The reverse-engineering algorithm calculates corrections to the Kohn-Sham electric field initially in the form of a stored but unused vector potential $\Delta A'_{\text{KS}}(x,t)$, yielding an additional electric field $\mathscr{E}_{\text{KS}}(x,t) = -\partial_t A'_{\text{KS}}(x,t)$ which is then implemented as a scalar potential

$$\Delta v_{\text{KS}}(x,t) = -\int_{-\infty}^{x} dx' \ \mathscr{E}_{\text{KS}}(x',t), \qquad (5.15)$$

effectively calculating the fields in the velocity gauge and then gauge-transforming to the Coulomb gauge. This gauge transform requires an additional integral over space which can be avoided by performing the whole calculation in the velocity gauge.

However, while the spatially ultranonlocal behaviour of the KS scalar potential is removed (since we are no longer integrating over the electric field), the transform introduces nonlocal temporal behaviour in the vector potential and its relationship to the charge density. Figure 5.11 shows the time-dependent charge density at five fixed positions for times $0 \leq t \leq 125\Delta t$ and the corresponding vector potential which reproduces it.
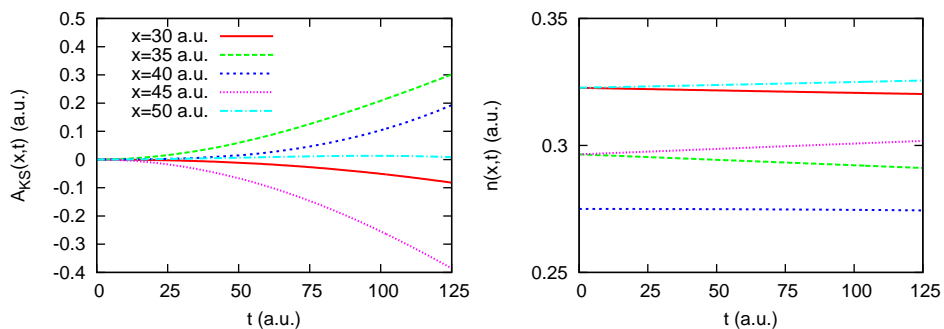
Figure 5.11: **The time-dependent vector potential and charge density.** An alternative KS description incorporates the time-dependence of the exact KS electric field as a vector, rather than scalar potential. While this removes the specific ultranonlocalities of the scalar potential, arising due to a spatial integral over the electric field, it introduces a temporal nonlocality, as evidenced here by, for example, the time-dependence of the vector potential at $x = 40$ a.u. where the density remains approximately time-independent.

One striking feature of the time-dependent vector potential is evident at position $x = 40$ a.u., where the charge density remains relatively constant for the first 125 timesteps, and yet the vector potential is gradually increasing with time. This is specific to the vector potential and can be explained by considering an approximately static but position-dependent scalar potential $v(x,t) \approx v(x)$ being gauge-transformed to a

vector potential:

$$A(x,t) = -\int_{-\infty}^{t} dt' \ \mathscr{E}(x,t') \approx \int_{0}^{t} dt' \ \partial_x v(x) \approx \partial_x v(x,t)t. \tag{5.16}$$

Thus we have traded one ultranonlocality for another. The question of how we might proceed to construct approximate functionals of the time-dependent charge and current density that implement the ultranonlocal behaviour of the exact KS potential is the subject of the next section.

5.4 The Kohn-Sham electric field

To date, all approximate functionals for modelling systems in the KS scheme are functionals for either the KS scalar potential or vector potential directly, since these are the quantities employed in the Schrödinger equation and thus the Kohn-Sham equations. As we have seen, local and even semilocal functionals of the charge and/or current density are unable to capture the correct physics of even a simple quantum transport scenario such as a single localised conduction electron propagating through a model semiconducting wire. In the Coulomb gauge, the exact scalar potential has been seen to have a spatially-ultranonlocal functional dependence on the densities, while in the velocity gauge the exact vector potential has a temporally-ultranonlocal functional dependence.

What these quantities have in common is that both are integrals (over the dimension they are nonlocal in) of the KS electric field:

$$\mathscr{E}_{\mathrm{KS}}(x,t) = -\frac{\partial}{\partial x} v_{\mathrm{KS}}(x,t) - \frac{\partial}{\partial t} A_{\mathrm{KS}}(x,t). \tag{5.17}$$

The additional KS electric field (relative to the ground state) associated with the scalar potential of Fig. 5.8 is shown in Fig. 5.12.

Examining the KS electric field, it is clear why the corresponding scalar potential has a time-dependent step: the electric field generally has a time-dependent nonzero average due to a relatively long-range spatial variation across the width of the quasiparticle. The field itself, however, is localised with the quasiparticle and, as such, is much more amenable to local or semilocal approximation in its functional dependence on the charge and current density.

In calculating the electric field, the reverse-engineering algorithm depended on both the local and semilocal charge and current density explicitly, suggesting that a local or
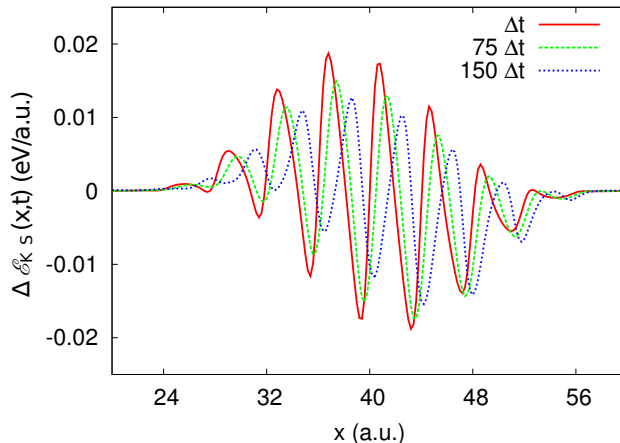
Figure 5.12: **The exact time-dependent KS electric field for the semiconducting nanowire.** The KS electric field required in addition to the ground-state KS electric field in order to reproduce the time-dependent charge and current density of the semiconducting nanowire exactly, corresponding to the additional KS scalar potential in Fig. 5.8, shown at the same snapshots in time: Δt (red solid), $75\Delta t$ (greed dashed) and $150\Delta t$ (blue dotted). The KS electric field is localised with the wavepacket and thus is more amenable to local or semilocal approximation than the scalar potential itself.

semilocal approximate functional may need to depend on both of these quantities. In fact, the functional dependence of the electric field is still strongly dominated by the charge density, having a smaller but certainly nonzero semilocal functional dependence on the current density.

The proof of the Runge-Gross theorem [104] employs the equation of motion of the current density of an electronic system which, in the absence of external magnetic fields and in one dimension, is given by

$$\frac{\partial j(x,t)}{\partial t} - \mathscr{E}(x,t)n(x,t) + P\left[n, |\Psi(t_0)\rangle\right] = 0, \qquad (5.18)$$

thus we expect $(1/n)\partial \mathbf{j}/\partial t$ to be a term in the electric field functional.

$P\left[n, |\Psi(t_0)\rangle\right]$ is the stress-momentum [106] of the system which is generally unknown but proven to be a unique functional of the time-dependent charge density and the initial state of the system, since all other quantities in Eq. 5.18 are also unique functionals of these quantities. The stress-momentum cannot depend entirely on the current density, since it is nonzero for all many-electron systems. The exact functional dependence of the quantity is not known; however, if we consider a generalised gradient approximation to it, one would expect terms that are local in $n(\mathbf{r})$ and its first spatial derivative. We find below that the gradient $\nabla n(\mathbf{r})$ is sufficient to, along with $\partial \mathbf{j}/\partial t$, uniquely determine the KS electric field.

Fig. 5.13 shows the local and instantaneous dependence of the total (including ground-state) KS electric field on the quantities $(\partial_x n(x,t))/n(x,t)$ and $(\partial_t j(x,t))/n(x,t)$ for four snapshots in time: $25\Delta t$, $50\Delta t$, $75\Delta t$ and $100\Delta t$. (For ease of reading, the 3D plot lines that pass through all data points are shown, rather than the data points themselves which clutter the figure.) What is striking is that, for the evolutionary history described above, the field $\mathscr{E}_{\mathrm{KS}}((\partial_t j)/n, (\partial_x n)/n)$ is single-valued and lies almost on a plane. The strong dependence of the electric field on the former is seen to dominate, especially in the central region where the gradient of the density is at its lowest, i.e. in the region of the system where the density is that of the ground state, as expected since $\partial\mathbf{j}/\partial t$ is zero and unvarying in this region. However, in the region of the wavepacket, the dependence of the electric field on the time-derivative of the current density becomes more clearer. Moreover, the electric field is largely independent of time: all four time-steps chosen have electric fields with almost identical dependence on these quantities. This suggests once again that the time-dependent KS electric field might be much more amenable to local and semilocal functional approximation than the KS scalar potential itself.
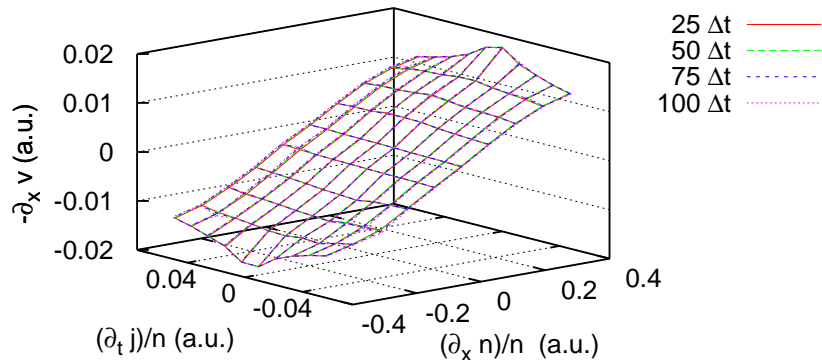
Figure 5.13: **The functional dependence of the KS electric field.** The total KS electric field $-\partial_x v(x,t)$ (top) is shown in atomic units at four snapshot in time: $25\Delta t$ (red solid), $50\Delta t$ (greed long-dashed), $75\Delta t$ (blue short-dashed) and $100\Delta t$ (purple dotted) as a local functional of $(\partial_x n(x,t))/n(x,t)$ and $(\partial_t j(x,t))/n(x,t)$. This semilocal functional dependence on the charge and current densities is approximately independent of time. Away from the wavepacket region, the dominant dependence is on the gradient of the charge density, but in the wavepacket region (where the current is nonzero) the dependence on the time-derivative of the current density becomes more important.

In conclusion, for the evolutionary history studied, KS functionals of the electric *field* rather than potentials appear to be much more amenable to local and semilocal approximation without losing some of the vital physics we have seen demonstrated in a simple quantum transport scenario. Unlike the scalar and vector potentials, the corresponding electric field is localised in both space and time, and in one dimension

is shown to have, to good approximation, a local and unique dependence on three quantities derivable from the time-dependent charge density: the charge density itself, the gradient of the charge density, and the time-derivative of the current density.

5.5 Finite lifetime effects

The true self-energy operator governing the nonequilibrium quasiparticle is generally complex, and the imaginary part of this energy is responsible for QP decay. Quasiparticle decay results from inelastic scattering between electrons in the system, wherein the initial QP energy is gradually lost to heating the electrons it interacts with as it propagates through the nanowire. This is generally a highly nonequilibrium and statistical situation; as such, we shall make several assumptions, simplifications and approximations.

First, in real excitations, the exponential character of the quasiparticle decay is seen to occur at times $t > \varepsilon_{\mathrm{QP}}/\varepsilon_{\mathrm{F}}$, where $\varepsilon_{\mathrm{QP}}$ is the quasiparticle energy and ε_{F} is the Fermi energy [154]. In our study, it is the long-time behaviour we are interested in, and so we approximate the decay as being exponential in character at all times.

Second, we assume that the excited state decays toward a Fermi-Dirac statistical distribution:

$$f(\varepsilon) = \frac{1}{e^{(\varepsilon-\mu)/kT} + 1}, \tag{5.19}$$

where $f(\varepsilon)$ is the average number of electrons occupying the state with energy ε, μ is the total chemical potential, k is Boltzmann's constant, and T is the temperature of the final state. The precise distribution can be obtained by physical considerations, namely conservations of energy, momentum and electron number.

Third, we model the decay of the quasiparticle into the background in the relaxation time approximation (RTA) [155; 156] for a homogeneous electron gas, i.e. we approximate the rate of this decay as being independent of where the quasiparticle is in the supercell. (One can include a localising correction to the RTA such that the decay rate attenuates with distance from the quasiparticle. However, for a moving quasiparticle wavepacket, conserving electron number in such a scheme would introduce so many complexities that differentiating the effects on the KS potential of the arbitrary means of doing so from those that we are interested in – namely exponential decay effects – would not be clear.) However, we specify only that the decay is uniform across the supercell under consideration, thus the transparent boundary conditions of the supercell must match those of a periodic system. (Once again, we may consider the infinite

wire to consist of an infinite number of such supercells, each of which has, at $t = 0$, an identical quasiparticle wavepacket added to it which decays identically toward the same Fermi-Dirac distribution.

Fourth, we shall include an additional ground-state electron in the lowest energy level of the conduction band, putting the system in a metallic (but periodic) state. Further, if necessary to conserve energy, momentum and electron number, excitations will be allowed across the band gap. As such, we shall approximate the one-dimensional dielectric function of the system as an all-electron function of a degenerate homogeneous electron gas in the random phase approximation.

Finally, in the evaluation of the quasiparticle lifetime, it is necessary to construct an approximate Coulomb interaction for a one-dimensional system that does not contain singularities, i.e. a softened Coulomb operator. We shall derive an approximate softening parameter from physical considerations. In addition, we shall evaluate the lifetime based on a linear response approach based on the random phase approximation (RPA).

The decay toward a statistical Fermi-Dirac ensemble demands a density matrix, where the initial matrix is given by

$$\rho(x, x', 0) = |\Psi(0)\rangle \langle \Psi(0)|, \tag{5.20}$$

the Liouville-von Neumann equation of motion in the RTA is

$$\frac{\partial}{\partial t} \rho(x, x', t) = -i \left[\hat{H}, \rho \right] + \frac{\rho_{\text{final}}(x, x') - \rho(x, x', t)}{\tau}, \tag{5.21}$$

where τ is the QP lifetime.

5.5.1 The quasiparticle background

Once the QP is injected into the system, the total system energy is

$$E_0 = E_{\text{GS}} + E_{\text{QP}}. \tag{5.22}$$

We take the zero of our energy scale to be the bottom of the valence band. For a supercell of 20 "atoms" of atomic separation 4 a.u. subject to the nonlocal self-energy operator described above and sampled at the Γ-point, the 21-electron ground-state energy is 79.95 eV. The additional electron quasiparticle wavepacket, constructed as a weighted sum over right-going Bloch states in the conduction band with the same

weightings as before, has energy 21.9 eV yielding a total system energy of $E = 101.85$ eV.

At $t = 0$, all of the momentum of the system is carried by the QP:

$$\langle p_0 \rangle = \langle \psi_{\mathrm{QP}} | \hat{p} | \psi_{\mathrm{QP}} \rangle = 1.16 \mathrm{a.u.}, \tag{5.23}$$

where $\hat{p} = -i\partial_x$ in one dimension, and the total electron number is 22.

The final distribution of the electrons in the system is an ensemble described in terms of a density matrix as

$$\rho(x, x') = \sum_k f(\varepsilon_k) |\Psi_k\rangle \langle \Psi_k| \tag{5.24}$$

in which the system has a probability $f(\varepsilon_k)$ of being measured in state $|\Psi_k\rangle$. The distribution must ensure that energy, momentum and electron number are conserved on the discretised grid:

$$\langle E_{\mathrm{final}} \rangle = \mathrm{Tr}\left[\hat{\rho}\hat{H}\right] = \sum_k f(\varepsilon_k)\varepsilon_k = E_0 \tag{5.25}$$

$$\langle p_{\mathrm{final}} \rangle = \mathrm{Tr}\left[\hat{\rho}\hat{p}\right] = \sum_k f(\varepsilon_k) \langle \Psi_k | \hat{p} | \Psi_k \rangle = \langle p_0 \rangle \tag{5.26}$$

$$N_{\mathrm{final}} = \mathrm{Tr}\left[\hat{\rho}\right] = \sum_k f(\varepsilon_k) \langle \Psi_k | \Psi_k \rangle = 22. \tag{5.27}$$

Via numerical optimisation using Basin's hopping technique [157] in conjunction with Powell's conjugate gradient method [148], we find the values of chemical potentials for the source and sink reservoirs and the final system temperature that yields the global minimum of

$$\epsilon = \alpha \left| \langle E'_{\mathrm{final}} \rangle - E_0 \right| + \beta \left| \langle p'_{\mathrm{final}} \rangle - p_0 \right| + \gamma \left| N'_{\mathrm{final}} - 22 \right|, \tag{5.28}$$

where $\beta > \gamma > \alpha$ are adjustable parameters to aid convergence, to be

$$\mu_L = 12.7 \text{ eV},$$
$$\mu_R = 12.4 \text{ eV},$$
$$k_{\mathrm{B}}T = 2.35 \text{ eV},$$

with the residual error $\epsilon = 0.01$ for $\alpha = 0.2$, $\beta = 1$, $\gamma = 0.1$, corresponding approximately to a 0.3% error in the energy, 0.8% error in the momentum, or 0.5% error

in electron number assuming all of the error to be in one of those quantities. The Fermi-Dirac distribution for $\mu = \mu_L - \mu_R$ and T is shown in Fig. 5.14 below.
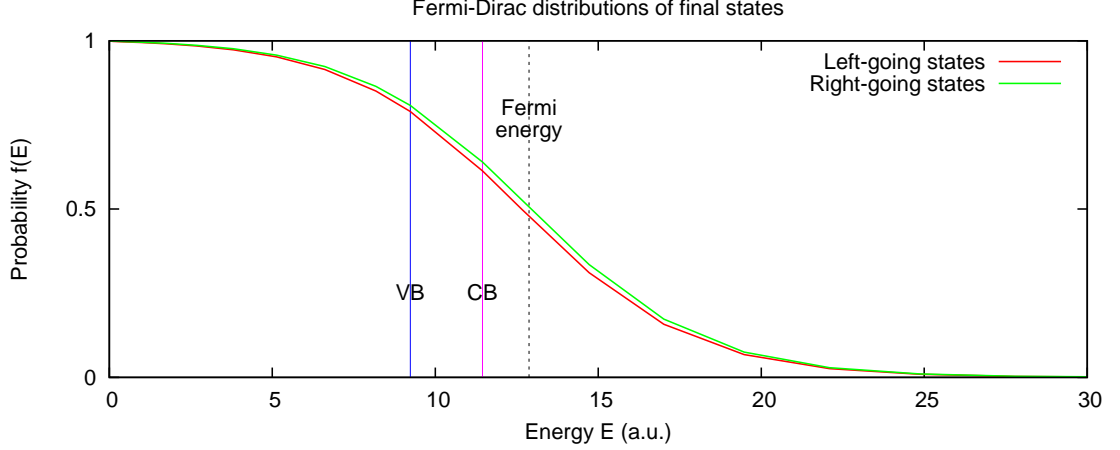
Figure 5.14: **Fermi distributions of final state:** The final Fermi-Dirac distributions of the left-going (red) and right-going (green) eigenstates of the interacting system after the added electron quasiparticle has decayed. The distributions are given by the left- and right-going chemical potentials and the final temperature of the supercell whose values are fixed by conservation of energy, momentum and electron number. The blue line denotes the top of the valence band, the purple line the bottom of the conduction band, and the dashed line is the Fermi energy.

5.5.2 Quasiparticle lifetime

The lifetime can be approximated on physical grounds. Starting with the imaginary part of the correlation energy for the homogeneous electron gas, calculated from GW theory in Ref. [158],

$$\text{Im } E_c(\mathbf{p}) = \int_{0 \leq E' \leq E} \frac{d\mathbf{k}}{(2\pi)^3} \frac{4\pi}{k^2} \text{ Im } \frac{1}{\epsilon(\mathbf{k}, E - E' + i\delta)}, \tag{5.29}$$

where $\mathbf{p}$ is the momentum of the electron in the gas, E its energy, $E' = \frac{1}{2}[\mathbf{p} - \mathbf{k}]^2$, and $\epsilon(\mathbf{p}, E)$ is the dielectric function, we construct a 1D approximation

$$\text{Im } E_c(p) = \int_{0 \leq E' \leq E} \frac{dk}{2\pi} W(k) \text{ Im } \frac{1}{\epsilon_{1D}(k, E - E' + i\delta)}, \tag{5.30}$$

where $W(k)$ is the softened 1D Coulomb interaction in reciprocal space, and ϵ_{1D} is a suitable approximate 1D dielectric function.

The 1D dielectric function in Eq. 5.29 needs to account for exchange and correlation

effects, and so we choose the 1D Lindhard function [159; 160] for the RPA [161]:

$$\epsilon(k, E) = 1 - W(k)\chi(k) \tag{5.31}$$

where $W(k)$ is the Coulomb interaction in Fourier space and the imaginary part of the electron response function is

$$\text{Im } \chi(k) = \begin{cases} -\frac{1}{2k} & \text{for } k^2 - 2k \leq E \leq k^2 + 2k, \\ 0 & \text{otherwise.} \end{cases} \tag{5.32}$$

where k_{F} is the Fermi momentum of the electron gas [160].

For the softened Coulomb interaction, we seek the constant parameter C of

$$W(x, x') = \frac{1}{\sqrt{(x - x')^2 + C^2}} \tag{5.33}$$

for the centre of a pseudo-one-dimensional waveguide modelled as a rotationally-invariant infinite potential well of diameter d. Evaluated at $x = x'$, this interaction is

$$\frac{1}{C} = \int_0^{d/2} dr \int_0^{2\pi} d\theta \ r \ \frac{1}{r} = \pi d. \tag{5.34}$$

The value of d is chosen to be as large as possible within the constraint that all electronic states consider are within the lowest-energy subband of the waveguide. Taking the top of the second conduction band as the highest considered energy $E_{\text{max}} \simeq 1.5$ Ha, we require that $d = \frac{1}{2\pi}\sqrt{2E_{\text{max}}}$, yielding

$$C = \sqrt{E_{\text{max}}/2} \simeq 0.866 \text{ a.u.} \tag{5.35}$$

In reciprocal space, the interaction is then

$$W(k) = \sqrt{\frac{2}{\pi}} K_0\left(C|k|\right) \tag{5.36}$$

where $K_0(x)$ is the zeroth-order modified Bessel function of the second kind.

Inserting Eqs. 5.36, 5.31 and 5.32 into Eq. 5.30 and integrating numerically gives an imaginary 1D correlation energy of $E_{\text{c}} = 0.009\ 35$ Ha, yielding a QP lifetime of $\tau \simeq 107$ a.u.

This is considerably larger than the simulation time of the wavepacket studied earlier in this chapter, and so one would not expect to see significant decay during

the study. However, due to the exponential character of the decay, we expect to see some significant *effects* on the time-dependent charge and current densities and on the Kohn-Sham potentials which reproduce them.

5.5.3 Quasiparticle decay

Fig. 5.15 shows the initial charge and current densities of the interacting system under two distinct approximations: the first, that decay occurs infinitesimally after the injection of the electron at $t = 0$ whereby the current density of the QP is identical to the system studied in the previous sections; the second, that decay begins at $t = 0$.
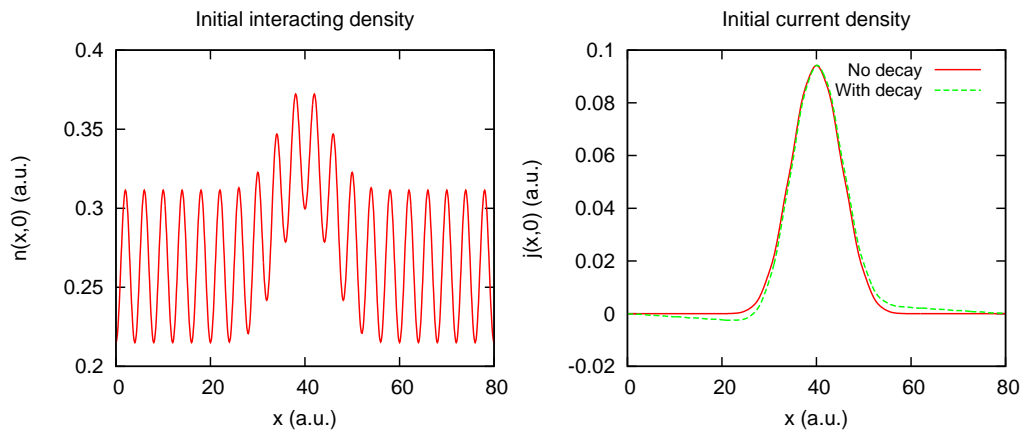
Figure 5.15: **Initial charge and current densities:** The initial charge density (left) of the interacting system with the additional electron occupying the lowest-energy state of the conduction band, and the current densities (right) with decay starting infinitesimally after $t = 0$ (red, solid) and decay starting exactly at $t = 0$ (green, dashed).

Fig. 5.16 shows snapshots of the QP density and Fig. 5.17 the current density calculated from the continuity equation and Eq. 5.21 at increments of $20\Delta t$, with $\Delta t = \frac{1}{2}\Delta x^2$ and $\Delta x = 0.2$ a.u. Periodic boundary conditions are maintained throughout the calculation.

The charge density is seen to attenuate with time in the region of the wavepacket and aggregate in the regions either side of it at a position-independent rate. The current density is qualitatively different from that which we have seen in the absence of decay due to the fact that the density is changing, however slowly, in the regions to the sides of the wavepacket. Furthermore, since the decay is exponential, the rate of change of the density is highest at $t = 0$, assuming the decay begins at this time. In the next two sections, we will look at the effects of this behaviour on the Kohn-Sham potential, and the implications for initial-state-dependence on the choice of when the decay begins.
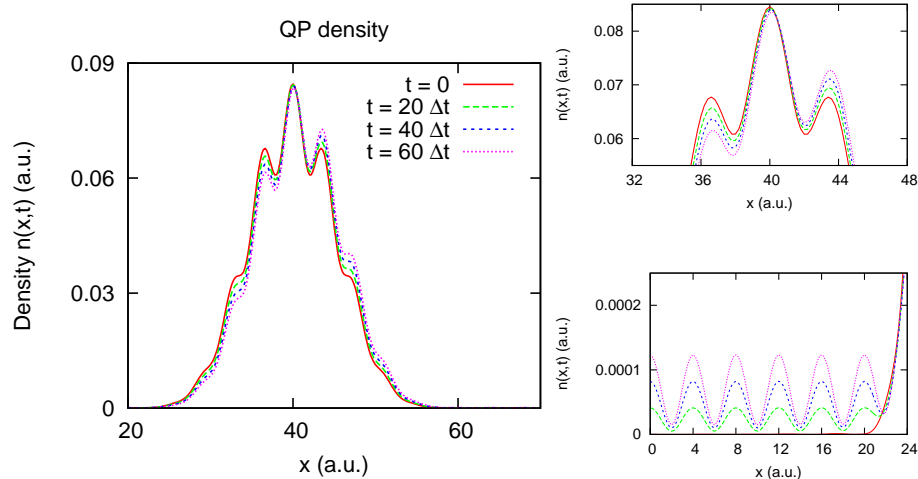
Figure 5.16: **Density of decaying quasiparticle:** Snapshots of the quasiparticle density as it decays with lifetime $\tau = 107$ a.u. (left) at multiples of $20\Delta t$. Decay can be seen most at the wavepacket peak (right, top) and the increasing charge at the edges (right, bottom).
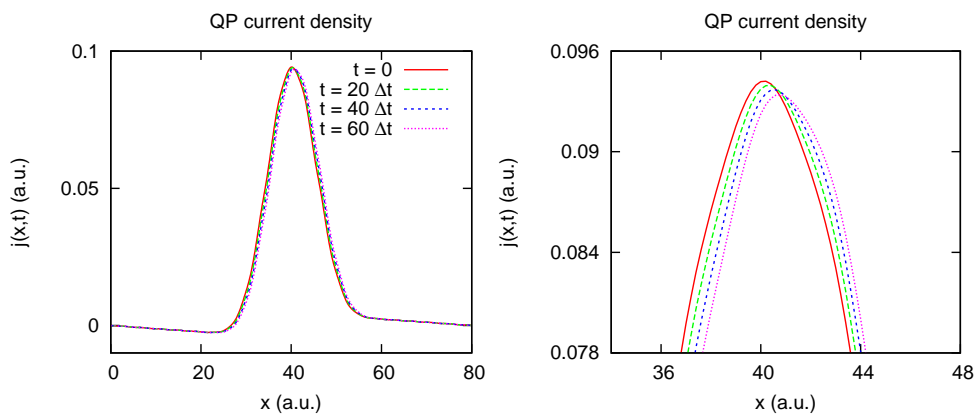
Figure 5.17: **Current density of decaying quasiparticle:** Snapshots of the quasiparticle current density as it decays with lifetime $\tau = 107$ a.u. (left) at multiples of $20\Delta t$. Detail of the current peak (right) shows the decay in addition to the translation of the current with time.

5.6 Incorporating decay in KS calculations

Due to the addition of the electron in the lowest-energy state of the conduction band in the ground state, the ground-state KS potential is calculated again using the van Leeuwen-Baerends procedure, this time with the additional occupied state at the bottom of the conduction band, and is shown in Fig. 5.18 for the first 10 unit cells along with the ground-state charge density. The first 21 eigenstates of this system are then occupied.
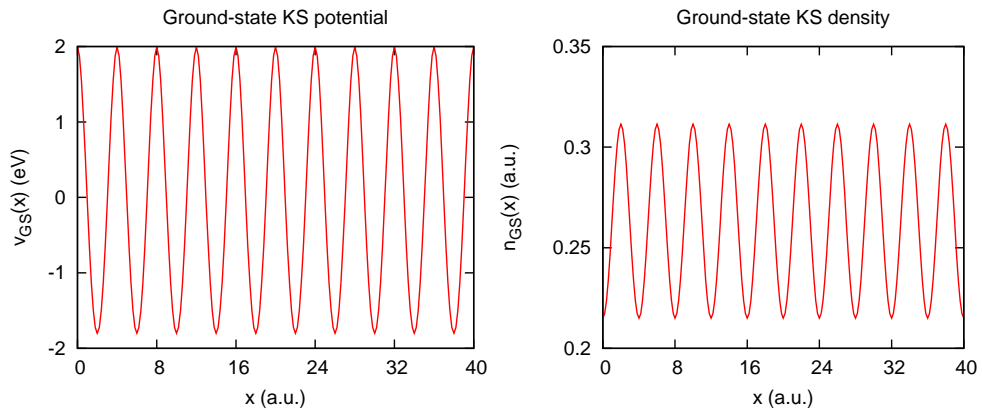
Figure 5.18: **Ground-state Kohn-Sham system:** The ground-state potential (left) and 21-electron charge density of the Kohn-Sham system reproducing the ground state of the interacting system to which the quasiparticle is added.

The 22$^{\text{nd}}$ electron is constructed as before to have the same charge and current density as the QP before decay:

$$\phi_{N+1}(z,0) = e^{i\lambda(z)}\sqrt{n_{\text{QP}}(z,0)} \tag{5.37}$$

with $\partial_z\lambda(z) = j(z,0)/n(z,0)$.

We assume that the quasiparticle decay begins infinitesimally after the injection of the QP wavepacket at $t = 0$. By constructing the system in this way, we can study the manner of KS potential that is required to induce exponential decay.

The time-dependent KS potential and electric field required to reproduce the time-dependent charge and current densities shown in Figs. 5.16 and 5.17 above are calculated via the nonequilibrium reverse-engineering algorithm of Sec. 3.7. The fields, including the ground-state contributions, at $t = \Delta t = \frac{1}{2}\Delta x^2$ with $\Delta x = 0.2$ a.u. are shown in Fig. 5.19 below.

As one can see, the fields required to induce decay in a QP system are very large,
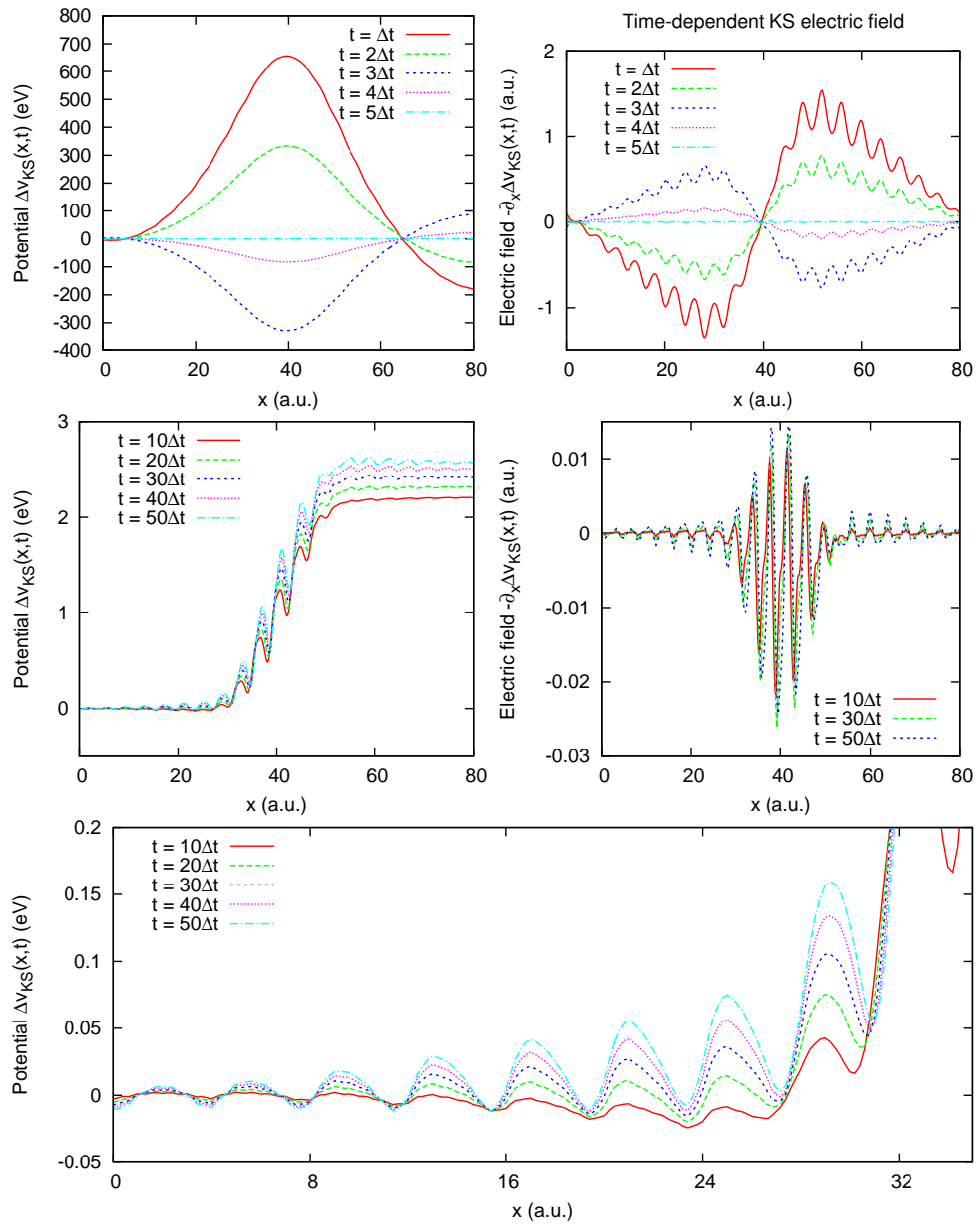
Figure 5.19: **Decay-inducing fields:** The first five timesteps of the additional (to the ground-state) time-dependent scalar potential (top left) and electric field (top right) that reproduce the time-dependent density of Fig. 5.16. The large potentials that induce decay quickly give way to smaller potentials that ensure the correct time-dependence thereafter, shown here in full (centre left) and in detail (bottom). The localised electric fields (centre right) are shown for fewer timesteps for visual clarity.

even compared with the ground-state potential. They consist of a very large potential barrier in the region of the wavepacket which pushes the quasiparticle density outward, and large x^2 potential wells either side of the wavepacket with a relative potential step in between.

The amplitudes of the large decay-inducing potential increases with decreasing time-step and decreasing quasiparticle lifetime τ. While the former makes the precise potential calculation-specific, it is an inevitable consequence of the exponential decay on any discretised timeline: the smaller Δt, the closer to $t = 0$ we sample the system at the first timestep, and the larger the rate of exponential decay. Further, from the reverse-engineering algorithm employed, the size of the corrections to the potential are proportional to the time-derivative of the current density. The assumption that decay begins infinitesimally after $t = 0$ means that the onset of the current density in the outer regions of the supercell is non-adiabatic, hence the electric fields required to reproduce that sudden onset are very large.

Despite the long-range behaviour, the associated XC electric field displays a semilocal functional dependence on the current density. Away from the wavepacket, the charge density is still periodic in space with a period equal to the unit cell length while the potential is very long range, demonstrating that it has an ultranonlocal dependence on the charge. The x^2 form of the potential wells can be understood in terms of the locally linear-in-x dependence of the current on position, yielding an electric field that is also linear in x and therefore a potential that goes as x^2.

Fig. 5.19 also shows the time-evolution of the KS potential after the larger perturbing field of the first few timesteps has attenuated, leaving four main features whose amplitudes are similar to the ground-state potential or smaller:

1. a small time-dependent potential step between the left and right regions of the supercell;

2. a small, long-range $-x^2$ component either side of the wavepacket;

3. increasingly large, asymmetric, periodic "buckets";

4. a large potential step in the central region of the supercell.

Feature 1 can be identified with the time-dependent potential step of the previous study, arising from the effects of the nonlocal hole and required to yield the correct wavepacket velocity, along with the spatial variance within the large potential step of feature 4, corresponding to the time-dependent potential barrier also seen in Fig. 5.8

Both from the start of the time-evolution, the long-range x^2 potential barriers on either side of the wavepacket are required to move charge density from the wavepacket itself to the outer regions. The largest of these potentials begins at $t = \Delta t$, and the potentials at subsequent times gradually reduce the amplitude of this initial potential as the system evolves toward a steady-state.

The presence of this long-range field would be expected to polarise the system, moving the electrons present in the N-electron ground-state away from their equilibrium positions. This unwanted polarisation is corrected by the asymmetric periodic "buckets" which act to "tilt" the electrons back into their equilibrium coordinates and with the correct shape.

The final feature – the large potential step in the region of the wavepacket – is necessary due to the asymmetry of the current density: since the QP is already moving to the right, a potential step is required to yield sufficient reflection to move some charge to the left region of the supercell, as well as allowing some tunnelling so as to aggregate charge in the right region. This step is distinct from the types of steps seen in stable quasiparticle case [147] and elsewhere in the literature (e.g. [162], [163]); whereas in those instances the step varies in sign and magnitude with time, the decay step is slowly varying (the variation of the step with time arises from the time-dependent step seen even in the absence of decay), and must decay to zero as the system approaches its final state.

As can be seen, the potential step is comparable to the band gap in size, as is required to excite the valence electrons of the ground-state wire into the conduction band as per the final QP state. It is also this band gap which stops the current-response of such a large potential step from generating large currents: close to the band gap, the current as a function of momentum decays quickly to zero.

Broadly, the KS potential consists of a component which governs the propagation of the decaying electron wavepacket along the wire as in the previous study, and one which governs the decay of the quasiparticle into the background. The second of these is exponential in character, i.e. at its most dominant at shortest times. At short times, therefore, this component is approximately independent of the relaxation time τ. (More generally, if one changes the relaxation time by a factor γ and correspondingly the timestep by a factor of γ, this component of the potential remains unchanged *at all times*. This has been confirmed computationally.) As such, the KS potential under varying relaxation time differs only in the relative phases of the time-dependent XC bias (along with the features local in the density, rather swamped here by the decay step) and the decay of the large central step (along with the growth of the buckets and

the decay of the small quadratic potential). As such, these features of the KS potential for a decaying QP wavepacket are highly robust.

5.7 Memory in quasiparticle decay

In the previous section, we studied the time-dependent KS potential that reproduces a quasiparticle wavepacket that is added to a ground-state system at $t = 0$ and, due to the non-Hermitian self-energy operator it is governed by, begins to decay exponentially infinitesimally after. In this section, we will assume that the QP decay begins at $t = 0$, and investigate the history-dependence of the time-dependent KS potential when describing QP decay.

In Sec. 5.6, as in Sec. 5.3, the initial KS wavepacket was injected into the system with the same charge and current densities as the QP itself. In this present study, the nonzero current density away from the wavepacket necessitates that some of the electron wavefunctions apart from the wavepacket carry some of the initial current density. One could still include all of the initial current in the conduction band due to the additional ground-state electron therein.

However, the fields responsible for inducing decay, calculated in Sec. 5.6, are felt by *all* electrons in the KS system. As such, it is sensible to share the initial current density of the QP across all of the electrons in the initial KS system. As such, the KS wavepacket is constructed as before, carrying the full current density of the nondecaying QP system, and yielding a putative current density of $j'_{\mathrm{KS}}(z)$ as in Fig. 5.15 (red curve).

Thus the entire KS system, including the valence band, is then further transformed as

$$\phi_k(z, 0) \rightarrow e^{i\lambda(z)}\phi_k(z, 0) \tag{5.38}$$

with

$$\frac{\partial}{\partial z}\lambda(z) = \frac{j_{\mathrm{QP}}(z, 0) - j'_{\mathrm{KS}}(z)}{n(z, 0)}, \tag{5.39}$$

and thus the whole KS system at $t = 0$ is in an excited state with respect to the ground state.

The time-dependent KS scalar potential and electric field are calculated using the nonequilibrium reverse-engineering algorithm of Sec. 3.7 and shown in Fig. 5.20. The time-dependent step between the left and right boundaries of the supercell, seen earlier for the non-decaying quasiparticle, remains significant in the presence of electron correlations.

As one would expect, the time-dependent KS potentials required to reproduce the
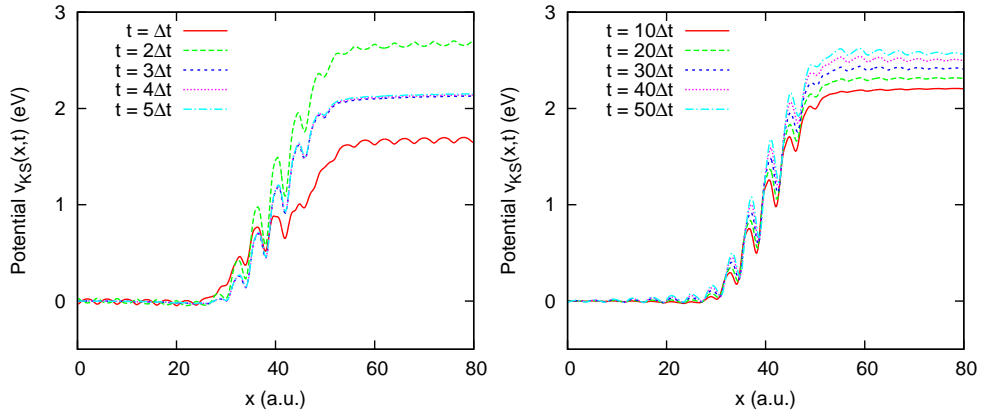
Figure 5.20:   **Time-dependent KS potentials and electric fields:** The time-dependent KS potentials for the first five timesteps (left) and at intervals of ten timesteps (right) yielded from initial KS states already constructed to reproduce quasiparticle decay. The qualitative form of the long-time potential of Fig. 5.19 is established immediately, and the two time-dependent potentials become identical within a small number of timesteps.

interacting charge and current densities are markedly different at the earliest times. The very large barriers and x^2 wells of Fig. 5.19 do not appear at all here, since the KS potential is no longer required to induce the dynamics representing quasiparticle decay. However, within the first few timesteps the potentials becomes insensitive to the history of the system and the potential at later times, shown in Fig. 5.20 at the same snapshots at intervals of $10\Delta t$, is identical to the potential at those snapshots in Fig. 5.19.

Using the nonequilibrium implementation of the reverse-engineering algorithms presented in Chapter 3, we have calculated the exact time-dependent Kohn-Sham potentials required to reproduce the time-dependent charge and current densities of four related but distinct systems. We have observed the characteristics of the potential required to introduce the nonlocality of the self-energy operator governing a quasiparticle wavepacket added to a semiconductor. Most notably, these potentials contain a time-dependent potential step either side of the wavepacket that is ultranonlocal in its functional dependence on the charge and current density.

We have found that such effects that are ultranonlocal for the KS scalar potential are semilocal for the KS electric field, strongly suggesting that future functionals should be in terms of the XC electric field rather than the XC potential. These effects are seen to be a robust feature of all calculations, independent of the precise nature of the self-energy operator or the initial interacting or Kohn-Sham states, so long as the

quasiparticle is localised and the self-energy operator nonlocal.

We have also studied the KS potentials that reproduce the effects of a decaying quasiparticle, governed by a self-energy operator that is energy-independent, but non-local and non-Hermitian. Once again, the potentials have an ultranonlocal dependence on the charge and current densities, but the corresponding electric fields are seen to depend only semilocally on the densities. The potentials required to induce decay are very large and vary very quickly. However, such the duration of such features in the potential is very short, and the potential demonstrates a remarkably short-ranged memory-dependence.

In conclusion, the central results of these studies, and those of the previous chapter are:

1. the reverse-engineering algorithms presented in Chapter 3 are successful at yielding the exact KS potentials required to describe both steady-state and nonequilibrium systems;

2. steady-state systems subject only to an external scalar potential are not generally noninteracting-V-representable without the inclusion of an exchange-correlation magnetic field. This magnetic field is observed to be uniquely determined by the charge and current densities of the interacting system;

3. the exact time-dependent KS potential that incorporates nonequilibrium many-body effects is generally ultranonlocal in its functional dependence on the charge and current density, however the KS electric field is much more amenable to approximation using semilocal density functionals;

4. excitation decay can be induced in a KS system with very large but simple potentials that depend on the target current density, and these potentials are short-lived;

5. we have seen that memory effects due to the differences in the initial charge distribution of the KS system can persist throughout the simulation time, while those that arise due to the differences in the initial current distribution may be short-lived, even if the potentials are initially qualitatively different. Furthermore, the main qualitative features of the exact time-dependent potential found in this study are robust.

The reverse-engineering algorithms of Chapter 3 may be employed to study a broader variety of systems and initial states, and these studies will be invaluable in

the construction of future approximate functionals. The particular systems studied in this Chapter already provide much insight into what form improved functionals may take, include the explicit definition of an exchange-correlation electric field functional that incorporates important many-body effects.

Chapter 6

Summary & Conclusions

The purpose of this research was to develop methods for calculating exact Kohn-Sham (KS) effective fields for systems of interest to quantum transport theory, both in the steady-state and nonequilibrium regimes. The investigation of the steady-state systems first required a more firm theoretical foundation for current-density functional theory (CDFT), including a choice of basic variables that yields unique external potentials and a method of constructing auxiliary KS systems that allows an energy-minimisation procedure, summarised in Sec. 6.1 below.

With a theoretical basis in place, a means of calculating exact KS potentials in the steady-state regime was formulated and extended to the nonequilibrium regime, as summarised in Sec. 6.2. These methods were then applied to steady-state and time-dependent current-carrying systems of both one and three dimensions whose charge and current densities were calculated from model self-energy operators that capture the nonlocal behaviour of quantum-mechanical electron-electron interactions. The KS potentials that reproduce these densities exactly were calculated and their functional dependencies on those densities were studied, as summarised in Sec. 6.3.

Sec. 6.4 will discuss how we may use the information gained from these studies in the construction of better density functionals, and Sec. 6.5 will discuss the applicability of these methods to ongoing and future studies.

6.1 Current-density functional theory

Existing formulations of CDFT have not been based on rigorous proofs of the bijectivity between the basic potentials and the basic variables of the theory. In the theory of Vignale and Rasolt (VR), the chosen basic variables (the charge and paramagnetic

current densities) do not reflect all of the physical consequences of a choice of basic potentials (scalar and vector), while in the theory of Pan and Sahni (PS) the gauge-invariance of the basic variables (the physical charge and current densities) does not allow for a Hohenberg-Kohn (HK) proof of uniqueness of the gauge-variant potentials.

The approach employed in this thesis took the necessary aspects of both previous formulations as its point of departure: the necessity of reflecting the gauge-dependence of the external potentials in the basic densities chosen to characterise the system of paramagnetic CDFT, and the necessity of reflecting all *physical* qualities in the chosen densities arising from the external electromagnetic fields.

That the basic variables need to reflect both gauge-variant and gauge-invariant phenomena means that they contain both the paramagnetic current density $\mathbf{j}_p(\mathbf{r})$ and the diamagnetic current density $\mathbf{j}_d(\mathbf{r})$ from which the physical current may be derived. Further, so long as the external vector potential does not vanish where the charge density is nonzero, the vector potential and diamagnetic current density uniquely determine the charge density, thus it need not be included as a basic variable.

The resulting HK theorem was

$$(v, \mathbf{A}) \xleftarrow{\quad\text{HK}\quad} (n, \mathbf{j}_p, \mathbf{j}_d)$$
$$A^{-1} \diagdown A \qquad B^{-1} \diagup B$$
$$(\lvert \Psi_0 \rangle, \mathbf{A}) \tag{6.1}$$

Chapter 3 contains the mathematical details of the proof, while the Appendix contains its extension to spin-polarised and degenerate ground-state systems (Sec. A.2). There is an additional uniqueness theorem that utilises equal numbers of density and potential variables, albeit at the expense of a straightforward minimisation procedure, also detailed in the Appendix, Sec. A.1.3.

One has some degree of choice in how one constructs a KS scheme, and Sec. 3.5 demonstrated that one could perform the minimisation procedure for a CDFT based on the paramagnetic and diamagnetic currents even when the KS system was defined to have the same *physical* charge and current densities as the interacting system and therefore, generally, different gauge-dependent densities. This allowed the construction of a scheme to calculate the ground-state densities of an interacting system by minimising its total energy with the use of a KS system with identical n and $\mathbf{j}$.

This research then established a practical scheme for calculating the densities of

interacting ground-state, current-carrying systems via an auxiliary system of noninteracting KS electrons subject to the effective external potentials

$$\mathbf{A}_{\mathrm{KS}}(\mathbf{r}) = \mathbf{A}_{\mathrm{ext}}(\mathbf{r}) + \mathbf{A}_{\mathrm{xc}}(\mathbf{r}) \tag{6.2}$$

$$v_{\mathrm{KS}}(\mathbf{r}) = v_{\mathrm{ext}}(\mathbf{r}) + v_{\mathrm{H}}(\mathbf{r}) + v_{\mathrm{xc}}(\mathbf{r}) + \tfrac{1}{2}\left[A_{\mathrm{KS}}^2(\mathbf{r}) - A_{\mathrm{ext}}^2(\mathbf{r})\right] \tag{6.3}$$

where $\mathbf{A}_{\mathrm{xc}}(\mathbf{r})$ and $v_{\mathrm{xc}}(\mathbf{r})$ are the exchange-correlation vector and scalar potentials respectively.

This formal basis is necessary for the calculation of exact KS systems that reproduce the charge and current densities of real, interacting systems, methods for which, both in the steady-state and nonequilibrium regimes, were derived in Chapter 3 and will be summarised in the next section. Other advantages of this approach is they it makes a connection with time-dependent current-density functional theory in the adiabatic limit, and employs Kohn-Sham systems that give predictions about physical densities.

6.2 The reverse-engineering algorithms

As discussed in the previous section, the auxiliary KS system is defined to have the same physical charge and current density as the real interacting system it represents, and yet neither interacting nor noninteracting potentials are uniquely defined by these quantities. In particular, $\mathbf{A}_{\mathrm{KS}}$ and v_{KS} are unique functionals of the Kohn-Sham gauge-variant current densities $\mathbf{j}_{\mathrm{p,KS}}$ and $\mathbf{j}_{\mathrm{d,KS}}$, which will generally differ from those of the interacting system.

The reverse-engineering algorithm for steady-state systems allows one to calculate corrections to the KS diamagnetic current density directly (and the paramagnetic current indirectly) in order to construct KS systems with the correct physical properties. The iterative scheme for calculating such potentials was detailed in Sec. 3.6, and was found to be convergent and have the correct stop-condition.

The algorithm was also simple to extend to the nonequilibrium regime, as was detailed in Sec. 3.7, which allows one to calculate the exact time-dependent KS scalar and vector potentials that reproduce the charge density of a nonequilibrium interacting system. The algorithm was tested for one-dimensional time-dependent systems subject to external scalar potentials only for which, once again, it has the correct stop-condition and was seen to be convergent.

This thesis has introduced two universal and tested schemes of calculating exact KS

potentials, including the XC term, for systems of known charge and current densities. These methods provide gain insight into the vital physics of exact KS systems, necessary for the future construction of better functionals.

6.3   Exact KS potentials for quantum nanowires

The time-independent form of the reverse-engineering algorithm was employed to study one-dimensional ground-state quantum wires to which current-carrying electron quasi-particles are added into the lowest-energy unoccupied state. The system under study was chosen to be free from any external magnetic fields for a variety of spin densities.

This algorithm was applied to a three-dimensional nanowire with the same electron occupancies and periodicity in the axial direction but strongly confined in the radial direction and with imposed cylindrical symmetry. It demonstrated rapid convergence to the potentials which reproduced the correct charge and current density. From studying the resulting time-dependent KS potential, it was concluded that:

- It is not generally possible to construct a 1D ground-state Kohn-Sham system that reproduces the charge and current density of a 1D ground-state interacting system as was found in Sec. 4.2;

- We can, however, calculate the exact KS scalar and vector potentials required to construct 2D and 3D ground-state Kohn-Sham systems that exactly reproduce the charge and current densities of interacting systems using the ground-state form of the reverse-engineering algorithm;

- Such KS systems were found in Sec. 4.3 to be subject to effective external magnetic fields or properties entirely, even if the interacting system they model is free from magnetic fields. These exchange-correlation magnetic fields are intrinsic to KS steady-state systems;

- The XC magnetic field can couple to the charge, current and magnetisation of the KS system. In particular, fields coupling to the magnetisation of the KS system can deform the charge density unless an additional KS scalar potential is included. This potential depends functionally on the charge, current and spin density of the system.

In time-dependent regime, we studied one-dimensional quantum wires based on silicon to which were added localised quasiparticle wavepackets with nonzero crystal

momentum, in the first instance governed by a nonlocal but Hermitian and energy-independent self-energy operator, as detailed in Sec. 5.1, and in the second case incorporating the quasiparticle decay associated to non-Hermitian self-energy operators implemented in the relaxation time approximation, as detailed in Sec. 5.5. The wavepacket was allowed to propagate through the wire due to its intrinsic momentum without the application of driving fields.

The algorithm was found to yield highly accurate KS systems very quickly and was indefinitely convergent. The following conclusions were drawn from the data produced in the first wavepacket study:

- The exact KS scalar potential contains a Hartree-like localised potential barrier, plus a periodic component that "tunes" the local band structure in the vicinity of the wavepacket

- The potential also contains a persistent time-dependent step demonstrating an ultranonlocal functional dependence of the potential on the charge and current density (see Sec. 5.3);

- It is the interplay of these three effects which is necessary to yield the correct wavepacket group velocity, a vital aspect of the time-dependent charge density;

- The potential demonstrates a strong and persistent functional dependence on the initial state of the KS system: two KS systems with the same time-dependent charge and current densities with only slightly different initial states were seen to have starkly different time-dependent KS potentials.

The reverse-engineering algorithm performed equally well for time-dependent quasi-particles undergoing exponential decay. In this case it was found that

- The time-dependent step due to the nonlocal (but Hermitian) part of the self-energy operator persists when the quasiparticle is allowed to decay;

- In addition, a much larger and more slowly-varying potential step arises across the quasiparticle width, allowing density to reflect and tunnel from the wavepacket region and aggregate across the wire;

- The potential also contains long-range components aiding the build-up of charge density in the quasiparticle background. These long-range potentials alone would polarise the charge density; as such, the potential was found to contain tilted "buckets" that forces the Kohn-Sham electron density to localise around the atomic sites;

- As well as describing its time-dependence correctly, it is possible to induce decay in Kohn-Sham systems with the use of exponentially large potentials whose spatial variation is nonetheless indicated by the semilocal charge and current density;

- In testing initial-state-dependence, it was found that the Kohn-Sham potential is very quickly insensitive as to whether the system is prepared in a state of decay or else the decay is induced afterwards.

One important conclusion of both studies of the one-dimensional time-dependent nanowire is that it is not feasible to construct local or semilocal functionals of the charge and/or current density for the scalar potential that capture the correct physics of nonequilibrium quantum transport, and that new types of functionals are required that allow for the introduction of nonlocal behaviours into the scalar potential. What kind of functionals one might seek to construct has been considered and will be summarised in the next section.

6.4   The KS electric and magnetic fields

In Chapter 4, the KS electric fields corresponding to the KS scalar potentials calculated for the nonequilibrium system were studied. It was found that the electric field $\Delta \mathscr{E}_{KS}$ needed *in addition* to the ground state was localised with the additional electron wavepacket, and that the nonlocal step in the potential was a consequence of the electric field having a time-dependent average. It was concluded that the electric field is much more amenable to local and semilocal approximation than the scalar potential itself, and indeed it was seen that the functional dependence of the electric field on the local quantities $\left(\partial_x n(x,t)\right)/n(x,t)$ and $\left(\partial_t j(x,t)\right)/n(x,t)$ was remarkably linear and local in time for the quasiparticle wavepacket scenario, as Sec. 5.4 demonstrates.

In the steady-state limit, $\dot{\mathbf{j}} = 0$, and the correct KS current density can no longer be achieved with an electric field alone. It was observed in Chapter 4 that a purely exchange-correlation *magnetic field* is required in order to yield KS systems with the correct physical densities, even in the absence of any external magnetic fields, and that mapping KS gauge-dependent densities onto their interacting counterparts does not introduce the correct physics. Generally, therefore, systems consisting of both steady-state and nonequilibrium components require both electric and magnetic XC fields, above that which is necessary to describe the steady-state charge density.

The usefulness of the electromagnetic fields as opposed to their corresponding potentials is two-fold: first, when mapping physical KS densities to their interacting

counterparts, the fields correctly lack the gauge-variance of the potentials which would be reflected in gauge-dependent densities; second, because the potentials are related to their corresponding fields via intergrals over space and/or time, the choice of the KS potential as a functional introduces ultranonlocalities that make local or semilocal functionals of the densities unfeasible or inaccurate. Thus the electromagnetic fields make for a logical choice for the construction of future functionals.

6.5   Ongoing and future developments

In order to construct improved functionals for current-density-functional and time-dependent density-functional approaches to quantum transport, one would need to calculate the exact KS potentials for many more systems to gather a more complete set of data upon which to base an analysis. The electric field's dependence on the gradient of the charge density suggests that more investigation of more rapidly-varying densities would be particularly important, and the data for the magnetic field strength in the central regions of current-carrying ground-state nanowires is presently limited.

The reverse-engineering algorithms should be employed once again to calculate the exact potentials and fields for systems with a broader range of parameters. Quasiparticle theory remains a highly effective and efficient method for studying systems where conduction is due to the introduction of a single electron, however at present we have studied only the spatially-nonlocal and non-Hermitian characteristics of the self-energy operator. The true self-energy operator is also energy-dependent: a property whose effect on the KS potential is not yet investigated. More realistic self-energy operators can be constructed from GW theory and employed in simulations of steady-state transport in a similar way.

For time-dependent transport, modifications to the model self energy operator should be considered to include energy-dependence and consider a broader range of nonequilibrium models. Beyond the one-electron approximation, much headway has already been made in exact continuum solutions of the time-dependent Schrödinger equation for two and three electrons and exact Hubbard model solutions for larger chains and electron numbers [141; 164] focusing on tunnelling transport absent in the research described in this thesis, the former employing the time-dependent reverse-engineering algorithm here.

Ultimately, suggested functionals must be tested with respect to experiment or experimentally-verified calculations, and it is the predictive power of functionals that

is of highest importance. Collaboration with other experimental and theory groups would provide a productive means of testing any new functional.

6.6 Concluding remarks

The purpose of this research was to develop methods for the calculation of exact Kohn-Sham potentials for quantum transport systems of known charge and current densities, particularly in the time-dependent regime. The result of these investigations was the reverse-engineering algorithms. So far, these algorithms have been found to be generally applicable, highly accurate for large numbers of time-steps and convergent, and we can propose their use as tools for calculating exact potentials with high confidence.

This provides a method for studying quantum transport (and, indeed, electronic systems in general), and not a means of calculating quantum transport systems from first principles. The ultimate aim of any such research is the construction of better, more accurate functionals. Some insight for how such functionals might be constructed has already been discovered, and a logical progression of this research would be to study the functional relationship between KS electromagnetic fields and the electronic charge and current densities in greater detail to advise the construction of such functionals.

The particular case of ground-state current-carrying systems has been put on a much firmer theoretical footing by the proof of unique relationships between particular ground-state densities (the paramagnetic and diamagnetic current densities) and the external potentials that yield them, and a practical scheme for the calculation of ground-state densities employing auxiliary Kohn-Sham systems of noninteracting electrons that have the same physical qualities as the interacting systems they represent. This approach can be employed to study the exact KS potentials for a broader range of systems and advise the construction of relevant approximate functionals.

Appendix A

Additional proofs

A.1 CDFT of balanced components

A.1.1 Hohenberg and Kohn revisited

Let us consider once more the proof of the Hohenberg-Kohn theorem with one minor and (as we shall see) inconsequential modification. One can consider ordinary DFT as a special case of any CDFT wherein $\mathbf{A}(\mathbf{r}) = \mathbf{0}$ always. We may consider now different special cases where $\mathbf{A}$ is similarly fixed in all instances, but is nonzero.

Let us state, then, that there exists two sets of external potentials $(v_1, \mathbf{A})$ and $(v_2, \mathbf{A})$ (where $v_2(\mathbf{r}) \neq v_1(\mathbf{r}) + C$ with C constant) that yield the same ground-state wavefunction:

$$(v_1, \mathbf{A}) \to |\Psi_0\rangle \leftarrow (v_2, \mathbf{A}). \tag{A.1}$$

The unique mapping between the potentials and their ground-state wavefunctions still holds as if $\mathbf{A}(\mathbf{r}) = \mathbf{0}$ since the Hamiltonians of the two systems differ only by the term $v_1(\mathbf{r}) - v_2(\mathbf{r})$, giving

$$(E_{v_1} - E_{v_2}) |\Psi_0\rangle = \left(\hat{H}_{v_1} - \hat{H}_{v_2} \right) |\Psi_0\rangle = (v_1(\mathbf{r}) - v_2(\mathbf{r})) |\Psi_0\rangle \tag{A.2}$$

and thus the two potentials are constrained to differ by no more than a constant equal to the differences in their respective ground-state energies.

Likewise the proof of a unique map between the potentials and the densities quickly

reduces to that of ordinary DFT. If $(v_1, \mathbf{A})$ and $(v_2, \mathbf{A})$ yield ground states $|\Psi_1\rangle$ and $|\Psi_2\rangle$ respectively, both having the same charge density, then their respective ground-state energies are

$$E_{v_1}\left[|\Psi_1\rangle\right] = F\left[|\Psi_1\rangle\right] + (\mathbf{j}_1 \mid \mathbf{A}) + \left(n \mid v_1 - \tfrac{1}{2}A^2\right) \tag{A.3}$$

$$E_{v_2}\left[|\Psi_2\rangle\right] = F\left[|\Psi_2\rangle\right] + (\mathbf{j}_2 \mid \mathbf{A}) + \left(n \mid v_2 - \tfrac{1}{2}A^2\right). \tag{A.4}$$

From the variational principle, we have

$$E_{v_i}\left[|\Psi_i\rangle\right] < \left\langle \Psi_j \left| \hat{H}_{v_i} \right| \Psi_j \right\rangle = E_j + (n \mid v_i - v_j) \tag{A.5}$$

where $i = 1, 2 \neq j = 2, 1$. Summing up over i yields the usual HK contradiction

$$E_1 + E_2 < E_2 + E_1. \tag{A.6}$$

Thus we see that the HK proof of DFT holds for *any* fixed vector potential, not just $\mathbf{A}(\mathbf{r}) = \mathbf{0}$.

A.1.2 Aims and terminology

The ideal scheme is one in which the number of basic densities and the number of basic potentials is balanced. In terms of uniqueness theorems, we are forced to dismiss $(n, \mathbf{j})$ and $(n, \mathbf{j}_{\mathrm{p}})$ as possible candidates. The remaining possibility is a CDFT that takes $(n, \mathbf{j}_{\mathrm{d}})$ as its basic densities. The previous section shows that such a choice of basic densities will yield a uniqueness theorem, since $(n, \mathbf{j}_{\mathrm{d}})$ together determine the external vector potential completely. What it did not show, however, is that a universal functional may be written in terms of $(n, \mathbf{j}_{\mathrm{d}})$.

First, we define the sets of data we wish to work with and the maps between them we wish to invert. The set $\mathscr{N}$ is the set of all possible combinations of V-representable charge densities $n(\mathbf{r})$ (ground-state densities of some external potentials $(v, \mathbf{A})$) and diamagnetic current densities $\mathbf{j}_{\mathrm{d}}(\mathbf{r})$ related to the charge density as $\mathbf{j}_{\mathrm{d}}(\mathbf{r}) = n(\mathbf{r})\mathbf{A}(\mathbf{r})$:

$$\mathscr{N} = \left\{n(\mathbf{r}), \mathbf{j}_{\mathrm{d}}(\mathbf{r})\right\}. \tag{A.7}$$

This is a subset of the set $\mathscr{J}$ of all possible combinations of charge and diamagnetic

current densities and whose elements are $(n, \mathbf{j}_\mathrm{d})$.

The set $\mathscr{S}$ is the set of all possible wavefunctions, together with any vector field $\mathbf{a}(\mathbf{r})$:

$$\mathscr{S} = \{\Psi, \mathbf{a}(\mathbf{r})\} \,. \tag{A.8}$$

Subsets of this set include the set $\mathscr{G}$ of all possible ground-state wavefunctions and any vector field:

$$\mathscr{G} = \{\Psi_0, \mathbf{a}(\mathbf{r})\} \,, \tag{A.9}$$

and the set $\mathscr{G}_A$ which is the set of all possible ground-state wavefunctions and the vector potential they are subject to:

$$\mathscr{G}_A = \{\Psi_0, \mathbf{A}(\mathbf{r})\} \tag{A.10}$$

whose elements are $(\Psi_0, \mathbf{A})$.

The set $\mathscr{V}$ is the set of all possible combinations of scalar and vector potentials:

$$\mathscr{V} = \{v(\mathbf{r}), \mathbf{A}(\mathbf{r})\} \tag{A.11}$$

whose elements are $(v, \mathbf{A})$.

A.1.3   Uniqueness theorem

The formal uniqueness theorem we wish to prove may be written as

$$
\begin{array}{ccc}
(v, \mathbf{A}) & \xleftarrow{\quad \text{HK} \quad}\dashrightarrow & (n, \mathbf{j}_\mathrm{d}) \\
& \underset{A^{-1}}{\overset{A}{\diagdown}} \quad \underset{B^{-1}}{\overset{B}{\diagup}} & \\
& (\left|\Psi_0\right\rangle, \mathbf{A}) &
\end{array} \tag{A.12}
$$

that is: a chosen element of $\mathscr{N}$ uniquely maps to an element of $\mathscr{V}$, and that element of $\mathscr{V}$ uniquely maps to the chosen element of $\mathscr{N}$. We establish this by first establishing unique and invertible maps between each of the elements in both sets and the elements of the intermediate set $\mathscr{G}_A$.

The map A is the solution of the time-independent Schrödinger equation and the

identity of the vector potential:

$$\left[\hat{H}\left[v, \mathbf{A}\right] - E_0\left[v, \mathbf{A}\right] \right]\Psi_0 = 0. \tag{A.13}$$

The map B is

$$n(\mathbf{r}) = \langle \Psi_0 \left| \hat{n}(\mathbf{r}) \right| \Psi_0 \rangle \tag{A.14}$$

$$\mathbf{j}_{\mathrm{d}}(\mathbf{r}) = \mathbf{A}(\mathbf{r}) \langle \Psi_0 \left| \hat{n}(\mathbf{r}) \right| \Psi_0 \rangle. \tag{A.15}$$

Map A^{-1} has been demonstrated in Sec. A.1.1, in particular Eq. A.2. We therefore need only to show that map B is invertible.

The energy of a state $|\Psi\rangle$ subject to external fields $(v, \mathbf{A})$ may be written as

$$E_{v,A} = \left\langle \Psi \left| \hat{T} + \hat{U} \right| \Psi \right\rangle + \int \frac{\mathbf{j}_{\mathrm{p}}\left[\Psi\right] \cdot \mathbf{j}_{\mathrm{d}} + \frac{1}{2}j_{\mathrm{d}}^2}{n} \, d\mathbf{r} + (n \,|\, v). \tag{A.16}$$

We suppose that there exist two different elements in $\mathscr{G}_A$ – $(\Psi_1, \mathbf{A}_1)$ and $(\Psi_2, \mathbf{A}_2)$ – corresponding to two different elements in $\mathscr{V}$, that yield the same $(n, \mathbf{j}_{\mathrm{d}})$ via map B.

Map B demands that

$$\mathbf{A}_1 = \mathbf{A}_2 = \frac{\mathbf{j}_{\mathrm{d}}}{n}. \tag{A.17}$$

Defining

$$\begin{aligned}
E'_{1,2} &= \left\langle \Psi_{1,2} \left| \hat{H}_{2,1} \right| \Psi_{1,2} \right\rangle_{1,2} \\
&= \left\langle \Psi_{1,2} \left| \hat{H}_{1,2} \right| \Psi_{1,2} \right\rangle + \left\langle \Psi_{1,2} \left| \hat{H}_{2,1} - \hat{H}_{1,2} \right| \Psi_{1,2} \right\rangle_{1,2} \\
&= E_{1,2} + (n \,|\, v_{2,1} - v_{1,2}) \\
&> E_{2,1}
\end{aligned}$$

and summing over both indices yields the usual contradiction

$$E_1 + E_2 > E_2 + E_1, \tag{A.18}$$

thus we have proved *reductio ad absurdum* that

$$|\Psi_0\rangle \;=\; |\Psi_0\rangle\,[n,\mathbf{j}_{\mathrm{d}}] \tag{A.19}$$

$$v(\mathbf{r}) \;=\; v\,[n,\mathbf{j}_{\mathrm{d}}]\,(\mathbf{r}) \tag{A.20}$$

which, together with the identity $\mathbf{A}(\mathbf{r}) = \mathbf{j}_{\mathrm{d}}(\mathbf{r})/n(\mathbf{r})$, ensures that all ground-state properties, including the paramagnetic current density $\mathbf{j}_{\mathrm{p}}(\mathbf{r})$, are unique functionals of $(n,\mathbf{j}_{\mathrm{d}})$.

A.1.4 Variational theorem

A uniqueness proof, the Rayleigh-Ritz theorem and Eq. A.16 allow us to construct a variational theorem

$$E_0\,[n,\mathbf{j}_{\mathrm{d}}] \leq E_{v,A}\,\left[n',\mathbf{j}_{\mathrm{d}}'\right], \tag{A.21}$$

where v denotes $v\,[n,\mathbf{j}_{\mathrm{d}}]\,(\mathbf{r})$, A denotes $\mathbf{A}\,[n,\mathbf{j}_{\mathrm{d}}]\,(\mathbf{r})$, and $\mathbf{j}_{\mathrm{d}}'$ is once again defined in terms of $\mathbf{A}$. This follows from the fact that

$$E_0\,[n,\mathbf{j}_{\mathrm{d}}] \leq \left\langle \Psi'\left[n',\mathbf{j}_{\mathrm{d}}'\right] \left| \hat{H}_{v,A} \right| \Psi'\left[n',\mathbf{j}_{\mathrm{d}}'\right] \right\rangle. \tag{A.22}$$

The variational theorem allows us, in principle, to construct an energy minimization scheme for finding the ground-state density n of a set of external potentials $(v,\mathbf{A})$. (Under fixed $\mathbf{A}$, once n is found, $\mathbf{j}_{\mathrm{d}}$ is once again fully determined.)

The second term on the right-hand side of Eq. A.16 is now a universal functional of our basic densities, thus we may define our energy in terms of a new functional

$$E_{v,A}\,\left[n',\mathbf{j}_{\mathrm{d}}'\right] = G\,\left[n',\mathbf{j}_{\mathrm{d}}'\right] + \left(n'\,|\,v\right) \tag{A.23}$$

where

$$G\,\left[n',\mathbf{j}_{\mathrm{d}}'\right] = F\,\left[n',\mathbf{j}_{\mathrm{d}}'\right] + \int \frac{\mathbf{j}_{\mathrm{p}}'\,\left[n',\mathbf{j}_{\mathrm{d}}'\right]\cdot\mathbf{j}_{\mathrm{d}}'(\mathbf{r}) + \tfrac{1}{2}j_{\mathrm{d}}'^2(\mathbf{r})}{n'(\mathbf{r})}\;d\mathbf{r} \tag{A.24}$$

The sole functional derivative of Eq. A.23 is then

$$\frac{\delta E_{v,A}}{\delta n'} = \frac{\delta G}{\delta n'} + v(\mathbf{r}). \tag{A.25}$$

While the functional dependence of $\mathbf{j}_p'$ on n' (for fixed $\mathbf{A}$) must be accounted for, such terms cancel and the minimization procedure quickly reduces to that of ordinary DFT:

$$\begin{aligned} \frac{\delta G}{\delta n'} &= \frac{\delta F}{\delta n'} + \mathbf{A} \cdot \frac{\delta \mathbf{j}_p'}{\delta n'} + \tfrac{1}{2}A^2 \\ &= \left(\frac{\delta F}{\delta n'}\right)_{\mathbf{j}_p'} + \frac{\delta \mathbf{j}_p'}{\delta n'} \cdot \left(\frac{\delta F}{\delta \mathbf{j}_p'}\right)_{n'} + \mathbf{A} \cdot \frac{\delta \mathbf{j}_p'}{\delta n'} + \tfrac{1}{2}A^2 \\ &= -v' - \tfrac{1}{2}A'^2 - \mathbf{A}' \cdot \frac{\delta \mathbf{j}_p'}{\delta n'} + \mathbf{A} \cdot \frac{\delta \mathbf{j}_p'}{\delta n'} + \tfrac{1}{2}A^2 \end{aligned}$$

yielding

$$\frac{\delta E_{v,A}}{\delta n} = v(\mathbf{r}) - v' \left[n', \mathbf{j}_d'\right](\mathbf{r}), \tag{A.26}$$

which gives the desired behaviour as $n' \to n$.

Thus we have shown that one may construct a CDFT with the same number of basic densities and basic potentials. The choice of $(n, \mathbf{j}_d)$ as basic densities is a counter-intuitive one, especially since, when minimizing the system energy under fixed external potentials, one does not consider the current density at all in this particular current-density functional theory.

Such a formulation is less an alternative approach to those of VR, Diener and PS, and more an extension of the original HK approach for ground-state DFT for a given vector potential. While $\mathbf{j}_d$ is not a measurable quantity, it is the current component that uniquely determines the external potentials, and the issue of non-physicality holds also for a choice of $\mathbf{j}_p$ as a basic density in nondegenerate systems. Further, since one does not actually employ $\mathbf{j}_d$ at all in the minimisation scheme beyond the evaluation of the universal functional, this is equivalent to dividing the universal functional into $\mathbf{A}$-dependent functionals, each uniquely defined by n only. Since $\mathbf{A}$ is always known in a minimization procedure, this is not problematic.

A.1.5 Practical minimisation and self-consistency schemes

It has been proven that a given ground-state charge and diamagnetic current density $(n_0(\mathbf{r}), \mathbf{j}_{d,0}(\mathbf{r}))$ uniquely determines the set of external scalar and vector potentials $(v(\mathbf{r}), \mathbf{A}(\mathbf{r}))$ that yield those densities as a nondegenerate ground state, and vice versa.

We have also seen that, in an ideal minimisation scheme under fixed external potentials where an expression (or at least a good approximation) for the universal functional $F[n(\mathbf{r}), \mathbf{j}_d(\mathbf{r})]$ is known, it is sufficient to vary only $n(\mathbf{r})$, since under fixed $\mathbf{A}(\mathbf{r})$, the

choice of a trial density n fixes the diamagnetic current density $\mathbf{j}_\mathrm{d}(\mathbf{r}) = \mathbf{A}(\mathbf{r})n(\mathbf{r})$.

For an interacting system, the energy functional of some set of trial densities subject to a fixed set of external potentials can be rewritten as

$$E_{v,A}[n(\mathbf{r}), \mathbf{j}_\mathrm{d}(\mathbf{r})] = F[n(\mathbf{r}), \mathbf{j}_\mathrm{d}(\mathbf{r})] + \int_{-\infty}^{\infty} d\mathbf{r}\, \frac{\mathbf{j}'[n(\mathbf{r}), \mathbf{j}_\mathrm{d}(\mathbf{r})](\mathbf{r}) \cdot \mathbf{j}_\mathrm{d}(\mathbf{r})}{n(\mathbf{r})}$$
$$+ \int_{-\infty}^{\infty} d\mathbf{r}\, n(\mathbf{r})u(\mathbf{r}) \tag{A.27}$$

where $u(\mathbf{r}) = v(\mathbf{r}) - \frac{1}{2}A^2(\mathbf{r})$. Nominally, the second term does not directly reference the external potentials. Here $\mathbf{j}'(\mathbf{r}) = \mathbf{j}'_\mathrm{p}(\mathbf{r}) + \mathbf{A}(\mathbf{r})n(\mathbf{r})$, where $\mathbf{j}'_\mathrm{p}(\mathbf{r})$ is the paramagnetic current density of the system whose ground-state basic densities are $(n, \mathbf{j}_\mathrm{d})$, and thus is uniquely determined by those densities.

As we can see, the reduction of the number of variable densities in a current-density functional theory to one (the charge) comes at the expense of increased complexity of the universal functional, and thus an increase of the number of terms therein that must be approximated: in addition to approximating the kinetic and Coulomb terms of the energy functional, one need also approximate how the current couples to the external fields.

However, the variational theorem of the previous section may easily be extended to include trial wavefunctions that are not the ground states of some set of external potentials $(u', \mathbf{A}')$. Consider the external potentials $(u, \mathbf{A})$ for which a ground-state solution is desired and for which, for conciseness, we define a (nonrelativistic) four-component vector

$$\mathbf{V}(\mathbf{r}) = (\mathbf{A}(\mathbf{r}), u(\mathbf{r})). \tag{A.28}$$

We then vary a trial wavefunction Ψ in order to find a minimum in the energy of the wavefunction when subject to $\mathbf{V}(\mathbf{r})$. By definition of the ground-state wavefunction, we have

$$\left\langle \Psi \left| \hat{H}_V \right| \Psi \right\rangle \geq \left\langle \Psi_0 \left| \hat{H}_V \right| \Psi_0 \right\rangle \tag{A.29}$$

irrespective of whether Ψ is itself the ground state of some other external potential $\mathbf{V}'(\mathbf{r})$.

The wavefunction Ψ uniquely determines the trial charge density $n(\mathbf{r})$ and the trial paramagnetic current density $\mathbf{j}_\mathrm{p}(\mathbf{r})$ and therefore defines, under fixed $\mathbf{V}$, the physical

current of the trial system. Defining basic and physical four-component vectors as

$$\mathbf{N}_\mathrm{d}(\mathbf{r}) = (\mathbf{j}_\mathrm{d}(\mathbf{r}), n(\mathbf{r})) \tag{A.30}$$

$$\mathbf{N}(\mathbf{r}) = (\mathbf{j}(\mathbf{r}), n(\mathbf{r})), \tag{A.31}$$

Eq. A.29 may be rewritten as

$$\left\langle \Psi \left| \hat{T} + \hat{W} \right| \Psi \right\rangle + (\mathbf{N}[\Psi, \mathbf{A}] \,|\, \mathbf{V}) >= \left\langle \Psi_0 \left| \hat{T} + \hat{W} \right| \Psi_0 \right\rangle + (\mathbf{N}_0[\Psi_0, \mathbf{A}] \,|\, \mathbf{V}) \tag{A.32}$$

where Ψ_0 is the ground state of $\mathbf{V}$ and $\mathbf{N}_0$ the corresponding density, and we have adopted the conventions

$$(a(\mathbf{r}) \,|\, b(\mathbf{r})) = \int_{-\infty}^{\infty} d\mathbf{r} \, a(\mathbf{r}) b(\mathbf{r}) \tag{A.33}$$

$$(\mathbf{A}(\mathbf{r}) \,|\, \mathbf{B}(\mathbf{r})) = \int_{-\infty}^{\infty} d\mathbf{r} \, \mathbf{A}(\mathbf{r}) \cdot \mathbf{B}(\mathbf{r}). \tag{A.34}$$

Because the diamagnetic current is fixed by $n(\mathbf{r})$ and $\mathbf{A}(\mathbf{r})$, a unique choice of Ψ is equivalent to a unique choice of $\mathbf{N}(\mathbf{r})$. (Note, this is *only* true under fixed $\mathbf{A}(\mathbf{r})$: generally, there are multiple wavefunctions that yield the same $\mathbf{N}(\mathbf{r})$.) As such, we may simultaneously move beyond the restriction that trial densities be the ground states of some external potential and incorporate aspects of the universal functional into the variation scheme.

The general energy functional may then be written as

$$E_V[\mathbf{N}_\mathrm{d}] = F[\mathbf{N}_\mathrm{d}] + (\mathbf{N}[\mathbf{N}_\mathrm{d}] \,|\, \mathbf{V}). \tag{A.35}$$

Defining the four-component density operators as

$$\hat{\mathbf{N}}_1(\mathbf{r}) = \left(\hat{\mathbf{j}}_\mathrm{p}(\mathbf{r}), \hat{n}(\mathbf{r}) \right) \tag{A.36}$$

$$\hat{\mathbf{N}}_2(\mathbf{r}) = (\hat{n}(\mathbf{r}) \mathbf{A}(\mathbf{r}), 0) \tag{A.37}$$

and noting that the first of these and the universal functional $F[\mathbf{N}_\mathrm{d}]$ do not depend on the external potential, the functional derivative of the energy functional with respect

to the external potential is evaluated as

$$
\begin{aligned}
\frac{\delta E_V}{\delta \mathbf{V}(\mathbf{r})} &= \frac{\delta F}{\delta \mathbf{V}(\mathbf{r})} + \frac{\delta}{\delta \mathbf{V}(\mathbf{r})} \left(\hat{\mathbf{N}}_1(\mathbf{r}') \,|\, \mathbf{V}(\mathbf{r}') \right) + \frac{\delta}{\delta \mathbf{V}(\mathbf{r})} \left(\hat{\mathbf{N}}_2(\mathbf{r}') \,|\, \mathbf{V}(\mathbf{r}') \right) \\
&= \left(\hat{\mathbf{N}}_1(\mathbf{r}') \,|\, \frac{\delta \mathbf{V}(\mathbf{r}')}{\delta \mathbf{V}(\mathbf{r})} \right) + \frac{\delta}{\delta \mathbf{V}(\mathbf{r})} \left(\hat{n}(\mathbf{r}') \,|\, \tfrac{1}{2}\mathbf{A}(\mathbf{r}') \cdot \mathbf{A}(\mathbf{r}') \right) \\
&= \left(\hat{\mathbf{N}}_1(\mathbf{r}') \,|\, \delta(\mathbf{r}, \mathbf{r}') \right) + \left(\hat{\mathbf{N}}_2 \,|\, \delta(\mathbf{r}, \mathbf{r}') \right) \\
&= (\mathbf{j}_{\mathrm{p}}(\mathbf{r}), n(\mathbf{r})) + (\mathbf{j}_{\mathrm{d}}(\mathbf{r}), 0) \\
&= \mathbf{N}(\mathbf{r}).
\end{aligned} \tag{A.38}
$$

Thus we see that the conjugate variable to the external potential is the four-component density, making it a sensible choice for the variable in a minimisation scheme.

Rearranging Eq. A.35, we have

$$
F[\mathbf{N}_{\mathrm{d}}] = E_{V'}[\mathbf{N}_{\mathrm{d}}] - \left(\mathbf{N}(\mathbf{r}') \,|\, \mathbf{V}'(\mathbf{r}') \right), \tag{A.39}
$$

where $\mathbf{V}'(\mathbf{r})$ is the potential which has $\mathbf{N}(\mathbf{r})$ as its ground-state density, and its functional derivative with respect to the physical density is

$$
\begin{aligned}
\frac{\delta F[\mathbf{N}_{\mathrm{d}}]}{\delta \mathbf{N}(\mathbf{r})} &= \frac{\delta E_V[\mathbf{N}_{\mathrm{d}}]}{\delta \mathbf{N}(\mathbf{r})} - \left(\delta(\mathbf{r}, \mathbf{r}') \,|\, \mathbf{V}'(\mathbf{r}') \right) - \left(\mathbf{N}(\mathbf{r}') \,|\, \frac{\delta \mathbf{V}'(\mathbf{r}')}{\delta \mathbf{N}(\mathbf{r})} \right) \\
&= \left(\frac{\delta E_V}{\delta \mathbf{V}'(\mathbf{r}')} \,|\, \frac{\delta \mathbf{V}'(\mathbf{r}')}{\delta \mathbf{N}(\mathbf{r})} \right) - \mathbf{V}'(\mathbf{r}) - \left(\mathbf{N}(\mathbf{r}') \,|\, \frac{\delta \mathbf{V}'(\mathbf{r}')}{\delta \mathbf{N}(\mathbf{r})} \right) \\
&= \left(\mathbf{N}(\mathbf{r}') \,|\, \frac{\delta \mathbf{V}'(\mathbf{r}')}{\delta \mathbf{N}(\mathbf{r})} \right) - \mathbf{V}'(\mathbf{r}) - \left(\mathbf{N}(\mathbf{r}') \,|\, \frac{\delta \mathbf{V}'(\mathbf{r}')}{\delta \mathbf{N}(\mathbf{r})} \right) \\
&= -\mathbf{V}'(\mathbf{r}).
\end{aligned} \tag{A.40}
$$

The universal functional may then be decomposed as

$$
F = T_{\mathrm{S}} + E_{\mathrm{H}} + E_{\mathrm{xc}} \tag{A.41}
$$

where T_{S} is the single-particle kinetic energy, E_{H} the Hartree energy as usual, and E_{xc} the exchange-correlation (XC) energy (i.e. remainder of the universal energy).

In standard DFT, T_{S} is defined as the kinetic energy of a system of noninteracting particles having the same charge density as the interacting system and as such is

uniquely determined by the density, while in the CDFT of Vignale and Rasolt, it is the kinetic energy of a noninteracting system having the same charge and paramagnetic current density as the interacting system. In both cases, since the noninteracting system is chosen to have the same basic densities as the interacting system, T_S is a unique functional of those densities. Here, however, the noninteracting and interacting systems do not share the same basic densities.

We may note that the universal functional $F[n, \mathbf{j}_d]$ is always exactly equal to a non-universal functional $F^A[\mathbf{N}]$ during energy minimisation:

$$F^A[\mathbf{N}] = F[\mathbf{N}_d]\big|_{\mathbf{j}_d = n\mathbf{A}}, \tag{A.42}$$

where A uniquely indexes the external vector potential $\mathbf{A}$, since knowledge of $\mathbf{N}(\mathbf{r})$ and $\mathbf{A}(\mathbf{r})$ yields $\mathbf{N}_d(\mathbf{r})$. Decomposing the $\mathbf{A}$-dependent functional as before, we have

$$F^A[\mathbf{N}] = T_S^A[\mathbf{N}] + E_H[\mathbf{N}] + E_{xc}^A[\mathbf{N}]. \tag{A.43}$$

We consider now a system of an equal number N of noninteracting electrons whose density $\mathbf{N}_{KS}(\mathbf{r})$ satisfies the identity

$$\mathbf{N}_{KS}(\mathbf{r}) = \mathbf{N}(\mathbf{r}) \tag{A.44}$$

via the equations

$$\left\{ \tfrac{1}{2} \left[\hat{\mathbf{p}} + \mathbf{A}_{KS}(\mathbf{r}) \right]^2 + v_{KS}(\mathbf{r}) \right\} \phi_i(\mathbf{r}) = \epsilon_i \phi_i(\mathbf{r}) \tag{A.45}$$

$$n_{KS}(\mathbf{r}) = \sum_{i=1}^{N} \langle \phi_i(\mathbf{r}) \, |\hat{n}(\mathbf{r})| \, \phi_i(\mathbf{r}) \rangle \tag{A.46}$$

$$\mathbf{j}_{KS}(\mathbf{r}) = \mathbf{A}_{KS}(\mathbf{r}) n_{KS}(\mathbf{r}) + \sum_{i=1}^{N} \left\langle \phi_i \left| \hat{\mathbf{j}}_p(\mathbf{r}) \right| \phi_i \right\rangle \tag{A.47}$$

$$\mathbf{N}_{KS}(\mathbf{r}) = (\mathbf{j}_{KS}(\mathbf{r}), n_{KS}(\mathbf{r})). \tag{A.48}$$

For the noninteracting system subject to the effective external field

$$\mathbf{V}_{KS}(\mathbf{r}) = (\mathbf{A}_{KS}(\mathbf{r}), u_{KS}(\mathbf{r})), \tag{A.49}$$

we require that

$$F^{A_{\mathrm{KS}}}[\mathbf{N}] = T_{\mathrm{S}}^{A}[\mathbf{N}].\tag{A.50}$$

Applying the Hellman-Feynman [137]-[138] theorem and taking the functional derivative of Eq. A.43 with respect to the physical density as before, we have that

$$\begin{aligned}
\frac{\delta F^{A}}{\delta \mathbf{N}} &= \frac{\delta F^{A_{\mathrm{KS}}}}{\delta \mathbf{N}} + \frac{\delta E_{\mathrm{H}}}{\delta \mathbf{N}} + \frac{\delta E_{\mathrm{xc}}^{A_{\mathrm{KS}}}}{\delta \mathbf{N}} = -\mathbf{V}'(\mathbf{r}) \\
&= -\mathbf{V}_{\mathrm{KS}}(\mathbf{r}) + (\mathbf{0}, v_{\mathrm{H}}(\mathbf{r})) + \mathbf{V}_{\mathrm{xc}}(\mathbf{r}) \\
&= -\mathbf{V}(\mathbf{r}),
\end{aligned}\tag{A.51}$$

where we have defined

$$\mathbf{V}_{\mathrm{xc}}(\mathbf{r}) = \frac{\delta E_{\mathrm{xc}}^{A_{\mathrm{KS}}}}{\delta \mathbf{N}}.\tag{A.52}$$

Thus we have an expression for the noninteracting potential

$$\mathbf{V}_{\mathrm{KS}}(\mathbf{r}) = \mathbf{V}(\mathbf{r}) + (\mathbf{0}, v_{\mathrm{H}}(\mathbf{r})) + \mathbf{V}_{\mathrm{xc}}(\mathbf{r})\tag{A.53}$$

which, from Eq. A.28, has scalar and vector components which defined the exchange-correlation potentials

$$\mathbf{A}_{\mathrm{KS}}(\mathbf{r}) = \mathbf{A}(\mathbf{r}) + \mathbf{A}_{\mathrm{xc}}(\mathbf{r})\tag{A.54}$$

$$u_{\mathrm{KS}}(\mathbf{r}) = u(\mathbf{r}) + v_{\mathrm{H}}(\mathbf{r}) + v_{\mathrm{xc}}(\mathbf{r})\tag{A.55}$$

and thus

$$v_{\mathrm{KS}}(\mathbf{r}) = v(\mathbf{r}) + v_{\mathrm{H}}(\mathbf{r}) + v_{\mathrm{xc}}(\mathbf{r}) + \tfrac{1}{2}\left[A_{\mathrm{KS}}^{2}(\mathbf{r}) - A^{2}(\mathbf{r})\right].\tag{A.56}$$

It should be noted that, while $\mathbf{V}_{\mathrm{KS}}(\mathbf{r})$ is a unique functional of

$$\mathbf{N}_{\mathrm{d,KS}}(\mathbf{r}) = n(\mathbf{r})\left(\mathbf{A}_{\mathrm{KS}}(\mathbf{r}), 1\right),\tag{A.57}$$

it is not a unique functional of $\mathbf{N}(\mathbf{r})$. The single-particle kinetic energy is only uniquely defined for a specific definition of E_{xc} and the condition that

$$F^{A}[\mathbf{N}] - E_{\mathrm{H}}[\mathbf{N}] = T_{\mathrm{S}}^{A}[\mathbf{N}] + E_{\mathrm{xc}}^{A}[\mathbf{N}].\tag{A.58}$$

Such a condition allows for a gauge-dependence in the XC functional. One can eliminate this entirely by implementing the further conditions that

$$\boldsymbol{\nabla} \cdot \mathbf{A}_{\mathrm{xc}}(\mathbf{r}) = 0 \qquad (A.59)$$

and that v_{xc} go to zero infinitely far from the system. This ensures that $\boldsymbol{\nabla} \cdot \mathbf{A}_{\mathrm{KS}}(\mathbf{r}) = \boldsymbol{\nabla} \cdot \mathbf{A}(\mathbf{r})$ and that $v_{\mathrm{xc}}(\mathbf{r})$ does not add an arbitrary constant to the energy of the trial density.

Beyond gauge-dependence, if there exist multiple choices of $\mathbf{V}_{\mathrm{xc}}[\mathbf{N}]$ that yield the same universal functional, all are equivalent since they do not effect energy minimisation. On the other hand, the XC functional must be constructed (e.g. from *ab initio* calculations) in such a way as that, if multiple choices of $\mathbf{V}_{\mathrm{xc}}[\mathbf{N}]$ exist that yield the same physical densities but different universal functionals, the correct one is selected.

A.2 Extensions to CDFT

A.2.1 Spin-polarised systems

The proof of uniqueness in Sec. 3.3 is valid for one-component ground-state wavefunctions, but does not generally hold for spinors. There are two approaches for incorporating spin into the theory. In paramagnetic CDFT, the charge and current densities are decomposed into their spin-up and spin-down components, as are the scalar and vector potentials that couple to them. All physical quantities can then be derived from the nonphysical spin-dependent components. An equivalent approach is to introduce the magnetization as a basic quantity, the benefit being that this is a physical quantity.

The magnetization of a system of N electrons is defined as

$$\mathbf{m}(\mathbf{r}) = \langle \Psi_0 \, | \hat{\mathbf{m}}(\mathbf{r}) | \, \Psi_0 \rangle \qquad (A.60)$$

where $\hat{\mathbf{m}}(\mathbf{r})$ is the magnetization operator

$$\hat{\mathbf{m}}(\mathbf{r}) = \mu_{\mathrm{B}} \sum_{i=1}^{N} \hat{\boldsymbol{\sigma}}_i \delta(\mathbf{r} - \mathbf{r}_i). \qquad (A.61)$$

where μ_{B} is the Bohr magneton. $\hat{\boldsymbol{\sigma}}$ is the spin operator, a vector operator whose three

spatial components are the Pauli spin matrices

$$\hat{\sigma}_x = \begin{bmatrix} 0 & 1 \\ 1 & 0 \end{bmatrix}, \hat{\sigma}_y = \begin{bmatrix} 0 & -i \\ i & 0 \end{bmatrix}, \hat{\sigma}_z = \begin{bmatrix} 1 & 0 \\ 0 & -1 \end{bmatrix}$$

The ground-state wavefunction is now a two-component spinor:

$$|\Psi_0\rangle = \begin{bmatrix} |\Phi_{0,\uparrow}\rangle \\ |\Phi_{0,\downarrow}\rangle \end{bmatrix} \tag{A.62}$$

and is the lowest-energy solution of the Pauli Hamiltonian

$$\hat{H} = \tfrac{1}{2}\left(\hat{\boldsymbol{\sigma}} \cdot [\hat{\mathbf{p}} + \mathbf{A}(\mathbf{r})]\right)^2 + v(\mathbf{r}) \tag{A.63}$$

which, in the absence of spin-orbit coupling, can be decomposed into the standard Hamiltonian for charges in external electromagnetic fields, plus a spin-dependent Stern-Gerlach term

$$\hat{H} = \tfrac{1}{2}\left[\hat{\mathbf{p}} + \mathbf{A}(\mathbf{r})\right]^2 + v(\mathbf{r}) - \mu_{\mathrm{B}}\hat{\boldsymbol{\sigma}} \cdot \mathbf{B}(\mathbf{r}) \tag{A.64}$$

where the external magnetic field, as usual, is given by $\mathbf{B}(\mathbf{r}) = \boldsymbol{\nabla} \times \mathbf{A}(\mathbf{r})$.

The ground-state energy of a system subject to potentials $(v, \mathbf{A})$ may then be written in several different ways:

$$E_0 = \left\langle \Psi \left| \hat{T} + \hat{U} \right| \Psi \right\rangle + \int d\mathbf{r} \ \left\{ \mathbf{j}_{\mathrm{p}} \cdot \mathbf{A} + n(v + \tfrac{1}{2}A^2) - \mathbf{m} \cdot \mathbf{B} \right\} \tag{A.65}$$

$$= \left\langle \Psi \left| \hat{T} + \hat{U} \right| \Psi \right\rangle + \int d\mathbf{r} \ \left\{ \mathbf{j} \cdot \mathbf{A} + n(v - \tfrac{1}{2}A^2) \right\} \tag{A.66}$$

$$= \left\langle \Psi \left| \hat{T} + \hat{U} \right| \Psi \right\rangle + \int d\mathbf{r} \ \left\{ (\mathbf{j}_{\mathrm{p}} + \nabla \times \mathbf{m}) \cdot \mathbf{A} + n(v + \tfrac{1}{2}A^2) \right\} \tag{A.67}$$

The number of external potentials has not changed from the current-density functional theory of Chapter 3, but the number of degrees of freedom the vector potential has to couple with the system has, due to the way that, via the associated magnetic field, it can couple to the magnetisation. For this reason, it is frequently the case that the external magnetic field is treated is independent of the external vector potential, a situation that is mathematically sound but physically only approximate. In Vignale-Rasolt theory [124], for instance, the imbalance is addressed first by noting that only

the scalar product of the magnetic field and magnetisation define the system, and second by decomposing the scalar and vector potentials into (nonphysical) spin-up and -down components, with

$$v(\mathbf{r}) = v_\uparrow(\mathbf{r}) + v_\downarrow(\mathbf{r}) \tag{A.68}$$

$$B_z(\mathbf{r}) = v_\uparrow(\mathbf{r}) - v_\downarrow(\mathbf{r}) \tag{A.69}$$

$$\mathbf{A}(\mathbf{r}) = \mathbf{A}_\uparrow(\mathbf{r}) = \mathbf{A}_\downarrow(\mathbf{r}). \tag{A.70}$$

The densities are then also decomposed into spin-up and -down components, with

$$n(\mathbf{r}) = n_\uparrow(\mathbf{r}) + n_\downarrow(\mathbf{r}) \tag{A.71}$$

$$m_z(\mathbf{r}) = n_\uparrow(\mathbf{r}) - n_\downarrow(\mathbf{r}) \tag{A.72}$$

$$\mathbf{j}_\mathrm{p}(\mathbf{r}) = \mathbf{j}_{\mathbf{p},\uparrow}(\mathbf{r}) + \mathbf{j}_{\mathbf{p},\downarrow}(\mathbf{r}) \tag{A.73}$$

with no spin-dependent coupling to the current. This yields a current- and spin-density functional theory (CSDFT) based on eight scalar potentials and eight scalar densities, wherein the magnetic field is introduced via the scalar potentials (and is independent of $\mathbf{A}$) and the magnetisation via the spin densities.

An alternative approach is to introduce the magnetisation as a vector via the current densities, exploiting the fact that the full physical current density is

$$\mathbf{j}(\mathbf{r}) = \mathbf{j}_\mathrm{p}(\mathbf{r}) + \mathbf{j}_\mathrm{d}(\mathbf{r}) + \nabla \times \mathbf{m}(\mathbf{r}). \tag{A.74}$$

The magnetic interaction is then introduced as the coupling of the last term in Eq. A.74 with the vector potential [95], with the true association between the vector potential and magnetic field intact.

It has already been proved [124] that the ground-state spinor of an N-electron system uniquely determines and is uniquely determined by the charge density $n(\mathbf{r})$ and the full paramagnetic current for magnetised systems

$$\mathbf{j}_\mathrm{g}(\mathbf{r}) = \mathbf{j}_\mathrm{p}(\mathbf{r}) + \nabla \times \mathbf{m}(\mathbf{r}) \tag{A.75}$$

thus one can rewrite the uniqueness theorem of Sec. 3.3 as

$$
\begin{array}{c}
(v, \mathbf{A}) \xleftarrow{\text{HK}} (n, \mathbf{j_g}, \mathbf{j_d}) \\[2mm]
\quad\; {}_{A^{-1}}\!\diagdown\!{}_{A} \qquad {}_{B^{-1}}\!\diagup\!{}_{B} \\[2mm]
(|\Psi_0\rangle, \mathbf{A})
\end{array}
\tag{A.76}
$$

Maps B and B^{-1} have already been discussed. As usual, map A is trivially proven by the definition of the Pauli Hamiltonian and the nondegeneracy of the system, and map B is given by the definitions of the charge density, diamagnetic current density and now the magnetisation in terms of the ground-state wavefunction and the vector potential. Map A^{-1} follows exactly as per current-density functional theory, since the magnetisation depends only on the wavefunction.

The energy functional of a set of trial densities $\mathbf{N} = \{n, \mathbf{j_g}, \mathbf{j_d}\}$ in terms of the physical current remains unchanged

$$
E_{v,A}[\mathbf{N}] = F[\mathbf{N}] + \int \, d\mathbf{r} \, \left\{ \mathbf{j}(\mathbf{r}) \cdot \mathbf{A}(\mathbf{r}) + n(\mathbf{r}) \left[v(\mathbf{r}) - \tfrac{1}{2}A^2(\mathbf{r}) \right] \right\}
\tag{A.77}
$$

$$
\geq E_{v,A}[\mathbf{N}_0] = F[\mathbf{N}_0] + \int \, d\mathbf{r} \, \left\{ \mathbf{j}_0(\mathbf{r}) \cdot \mathbf{A}(\mathbf{r}) + n_0(\mathbf{r}) \left[v(\mathbf{r}) - \tfrac{1}{2}A^2(\mathbf{r}) \right] \right\}
$$

where $\mathbf{N}_0 = \{n_0, \mathbf{j}_{g,0}, \mathbf{j}_{d,0}\}$ and $\mathbf{j}_0(\mathbf{r}) = \mathbf{j}_{g,0}(\mathbf{r}) + \mathbf{j}_{d,0}(\mathbf{r})$.

Functional derivatives of the universal functional are then taken with respect to the current density $\mathbf{j}_g(\mathbf{r})$ to yield a practical Kohn-Sham scheme for energy minimisation.

Thus current-density functional theory may be extended to include spin polarisation with no increase in the number of basic potentials or basic densities. Only the number of intermediate variables has changed, since $|\Psi\rangle$ is now a two-component spinor.

A.2.2 Degenerate ground states

As with standard ground-state DFT (i.e. for systems in the absence of a vector potential), the HK-like proof for a CDFT based on the paramagnetic and diamagnetic current densities relies on the Ritz variational procedure such that if $|\Psi_0\rangle$ is the ground state of Hamiltonian $\hat{H}$, any state $|\Psi'\rangle \neq |\Psi_0\rangle$ obeys the inequality

$$
\left\langle \Psi' \left| \hat{H} \right| \Psi' \right\rangle > \left\langle \Psi_0 \left| \hat{H} \right| \Psi_0 \right\rangle,
\tag{A.78}
$$

i.e. it only holds for nondegenerate systems. For a Hamiltonian that has more than one ground state, the above inequality does not hold and the HK theorems remain unproven.

There are two distinct types of state that might have a different wavefunction but the same energy when subject to a given set of potentials: *pure* states, where the wavefunction is any linear combination of degenerate ground states, and *mixed* states, where the system is in a statistical ensemble of unmixed ground states. We have discussed the representation of mixed-state ensembles in Chapter 3. In this section, we shall concern ourselves with pure states only.

Defining the set of all possible potentials $\mathscr{V}$ as before:

$$\mathscr{V} : \{v(\mathbf{r}), \mathbf{A}(\mathbf{r})\} \tag{A.79}$$

then from the set of all ground states, $\mathscr{G}$, we can define the particular set of degenerate ground states, together with their corresponding vector potential, for a particular combination of scalar and vector potentials as

$$\mathscr{G}_v : \left\{ |\Psi_0\rangle = \sum_{i=1}^{G} c_i |\Psi_{0,i}\rangle , \mathbf{A} \right\} \tag{A.80}$$

where $\{|\Psi_{0,i}\rangle\}$ are the G degenerate ground states of the fixed scalar and vector potentials $v(\mathbf{r})$ and $\mathbf{A}(\mathbf{r})$. We can likewise define, from the set of all ground-state basic densities $\mathscr{N}$, the set of densities

$$\mathscr{N}_v : \{n, \mathbf{j}_\mathrm{p}(\mathbf{r}), \mathbf{j}_d(\mathbf{r})\} . \tag{A.81}$$

The maps we then wish to prove unique are shown schematically in Eq. A.82.

$$
\begin{array}{ccc}
\mathscr{V} & \xleftarrow{\quad\text{HK}\quad}\dashrightarrow & \mathscr{N}_v \\[2pt]
A^{-1}\diagdown A & B^{-1}\diagup B & \\
 & \mathscr{G}_v &
\end{array}
\tag{A.82}
$$

If map A is false, then there exist other ground-state solutions of the Hamiltonian specified by potentials v and $\mathbf{A}$ that are not in $\mathscr{G}_v$, since the vector potential in $\mathscr{G}_v$ is

that of $\mathscr{V}$ by definition. This existence of other ground states is not possible since $\mathscr{G}_v$ is defined from the complete set of degenerate ground states of that Hamiltonian. Map B is also trivially shown to be true from the definition $\mathscr{N}_v$ in Eq. A.81.

If map A^{-1} is false, then there exists a state $|\Psi_0\rangle$ that can be constructed from the degenerate ground states of two different sets of potentials $(v_1, \mathbf{A}_1)$ and $(v_2, \mathbf{A}_2)$ with corresponding Hamiltonians $\hat{H}_1$ and $\hat{H}_2$ and energies given by

$$E_1 |\Psi_0\rangle = \hat{H}_1 |\Psi_0\rangle$$
$$E_2 |\Psi_0\rangle = \hat{H}_2 |\Psi_0\rangle,$$

thus

$$(E_1 - E_2) |\Psi_0\rangle = \left[\hat{H}_1 - \hat{H}_2\right] |\Psi_0\rangle. \tag{A.83}$$

Since the set $\mathscr{G}_v$ determines the vector potential $\mathbf{A}$ by definition, we have that $\mathbf{A}_2 = \mathbf{A}_1$ and thus

$$(E_1 - E_2) = [v_1 - v_2] |\Psi_0\rangle \tag{A.84}$$

which holds for all positions only if

$$v_1(\mathbf{r}) - v_2(\mathbf{r}) = E_1 - E_2, \tag{A.85}$$

i.e. if the two potentials differ only by a constant. Thus map A^{-1} is unique up to an additive constant in $v(\mathbf{r})$.

Finally, if map B^{-1} is false, then two sets of degenerate ground states and corresponding vector potentials can yield the same basic densities:

$$(|\Psi_1\rangle, \mathbf{A}_1) \to (n, \mathbf{j}_\mathrm{p}, \mathbf{j}_d) \leftarrow (|\Psi_2\rangle, \mathbf{A}_2). \tag{A.86}$$

Again, the set $\mathscr{G}_v$ uniquely determines the vector potential:

$$\mathbf{A}_2(\mathbf{r}) = \mathbf{A}_1(\mathbf{r}) = \mathbf{A}(\mathbf{r}) \tag{A.87}$$

where $\mathbf{j}_d(\mathbf{r})$ and $n(\mathbf{r})$ are as defined in Eq. A.81. The proof of map A means that the two states $|\Psi_1\rangle$ and $|\Psi_2\rangle$ must be constructed from the degenerate ground states of two

different sets of external potentials. From the Ritz variational principle, we have that

$$E_1' = \left\langle \Psi_1 \left| \hat{H}_2 \right| \Psi_1 \right\rangle = \left\langle \Psi_1 \left| \hat{H}_1 \right| \Psi_1 \right\rangle + \left\langle \Psi_1 \left| \hat{H}_2 - \hat{H}_1 \right| \Psi_1 \right\rangle$$

$$= E_1 + \int d\mathbf{r} \, n(\mathbf{r}) \left[v_2 - v_1 \right] > E_2 \tag{A.88}$$

$$E_2' = E_2 + \int d\mathbf{r} \, n(\mathbf{r}) \left[v_1 - v_2 \right] > E_1. \tag{A.89}$$

Summing the two inequalities leads to the contradiction

$$E_1 + E_2 > E_2 + E_1 \tag{A.90}$$

and thus map B^{-1} has been proven *reductio ad absurdum*. Thus there exists a one-to-one relationship between the external potentials $(v, \mathbf{A})$ and the degenerate ground-state densities $(n, \mathbf{j}_d)$, although not *individual* degenerate combinations of particular charge and diamagnetic current densities. Thus we may write the external scalar and vector potentials as unique functionals of the densities:

$$v(\mathbf{r}) = v\left[n, \mathbf{j}_\mathrm{p}, \mathbf{j}_d \right](\mathbf{r})$$
$$\mathbf{A}(\mathbf{r}) = \mathbf{A}\left[n, \mathbf{j}_\mathrm{p}, \mathbf{j}_d \right](\mathbf{r}). \tag{A.91}$$

References

[1] M. A. Reed, C. Zhou, C. J. Muller, T. P. Burgin, and J. M. Tour, "Conductance of a molecular junction," *Science*, vol. 278, p. 252, 1997. vi, 3

[2] V. Rodrigues and D. Ugarte, "Real-time imaging of atomistic process in one-atom-thick metal junctions," *Phys. Rev. B*, vol. 63, p. 073405, 2001. vi, 3

[3] J. M. Cowley, *Diffraction Physics*. Amsterdam: Elsevier, 1975. vi, 4

[4] H. Ohnishi, Y. Kondo, and K. Takayanagi, "Quantized conductance through individual rows of suspended gold atoms," *Nature*, vol. 395, pp. 780–783, 1998. vi, 4

[5] C. W. J. Beenakker, "Theory of Coulomb-blockade oscillations in the conductance of a quantum dot," *Phys. Rev. B*, vol. 44, pp. 1646–1656, 1991. vi, 10

[6] J. Park, "Coulomb blockade and the Kondo effect in single-atom transistors," *Nature*, vol. 417, pp. 722–725, 2002. vi, 11

[7] S. Kurth, G. Stefanucci, E. Khosravi, C. Verdozzi, and E. K. U. Gross, "Dynamical Coulomb Blockade and the Derivative Discontinuity of Time-Dependent Density Functional Theory," *Phys. Rev. Lett.*, vol. 104, p. 236801, 2010. vii, 18, 19

[8] J. E. Hirsch, "Superconductivity from hole undressing," *Physica C: Superconductivity*, vol. 364-365, pp. 37–42, 2001. vii, 23

[9] J. Rammer and H. Smith, "Quantum field-theoretical methods in transport theory of metals," *Rev. Mod. Phys.*, vol. 58, pp. 323–359, 1986. vii, 27

[10] C. Toher, A. Filippetti, S. Sanvito, and K. Burke, "Self-Interaction Errors in Density-Functional Calculations of Electronic Transport," *Phys. Rev. Lett*, vol. 95, p. 146402, 2005. vii, 42, 43

[11] C. A. Ullrich, "TDCDFT: Basic formalism (Lecture 1)." `http://www.tddft.org/TDDFT2012/school/Ullrich2.pdf`, January 2012. vii, 45

[12] G. E. Moore, "Cramming more components onto integrated circuits," *Electronics*, vol. 38, p. 114, 1965. 1

[13] K. Jain, C. G. Wilson, and B. J. Lin, "Ultrafast deep UV Lithography with excimer lasers," *IEEE Electronic Device Lett.*, vol. 3, pp. 53–55, 1982. 1

[14] A. von Hippel, "Molecular engineering," *Science*, vol. 123, p. 315, 1956. 1

[15] J. C. Cuevas and E. Scheer, *Molecular Electronics: An Introduction to Theory and Experiment.* Singapore: World Scientific, 2010. 3, 5, 23, 25

[16] B. J. van Wees, H. van Houten, C. W. J. Beenakker, J. G. Williamson, L. P. Kouwenhoven, D. van der Marel, and C. T. Foxon, "Quantized conductance of point contacts in a two-dimensional electron gas," *Phys. Rev. Lett.*, vol. 60, pp. 848–850, 1988. 3

[17] B. J. van Wees, L. P. Kouwenhoven, H. van Houten, C. W. J. Beenakker, J. E. Mooij, C. T. Foxon, and J. J. Harris, "Quantized conductance of magnetoelectric subbands in ballistic point contacts," *Phys. Rev. B*, vol. 38, pp. 3625–3627, 1988. 3

[18] D. A. Wharam, T. J. Thornton, R. Newbury, M. Pepper, H. Ahmed, J. E. F. Frost, D. G. Hasko, D. C. Peacock, D. A. Ritchie, and G. A. C. Jones, "One-dimensional transport and the quantisation of the ballistic resistance," *J. Phys. C*, vol. 21, p. L209, 1988. 3

[19] L. Venkataraman, J. E. Klare, I. W. Tam, C. Nuckolls, M. S. Hybertsen, and M. L. Steigerwald, "Single-Molecule Circuits with Well-Defined Molecular Conductance," *Nano. Lett.*, vol. 6, p. 458, 2006. 4

[20] F. von Wrochem, D. Gao, F. Scholz, H.-G. Nothofer, G. Nelles, and J. M. Wessels, "Efficient electronic coupling and improved stability with dithiocarbamate-based molecular junctions," *Nature Nanotechnology*, vol. 5, p. 618, 2010. 4

[21] J. K. Sørensen, J. Fock, A. H. Pedersen, A. B. Petersen, K. Jennum, K. Bech-gaard, K. Kilsa, V. Geskin, J. Cornil, T. Bjørnholm, and M. B. Nielsen, "Fulleropyrrolidine End-Capped Molecular Wires for Molecular Electronics-Synthesis, Spectroscopic, Electrochemical, and Theoretical Characterization," *The Journal of Organic Chemistry*, vol. 76, p. 245, 2011. 4

[22] A. Mishchenko, L. A. Zotti, D. Vonlanthen, M. Bürkle, F. Pauly, J. C. Cuevas, M. Mayor, and T. Wandlowski, "Single-Molecule Junctions Based on Nitrile-Terminated Biphenyls: A Promising New Anchoring Group," *J. Am. Chem. Soc.*, vol. 133, p. 184, 2011. 4

[23] D. R. Ward, N. J. Halas, J. W. Ciszek, J. M. Tour, Y. Wu, P. Nordlander, and D. Natelson, "Simultaneous Measurements of Electronic Conduction and Raman Response in Molecular Junctions," *Nano Lett.*, vol. 8, p. 919, 2008. 4

[24] C. R. Arroyo, T. Frederiksen, G. Rubio-Bollinger, M. Vélez, A. Arnau, D. Sánchez-Portal, and N. Agraït, "Characterization of single-molecule pen-tanedithiol junctions by inelastic electron tunneling spectroscopy and first-principles calculations," *Phys. Rev. B*, vol. 81, p. 075405, 2010. 4

[25] L. Venkataraman, Y. S. Park, A. C. Whalley, C. Nuckolls, M. S. Hybertsen, and M. L. Steigerwald, "Electronics and Chemistry: Varying Single-Molecule Junction Conductance Using Chemical Substituents," *Nano Lett.*, vol. 7, p. 502, 2007. 4

[26] A. Mishchenko, D. Vonlanthen, V. Meded, M. Bürkle, C. Li, I. V. Pobelov, A. Bagrets, J. K. Viljas, F. Pauly, F. Evers, M. Mayor, and T. Wandlowski, "Influence of Conformation on Conductance of Biphenyl-Dithiol Single-Molecule Contacts," *Nano Lett.*, vol. 10, p. 156, 2010. 4

[27] R. Landauer, "Spatial variation of currents and fields due to localized scatterers in metallic conduction," *IBM J. Res. Develop.*, vol. 1, pp. 223–231, 1957. 5

[28] Y. V. Nazarov and Y. M. Blanter, *Quantum Transport: Introduction to Nanoscience.* Cambridge: Cambridge University Press, 2009. 5, 6, 8, 14, 116

[29] M. Di Ventra, *Electrical Transport in Nanoscale Systems.* Cambridge: Cambridge University Press, 2008. 5, 10, 25

[30] R. Landauer, "Electrical transport in open and closed systems," *Z. Phys. B*, vol. 68, pp. 217–228, 1987. 5

[31] A. M. Kriman, N. C. Kluksdahl, and D. K. Ferry, "Scattering states and distribution functions for microstructures," *Phys. Rev. B*, vol. 36, pp. 5953–5959, 1987. 6

[32] A. D. Stone and A. Szafer, "What is measured when you measure resistance? – the landauer formula revisited," *IBM J. Res. Develop.*, vol. 32, pp. 384–413, 1988. 9

[33] A. D. Benoit, S. Washburn, C. P. Umbach, R. B. Laibowitz, and R. A. Webb, "Asymmetry in the Magnetoconductance of Metal Wires and Loops," *Phys. Rev. Lett.*, vol. 57, p. 1765, 1986. 9

[34] Y. Isawa, H. Ebisawa, and S. Maekawa, "Effects of Non-Locality on Quantum Transport Phenomena in Microstructures," *Jpn. J. Appl. Phys.*, vol. 26-3, p. 25, 1987. 9

[35] H.-L. Engquist and P. W. Anderson, "Definition and measurement of the electrical and thermal resistances," *Phys. Rev. B*, vol. 24, pp. 1151–1154, 1981. 9

[36] M. Büttiker, Y. Imry, R. Landauer, and S. Pinhas, "Generalized many-channel conductance formula with application to small rings," *Phys. Rev. B*, vol. 31, pp. 6207–6215, 1985. 9

[37] M. Büttiker, "Symmetry of electrical conduction," *IBM J. Res. Dev.*, vol. 32, pp. 317–334, 1988. 9

[38] H. D. Cornean, A. Jensen, and V. Moldoveanu, "A rigorous proof of the Landauer-Büttiker formula," *J. Math. Phys.*, vol. 46, p. 042106, 2005. 10

[39] M. Büttiker, "Transmission Probabilities and the Quantum Hall Effect," *Phys. Rev. Lett.*, vol. 62, p. 229, 1989. 10

[40] P. Streda, J. Kucera, and A. H. MacDonald, "Edge states, transmission matrices, and the Hall resistance," *Phys. Rev. Lett.*, vol. 59, p. 1973, 1987. 10

[41] B. J. van Wees, E. M. M. Willems, C. J. P. M. Harmans, C. W. J. Beenakker, H. van Houten, J. G. Williamson, C. T. Foxon, and J. J. Harris, "Anomalous integer quantum Hall effect in the ballistic regime with quantum point contacts," *Phys. Rev. Lett.*, vol. 62, pp. 1181–1184, 1989. 10

[42] S. Washburn, A. B. Fowler, H. Schmid, and D. Kern, "Quantized Hall Effect in the Presence of Backscattering," *Phys. Rev. Lett.*, vol. 61, pp. 2801–2804, 1988. 10

[43] Y. Imry, "Active Transmission Channels and Universal Conductance Fluctuations," *Europhys. Lett.*, vol. 1, p. 249, 1986. 10

[44] Y. Aharonov and D. Bohm, "Significance of electromagnetic potentials in quantum theory," *Phys. Rev.*, vol. 115, pp. 485–491, 1959. 10

[45] S. Washburn and R. A. Webb, "Aharonov-Bohm Effect in Normal Metal Quantum Coherence and Transport," *Adv. Phys.*, vol. 35, p. 375, 1986. 10

[46] M. C. Payne, "Electrostatic and electrochemical potentials in quantum transport," *J. Phys.: Condens. Matter*, vol. 1, p. 4931, 1989. 11

[47] G. Vignale and M. D. Ventra, "Incompleteness of the Landauer formula for electronic transport," *Phys. Rev. B*, vol. 79, p. 014201, 2009. 11

[48] N. Sai, M. Zwolak, G. Vignale, and M. D. Ventra, "Dynamical Corrections to the DFT-LDA Electron Conductance in Nanoscale Systems," *Phys. Rev. Lett.*, vol. 94, p. 186810, 2005. 11

[49] J. Jung, P. Bokes, and R. W. Godby, "Comment on "Dynamical Corrections to the DFT-LDA Electron Conductance in Nanoscale Systems"," *Phys. Rev. Lett.*, vol. 98, p. 259701, 2007. 11

[50] E. Wigner, "On the Quantum Correction For Thermodynamic Equilibrium," *Phys. Rev.*, vol. 40, p. 749, 1932. 14

[51] J. M. Ziman, *Principles of the Theory of Solids*. Cambridge: Cambridge University Press, 1972. 15

[52] D. S. Fisher and P. A. Lee, "Relation between conductivity and transmission matrix," *Phys. Rev. B*, vol. 23, pp. 6851–6854, 1981. 16

[53] D. C. Langreth and E. Abrahams, "Derivation of the Landauer conductance formula," *Phys. Rev. B*, vol. 24, pp. 2978–2984, 1981. 16

[54] H. P. Breuer and F. Petruccione, *The Theory of Open Quantum Systems*. Oxford: Oxford University Press, 2002. 17

[55] A. Atland, *Condensed Matter Field Theory.* Cambridge: Cambridge University Press, 2006. 18

[56] T. N. Todorov, G. A. D. Briggs, and A. P. Sutton, "Elastic quantum transport through small structure," *J. Phys.: Condens. Matter*, vol. 5, p. 2389, 1993. 18

[57] T. N. Todorov and G. A. D. Briggs, "Effects of compositional impurities and width variation on the conductance of a quantum wire," *J. Phys.: Condens. Matter*, vol. 6, p. 2559, 1993. 18

[58] J. F. Janak, "Proof that $\partial E / \partial n_i = \epsilon_i$ in density-functional theory," *Phys. Rev. B*, vol. 18, p. 7165, 1978. 19

[59] L. Hedin, "New Method for Calculating the One-Particle Green's Function with Application to the Electron-Gas Problem," *Phys. Rev.*, vol. 139, pp. A796–A823, 1965. 21

[60] G. Stefanucci and R. van Leeuwen, *Nonequilibrium Many-Body Theory of Quantum Systems.* Cambridge: Cambridge University Press, 2013. 22, 23

[61] G. Onida, L. Reining, R. W. Godby, R. D. Sole, and W. Andreoni, "*Ab initio* calculations of the quasiparticle and absorption spectra of clusters: The sodium tetramer," *Phys. Rev. Lett.*, vol. 75, pp. 818–821, 1995. 23

[62] S. Albrecht, G. Onida, and L. Reining, "Ab initio calculation of the quasiparticle spectrum and excitonic effects in Li_2O," *Phys. Rev. B*, vol. 55, pp. 10278–10281, 1997. 23

[63] J. Yan, K. W. Jacobsen, and K. S. Thygesen, "Optical properties of bulk semiconductors and graphene/boron nitride: The Bethe-Salpeter equation with derivative discontinuity-corrected density functional energies," *Phys. Rev. B*, vol. 86, p. 045208, 2012. 23

[64] Y. Ping and D. Rocca, "*Ab initio* calculations of absorption spectra of semiconducting nanowires within many-body perturbation theory," *Phys. Rev. B*, vol. 85, p. 035316, 2012. 23

[65] D. A. Ryndyk, R. Gutiérrez, B. Song, and G. Cuniberti, *Energy Transfer Dynamics in Biomaterial Systems.* Berlin: Springer, 2009. 23

[66] M. Strange, C. Rostgaard, H. Häkkinen, and K. S. Thygesen, "Self-consistent GW calculations of electronic transport in thiol- and amine-linked molecular junctions," *Phys. Rev. B*, vol. 83, p. 115108, 2011. 24

[67] L. P. Kadanoff and G. Baym, *Quantum Statistical Mechanics*. Menlo Park: W.A. Benjamin, 1962. 26

[68] S. Schmitt-Rink, D. S. Chemla, and H. Haug, "Nonequilibrium theory of the optical Stark effect and spectral hole burning in semiconductors," *Phys. Rev. B*, vol. 37, pp. 941–955, 1988. 26

[69] K. Henneberger and H. Haug, "Nonlinear optics and transport in laser-excited semiconductors," *Phys. Rev. B*, vol. 38, pp. 9759–9770, 1988. 26

[70] M. F. Pereira and K. Henneberger, "Microscopic theory for the influence of Coulomb correlations in the light-emission properties of semiconductor quantum wells," *Phys. Rev. B*, vol. 58, pp. 2064–2076, 1998. 27

[71] L. V. Keldysh, "Diagram technique for nonequilibrium processes," *Sov. Phys. JETP*, vol. 20, p. 1018, 1965. 27

[72] C. Caroli, R. Combescot, P. Nozieres, and D. Saint-James, "Direct calculation of the tunnelling current," *J. Phys. C: Solid St.*, vol. 4, p. 916, 1971. 29

[73] C. Caroli, R. Combescot, D. Lederer, P. Nozieres, and D. Saint-James, "Direct calculation of the tunnelling current. II. Free electron description," *J. Phys. C: Solid St.*, vol. 4, p. 2598, 1971. 29

[74] Y. Meir and N. S. Wingreen, "Landauer Formula for the Current through an Interacting Electron Region," *Phys. Rev. Lett.*, vol. 68, pp. 2512–2515, 1992. 29

[75] M. Cini, "Time-dependent approach to electron transport through junctions: General theory and simple applications," *Phys. Rev. B*, vol. 22, p. 5887, 1980. 29, 43

[76] G. Stefanucci and C.-O. Almbladh, "Time-dependent partition-free approach in resonant tunneling systems," *Phys. Rev. B*, vol. 69, p. 195318, 2004. 29

[77] T. K. Ng and P. A. Lee, "On-Site Coulomb Repulsion and Resonant Tunneling," *Phys. Rev. Lett.*, vol. 61, pp. 1768–1771, 1988. 29

[78] H. Ness, L. K. Dash, and R. W. Godby, "Generalization and applicability of the Landauer formula for nonequilibrium current in the presence of interactions," *Phys. Rev. B*, vol. 82, p. 085426, 2010. 29

[79] A. Ferretti, A. Calzolari, R. Di Felice, F. Manghi, M. J. Caldas, M. B. Nardelli, and E. Molinari, "First-Principles Theory of Correlated Transport through Nanojunctions," *Phys. Rev. Lett.*, vol. 94, p. 116802, 2005. 29

[80] A. Ferretti, A. Calzolari, R. Di Felice, F. Manghi, M. J. Caldas, M. B. Nardelli, and E. Molinari, "Erratum: First-Principles Theory of Correlated Transport through Nanojunctions [Phys. Rev. Lett. 94, 116802 (2005)]," *Phys. Rev. Lett.*, vol. 94, p. 179901(E), 2005. 29

[81] L. K. Dash, H. Ness, and R. W. Godby, "Nonequilibrium electronic structure of interacting single-molecule nanojunctions: Vertex corrections and polarization effects for the electron-vibron coupling," *J. Chem. Phys.*, vol. 132, p. 104113, 2010. 29

[82] L. K. Dash, H. Ness, and R. W. Godby, "Nonequilibrium inelastic electronic transport: Polarization effects and vertex corrections to the self-consistent Born approximation," *Phys. Rev. B*, vol. 84, p. 085433, 2011. 29

[83] N. Sergueev, Qing-feng Sun, H. Guo, B. G. Wang, and J. Wang, "Spin-polarized transport through a quantum dot:Anderson model with on-site Coulomb repulsion," *Phys. Rev. B*, vol. 65, p. 165303, 2002. 29

[84] R. Lake and S. Datta, "Nonequilibrium Green's-function method applied to double-barrier resonant-tunneling diodes," *Phys. Rev. B*, vol. 45, pp. 6670–6685, 1992. 29

[85] T. Yamamoto and K. Watanabe, "Nonequilibrium Green's Function Approach to Phonon Transport in Defective Carbon Nanotubes," *Phys. Rev. Lett.*, vol. 96, p. 255503, 2006. 29

[86] J. Taylor, H. Guo, and J. Wang, "*Ab initio* modeling of quantum transport properties of molecular electronic devices," *Phys. Rev. B*, vol. 63, p. 245407, 2001. 29

[87] N. E. Dahlen and R. van Leeuwen, "Solving the Kadanoff-Baym Equations for Inhomogenous Systems: Application to Atoms and Molecules," *Phys. Rev. Lett.*, vol. 98, p. 153004, 2007. 29

[88] A. Marini, "Competition between the electronic and phonon-mediated scattering channels in the out-of-equilibrium carrier dynamics of semiconductors: an ab-initio approach," *J. Phys.: Conf. Ser.*, vol. 427, p. 012003, 2013. 29

[89] L. H. Thomas, "The calculation of atomic fields," *Proceedings of Cambridge Philosophical Society*, vol. 23, pp. 542–548, 1927. 31

[90] E. Fermi, "Un Metodo Statistico per la Determinazione di alcune Prioprietá dell'Atomo," *Rend. Accad. Naz. Lincei*, vol. 6, pp. 602–607, 1927. 31

[91] P. Hohenberg and W. Kohn, "Inhomogeneous electron gas," *Phys. Rev.*, vol. 136, pp. B864–B871, 1964. 31, 32

[92] W. Ritz, "Über eine neue Methode zur Lösung gewisser Variationsprobleme der mathematischen Physik," *Journal für die Reine und Angewandte Mathematik*, vol. 135, pp. 1–61, 1909. 32

[93] M. Levy, "Electron densities in search of Hamiltonians," *Phys. Rev. A*, vol. 26, pp. 1200–1208, 1982. 34, 72

[94] E. H. Lieb, "Density functionals for coulomb systems," *Int. J. Quantum Chem.*, vol. 24, pp. 243–277, 1983. 34, 72

[95] E. Engel and R. M. Dreizler, *Density Functional Theory: An Advanced Course.* New York: Springer-Verlag, 2011. 35, 52, 79, 165

[96] R. O. Jones and O. Gunnarsson, "The density functional formalism, its applications and prospects," *Reviews of Modern Physics*, vol. 61, pp. 689–746, 1989. 35, 36

[97] W. Kohn and L. J. Sham, "Self-Consistent Equations Including Exchange and Correlation Effects," *Phys. Rev.*, vol. 140, p. A1133, 1965. 35

[98] R. G. Parr and W. Yang, *Density-Functional Theory of Atoms and Molecules.* Oxford: Oxford University Press, 1994. 36

[99] D. C. Langreth and M. J. Mehl, "Beyond the local-density approximation in calculations of ground-state electronic properties," *Phys. Rev. B*, vol. 28, p. 1809, 1983. 36

[100] D. C. Langreth and M. J. Mehl, "Erratum: Beyond the local-density approximation in calculations of ground-state electronic properties," *Phys. Rev. B*, vol. 29, p. 2310, 1984. 36

[101] J. P. Perdew and K. Burke and M. Ernzerhof, "Generalized Gradient Approximation Made Simple," *Phys. Rev. Lett.*, vol. 77, p. 3865, 1996. 36

[102] J. P. Perdew and K. Burke and M. Ernzerhof, "Erratum: Generalized Gradient Approximation Made Simple [Phys. Rev. Lett. 77, 3865 (1996)]," *Phys. Rev. Lett.*, vol. 78, p. 1396, 1997. 36

[103] K. Burke, J. P. Perdew, and D. C. Langreth, "Is the Local Density Approximation Exact for Short Wavelength Fluctuations?," *Phys. Rev. Lett.*, vol. 73, pp. 1283–1286, 1994. 36

[104] E. Runge and E. K. U. Gross, "Density-Functional Theory for Time-Dependent Systems," *Phys. Rev. Lett.*, vol. 52, pp. 997–1000, 1984. 37, 127

[105] T. K. Ng and K. S. Singwi, "Time-Dependent Density-Functional Theory in the Linear-Response Regime," *Phys. Rev. Lett.*, vol. 59, pp. 2627–2630, 1987. 38

[106] R. van Leeuwen, "Key Concepts in Time-Dependent Density-Functional Theory," *Int. J. Mod. Phys. B*, vol. 15, p. 1969, 2001. 39, 127

[107] N. T. Maitra, T. N. Todorov, C. Woodward, and K. Burke, "Density-potential mapping in time-dependent density-functional theory," *Phys. Rev. A*, vol. 81, p. 042525, 2010. 39

[108] M. Ruggenthaler and R. van Leeuwen, "Global fixed-point proof of time-dependent density-functional theory," *Eur. Phys. Lett.*, vol. 95, p. 13001, 2011. 39, 40

[109] R. van Leeuwen, "Mapping from Densities to Potentials in Time-Dependent Density-Functional Theory," *Phys. Rev. Lett.*, vol. 82, pp. 3863–3866, 1999. 40, 119

[110] N. T. Maitra, K. Burke, and C. Woodward, "Memory in Time-Dependent Density Functional Theory," *Phys. Rev. Lett.*, vol. 89, p. 023002, 2002. 41, 110

[111] V. U. Nazarov and G. Vignale, "Optics of Semiconductors from Meta-Generalized-Gradient-Approximation-Based Time-Dependent Density-Functional Theory," *Phys. Rev. Lett.*, vol. 107, p. 216402, 2011. 42

[112] C. A. Ullrich, U. J. Gossmann, and E. K. U. Gross, "Time-Dependent Optimized Effective Potential," *Phys. Rev. Lett.*, vol. 74, pp. 872–875, 1995. 42

[113] K. Hirose and M. Tsukada, "First-Principles Theory of Atom Extraction by Scanning Tunneling Microscopy," *Phys. Rev. Lett.*, vol. 73, pp. 150–153, 1994. 42

[114] N. D. Lang, "Resistance of atomic wires," *Phys. Rev. B*, vol. 52, pp. 5335–5342, 1995. 42

[115] B. A. Lippman and J. Schwinger, "Variational Principles for Scattering Processes. I," *Phys. Rev.*, vol. 79, pp. 469–480, 1950. 42

[116] R. W. Godby and R. J. Needs, "Metal-Insulator Transition in Kohn-Sham Theory and Quasiparticle Theory," *Phys. Rev. Lett*, vol. 62, pp. 1169–1172, 1989. 42, 90

[117] J. P. Perdew, R. G. Parr, M. Levy, and J. L. Balduz, Jr., "Density-Functional Theory for Fractional Particle Number: Derivative Discontinuities of the Energy," *Phys. Rev. Lett.*, vol. 49, pp. 1691–1694, 1982. 43

[118] J. P. Perdew and M. Levy, "Physical Content of the Exact Kohn-Sham Orbital Energies: Band Gaps and Derivative Discontinuities," *Phys. Rev. Lett.*, vol. 51, pp. 1884–1887, 1983. 43, 95

[119] S. Kurth, G. Stefanucci, C.-O. Almbladh, A. Rubio, and E. K. U. Gross, "Time-dependent quantum transport: A practical scheme using density functional theory," *Phys. Rev. B*, vol. 72, p. 035308, 2005. 43

[120] P. S. Damle, A. W. Ghosh, and S. Datta, "Unified description of molecular conduction: From molecules to metallic wires," *Phys. Rev. B*, vol. 64, p. 201403, 2001. 44

[121] X. Antoine, A. Arnold, C. Besse, M. Ehrhardt, and A. Schädle, "A review of transparent and artificial boundary conditions techniques for linear and nonlinear schrodinger equations," *Commun. Comput. Phys.*, vol. 4, pp. 729–796, 2008. 44

[122] S. K. Ghosh and A. K. Dhara, "Density-functional theory of many-electron systems subjected to time-dependent electric and magnetic fields," *Phys. Rev. A*, vol. 38, pp. 1149–1158, 1988. 46

[123] G. Vignale, "Mapping from current densities to vector potentials in time-dependent current density functional theory," *Phys. Rev. B*, vol. 70, p. 201102(R), 2004. 47

[124] G. Vignale and M. Rasolt, "Current- and spin-density-functional theory for inhomogeneous electronic systems in strong magnetic fields," *Phys. Rev. B*, vol. 37, p. 10685, 1988. 48, 51, 55, 60, 74, 108, 164, 165

[125] G. Vignale and W. Kohn, "Current-Dependent Exchange-Correlation Potential for Dynamical Linear Response Theory," *Phys. Rev. Lett.*, vol. 77, pp. 2037–2040, 1996. 48, 49

[126] I. V. Tokatly, "A unified approach to the density-potential mapping in a family of time-dependent density functional theories," *Chem. Phys.*, vol. 391, pp. 78–82, 2011. 49

[127] K. Capelle and G. Vignale, "Nonuniqueness and derivative discontinuities in density-functional theories for current-carrying and superconducting systems," *Phys. Rev. B*, vol. 65, p. 113106, 2002. 52, 55, 79

[128] X. Pan and V. Sahni, "Density and Physical Current Density Functional Theory," *International Journal of Quantum Chemistry*, vol. 110, pp. 2833–2843, 2010. 54, 63

[129] G. Vignale, C. A. Ullrich, and K. Capelle, "Comment on density and physical current density functional theory by Xiao-Yin Pan and Viraht Sahni," *International Journal of Quantum Chemistry*, vol. 113, pp. 1422–1423, 2013. 55

[130] E. I. Tellgren, S. Kvaal, E. Sagvolden, U. Ekström, A. M. Teale, and T. Helgaker, "Choice of basic variables in current-density-functional theory," *Phys. Rev. A*, vol. 86, p. 062506, 2012. 55, 63

[131] G. Diener, "Current-density-functional theory for a nonrelativistic electron gas in a strong magnetic field," *J. Phys.: Condens. Matter*, vol. 3, pp. 9417–9428, 1991. 56, 63

[132] G. Vignale and M. Rasolt and D. J. W. Geldart, "Diamagnetic susceptibility of a dense electron gas," *Phys. Rev. B*, vol. 37, pp. 2502–2507, 1988. 60

[133] T. L. Gilbert, "Hohenberg-Kohn theorem for nonlocal external potentials," *Phys. Rev. B*, vol. 12, pp. 2111–2120, 1975. 72

[134] J. E. Harriman, "Orthonormal orbitals for the representation of an arbitrary density," *Phys. Rev. A*, vol. 24, pp. 680–682, 1981. 72

[135] G. Zumbach and K. Maschke, "New approach to the calculation of density functionals," *Phys. Rev. A*, vol. 28, pp. 544–554, 1983. 72

[136] G. Zumbach and K. Maschke, "Erratum: New approach to the calculation of density functionals," *Phys. Rev. A*, vol. 29, pp. 1585–1587, 1984. 72

[137] P. Güttinger, "Das Verhalten von Atomen im magnetischen Drehfeld," *Z. Phys.*, vol. 73, pp. 3–4, 1932. 77, 162

[138] R. P. Feynman, "Forces in molecules," *Phys. Rev.*, vol. 56, p. 340, 1939. 77, 162

[139] R. van Leeuwen and E. J. Baerends, "Exchange-correlation potential with correct asymptotic behavior," *Phys. Rev. A*, vol. 49, p. 2421, 1994. 80, 94

[140] K. Peirs, D. V. Neck, and M. Waroquier, "Algorithm to derive exact exchange-correlation potentials from correlated densities in atoms," *Phys. Rev. A*, vol. 67, p. 012505, 2003. 80

[141] M. J. P. Hodgson, J. D. Ramsden, J. B. J. Chapman, P. Lillystone, and R. W. Godby, "Exact time-dependent density-functional potentials for strongly correlated tunneling electrons," *Phys. Rev. B*, vol. 88, p. 241102(R), 2013. 80, 150

[142] R. W. Godby and M. Schlüter and L. J. Sham, "Self-energy operators and exchange-correlation potentials in semiconductors," *Phys. Rev. B*, vol. 37, pp. 10159–10175, 1998. 90

[143] J. P. Perdew and A. Zunger, "Self-interaction correction to density-functional approximations for many-electron systems," *Phys. Rev. B.*, vol. 23, p. 5048, 1981. 90

[144] P. Sanchez-Friera and R. W. Godby, "Efficient Total Energy Calculations from Self-Energy Models," *Phy. Rev. Lett.*, vol. 85, pp. 5611–5614, 2000. 91

[145] J. D. Ramsden and R. W. Godby, "Intrinsic exchange-correlation magnetic fields in exact current density functional theory for degenerate systems," *Phys. Rev. B*, vol. 88, p. 195115, 2013. 94

[146] J. D. Ramsden, M. J. P. Hodgson, T. Durrant, and R. W. Godby, "Dynamical steps in the nonlocal exchange-correlation potential: derivative discontinuity, nonlocal currents and excited-state decay." In preparation. University of York, Department of Physics, 2011. 94

[147] J. D. Ramsden and R. W. Godby, "Exact Density-Functional Potentials for Time-Dependent Quasiparticles," *Phys. Rev. Lett.*, vol. 109, p. 036402, 2012. 111, 139

[148] M. J. D. Powell, "An efficient method for finding the minimum of a function of several variables without calculating derivatives," *Computer Journal*, vol. 7, pp. 155–162, 1964. 112, 131

[149] J. Crank and P. Nicolson, "A practical method for numerical evaluation of solutions of partial differential equations of the heat conduction type," *Proceedings of the Cambridge Philosophical Society*, vol. 43, pp. 50–67, 1947. 114

[150] Y. Pinchover and J. Rubinstein, *An Introduction to Partial Differential Equations.* Cambridge: Cambridge University Press, 2005. 114

[151] W. H. Press, B. P. Flannery, S. A. Teukolsky, and W. T. Vetterling, *Numerical Recipes.* Cambridge: Cambridge University Press, 1992. 114

[152] J. W. Thomas, *Numerical Partial Differential Equations: Finite Difference Methods.* New York: Springer-Verlag, 1995. 114

[153] J. P. Perdew, A. Ruzsinszky, G. I. Csonka, O. A. Vydrov, G. E. Scuseria, V. N. Staroverov, and J. Tao, "Exchange and correlation in open systems of fluctuating electron number," *Phys. Rev. A*, vol. 76, p. 040501(R), 2007. 116

[154] P. Nozières and C. T. De Dominicies, "Singularities in the X-Ray Absorption and Emission of Metals. III. One-Body Theory Exact Solution," *Phys. Rev.*, vol. 178, p. 1097, 1969. 129

[155] A. K. Das, "The relaxation-time approximation in the RPA dielectric formulation," *J. Phys. F: Metal Phys.*, vol. 5, pp. 2035–2040, 1975. 129

[156] H. Mizuta and C. J. Goodings, "Transient quantum transport simulation based on the statistical density matrix," *J. Phys.: Condens. Matter*, vol. 3, pp. 3739–3756, 1991. 129

[157] D. J. Wales and J. P. K. Doye, "Global optimization by basin-hopping and the lowest energy structures of lennard-jones clusters containing up to 110 atoms," *J. Phys. Chem.*, vol. 101, p. 5111, 1997. 131

[158] J. J. Quinn and R. A. Ferrell, "Electron Self-Energy Approach to Correlation in a Degenerate Electron Gas," *Phys. Rev.*, vol. 112, pp. 812–827, 1958. 132

[159] J. Lindhard, "On the properties of a gas of charged particles," *Matematisk-fysike Meddlelser*, vol. 28, p. 8, 1954. 133

[160] G. F. Giuliani and G. Vignale, *Quantum Theory of the Electron Liquid*. Cambridge: Cambridge University Press, 2005. 133

[161] N. W. Ashcroft and N. D. Mermin, *Solid State Physics*. Toronto: Thomson, 1976. 133

[162] P. Elliott and N. T. Maitra, "Propagation of initially excited states in time-dependent density-functional theory," *Phys. Rev. A*, vol. 85, p. 052510, 2005. 139

[163] K. Luo, J. I. Fuks, E. D. Sandoval, P. Elliott, and N. T. Maitra, "Kinetic and interaction components of the exact time-dependent correlation potential," *J. Chem. Phys.*, vol. 140, p. 18A515, 2014. 139

[164] L. Mancini, J. D. Ramsden, M. J. P. Hodgson, and R. W. Godby, "Adiabatic and local approximations for the Kohn-Sham potential in time-dependent Hubbard chains." Submitted. University of York, Department of Physics, 2013. 150